Distribution Category:
General, Miscellaneous and
Progress Reports (Nonnuclear)
(UC-13)

ANL-79-22

ARGONNE NATIONAL LABORATORY
9700 South Cass Avenue
Argonne, Illinois 60439

CHEMICAL ENGINEERING DIVISION

RESEARCH HIGHLIGHTS

1978

L. Burris	Division Director
D. S. Webster	Deputy Division Director
D. L. Barney	Associate Division Director
F. A. Cafasso	Associate Division Director
A. A. Jonke	Associate Division Director
M. J. Steindler	Associate Division Director

NOTICE
This report was prepared as an account of work sponsored by the United States Government. Neither the United States nor the United States Department of Energy, nor any of their employees, nor any of their contractors, subcontractors, or their employees, makes any warranty, express or implied, or assumes any legal liability or responsibility for the accuracy, completeness or usefulness of any information, apparatus, product or process disclosed, or represents that its use would not infringe privately owned rights.

June 1979

TABLE OF CONTENTS

TABLE OF CONTENTS (contd)

TABLE OF CONTENTS (contd)

TABLE OF CONTENTS (contd)

TABLE OF CONTENTS (contd)

TABLE OF CONTENTS (contd)

CHEMICAL ENGINEERING DIVISION
RESEARCH HIGHLIGHTS
1978

ABSTRACT

Highlights of the research and development activities in Argonne's Chemical Engineering Division (CEN) during 1978 are presented. In the program on high-temperature lithium/metal sulfide batteries for vehicle propulsion and stationary energy storage, industrial firms were subcontracted to design and fabricate Li-Al/FeS and Li-Al/FeS_2 battery cells, which were tested by the contractors and by CEN; a Li-Al/FeS battery is being fabricated and will be tested in a van during 1979. The in-house program also includes cell and battery engineering development, materials development, and cell chemistry studies. CEN's Office for Electrochemical Project Management managed subcontracted efforts and conducted supporting research on development of ambient-temperature batteries (lead-acid, nickel/zinc, and nickel/iron); operated the National Battery Test Laboratory, a facility for testing cells and batteries developed in the Department of Energy's battery program; and managed a program to develop methods for increasing the energy efficiency of industrial electrolytic processes, e.g., production of aluminum and chlorine-caustic. Work on molten-carbonate fuel cells included program management activities, as well as in-house research on electrolyte structures. The Division's efforts on coal technology were mainly centered on pressurized fluidized-bed combustion in the presence of an SO_2 sorbent and regeneration of the sorbent for reuse; other work was in the areas of underground gasification of coal and open-cycle magnetohydrodynamics. In the solar energy program, work on the development and application of nonimaging collectors was continued. Fast reactor safety studies included investigations of the high-temperature physical properties of reactor fuels and materials and of reactions related to post-accident heat removal. Recent studies of the behavior of fission products in irradiated fuel focused on development of a model for the reaction of cesium with stainless steel cladding. Efforts in sodium technology included modeling studies of the transport of tritium in LMFBRs and investigations of methods for processing radioactive sodium for disposal or reuse. The program on reprocessing of nuclear fuels involved technical management of subcontracts and in-house research activities on nonaqueous reprocessing in molten metal and salt systems, as well as development of advanced techniques and systems for solvent extraction in centrifugal contactors. Waste management R&D included studies on the disposal of radioactive waste as fragments encapsulated in a metal such as lead and on the migration behavior of radionuclides in geologic formations. Other work on fuel cycle technology included participation in a program to determine the breeding ratio of the Light Water Breeder Reactor. Magnetic fusion energy research was directed toward development of technology for processing lithium from a fusion-reactor blanket, investigation of the behavior of hydrogen (and tritium) in reactor structural materials, and neutron-radiation dosimetry and damage analyses. The CEN program in basic energy science encompassed research in the areas of homogeneous catalysis, thermodynamics of metal and salt systems, thermochemistry, environmental chemistry, physical properties of associating gases and salt vapors, and electrochemistry.

I. OVERVIEW

A. Introduction

The Chemical Engineering Division (CEN) is a multidisciplinary research organization in which engineers and scientists of diversified talents seek solutions to a wide variety of problems, nearly all of which are related to the nation's energy and environmental needs. For some years after the formation of the Division in 1947, efforts were focused predominantly on development of processes for the recovery of spent nuclear-reactor fuels. More than a decade ago, the scope of the Division's work expanded; while still maintaining strong programs in fuel-cycle technology, we undertook programs on sodium technology, reactor safety, reactor-fuel synthesis by pyrochemical and fluidized-bed techniques, the chemistry of irradiated nuclear fuels, measurements of nuclear constants and fuel burnup, and the direct conversion of heat (from nuclear reactors) to electrical energy. Later, when the function of the national laboratories was broadened to allow research in nonnuclear areas, CEN programs became increasingly diversified. Although we have retained the name "Chemical Engineering," our work is probably best characterized by the term "chemical technology."

Currently, the Division conducts research and development in the following areas: (1) high-temperature, rechargeable lithium/metal sulfide batteries for electric vehicles and off-peak energy storage; (2) ambient-temperature batteries--improved lead-acid, nickel/zinc, and nickel/iron--for near-term electric vehicles; (3) molten-carbonate fuel cells for use by electric utilities; (4) coal technology--mainly pressurized fluidized-bed combustion of coal in the presence of an SO_2 sorbent of limestone; (5) magneto-hydrodynamics; (6) solar energy collectors and concentrators; (7) fast breeder reactor chemistry research--chemical support of reactor safety studies, chemistry of irradiated fuels, and sodium technology; (8) fuel cycle tech-nology--reprocessing of spent fuels, management of nuclear wastes, and nuclear safeguards; (9) magnetic fusion research--lithium processing technology and materials research; and (10) basic energy sciences--homogeneous catalysis, thermodynamics of metal and salt systems, thermochemistry, environmental chemistry, electrochemistry, and physical properties of associating gases and vapors. In addition, the Division operates ANL's Central Analytical Chemistry Laboratory.

The total funding of the Division for FY 1979 is about $31 million, as compared with $25 million for FY 1978. A substantial fraction of the total (about 40%) is "pass through" funding, i.e., funding for work for the Depart-ment of Energy (DOE) that is managed by CEN but is performed outside CEN. The Division's largest programmatic area (58% of the total funding) is electro-chemical technology--mainly, development of batteries and fuel cells; fission-related programs also comprise a significant segment (23%) of the total effort. At the end of 1978, about 285 people were employed in CEN; little growth is expected during 1979.

Management of industrial contracts for research and development continued to occupy a substantial portion of CEN's manpower during the past year. The management responsibilities, which cover development of both ambient- and high-temperature batteries, nonaqueous reprocessing of nuclear fuels, and development of molten-carbonate fuel cells, are in line with DOE policy to place programmatic management "in the field." We also perform R&D work in all these areas, thereby enabling us to maintain a high level of expertise and to be sensitive to programmatic needs and problems. In the programs on battery development, Argonne has been designated by DOE as having the "lead mission" assignment; that is, Argonne has the major responsibility for planning and managing the programs within the policy guidelines and funding established by DOE.

The Division's scientific staff consists principally of chemists and chemical engineers, but includes other types of engineers as well as scientists of other disciplines, e.g., physicists and metallurgists; support personnel effectively round out the Division's capabilities. In addition to its permanent members, CEN also employs some personnel on a temporary basis--post-doctoral appointees, research associates, visiting scientists, and students. In general, 10 to 20 such people may be working in the Division at any given time; however, in the summer, there may be as many as 40--mainly students and professors. In addition, CEN also has contractual relations with consultants from universities and industry.

In summary, the diversity of the Division's programs and the capability to accommodate a wide variety of work help to assure stability. Although the Division's work consists largely of applied technology, the research effort in basic energy science provides a balance of activities and is a rich resource for the applied programs. Along with the basic and applied research efforts, management activities now constitute a significant part of the Division's work.

B. Current Programs

Current programs within the Division are summarized below. These programs are discussed individually in the remainder of the report.

1. Lithium/Metal Sulfide Batteries

Lithium/metal sulfide batteries have the potential of providing energy and power densities that are perhaps five times higher than state-of-the-art lead-acid batteries. Development efforts in CEN are directed principally to electric-vehicle propulsion and stationary energy storage. Although specific energy and power requirements are less demanding for stationary energy storage than for electric vehicles, the high energy densities of lithium/metal sulfide batteries may provide a cost advantage over other battery systems for stationary energy storage.

The ultimate goal of the ANL program is a competitive, self-sustaining industry for production of lithium/metal sulfide batteries for both applications. Thus, transfer of technology to industry is vital. Since 1975, industrial firms have participated in the program, initially by sending employees to ANL to work for times up to one year and, subsequently, by performing subcontracted programs. Work representing about half of the funding of the program is now subcontracted to industrial firms for fabrication and testing of cells, batteries, and hardware.

The program on electric-vehicle batteries consists of a three-step progression to a battery suitable for powering passenger automobiles. The first step involves the development, fabrication, and testing of a 40-kW·h battery, designated Mark IA, to evaluate the general technical feasibility of the lithium/metal sulfide system for vehicle propulsion. This battery, currently being fabricated by Eagle-Picher Industries, Inc., is scheduled for testing in the laboratory and in a van during early to mid-1979. The next step entails the development, fabrication, and testing of a 50-kW·h battery, Mark II, which has somewhat higher performance goals than Mark IA; in addition, materials and fabrication methods amenable to low-cost mass production will be used for Mark II. The performance goals of Mark II are consistent with requirements for powering electric vans or buses. The final step is the development of a high-performance, cost-competitive passenger-car battery, Mark III. The cells in the Mark IA and Mark II batteries will have positive electrodes of FeS. A decision has not yet been made on the positive electrode material for the Mark III battery; however, it will probably be FeS_2, which has a higher energy potential but requires further development.

For electric-vehicle use, the lithium/metal sulfide battery will be contained within a lightweight case that is insulated to limit heat losses at the cell operating temperature of about 450°C. Another important component, now being tested, is a charging system that maintains very close control of individual cell voltages during charge.

Supporting research and development in CEN includes commercialization studies, testing of cells and batteries produced by industrial contractors, cell and battery engineering development, materials development and testing, post-test examination of cells, and cell-chemistry studies. A facility for lifetime testing of up to 50 cells has been constructed and initial operations have commenced; another facility is being prepared and equipped for testing full-scale batteries. In the area of cell and battery development, efforts are directed to advancing cell technology, particularly to improvement of the lifetime and specific energy at high discharge currents. Tests of Li-Al/FeS cells have demonstrated that improved performance is obtained by using LiCl-KCl electrolyte richer in LiCl than the electrolyte composition normally used, or by adding 15 mol % Cu_2S to the FeS electrode. Work is also proceeding on the development of FeS_2 electrodes, which may be used in the Mark III battery; carbon-bonded, paste-like electrodes as an alternative to the present electrodes fabricated by pressing powders; improved separators of boron nitride; and alternative, lower-cost separators formed by pressing powders (e.g., MgO, AlN, β-Si_3N_4).

Post-test examinations of cells continue to provide information on the behavior of cell components that serves as a guide for improving cell design and performance. Cell-chemistry studies are focused on chemical and electrochemical problems that are encountered in cell development and on advancing our understanding of the electrochemical processes. In a separate program, we are also investigating cells that use less expensive and more abundant materials than lithium; present emphasis is on development of calcium-containing negative electrodes.

2. Office for Electrochemical Project Management

The Office for Electrochemical Project Management (OEPM) was established in CEN in 1977 to assist DOE in the planning and management of certain parts of DOE's electrochemical program. The principal activities of the OEPM are (1) management of research and development contracts on near-term, ambient-temperature batteries for electric vehicles; (2) operation of the National Battery Test Laboratory (NBTL), a facility for performance verification and qualification testing of batteries developed in DOE programs; (3) in-house applied and basic research in support of the ambient-temperature battery program; and (4) planning of, and in-house research on, programs related to energy conservation in industrial electrolytic processes.

The ambient-temperature batteries selected for further development and accelerated commercialization are improved lead-acid, nickel/iron, and nickel/zinc. In early 1978, eight major contracts were made with industrial firms for the development work. In addition to management of the contracts, the managerial effort also includes cost and performance studies, establishment of battery specifications and testing procedures, and assessment of thermal management and battery maintenance requirements. The NBTL became fully operational in mid-1978 when the first battery modules (lead-acid and nickel/zinc) were received from contractors and placed under test. The NBTL has the capability for testing about 120 cells and five or six full-size batteries.

In-house research supporting the industrial-contract efforts largely consists of theoretical and experimental work related to electrode reactions in ambient-temperature batteries. During the past year, a three-dimensional model was developed to describe temperature, potential, and reactivity variations occurring over both electrodes of a nickel/zinc electric-vehicle battery. A special porous electrode was used to study the cause of performance-limiting maldistribution of zinc on the anodes of nickel/zinc cells during cycling.

The goal of the program on industrial electrolytic process technology is to increase the energy efficiency of industrial electrolytic processes, e.g., production of aluminum and chlorine-caustic. Studies of electrolytic processes by industrial firms under contract to Argonne will serve as the basis for preparation of a long-range R&D program for DOE. An ad hoc advisory committee that was formed to promote interactions between government, industry, and universities will participate in identifying areas to be studied. In studies at ANL, energy and cost relationships were calculated for improved or alternative electrochemical processes, and new processing concepts were investigated; the latter included production of aluminum using aluminum sulfide as an intermediate species, and copper refining from a

cuprous instead of a cupric medium. These processes show good potential for energy savings, but considerably more development is needed before firm judgments can be made.

3. Molten-Carbonate Fuel Cell Development

The Division provides technical management of DOE's program on molten-carbonate fuel cells by planning and coordinating the work among several organizations--General Electric, Co., Institute of Gas Technology, Oak Ridge National Laboratory, Energy Research Corp., and Argonne National Laboratory. Control of funding is not included in this arrangement. In the overall program, the effects on cell performance of gas pressure, composition, and contaminants have been defined; advances have been made in electrode and electrolyte performance; and a prototype plant-scale module will soon be fabricated.

The primary effort in CEN has centered on improving the performance and decreasing the cost of the electrolyte, which is a composite of lithium-potassium carbonates and lithium aluminate ($LiAlO_2$), through which carbonate ions are conducted between the two electrodes. Several methods have been devised for producing β- and γ-$LiAlO_2$. One such process, which uses a much less expensive starting material than was previously used, has been adopted by most of the industrial partners. Studies of the transformation of $LiAlO_2$ among its three allotropic forms (alpha, beta, and gamma) showed that α- and β-$LiAlO_2$ are transformed to γ-$LiAlO_2$ at cell operating temperatures (925 K), and that the shift is accelerated by the presence of molten Li_2CO_3-K_2CO_3 electrolyte and oxygen. During transformation, particle growth occurs and the resulting decrease of surface area leads to decreases in strength of the tile and in electrolyte retention. Deformation tests have verified the importance of high surface area for high strength. These results suggest that the use of γ-$LiAlO_2$ in the tiles would be advantageous, because the γ-form is stable at the cell operating temperature. The laboratory studies of the properties of $LiAlO_2$ are complemented by in-cell testing of the stability and performance of electrolyte tiles.

4. Utilization of Coal

The CEN effort in coal technology continues to center on fluidized-bed combustion (FBC). This technology is considered to be a top-priority route to near-term clean utilization of coal, and DOE is pressing to bring it quickly to the point of commercial acceptance. DOE has decided to give first priority to commercializing industrial, rather than utility, applications. In the resulting program revision, further ANL work on the large, pressurized Component Test and Integration Unit was halted, and the planned work will be done in other facilities. Continuing work in CEN on laboratory support studies and bench-scale process development is in three general areas: regeneration of the limestone used for SO_2 sorption; studies of limestone sources and reactivity enhancement; and cleaning of gas from a pressurized fluidized-bed combustor before it enters the turbine.

Data on reductive regeneration of sulfated limestone using gases from partial combustion of coal were incorporated into a mathematical model of the process that allowed prediction of performance and cost under a variety of conditions; the results indicated that sorbent cost (including disposal) was the most important cost factor and identified conditions under which regeneration would be economical. Studies recently completed on the behavior of trace elements in coal during cyclic combustion and regeneration showed that emissions are lower than from conventional combustion of pulverized coal, and that the trace elements are retained mostly by the ash rather than the sorbent; the emission advantage is attributed to the lower combustion temperature. Regeneration tests with an externally fired rotary kiln in place of the fluidized bed gave good yields of CaO and SO_2, but the kiln was considered an unsuitable substitute because of marked corrosion and the need for clean fuel for exterior firing.

A thermogravimetric test of limestone sorption capacity for SO_2 was developed, correlated with results from FBC data on seven different stones, and used to evaluate a total of fifty-seven stones from around the U.S. Although further refinement of the method is needed, it is adequate to show a large availability of reactive limestones in the country. Enhancement of limestone-sorption capacity by the addition of small quantities of NaCl or $CaCl_2$ to the bed was shown to involve trace amounts of molten salt that accelerate migration of pores into larger pores, thereby allowing easier movement of gases to and from reactive inner surfaces. Study of the enhancement of sorption, as well as the corrosion of equipment, by salt is proceeding in a small combustor unit equipped with corrosion coupons.

The combustion gas from a pressurized fluidized-bed combustor will enter a gas turbine, where erosion of the turbine blades by particulates and corrosion by gaseous alkali compounds must be controlled. The use of a granular-bed filter containing spent sorbent from the FBC process, downstream from a conventional cyclone collector, provided nearly sufficient reduction in the loading of particulates to meet the acceptable range for turbine operation. Complementary tests with a special cyclone (TAN-JET), which gave better performance than conventional cyclones, indicated that a combination of cyclones and a granular-bed filter will be adequate to meet the acceptable range. Acoustic agglomeration of particles is being investigated as yet another approach to gas clean-up, but is farther from realization. The gaseous alkali compounds can be removed by beds of diatomaceous earth or activated bauxite; optimum conditions and likely costs are being studied, as well as alternative bed materials.

In other work, measurements are being continued of the kinetics of the reaction between steam and chars for use in studies by others of mathematical modeling related to underground (in situ) gasification of coal. Previously obtained kinetic data on subbituminous coal were correlated during the past year and new data were gathered on a typical bituminous coal (Pittsburgh seam); the data-correlation effort will be expanded to include the reaction of chars with CO_2 as well as steam. The Division also has several small activities involving technical assistance to DOE in the form of assessments, planning, or monitoring of programs; these include control of NO_x from coal-fired boilers, and utilization of alternatives (e.g., coal liquids) to petroleum and natural gas in fuel cells and transportation.

5. Magnetohydrodynamics

The Chemical Engineering Division is one of several divisions at ANL working on the development of open-cycle magnetohydrodynamics (MHD) for the generation of electricity from coal combustion. CEN's particular concerns are the processes downstream from the magnetic channel, where the remaining heat must be utilized for steam-turbine generation of electricity--despite the presence of volatilized and entrained slag in the combustion gas and the need to efficiently recover the potassium seed that is added to raise the electrical conductivity of the gas (plasma) flowing through the MHD channel.

In studies of seed/slag chemistry, results of a computer program for predicting partial pressures and condensed-phase compositions for mixtures of combustion gases, seed, and slag have shown reasonable agreement with measurements of potassium partial pressure made on a seed/slag sample. The code has also been used to predict conditions in the process under which sulfur emissions might be unacceptable and the nature of potassium permeation from the gas through a slag layer on component surfaces.

An assessment was made of potential methods for recovering seed (as K_2CO_3) from the mixture of seed and slag removed from the combustion gas. One process (reduction with CO and H_2) has been successfully applied to sodium systems in a flue-gas scrubbing process and in a process for recovery of paper-pulping liquor. Another process (reduction by CO in the presence of $Ca(OH)_2$--the "formate process") is used industrially to make K_2CO_3 from K_2SO_4. More exact data are needed for evaluation of process suitability in the MHD application; experiments are under way to determine the rate and extent of reactions in the direct reduction process.

A major MHD activity in which CEN has a part is the testing of steam-generator components under typical MHD conditions. The experiments will be conducted in a recently completed 2-MW test facility. CEN has a lead role in planning, design, and execution of the tests, and interpretation of the results. The experiments will include heat-transfer measurements, studies of seed and slag behavior, and corrosion testing of construction materials.

6. Solar Energy

Our efforts are continuing on development and application of nonimaging solar collectors. The first phase of this program has been successfully completed, as signaled by construction of 1.5x stationary concentrating collectors by two of our "client" companies; the temperature capabilities (100-250°C) of this simple unit are adequate for space cooling as well as space heating. Higher temperature collectors (250-300°C), suitable for providing industrial process heat or electrical generation plus by-product heat, require 3x to 5x configurations and periodic tilt adjustment. Although the optical and thermal theories are worked out, improved materials are needed: stable selective-absorption surfaces, stable heat-transfer fluids, and more highly reflective collector surfaces. A well-instrumented outdoor facility was built and is being used to test components and finished assemblies.

A concept is being explored for summer space cooling with ice produced and stored during the winter. A buried, insulated tank (perhaps 15 x 15 ft) is equipped with freezing units near the bottom that can flex to free the ice, which floats upward. The units are cooled by evaporation of ammonia; the vapor rises to air-cooled condensers and liquid returns to the freezing units. (Similar "heat pipes" are used to keep the tundra frozen along the Alaska pipeline.) The cooling capacity of the stored ice is tapped in the summer by another system of pipes. We have started a literature review on heat pipes and are discussing them with manufacturers; equipment for experiments on ice formation and release is being assembled.

The Division is also involved in support work for the National Solar Energy Demonstration Program, largely in the form of evaluations and design reviews for commercial and residential systems.

7. Fast Reactor Chemistry Research

Reactor Safety. The Division's ongoing chemical program in fast reactor safety is focused on two major areas of study: (1) high-temperature (up to 6000 K) physical properties, which are needed in reactor-safety analysis, and (2) post-accident heat removal, which involves heat-transfer modeling, calculations of chemical equilibria, and experimental studies of reactions of sodium and fuel with concrete, steel, and graphite.

In high-temperature physical-property studies, values of the thermodynamic and transport properties of sodium were updated and incorporated in a revision of the sodium section of a previously compiled handbook, "Properties for LMFBR Safety Analysis." Studies of thermophysical characteristics of reactor materials have focused mainly on oxide fuels, with some attention being given to carbides and nitrides. Thermodynamic functions of fuel-vapor species are calculated from spectroscopic data on molecular energy levels obtained by a matrix-isolation technique. Data for thorium nitride were obtained during the past year. Calculational studies included the assessment of several models of electronic structure to derive "best estimates" of the thermodynamic functions of UO_2.

One of the findings in a study of post-accident heat removal in gas-cooled fast reactors was that the high-temperature (2400 K) reaction between UO_2, graphite, and stainless steel is exothermic. Accordingly, the heat evolution from this reaction must be included in calculations of post-accident heat removal and in the design of fuel-debris containments.

Reactor Fuels Chemistry. In an ongoing program in support of gas-cooled fast-reactor (GCFR) technology, we are investigating the transport and reaction of fission products in irradiated fuels. Because GCFRs and LMFBRs both use mixed uranium-plutonium oxide fuel, GCFR technology relies heavily on LMFBR base technology, but requires assessment of the impacts of using vented instead of nonvented fuel pins, and helium instead of sodium as a coolant. During the past year, study of the role of cesium in cladding attack was continued. A model was developed that is based on the formation of a cesium-fuel compound at the relatively cool fuel surface and the formation of a cesium chromate compound on the cladding inner surface. The model, which should be applicable to both LMFBR and GCFR fuels, predicts that the local temperature difference between the fuel outer surface and the cladding inner surface is the most important factor in cladding attack and that the maximum

depth of cladding attack will occur at the axial midpoint of the fuel. The nature of cladding attack observed in irradiated fuel from French and British fast reactors is consistent with the model.

Sodium Technology. For over ten years the Division has conducted programs in sodium chemistry and sodium purification. During the past year, work was concentrated in three areas: (1) tritium behavior in LMFBRs; (2) processing of radioactive sodium for recovery or disposal; and (3) development of improved cold traps for in-reactor purification of sodium.

Tritium, which is produced in reactors mainly by ternary fission and by activation of boron in control rods, readily diffuses through stainless steel cladding into the sodium coolant. Although more than 99% is deposited in side-stream cold traps, a small quantity can escape to the environment. In a recently completed CEN study, a computer model was developed for calculating tritium transfer rates and concentrations throughout LMFBR systems; model predictions were verified by tritium measurements in EBR-II. A major conclusion of the study was that tritium release to the environment from the Fast Flux Test Facility or the Clinch River Breeder Reactor would be within acceptable limits.

Fractional distillation is being investigated as a method for processing radioactive sodium for recovery and reuse. Experiments are being conducted in a recently completed, small distillation column to test the separation of fission products (e.g., cesium and strontium) from sodium. Two methods were found to be promising as first steps for converting radioactive sodium waste into compounds suitable for further processing to desired waste forms: (1) reaction with molten NaOH and (2) direct calcination of sodium on silica particles to yield a SiO_2-Na_2O product that could be readily melted to form a glass.

Mechanisms of impurity deposition in sodium cold traps are poorly understood. Accordingly, a small, experimental cold trap has been installed in a sodium loop to study deposition of impurities, principally hydrogen and oxygen, and to test models proposed for representing impurity behavior in cold traps.

8. Fuel Cycle Studies

Reprocessing of Nuclear Fuels. The Division is managing a program on nonaqueous methods of reprocessing nuclear fuels as part of the national effort to reduce the potential for weapons proliferation. The program, which initially included processing of both light water and fast breeder reactor fuels, is now focused only on fast breeder fuels; as a result, some subcontracted work has been terminated. However, the technologies being explored by CEN are suitable for breeder fuels, and are being continued. One study deals with direct approaches to carbide fuels: processing in molten bismuth or chlorinating in molten salt with $CdCl_2$, followed by reduction of some constituents to metal with Cd-Mg alloy (to be partitioned later by a salt-transport process). Salt-transport processes are being investigated for processing Th-U-Pu fuels. In such a process, elements dissolved in a "donor" alloy are contacted with molten salt, oxidized, and transported by the salt to an "acceptor" alloy, where they are reduced. We are also testing the feasibility of reprocessing waste salt containing CaO

(from reduction of oxide fuel by calcium metal) by electrolytic reduction of the CaO back to metal.

Our program on advanced solvent-extraction techniques centers on the ANL centrifugal contactor. Because of the intensity of phase mixing and separation in centrifugal contactors, they are small relative to conventional gravity-settling units and consequently offer advantages in avoiding criticality hazards and radiation damage to solvent. The ANL design, a modified version of the established Savannah River Plant (SRP) design, has potential for lower cost and easier maintenance. In work funded by SRP, a single-stage unit (25-cm-dia rotor) is being built that will have sufficient capacity for extraction of 10 metric tons of LWR fuel per day. A smaller unit (9-cm-dia), built with funding from Oak Ridge National Laboratory (ORNL) and capable of processing 0.5 metric ton of LMFBR fuel per day, has been thoroughly characterized during the year, showing, e.g., extraction efficiencies >98%. An eight-stage bank of these units will eventually be constructed for use at ORNL. To characterize the performance of the contactor concept with radioactive solutions, two eight-stage minicontactors (about 50 mL/min) have been built and used for various tasks: demonstrating an actinide partitioning process for the Chemistry Division; exploring a method to diminish extraction of fission-product ruthenium; and (using a single stage) developing improved methods of cleaning used solvent.

Management of Nuclear Wastes. Suitable means for safe disposal of radioactive wastes must be found if public acceptance of nuclear power is to be achieved. The physical form of the waste is one area that needs further study. We have continued previous work on encapsulation of ceramic waste pellets in lead or aluminum as an alternative to incorporation of waste in monolithic glass forms. We have demonstrated a procedure for void-free encapsulation of waste pellets in lead, and defined the conditions necessary for testing impact resistance (dispersion) of small canisters so that the results are scalable to full size. Preliminary cost comparisons of our process and the glass process have started.

The role of geological formations in retarding migration of radionuclides from a repository is another important factor in safe disposal of waste. Our studies deal with the physical-chemical interactions among radionuclides, rock, and rock water (aspects of migration such as hydrodynamic dispersion are being handled by other laboratories). In our experiments, simulated groundwater containing radionuclides is forced through porous rock or through a fissure in impermeable rock. Interaction is usually considered to be of an ion-exchange type, but our studies indicate that it can be complicated by irreversible precipitation (which immobilizes) and colloid formation (which does not immobilize). One study showed that the distribution coefficient for cesium between water and kaolinite (a mineral typical of the weathered surface of many rocks) decreases more at high temperatures (about 200°C) than previously believed; this finding has an impact on the use of clay backfills in repositories.

Evaluations and Studies. We continue to have a part in the national program to lessen the possibility of nuclear weapons proliferation by diversion of fissionable material from power reactor systems. In our studies, which are on fuel reprocessing, preliminary findings indicate that even major changes and costs will produce only marginal benefits.

As a follow-on to our previous work on the pyrophoricity of Zircaloy cladding, we developed criteria for the management of these waste hulls. The use of "criterion functions," applied separately to a number of factors pertaining to hull management, provides a valuable means of assessing hazards under normal and abnormal operations.

LWBR Proof-of-Breeding Analytical Support. Our program for chemical analysis of segments of irradiated ThO_2-$^{233}UO_2$ fuel from the Light Water Breeder Reactor (Division of Naval Reactors) will allow calibration of a nondestructive assay gauge currently under development by Bettis Atomic Power Laboratory; the gauge will be used on fuel discharged from the reactor in mid-1981 to determine the reactor breeding ratio. After a difficult and protracted period of revision of equipment and procedures, necessitated by the extreme requirements for precision, satisfactory results were obtained on segments of irradiated fuels.

The foregoing phase of work was carried out with a pilot-scale shear and pressurized dissolver initially developed by Bettis. Since we will have to analyze at least 50 fuel rods during 1982 as a check on the fuel assay gauge, the second phase of the program consists of design, procurement, installation, and testing of full-scale equipment during the next two years. This work, which has been started, will provide a precision shear (capable of handling four different rod diameters), a multiple-unit dissolver system, and procedures and equipment for disposing of the waste generated.

9. Magnetic Fusion Energy Research

CEN's participation in ANL's Magnetic Fusion Energy program involves the following activities: (1) lithium processing technology, including measurement and control of impurity elements and extraction of tritium; (2) materials research; and (3) neutron-radiation dosimetry and damage analyses.

During 1978, the 50-gallon stainless steel (Type 304) Lithium Processing Test Loop logged more than 5000 hours with no serious difficulties. Cold-trapping and getter-trapping are being studied as methods for removing oxygen, nitrogen, carbon, hydrogen, and deuterium from liquid lithium. Results to date show that cold-trapping removes carbon and provides moderately effective oxygen control. Preliminary work shows that gettering by zirconium may be effective in controlling nitrogen.

Factors that influence hydrogen permeation, and hence tritium permeation, through structural metals and alloys are being investigated to provide data for the design and analysis of fusion reactor systems. Completed during the past year were measurements of hydrogen permeation rates through candidate austenitic, nickel, and refractory metal-base alloys over a wide range of temperatures and hydrogen driving pressures. Aluminum in nickel alloys imparted a roughly tenfold increase in resistance to permeation by forming an aluminum oxide layer on the alloy surface. The permeability of a titanium alloy sample was about 1000 times greater than that of typical 300-series stainless steels.

In the program on dosimetry and damage analysis, we are developing methods for characterizing the neutron field (flux and spectrum) in test facilities (reactors and accelerators) and for calculating damage parameters. We also provide dosimetry services at the various irradiation facilities. During 1978, the neutron fields of four irradiation facilities were characterized, the most important being the Oak Ridge Research Reactor, which has been designated the primary reactor for fusion materials research for the next three to five years. Computer codes for damage analysis calculations were also upgraded.

10. Basic Energy Science

The Division's research program in basic energy science effectively complements the applied programs by providing contiguous efforts of a basic research nature. Major activities in basic energy science research are described below.

Homogeneous Catalysis. In this research area, current work is devoted to an elucidation of the kinetics and mechanism of the homogenously catalyzed hydrogenation of carbon monoxide. This recently discovered hydrogenation reaction is of interest not only because it may provide a route for the production of chemical feedstock from fossil fuels (e.g., coal), but also because it may help to understand related heterogeneous processes. In a recently completed companion study, the kinetics and mechanism of the catalyzed isomerization of norboradiene to quadrocyclane were studied. The simplicity of this system makes it especially useful for the development of the science of homogeneous catalysis. It is also of interest because, in combination with the reverse reaction, it represents a cycle whereby solar energy may be stored and released on demand.

Thermodynamics of Metal and Salt Systems. The effort in this area includes both theoretical and experimental studies. A statistical-mechanical theory, developed for ternary solutions dilute in one component, more accurately describes the relation of activity coefficient to concentration for a dilute solute in a binary solvent than do other available theories. A computer-assisted analysis of the thermodynamics of cryolite-based systems ($NaF-AlF_3-CaF_2-LiF-MgF_2-Al_2O_3$) is being carried out to extend our knowledge of the phase diagrams; this information is pertinent to the electrolytic production of aluminum by the Hall-Heroult process. Study of the complex equilibria between a multi-component gas phase and condensed phases has started with the development of a computer program that can handle solution phases having up to twelve components.

Study of the thermodynamic and phase relationships in lithium alloys continued with measurement of the thermodynamic properties and phases in the lithium-lead system by a hydrogen titration method. Lithium alloys are important in high-energy battery systems and as fusion-reactor blanket materials. Measurements of the solubility of carbon in liquid lithium were completed. Resistivity measurements as a function of the concentration of impurities in lithium (e.g., Li_3N, Li_2C_2, Li_2O, LiH, and LiBr) are being made to provide an indication of gross impurity levels and to permit studies of interaction between impurities or with getters.

Thermochemistry. The thermochemistry program is an ongoing effort in the Division in which measurements are made of heats of formation and enthalpy increments of substances important to science and technology. Studies during the past year concentrated on measuring enthalpies of formation of heteroatomic polyaromatic "building block" molecules of coal, the thermodynamic properties of sulfide minerals that are of interest in the geothermal energy program, and the enthalpy of hydrogen absorption in $LaNi_x$ and related alloys. The latter are under consideration for use in heat pumps, hydrogen storage, and gettering of tritium in fusion reactor systems.

Environmental Chemistry. In the Division's four-year-old environmental chemistry program, the chemical composition and behavior of condensed material in the atmosphere are studied, techniques for sampling and characterizing particulate emissions from energy-production systems are developed, and mechanisms for formation of primary (at the source) and secondary (in the atmosphere) sulfates, nitrates, and other pollutants are determined. In addition, we are participating in a major field program, the Multistate Atmospheric Power Production Pollution Study (MAP3S) to study atmospheric aerosols. In our studies of the mechanisms of formation of sulfate in the atmosphere, the technique of measuring changes in the ratios of $^{18}O/^{16}O$ continues to be a useful tool. Studies of sulfur-emissions-control chemistry are directed toward determining the kinetics and mechanisms of reactions that are significant in the cyclic use of SO_2 sorbents in fossil fuel combustion, with emphasis this past year on regeneration of CaO from sulfated dolomite.

Physical Properties of Associating Gases and Salt Vapors. Studies continued on the properties of associating gases that are promising candidates for heat-transfer and power-cycle working fluids. In recent experimental work, thermal conductivity measurements were made on mixtures of water with methanol and with trifluoromethanol; this work is augmented by *ab initio* molecular orbital calculations. Spectroscopic studies of stable gaseous complexes formed between nonvolatile transition-metal halides and acidic gases were continued; formation of these vapor complexes provides a potentially useful method for converting nonvolatile halides to a volatile form. A theory was developed for calculating free-energy functions and entropies of unknown substances from the known properties of a few; *ab initio* molecular orbital theory was used to obtain information on structures, energies, and bonding for different molecules.

Electrochemistry. Work in this area consists of emf studies of sulfide solubilities in molten-salt systems, electrocatalysis, and electrode reaction kinetics. The solubilities of lithium sulfide and lead sulfide in LiCl-KCl and LiCl-LiF eutectics were measured. In the area of electrocatalysis, work has started on a study of the kinetics and mechanism of the electroreduction of oxygen on carbon-supported iron phthlocyanine. Also under way are measurements of the exchange current density of iron in LiCl-KCl eutectic using a double-pulse relaxation technique.

11. Analytical Chemistry Laboratory

Operated on a full-cost recovery basis by CEN, the Analytical Chemistry Laboratory (ACL), with a staff of 30 people, supports ANL's scientific and engineering programs by performing routine chemical analyses, developing new or improved analytical methods and equipment, and consulting

with experimenters. A major effort of the ACL during the past year has been the analytical work associated with CEN's Proof-of-Breeding Project. An expanding area of analytical work is the analysis of effluent streams from coal conversion and combustion processes for organic constituents. The analyses, performed in support of an ANL coal toxicology program, have aided in assessment of the biological hazards of coal utilization processes. In a DOE-funded development program, we have acquired the components for a gas-chromatograph/mass-spectrometer/data-acquisition system, which will markedly improve our analytical capability for organic materials. Also acquired during the past year were an ion chromatograph, a scanning electron microscope, and an apparatus for measuring surface area. A plutonium analytical facility, under construction for the past two years, was placed in operation.

12. Computer Applications

A computer-applications group, composed of four people, assists the Division's staff in all phases of computer-related activities, the major areas being computer modeling and calculation, laboratory automation, data-base development, and general support. During the past year, mathematical models were developed for various CEN programs and extensive support in laboratory automation was provided to the National Battery Test Facility, the ambient-temperature and lithium/metal sulfide battery programs, and the ion-microprobe facility.

13. Other Programs

The Division also has several small programs, not discussed further in this report, that are funded by organizations other than DOE. These are (1) a program to develop highly sensitive neutron detectors for characterization of low-intensity, moderated neutron sources; (2) a small program for NASA on experimental and theoretical studies to test theories of the origin of meteorites; and (3) a program for Exxon, Inc. to perform post-irradiation physical and chemical analyses of plutonium recycle fuel from the Big Rock Point Reactor in Michigan. In addition, the Division accommodates numerous ad hoc assignments from other organizations or other divisions of the Laboratory on a purchase-order basis.

II. LITHIUM/METAL SULFIDE BATTERIES

A. Overview of Battery Program

The lithium/metal sulfide battery program at ANL is concerned with the development of high-performance, electrically rechargeable batteries for electric-vehicle propulsion and for stationary energy-storage devices. The widespread use of electric vehicles would conserve petroleum fuels, since the energy for charging the batteries could be provided by coal, nuclear, hydroelectric, or other energy sources; a side-benefit would also be realized in decreased air pollution in congested urban areas. The use of stationary energy-storage batteries for load leveling on electric-utility systems could save petroleum by reducing the need for gas turbines to meet peak power demands. The stationary storage batteries may also find application in systems involving solar, wind, or other cyclic or intermittent energy sources.

The battery cells that are currently under development consist of a lithium-aluminum or lithium-silicon negative electrode, an FeS or FeS_2 positive electrode, a separator to provide electrical isolation of the electrodes, and molten LiCl-KCl electrolyte. The melting point of the electrolyte (352°C at the eutectic composition of 58.2 mol % LiCl) requires a battery operating temperature in the range of about 400-500°C. The overall electrochemical reaction for the Li-Al/FeS cell can be written as follows:

$$2LiAl + FeS \overset{2e^-}{\rightleftharpoons} Li_2S + Fe + 2Al \qquad (1)$$

The theoretical specific energy for reaction 1 is about 460 W·h/kg, and the voltage *vs.* capacity curve has a single voltage plateau at about 1.3 V. The reaction is actually much more complex than shown; for example, an intermediate compound, $LiK_6Fe_{24}S_{26}Cl$ (J phase), is formed through a reaction with the KCl in the electrolyte (see Section II.G). The overall reaction for the Li-Al/FeS_2 cell can be written in two steps:

$$2LiAl + FeS_2 \overset{2e^-}{\rightleftharpoons} Li_2S + FeS + 2Al \qquad (2)$$

$$2LiAl + FeS \overset{2e^-}{\rightleftharpoons} Li_2S + Fe + 2Al \qquad (3)$$

The total theoretical specific energy for reactions 2 and 3 is approximately 650 W·h/kg. The voltage *vs.* capacity curve has two voltage plateaus, one at about 1.7 V (reaction 2) and the other at 1.3 V (reaction 3). The Li-Al/FeS_2 cells are often designed to operate only on the upper voltage plateau; these are referred to as "upper plateau" cells. Reactions 2 and 3 also involve several complex intermediate phases (generally compounds of lithium, iron, and sulfur).

Most of the cells that have been fabricated until recently have been of a prismatic, bicell design with a central positive electrode and two facing negative electrodes. Recently, multiplate cells (see Fig. II-1), which have two or more positive electrodes and facing negative electrodes, have been developed. Testing of multiplate cells has shown that they can achieve higher specific energy and specific power than the bicells.

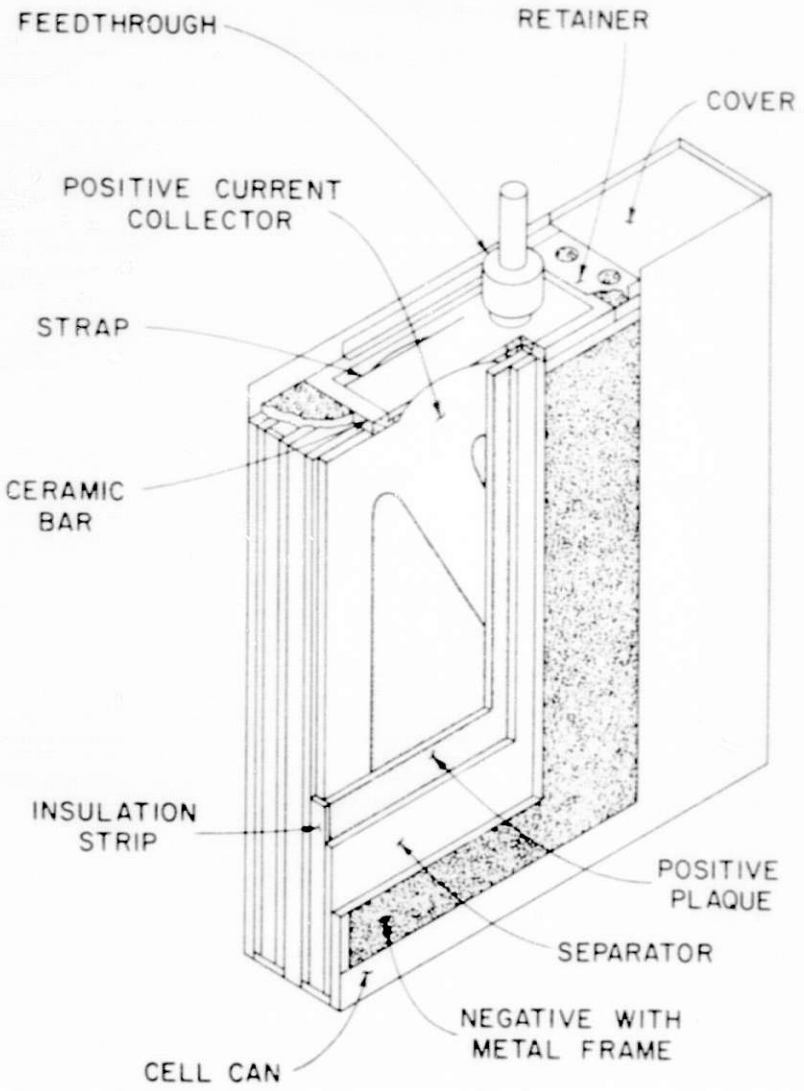

Fig. II-1. Multiplate Cell Design

In the lithium/metal sulfide cell, porous separator sheets between the electrodes serve as electronic insulators, while at the same time providing a path for the migration of lithium ions through the electrolyte absorbed in the separator material. Since both the negative and positive electrodes consist of particle beds or porous structures of the active material filled with electrolyte, screens or cloths are often used on the electrode faces to prevent the escape of particulate material from the electrodes into the separator. To enhance the electronic conductivity of the electrodes, metallic current collectors are used to provide a low-resistance current path from all areas of the electrode to the terminal. In nearly all of the present cell designs, the negative electrodes are grounded to a steel can or housing, and the terminal of the positive electrode extends through the top of the cell can via an electrically insulating feedthrough. The top of the cell can is also provided with a tube, which is closed off later by a weld, to permit the addition of electrolyte to the cell after assembly. In many of the cells, "picture-frame" structures around the perimeter of the electrodes are used to hold the electrode components together as a unit.

The lithium/metal sulfide cell can be assembled in a charged, uncharged, or partially charged state. To assemble a Li-Al/FeS or Li-Al/FeS_2 cell in the charged state, the negative electrodes are normally cold- or hot-pressed from Li-Al powder (usually 46-50 at. % lithium), which may or may not be mixed with some of the LiCl-KCl electrolyte powder. The positive electrodes are formed similarly by cold- or hot-pressing FeS or FeS_2 powder with or without added electrolyte powder. In the case of the uncharged cells, the electrode plaque is pressed from a mixture of Li_2S and iron powder in the appropriate proportions; the negative electrode in this case is an aluminum structure (e.g., pressed wire, porous metal, solid plate) which is converted to the Li-Al alloy electrochemically when the cell is charged. Partially charged cells can be fabricated from mixtures of the above materials in intermediate ratios.

In general, the electric-vehicle battery must have a high specific energy to permit an adequate driving range, and a high specific power to maintain normal highway speeds and to provide sufficient power for passing and hill climbing. The volumetric energy and power densities must also be high because of the limited space available in most vehicles for installation of the battery. For large-scale application in electric vehicles, the battery will probably have to have a maximum cost of \$40-50/kW·h and a minimum lifetime of 1000 equivalent deep-discharge cycles. The performance and lifetime goals for the electric-vehicle battery are presented in Table II-1. The progression of performance goals shown in the table is based on specific improvements that are anticipated in the cell and battery designs as the technology is developed.

The most significant event in the development of the electric-vehicle battery during the past year has been the initiation of a contract with Eagle-Picher Industries, Inc. for the development, design, and fabrication of a 40-kW·h battery, designated Mark IA, which is scheduled for an in-vehicle test in early to mid-1979. The Mark IA battery will consist of multiplate Li-Al/FeS cells, and will be tested primarily to evaluate the technical feasibility of the lithium/metal sulfide system for use in electric vehicles. In the original plan for the electric-vehicle battery, the Mark IA battery was to be followed by Mark IB and IC versions, which would fully meet the Mark I goals (presented in last year's report). However, the advances in the technology, particularly in the development of separators, have been such that a decision was made to proceed directly from the Mark IA to the Mark II battery. The Mark II battery will also consist of multiplate Li-Al/FeS cells, but will have somewhat higher performance than Mark IA. The primary purpose of the Mark II battery is to develop materials and fabrication methods that have a low cost in mass production. Cost and design studies on the Mark II battery were completed by Eagle-Picher Industries, Inc., Gould Inc., and Rockwell International in November 1978. In addition, a request for proposals for development work and fabrication of a 50-kW·h Mark II battery was issued in October 1978. The Mark III program, which is aimed at a high-performance battery for passenger automobiles, is expected to begin in 1981. The type of cells for the Mark III battery has not yet been determined, but they will probably be multiplate Li-Al/FeS_2 cells.

Table II-1. Program Goals for Lithium/Metal Sulfide Electric-Vehicle Batteries

	Mark IA	Mark II	Mark III	Long Range
Specific Energy,[a] W·h/kg				
Cell (average)	80	125	160	200
Battery	60	100	130	155
Energy Density,[a] W·h/L				
Cell (average)	240	400	525	650
Battery	100	200	300	375
Peak Power, W/kg				
Cell (average)	80	125	200	250
Battery	60	100	160	200
Heat Loss through Jacket, W	400	150	125	75-125
Lifetime				
Deep Discharges[b]	200	500	1000	1000
Equivalent Distance, km	30,000	100,000	200,000	300,000
Target Dates				
Battery Test	1979	1981	1983	-
Pilot Manufacture	-	1983	1985	1990

[a] Calculated at the 4-h discharge rate.

[b] Utilization of more than 50% of the theoretical capacity every 10 cycles.

The goals for the stationary energy-storage battery are listed in Table II-2. The specific-energy and specific-power requirements for this application are less demanding than those for the electric-vehicle battery, but low cost (about $40-50/kW·h) and long lifetime are essential. Most of the effort during the past year on the stationary energy-storage battery has involved conceptual design studies of a 100-MW·h energy-storage plant. These studies, which were conducted as a cooperative effort between the Energy Systems Group of Rockwell International and ANL, have provided a general basis for a design of a multiplate LiSi/FeS cell with a capacity of 2.5 kW·h.

A major objective of the program at ANL is to transfer the technology to interested commercial organizations as it is developed, with the ultimate goal of a competitive, self-sustaining industry for the production of lithium/metal sulfide batteries. Technology transfer is implemented by various means, including the assignment of engineers or scientists from industrial companies to ANL on a cost-sharing basis, and the subcontracting of development work on cells, batteries, and auxiliary items to industrial firms. Cost, design, and marketing studies are also conducted with the assistance of subcontractors and consultants. Various academic institutions are also involved in the program through temporary student and faculty assignments, subcontracts, and

Table II-2. Program Goals for Lithium/Metal Sulfide Stationary Energy-Storage Batteries

Goal	BEST[a] 1983	Demonstration 1987
Battery Performance		
Energy Output, kW·h	5,000	100,000
Peak Power, kW	1,500	25,000
Sustained Power, kW	1,000	10,000
Cycle Life	500-1,000	3,000
Discharge Time, h	5	5-10
Charge Time, h	10	10
Cell Performance		
Specific Energy, W·h/kg	60-80	60-150
Specific Power, W/kg	12-20	12-20
Cell Cost, $/kW·h	30-35[b]	25-30[b]

[a] Battery Energy Storage Test Facility. This facility, which is being constructed under joint sponsorship by the U.S. Department of Energy, the Electric Power Research Institute, and the Public Service Co. of New Jersey, will be used to test various types of batteries as load-leveling devices on an electric utility system.

[b] Projected cost for a production rate of 2000 MW·h/y in 1979 dollars.

consultants, mainly in the area of electrode modeling. At the present time, approximately one-half of the funding for this program is used for subcontracted work.

The research and development work at ANL includes cell and battery testing, post-test examinations of cells, cell and battery engineering development, materials development and testing, cell chemistry studies, and commercialization studies. As improvements are made in the ANL cell materials and designs, they are incorporated into the cells fabricated by the subcontractors.

In addition to the research and development program on lithium/metal sulfide batteries, a small effort on alternative cell systems has been maintained under a separate budget activity. The objective of this work is to develop a new battery system that uses abundant, low-cost materials while maintaining the performance levels required for electric vehicles or stationary energy storage. During the past year, this program has been focused on the use of calcium alloys as the negative electrode material.

B. Commercialization Studies

The objective of the commercialization studies at ANL is to provide data on the manufacturing cost and market requirements for the lithium/metal sulfide battery. The commercialization studies are conducted at ANL with assistance

from industrial subcontractors and consultants. These studies involve the identification of potential markets, manufacturing cost analyses, financial plans, and evaluations of competing technologies.

The first commercial production of lithium/metal sulfide batteries will probably be for limited (low volume and high cost) markets such as postal vans, buses, mining vehicles, and submarines. In these near-term (1982-1990) markets, the relatively high price of the batteries should be offset by their favorable performance characteristics.

The bus market is of special interest to potential electric-vehicle manufacturers, both in the U.S. and throughout the world, because the cost of purchasing buses is very often subsidized by national or local governments. In the U.S., the Urban Mass Transportation Authority provides an 80% federal subsidy for bus purchases. An analysis has shown that a significant bus market of about 40 MW·h/y could be achieved by 1982; this market could then rapidly expand to about 580 MW·h/y in 1987 and to about 934 MW·h/y in 1990, which is enough to support the output from one automated battery plant.

The van market after 1987 could become very large. An estimate has been made that this market could support 300,000 battery-powered vans per year, which would require 18,900 MW·h/y of plant capacity. This market alone would require the output from about 17 automated battery plants rated at 1,100 MW·h/y.

Another potential near-term market for the Li/MS_x battery is fork-lift trucks for the U.S. Army. Eagle-Picher Industries, Inc. has been contracted to deliver several cells and a 6-V battery module to Fort Belvoir for test evaluation.

Institutional agencies with responsibilities in resource surveillance and management are interested in the effect of mass production of lithium/metal sulfide batteries on world lithium resources. Consequently, we determined the projected lithium requirements for use in lithium/metal sulfide batteries for electric-vehicle and stationary energy-storage applications by the year 2000. The results showed that a significant production of utility and electric-vehicle batteries, about 110 GW·h by the year 2000, would require about 15% of the U.S. reserves or about 5% of the world reserves.

C. Testing of Industrial Cells and Batteries

Three major subcontractors--Eagle-Picher Industries, Inc., Gould Inc., and Rockwell International's Energy Systems Group--are developing manufacturing procedures as well as fabricating and testing cells. In addition, some of the industrially fabricated cells are being tested at CEN's testing facilities.

Eagle-Picher and Gould fabricated Li-Al/FeS and Li-Al/FeS_2 cells. These cells were assembled in the charged and uncharged states, with pressed negative and positive electrodes of approximately equal capacity (A·h) or with some excess capacity (10-50%) in the negative electrodes.

For the past several years, Cu_2S has been added to the positive electrode of Li-Al/FeS cells to eliminate the formation of J phase, which produces diffusional overvoltage and poor electrical performance. Post-test examinations of cells of this type at ANL (see Table II-9) have indicated, however, that cell failure is sometimes caused by deposition of copper in the separator.* Recent cell-chemistry studies (see Section II.G) indicated that the formation of J phase can be inhibited by either increasing the LiCl content above that of the eutectic electrolyte, or operating the cell at high temperatures (about 500°C).† Both of these approaches have been tested in recent industrial cells.‡ In the case of Li-Al/FeS_2 cells, cobalt sulfides of various sulfur-to-metal ratios have been added to the FeS_2 electrode to increase its electronic conductivity; however, the effectiveness of the cobalt sulfide additive in improving cell performance has not yet been clearly demonstrated.

Boron nitride fabric has been used as the separator material in most of the Eagle-Picher and Gould cells fabricated thus far. Recently, improvements have been made in boron nitride felts, and this material is now being used successfully in cells. The felts offer significant advantages over the fabric both in improved cell performance and lower cost. Various materials, including metal screens, Y_2O_3 cloth, and ZrO_2 cloth have been used as particle retainers at the electrode faces. In most current cells, particle retainers of stainless steel screen are used; however, there appears to be a good chance that the particle retainers can be eliminated completely in future cell designs. A wide variety of current collector designs has been used in these industrial cells, including flat sheets and honeycombs. Iron is a satisfactory current collector material in Li-Al electrodes, and can be used for a limited period (<1 y) in FeS electrodes; nickel, iron-based alloys, and several other materials show promise for longer-term use in FeS electrodes. The only current-collector material that has been used successfully in FeS_2 electrodes to date is molybdenum, which is expensive and difficult to fabricate; alternatives such as protective coatings for inexpensive metals are under investigation at ANL (see Section II.F.3).

During the past year, Rockwell International fabricated Li-Si/FeS cells. These cells were assembled in the uncharged state, and usually had a eutectic LiCl-KCl electrolyte. Most of these cells had the following cell components: separator, AlN powder; positive current collector, nickel honeycomb; negative current collector, steel honeycomb; and particle retainer, porous nickel sheet or nickel screen. Other types of cell components were also tested in these cells.

---

*Significant copper deposition does not occur until after the cell has operated for a long period of time; consequently, copper deposition is not expected to be a problem in batteries for which the required cell lifetime is relatively short, such as the Mark IA.

†Industrial cells have normally been operated at 400-450°C.

‡Before testing LiCl-rich electrolyte in industrial cells, it was first tested in small-scale ANL cells (see Section II.D.1).

The results of the industrial cell testing are briefly summarized below.

1. Eagle-Picher Industries, Inc.

Over the past two years, Eagle-Picher has fabricated about sixty Li-Al/FeS-Cu_2S and Li-Al/FeS_2-CoS_2 bicells with many variations in design (e.g., electrode thickness, electrode capacity loading, and current collector designs). These electric-vehicle cells were tested at ANL and evaluated using a standardized procedure that permits a comparison of the performance of cells with different designs. During the past year, five Li-Al/FeS-Cu_2S bicells were cycled, and all but one operated for between 500 and 1200 cycles. However, the specific energy and specific power of these cells were significantly below the goals set for the Mark IA battery (see Table II-1). Operation of a few of these FeS cells at high temperatures (450-500°C) produced a significant improvement in performance; but operation at these high temperatures for long periods is expected to increase the corrosion rates of the FeS cell components, thereby shortening the cell lifetime.

In this same period, eighteen Li-Al/FeS_2-CoS_2 bicells were tested at ANL, and most of these cells attained very high specific energy and specific power, but operated for less than 250 cycles. Table II-3 gives the design characteristics and performance data of two recently tested FeS_2 cells (I8H and I8L) and two baseline cells. As can be seen in this table, an increase in electrode loading resulted in a significant increase in specific energy. In addition, Cells I8H and I8L had an improved honeycomb design for the positive current collector, which reduced cell resistance and consequently increased power.

Eagle-Picher was awarded a contract in February 1978 for the development, design, and fabrication of the 40-kW·h Mark IA battery. The technical goals for the Mark IA battery are given in Table II-4. On the basis of previous test results from Li-Al/FeS and Li-Al/FeS_2 bicells, Eagle-Picher selected a Li-Al/FeS multiplate cell design (three positive and four negative electrodes) for this battery. As of the end of 1978, about 130 multiplate cells had been fabricated; and most of these cells have been or are being tested by either Eagle-Picher or ANL to determine the effect on performance of the following design variables: method of particle retention, current collector design, additives to the positive electrode, and LiCl content of the electrolyte. Some of the cells have achieved very high specific energies--greater than 100 W·h/kg at the 4-h rate; however, several problems were encountered during the development phase of this program, including high cell resistance, loss of capacity during cycling, and poor wetting of the separator by the electrolyte. These problems appear to have been resolved through intensive efforts both at ANL and at Eagle-Picher. The test results from individual cells indicate that the Mark IA cells, which will be fabricated in early 1979, will meet the performance and lifetime goals listed in Table II-1.

The Mark IA battery will consist of two 20-kW·h modules, each module having 60 multiplate cells connected in series and housed in a thermally insulated case (see Fig. II-2). After the Mark IA has been fabricated, it will undergo laboratory and in-vehicle testing at ANL (scheduled for early to mid-1979). Prior to these tests, however, a small (1.8 kW·h) Li-Al/FeS battery,

Table II-3. Test Results from Eagle-Picher Li-Al/FeS_2-CoS_2 Cells

	2A5[a]	2B4[a]	I8H	I8L
Electrode Thickness, mm				
Positive[b]	3.4	6.3	2.8	5.1
Negative	3.3	6.8	4.2	7.6
Cell Capacity, A·h				
Positive Electrode	70	155	117	220
Negative Electrode	70	155	148	290
Electrode Loading, A·h/cm^3				
Positive	0.67	0.79	1.35	1.39
Negative	0.67	0.73	1.10	1.21
Specific Energy,[c] W·h/kg	44.0	54.5	83.8	99.1
Peak Power, W	84.5	97.5	136	106
Peak Power Flux,[d] W/cm^2	0.22	0.21	0.25	0.19
Cell Resistance, mΩ	8.5	7.5	5.3	6.6

[a]Baseline cells.

[b]Because the cells have two negative electrodes and one positive electrode, the positive electrode is considered to consist of two halves, each having the thickness given here.

[c]Calculated at a current density of 80 mA/cm^2.

[d]Calculated at 50% discharge.

Table II-4. Technical Goals for the Mark IA Battery

Battery Characteristics	Goals
Energy Output,[a] kW·h	40
Power Output,[b] kW	30
Maximum Weight, kg	667
Maximum Volume, L	400
Specific Energy, W·h/kg[a]	60
Energy Density,[a] W·h/L	100
Operating Temperature, °C	400-500
Maximum Heat Loss, W	400
Battery Voltage, V	144
Cycle Life[c]	200

[a]Discharge to 1.0 V/cell at the 4-h rate.

[b]15-s pulse at 50% discharge.

[c]To 20% loss of the design capacity.

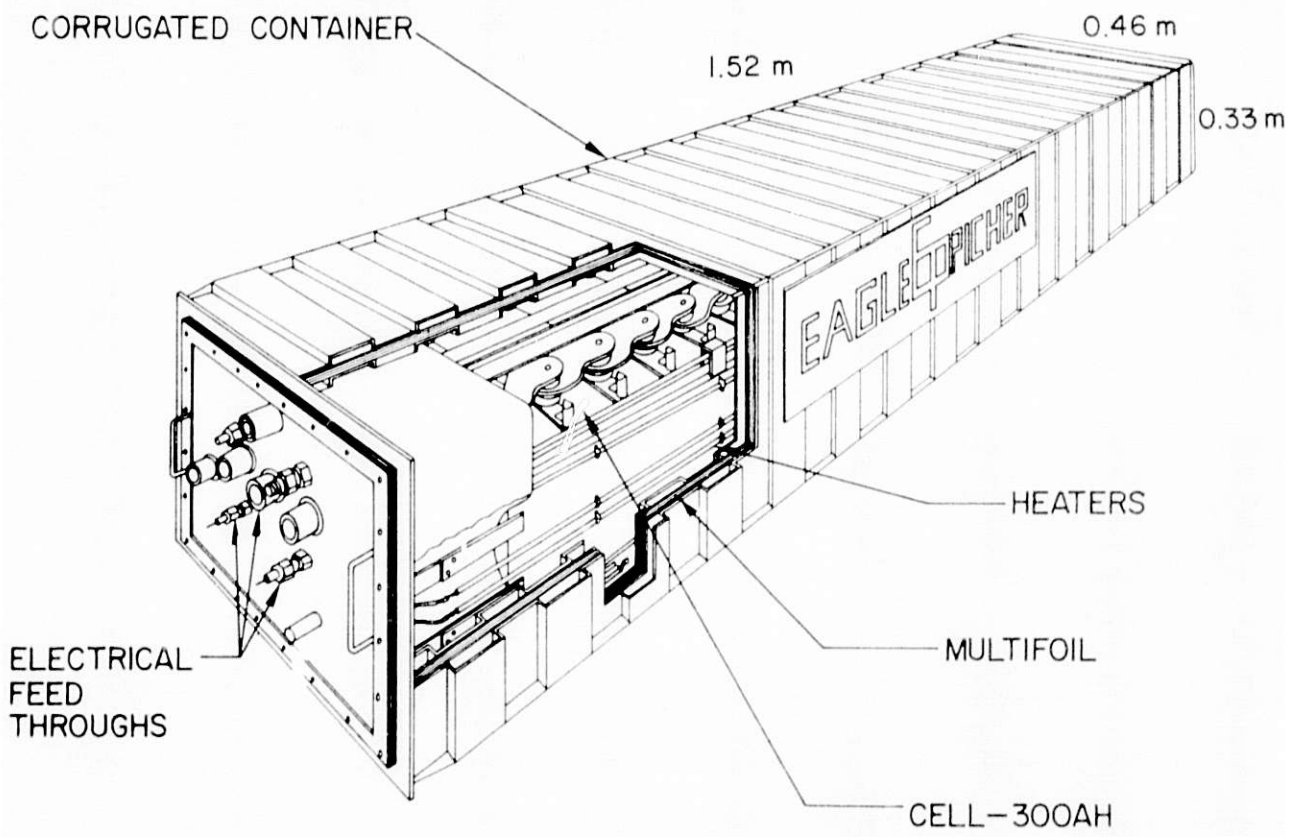

Fig. II-2. Battery Case for a 20-kW·h Battery Module

also fabricated by Eagle-Picher, will be tested at ANL in a Volkswagen van presently powered by twelve 1.8-kW·h lead-acid batteries; testing of this battery will aid in developing the final design for the Mark IA.

2. Gould Inc.

During the past year, Gould fabricated and tested about 40 electric-vehicle bicells with FeS electrodes. The testing of these cells indicated that the cell resistance could be reduced by two design modifications: the substitution of BN felt for the previously used BN cloth separator, and the substitution of a thin nickel sheet for the iron sheet previously used as the current collector. In addition, a Li-Al/FeS cell having carbon, cobalt, and excess iron added to the positive electrode and a LiCl-KCl electrolyte with a high LiCl content (62.8 mol % LiCl) showed a 35% higher positive-electrode utilization than that of a baseline Li-Al/FeS-Cu_2S cell. The test results to date indicate that the near-term (1978-1981) performance goals for the electric-vehicle battery can probably be met or exceeded with the Li-Al/FeS system.

During 1977-1978, Gould Inc. fabricated 55 upper-plateau electric-vehicle bicells with FeS_2 electrodes. These cells are being tested at ANL to determine the effect on performance of the following design features: method of particle retention, thickness and electrolyte content of the positive

electrode, lithium content in the negative electrode, and design of the current collector. The following conclusions were reached from the testing of these cells. First, the use of more than 30 vol % electrolyte in the FeS_2 electrode does not appear to offer any benefit in cell performance. Second, for FeS_2 electrodes that are more than 5.6-mm thick, an increase in the electrode thickness results in a decrease in the utilization of the active material. Third, to attain optimum capacity, the cell should be designed to have 50 at. % lithium and to utilize 70% of the lithium in the negative electrode. In cells designed for negative-electrode utilization higher than 70%, the capacity becomes limited by the negative electrode. In cells designed for negative-electrode utilizations less than 70%, greater than 85% utilization of the positive electrode was achieved at high current densities (100 mA/cm^2). Even though not designed for minimum weight, cells built in this manner have attained specific energies of 75 W·h/kg at the 4-h rate. Testing of the Gould cells will continue in 1979.

3. Rockwell International

The Energy Systems Group at Rockwell International (RI) is developing Li-Si/FeS cells for electric-vehicle and stationary energy-storage applications.

During 1978, a Li-Si/FeS multiplate cell (capacity, 2.5 kW·h) for stationary energy-storage applications was fabricated and tested at RI. This cell, which was operated at about 460°C, had nine negative and eight positive electrodes (23 x 23 cm) and LiCl-KCl eutectic electrolyte; this is believed to be the largest lithium/metal sulfide cell ever operated (see Fig. II-3). The cell operated for a short time (<35 cycles), and post-test examinations revealed that the particle retainer for the positive electrode (porous nickel sheet) had ruptured in many places, the particle retainer for the negative electrode (nickel screen) had allowed material to escape, and the separator (AlN powder) had not been sufficiently wet by the electrolyte. Another 2.5-kW·h cell is presently under development.

Testing of sixteen Li-Si/FeS bicells for electric-vehicle applications was also completed at RI. These cells showed significant improvements in performance, similar to those of the Li-Al/FeS bicells, when operated at high temperatures (between 450 and 500°C) or when the LiCl-KCl electrolyte had a high LiCl content. Although substantial progress has been made at RI in the development of an electric-vehicle Li-Si/FeS cell, further work is needed to attain the required cost and performance goals.

4. Industrial Cell and Battery Testing Facilities

A major effort at ANL is directed toward performance and lifetime testing of cells fabricated by industrial contractors. Additional facilities are being installed at ANL both for cell lifetime tests and for laboratory tests of electric-vehicle batteries.

a. Fifty-Cell Lifetime Test Facility

Construction of a facility for simultaneous lifetime testing of up to 50 cells for the electric-vehicle program is nearing completion. Part of the facility is now in operation; its completion and full-scale

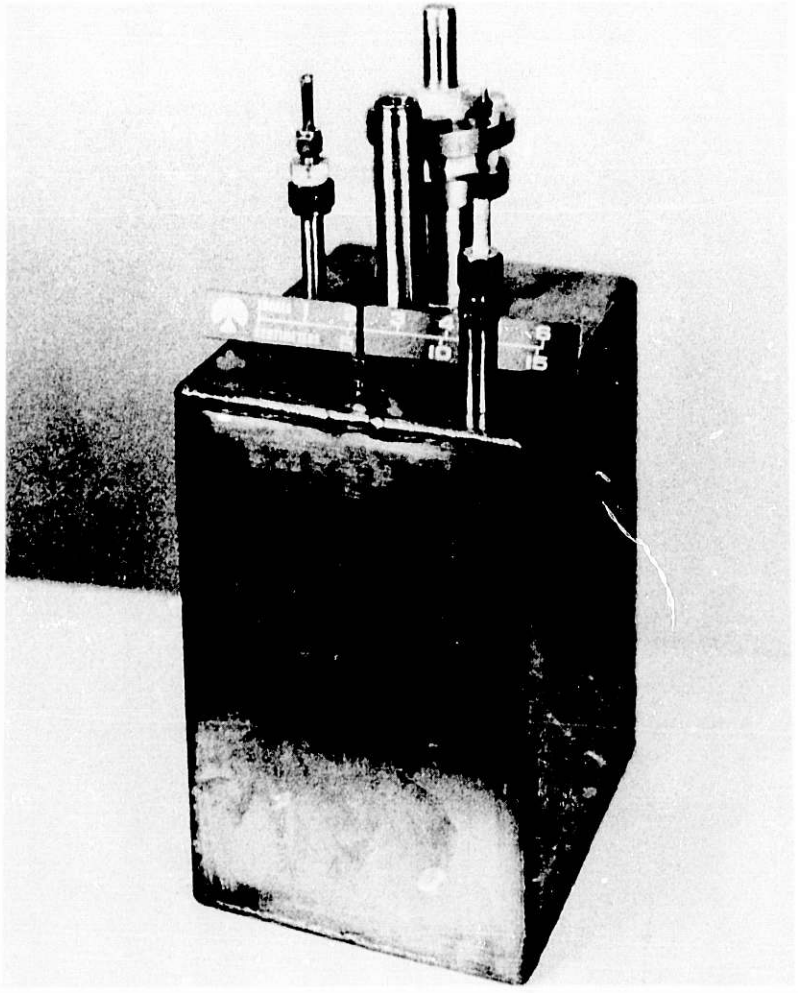

Fig. II-3. Load-Leveling Cell (2.5 kW·h)

operation are scheduled for early 1979. Emphasis will be placed on the testing of cells fabricated by industrial contractors to acquire statistical data on cell performance and lifetime.

Each cell test-station is a module consisting of an open relay rack which contains a furnace, a furnace temperature-control panel, a cell cycler, and a power supply. Figure II-4 is a view of a completed module. The furnaces are 114-L (30-gal) steel drums containing a rigid insulating material and heating elements. The cell under test is suspended from the lid of the drum along with heat shields and insulating materials. All of the furnaces are connected to a low-pressure manifold that provides an argon blanket at positive pressure to minimize atmospheric corrosion. After a prototype cell cycler for this facility had been designed and built by the ANL Electronics Division, the required number of cyclers were ordered from a commercial vendor.*

*Paraplegic Manufacturing Co., Inc., Bensenville, Illinois.

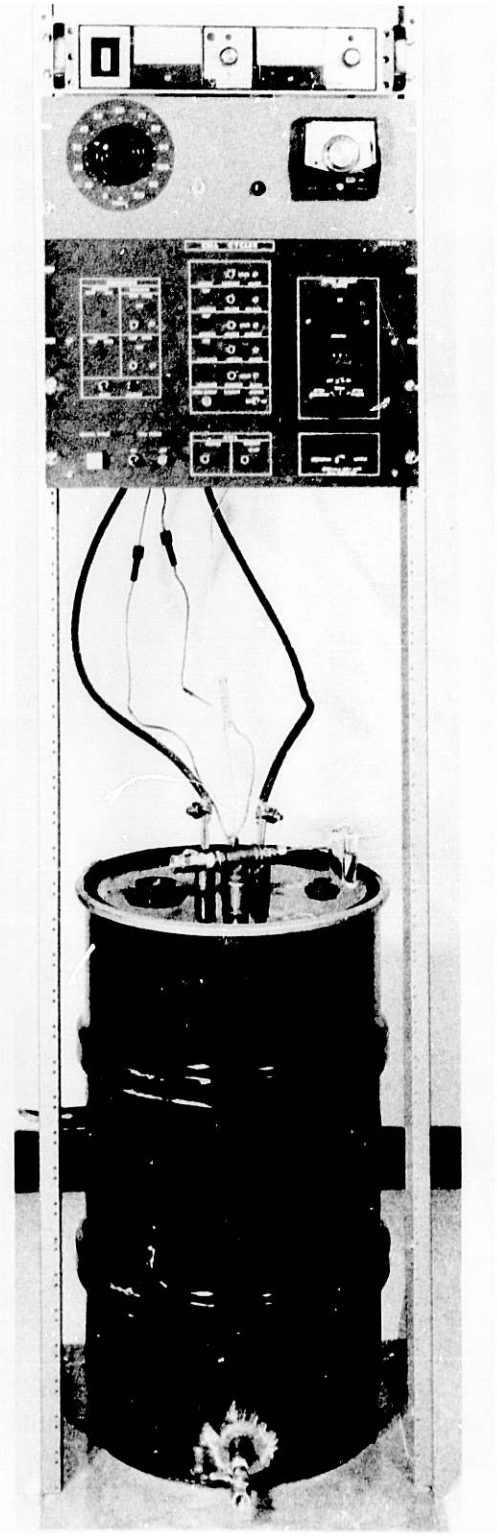

Fig. II-4.

Individual Cell Testing Module

All data from the 50-cell test facility will be fed to a data-acquisition computer system that will store and compute the desired information on cell performance. The data will be sent to a PDP 11/34 computer, which will process the information into the required form. The following data on cell performance will be available: capacity (A·h), energy (W·h), elapsed time (h), voltage (V), current (A), and temperature (°C).

b. Electric-Vehicle Battery Test Facility

A laboratory is being prepared and equipped for testing of two full-scale (up to 60 kW·h) electric-vehicle batteries. Provisions are being made to test the batteries under a variety of modes, e.g., discharges and charges at constant current or constant power; discharges that follow a driving schedule such as a SAE J-227 profile;[1] and charges at constant voltage followed by cell equalization after bulk charging.

The electric-vehicle battery test facility employs computer-controlled power supplies. A block diagram of the system is shown in Fig. II-5. Robicon programmable power supplies* (shown as "cycler" in Fig. II-5) provide the means for charging and discharging the battery. These units are capable of charge currents up to 300 A and discharge currents up to 1200 A; the maximum voltage is 250 V. The current is controlled by a micro-computer (Plessey Micro-1), which permits operation in various modes. The computer also provides safety monitoring of the battery under test and switching of modes of operation. Battery and cell voltages, battery current, and battery temperatures are monitored on a periodic basis, using multiplexers and analog-to-digital (A/D) converters coupled to a CAMAC system.† Data from this system enter the computer for comparison, integration, and processing. A 20-K core memory and 5-megabyte disc memory provide storage for the programs, data acquisition, and data reduction. A visual display is provided by a Decscope‡ and hard copy by a Decwriter.‡

For the first full-scale, electric-vehicle battery (Mark IA), it is anticipated that cell equalization will be required after about ten cycles to bring all cells to the same state of charge. An individual power supply for each cell is provided for this purpose. These power supplies have a current limit of 10 A at a constant voltage (adjustable) of about 1.62 V, and each has its own voltage-sensing leads. The power supplies have been assembled in two modules, each containing 60 power supplies. The modules can be controlled independently, or together as a complete system.

---

*Manufactured by the Robicon Corp., Pittsburgh, PA.

†The CAMAC system is an international, modular data-acquisition and control standard which, when interfaced to a computer, allows the use of remote stations to gather data and control various types of equipment used in industrial and specialized research applications.

‡Manufactured by Digital Equipment Corp., Maynard, MA.

[1]U.S. Energy and Development Administration (ERDA), Office of Electric and Hybrid Vehicles, Test and Evaluation Procedures for Electric Vehicles (1976).

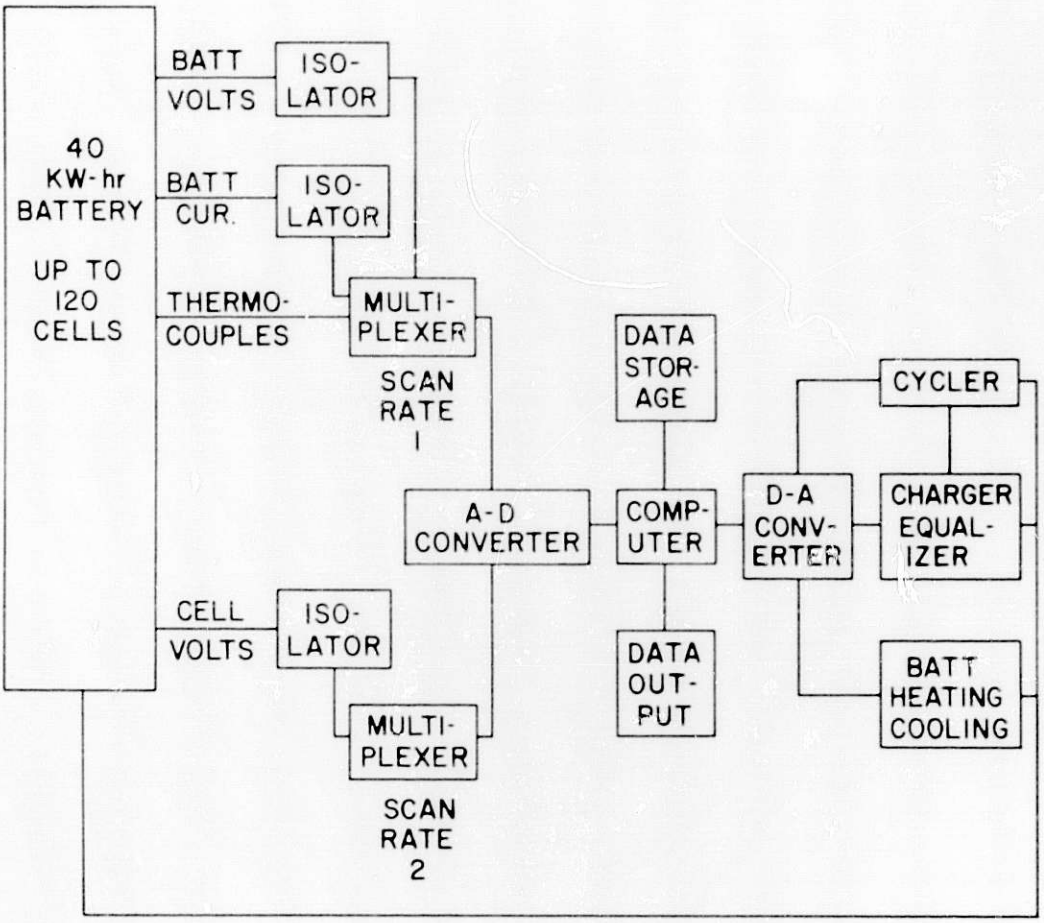

Fig. II-5. Computer Control and Data-Acquisition System for Testing of Electric-Vehicle Batteries

This test facility will be used for laboratory tests of the Mark IA battery. It will also be used to charge the battery for in-vehicle tests.

D. Testing of ANL Cells

Over the past year, ANL has fabricated and tested nearly 40 lithium/metal sulfide engineering-scale bicells. These cells were assembled in the charged, uncharged, or partially charged state. For most of the ANL cells, the electrodes are pressed mixtures of active materials and electrolyte, the separators are a felt material (BN or Y_2O_3), and the electrolyte is LiCl-KCl eutectic. The ANL cells have designs that are expected to reduce cost, or improve lifetime and specific energy at high discharge current densities (>75 mA/cm^2). Whenever advances in cell technology are demonstrated, these advances are incorporated as quickly as possible into the industrial contractors' cells.

1. Small-Scale Cells

Cell-chemistry studies have indicated that the formation of J phase ($LiK_6Fe_{24}S_{26}Cl$) in FeS electrodes has an adverse effect on the electrode kinetics, and that J-phase formation can be decreased by increasing the LiCl content of the LiCl-KCl eutectic (Section II.G). Accordingly, tests were performed on two small-scale FeS cells (15-cm^2 electrode area) to determine the effect of electrolyte composition on positive-electrode utilization. The following electrolyte compositions were tested: 53, 58, 61, 65, and 67 mol % LiCl (liquidus temperatures, 415, 350, 375, 400, and 425°C, respectively). The results indicated that positive-electrode utilization increases significantly with increased LiCl content in the electrolyte of FeS cells. The positive electrode in the cell with the 53 mol % LiCl had the lowest utilization--25%. When an electrolyte of 67 mol % LiCl was used, a positive-electrode utilization of 80% was achieved. In another series of tests, the peak power density (W/cm^2) in small-scale FeS cells was found to be significantly increased by the use of a 67 mol% LiCl-33 mol % KCl electrolyte.

2. Cells with Pressed Electrodes

Over the past year, about ten engineering-scale Li-Al/FeS cells with pressed electrodes were tested in a continuing effort to determine the effect on performance of the Cu_2S positive-electrode additive and the LiCl-rich electrolyte. Performance data for five of the cells are given in Table II-5. These five "M-series" cells* were also tested to determine the effect of a high positive-electrode loading (1.6 A·h/cm^3) on cell performance. As can be seen in the table, both the Cu_2S additive and the LiCl-rich electrolyte improved the performance of the Li-Al/FeS cell. In addition, the use of a high positive-electrode loading appeared to result in somewhat better cell performance.

In the past, although FeS_2 cells have achieved high specific energy and specific power, they have generally had limited lifetimes (<200 cycles). Studies by the cell-chemistry group have shown that gradual loss of capacity in Li-Al/FeS_2 cells may result from irreversibility of the FeS_2 electrode. As a potential solution to this problem, a lower sulfur-to-metal ratio, 1.44, was tested in the positive electrode of two engineering-scale cells--M-4 and M-7. These two cells differed in capacity loading of both electrodes and in lithium content of the negative electrode. The capacity that Cell M-4 could achieve was limited by the capacity of the negative electrode (165 A·h vs. 267 A·h for the positive), whereas the capacity of Cell M-7 was limited by the capacity of the positive electrode (233 A·h vs. 194 A·h). The lithium content of the negative electrode was 48 at. % in Cell M-4 and 55 at. % in Cell M-7.

As shown in Table II-6, the specific energy and specific power in both of these cells were high. After 255 cycles of operation, the capacity of Cell M-4 had declined by only 11%, from 107 to 95 A·h. The stable performance of this cell is very encouraging. Because of the limiting capacity of the negative electrode, the positive-electrode utilization was typically about

*The basic design for this type of cell was presented in last year's report.

Table II-5. Cell Characteristics and Performance Data for Five M-Series FeS Cells

	M-6	M-8	M-9	M-10	M-11
Cu_2S Addition to FeS, mol %	16	0	16	0	0
LiCl Content of Electrolyte, mol %	58[a]	67	58[a]	58[a]	67
Pos. Electrode Loading, A·h/cm^3	0.7	1.4	1.6	1.4	1.6
Specific Energy,[b] W·h/kg	54	59	65	42	53
Specific Power,[c] W/kg	51	62	76	66	75
Cycle Life	64	347	244	300	365

[a]Eutectic composition.

[b]Measured at a current density of 75 mA/cm^2.

[c]Peak power sustainable for 15 s at 50% discharge.

Table II-6. Performance Data for Two M-Series FeS_2 Cells

	Cell M-4[a]	Cell M-7[b]
Specific Energy,[c] W·h/kg	87	97
Specific Power,[d] W/kg	90	125
Cycle Life	300	138

[a]Capacity loading: 165 A·h (neg.)/267 A·h.(pos.).

[b]Capacity loading: 233 A·h (neg.)/194 A·h.(pos.).

[c]Calculated at a current density of 93 mA/cm^2.

[d]Peak power sustainable for 15 s at 50% discharge.

38%. The reserve of active material in the positive electrode may have been partly responsible for its extended operation. Cell M-7 demonstrated similar performance stability for about 135 cycles, and achieved a positive-electrode utilization of about 42% (85 A·h); operation of the cell was terminated, however, because of a sharp decrease in its coulombic efficiency. These results suggest that the use of sulfur-to-metal ratios that are somewhat less than 2.0 in Li-Al/MS_x cells probably stabilizes cell capacity for at least a few hundred cycles.

During 1977, in a number of Li-Al/MS_x cells, NiS_2 was substituted for iron sulfide as the active material in the positive electrode or was used as an additive to improve cell lifetime (see last year's report). Testing of these cells indicated that the relatively small benefit in lifetime resulting from the use of nickel sulfide is not offset by the high cost of nickel. Therefore, testing of this type of cell has been discontinued.

3. Cells with Carbon-Bonded Electrodes

Carbon-bonded positive electrodes are being developed as an alternative to those made by pressing techniques. In the carbon-bonded electrode, the particulate active material is supported in a pyrolyzed-carbon matrix having a void volume of 95%. This structure is formed by the pyrolysis (at 450-550°C) of a paste-like mixture consisting of active material (e.g., FeS or FeS_2), a volatile pore-forming agent (ammonium carbonate), a binder (furan resin), and a carbonaceous filler. In an investigation of potential manufacturing methods for carbon-bonded electrodes, the use of a heat-activated catalyst (1 wt % maleic anhydride) to polymerize the furan resin was found to reduce the curing time. A successful attempt to extrude the paste indicated that extrusion is a potential fabrication method.

Tests have been conducted on three engineering-scale cells having carbon-bonded positive electrodes (one of FeS and the other two of FeS_2) and a design similar to that of the M-series cells. These tests have shown that carbon-bonding is a promising alternative to cold- or hot-pressing techniques for the fabrication of electrodes and that the electrodes have good electrical performance characteristics. A choice between carbon bonding and pressing probably will depend primarily on relative costs and adaptability to mass production.

4. Cells with Powder Separators

Earlier work (see last year's report) had indicated that nonconductive ceramic powders are possible low-cost alternatives to the BN fabric and felt that are currently being used as electrode separators in lithium/metal sulfide cells. The use of MgO-powder separators has now been evaluated in eight engineering-scale Li-Al/FeS cells. Two techniques, vibratory compaction and hot pressing, were used to form the powder separators. The vibratory-compaction procedure consists of vibrating the MgO into the space between the electrodes, which are separated by temporary spacers. The hot-pressed separator is formed by premixing the insulating powder with electrolyte and hot-pressing the mixture onto a previously fabricated positive electrode.

In general, the cells with powder separators have a high coulombic efficiency (>99%) and stable capacity after break-in cycling; and the method of formation of the powder separators has little, if any, effect on the performance characteristics of the cells. The results of these cell tests indicate that powder separators may be an alternative to BN felt or fabric. They offer several potential advantages--ease of fabricating various shapes, the possibility of using a variety of different ceramic powders, and low cost. It is also possible that a thinner powder separator can be developed, with a resulting decrease in the weight of the cell and an improvement in power characteristics. Further work is needed to demonstrate the long-term stability of powder separators, particularly when the cell is being rapidly vibrated, and to develop multiplate cell designs that can accommodate powder separators.

E. Systems Design and Development

The approaches taken in the design of the battery components other than cells differ significantly for the electric-vehicle and stationary-storage applications. The work done on the design and development of this equipment is discussed below; also discussed is a model developed for optimization of the electric-vehicle cell design.

1. Electric-Vehicle Propulsion

Eagle-Picher Industries, Inc. has designed a thermally insulated case for the Mark IA battery based upon a conceptual design devised at ANL. This case will consist of double-walled metal (Inconel 718) with multilayered foil in the evacuated space (see Fig. II-2), and will enclose 60 cells with a total capacity of 20 kW·h. Eagle-Picher has contracted two firms--Thermo Electron Corp. and Budd Co.--to construct the case, and this task is nearly complete. Other Mark IA hardware is also being designed and fabricated by Eagle-Picher. This hardware includes a cell tray, temperature-control and fail-safe equipment, and electrical/electronic components. Great care has been taken to minimize hardware weight without adversely affecting battery performance.

During the past year, ANL constructed a charging system for electric-vehicle batteries that also provides individual cell-capacity equalization with very close control of individual cell voltages. (Close voltage control is important in ensuring long cell life.) The ANL charger/equalizer, shown in Fig. II-6, is based on a design which TRW Systems developed under a contract with ANL; the unit can be preset to charge battery systems containing from one to six cells. The test unit has performed accurately and reliably over a variety of operating conditions.

Two studies on the thermal management of Li/MS_x batteries have been initiated at ANL. In one of these studies, an assessment was made of the optimal shape for a 50-kW·h battery case, rectangular or cylindrical. The results, although still preliminary, indicate that the cylindrical shape has advantages over the rectangular one with respect to weight and volume, heat loss, and manufacturing cost. In the second study, an experimental method was devised for calculating the reversible heating ($T\Delta S$) of Li-Al/FeS cells. The information obtained from these calculations will be used in the design of future electric-vehicle battery cases.

Engineering modeling studies are being conducted at ANL with the objective of developing empirical equations that relate cell performance to the physical and chemical characteristics of the cell and the mode of cell operation. Very general equations have been developed to fit FeS and FeS_2 bicells and multiplate cells; the coefficients in the equations are determined by multiple regression analysis. Operating and performance data of 26 cells* were used to develop the model, and data from a second group of 16 cells* were

*Fabricated by Eagle-Picher, Gould, and ANL.

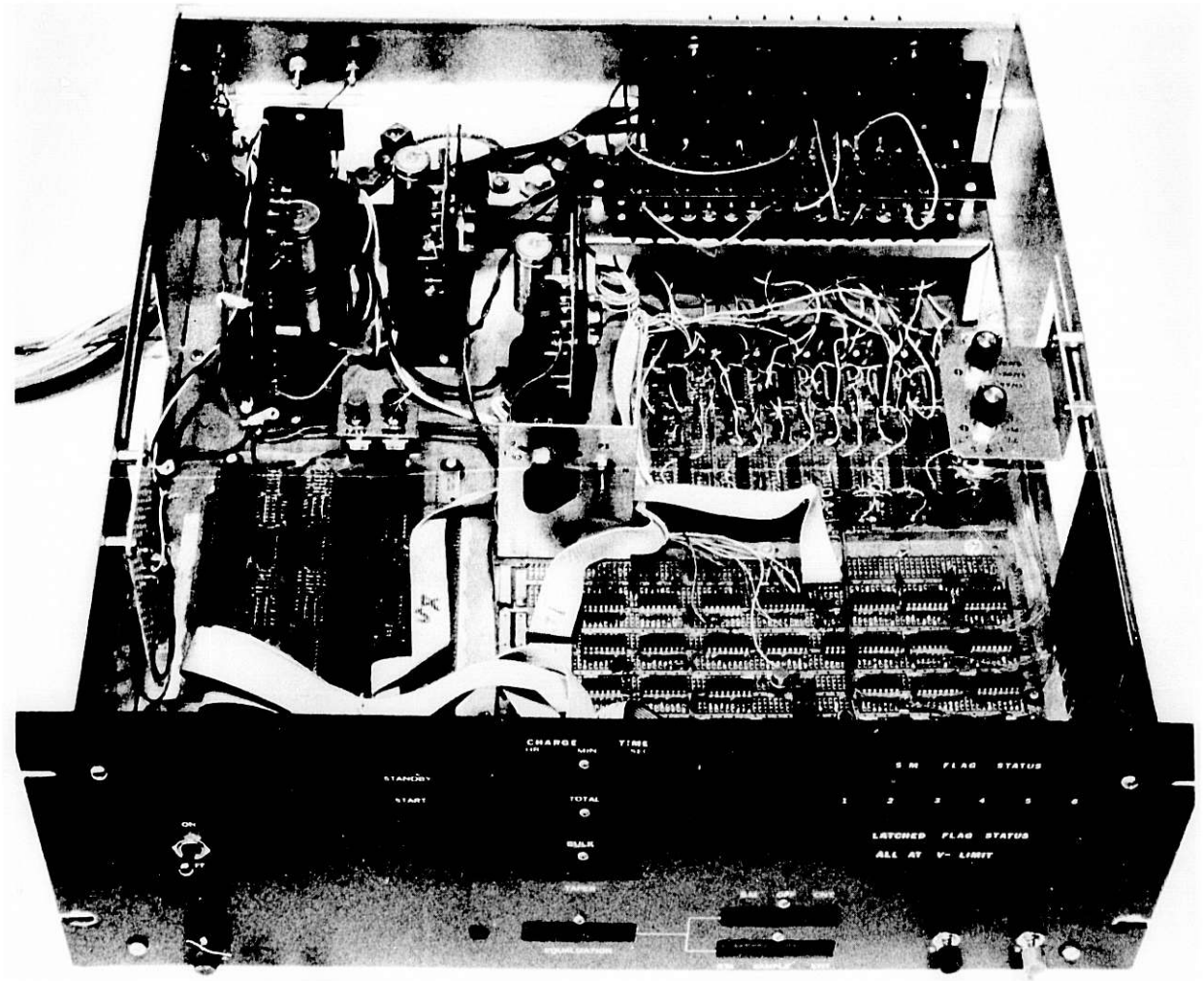

Fig. II-6. ANL Charger/Equalizer

used as a subsequent check of the model. Good agreement has been obtained between predicted and actual cell performance. The model will be very useful in the optimization of the electric-vehicle cell design.

2. Stationary Energy Storage

Rockwell International (RI) has been performing conceptual design studies of a 100-MW·h energy-storage plant; recently, this design was combined with a conceptual design conceived at ANL. The cell chosen for this plant is the 2.5-kW·h multiplate cell (see Section II.C.3). In the RI/ANL design, four of these cells will be electrically connected (in parallel)

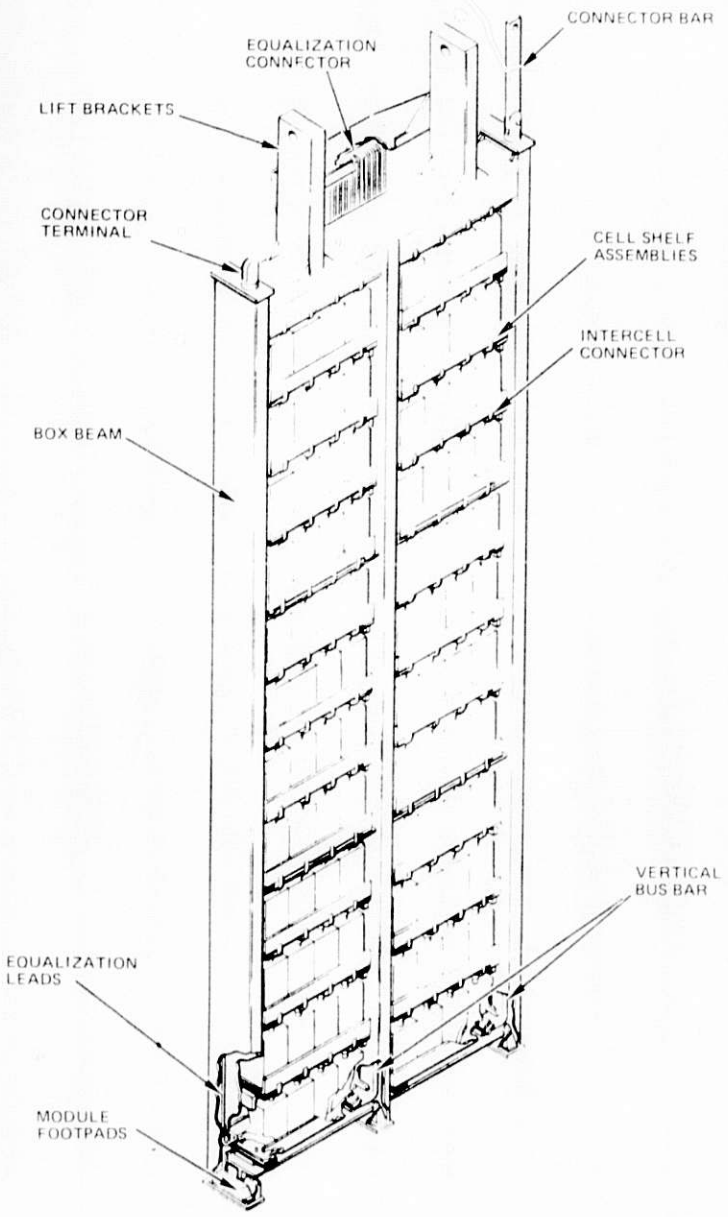

Fig. II-7. Submodule for the Stationary Energy-Storage Plant

to form a 10-kW·h assembly, which will be the basic replaceable unit of the plant. Twenty-four such assemblies will be stacked in two sets of twelve to form a submodule (see Fig. II-7). A module will consist of six rows of six submodules each (a total of 864 cell assemblies) connected in series. Nominal dimensions for an uninsulated, assembled module are 12 x 2.8 x 6 m. Fiberglass insulation panels, 43 cm thick, will be attached to the sides of the module to reduce heat losses.

The 100-MW·h facility design (Fig. II-8) contains two groups of six modules (designated a "battery bank") arranged on either side of an electrical-power processing center. This central area contains ac-dc converters, circuit breakers, and transformers interfacing with the utility distribution or transmission system. Each module group has a 10-MW converter; interties permit

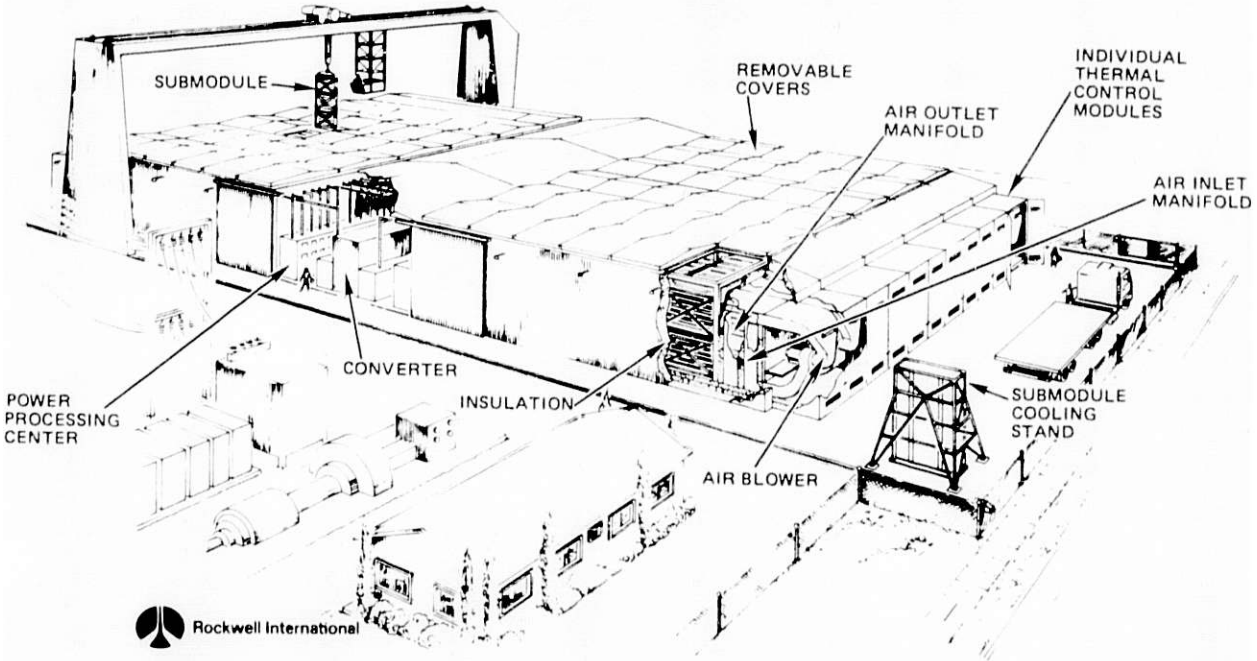

Fig. II-8. 100-MW·h Stationary Energy-Storage Plant

reassignment of the converters to alternate battery banks. Also in the central area are ancillary buildings (sheet-metal sheds) which house switchgear, equalizer electronics, and other instrumentation. Centrifugal blowers for the thermal management system are housed in sheet-metal structures on the outside of each bank. A gantry spans the 23-m width of the plant for loading or replacing the submodules. The submodules can be trucked to the plant site and brought up to operating temperature in an external furnace on site.

Cost estimates for the plant are being prepared by ANL and RI. Preliminary cost estimates by ANL suggest that the cost of the battery plant as presently described (including cells but excluding ac/dc converters) is well over the battery cost goal of \$50/kW·h.* During the next fiscal year, ANL and RI will try to find a way to reduce this cost.

F. Materials Development

Efforts in the materials program are directed toward the development of various cell components (electrode separators, current collectors, and cell hardware), testing and evaluation of potential cell materials (for corrosion and wettability), and post-test examinations of cells to evaluate the behavior of the electrodes and construction materials. The results of these studies form the basis for recommending materials, components, and cell designs.

*A cell cost of \$30/kW·h was assumed for this estimate.

1. Testing of Electrode Separators

The separator is a key component of the cell, and it must meet several requirements, including compatibility with the electrode materials and electrolyte, good wettability by the electrolyte, adequate mechanical strength, acceptable cost, suitable porosity and thickness, and lack of electronic conductivity.

In the past, BN fabric has been used successfully in engineering cells; however, the projected cost for mass production precludes its use in commercial cells. Consequently, three types of potentially low-cost separators have been under study: felts, ceramic powders, and sintered porous ceramics. The ceramic-powder and sintered-ceramic separators have the advantages of utilizing materials that are not available in fibrous form (e.g., AlN, MgO, and β-Si_3N_4) and are amenable to low-cost mass production. The primary disadvantage of the ceramic separators is their low porosity (ceramic powder, 40-50% porosity; sintered ceramic, 50-70% porosity; felt, 90-93% porosity), which restricts ionic transport at high current densities (>75 mA/cm^2).

Testing of experimental cells has demonstrated the technical feasibility of each type of separator. The separators being tested had thicknesses between 0.9 and 1.6 mm. At low current densities (<40 mA/cm^2),the thickness and porosity of the separator had little effect on the utilization of the active material. However, at high current densities, the utilization of cells with powder or sintered separators (i.e., low porosity) was significantly lower than that of cells with felt separators. In addition, at high current densities, utilization was lower in cells with thicker separators. Efforts are continuing on the optimization of the design of ceramic-powder and sintered-ceramic separators; felt separators are being tested in contractor-fabricated cells.

2. Electrolyte Wetting Studies

In the operation of a cell, the separator and active materials must be well wet by the electrolyte; the internal resistance is determined, in part, by the extent to which these components are filled with electrolyte. Therefore, over the past few years studies have been conducted to determine the wettability by molten LiCl-KCl of candidate separator materials and active materials. For these studies, the advancing and receding contact angles of molten LiCl-KCl electrolyte were measured on the following cell materials: LiAl, Al, FeS_2, FeS, Li_2S (active materials), Type 304 stainless steel, Y_2O_3, MgO, BN, Al_2O_3, C, and ZrO_2 (candidate materials for separators and particle retainers). Only the LiAl, Al, Type 304 SS, and Y_2O_3 were easily wet by the electrolyte.

Owing to the difficulty of wetting most of the above materials, studies are being conducted to identify pretreatment processes to improve wettability. This effort has identified $LiAlCl_4$ as an effective wetting agent for separator materials. At room temperature, a low concentration of $LiAlCl_4$ is added to the separator material in the form of a powder; at temperatures above 150°C, this powder melts and spreads over the separator material, thereby producing a material that can be easily penetrated by molten LiCl-KCl. This wetting agent has been successfully tested in engineering-scale cells.

3. Corrosion Studies

Corrosion testing is an integral part of the selection of suitable materials of construction for lithium/metal sulfide cells. Initial evaluations are made on the basis of static corrosion tests, and the more promising materials are tested further in experimental cells.

The search for construction materials for FeS and FeS_2 electrodes is being continued. Results of static corrosion tests have indicated that a number of nickel-base alloys (Hastelloys B and C and some of the Inconel alloys) should have low corrosion rates (<5 μm/y) in the FeS electrode. Iron-base alloys developed at ANL have also looked promising in static tests. However, all these alloys have higher resistivities than those of nickel and iron, and are thus less desirable. For the FeS_2 electrode, corrosion tests have shown that only molybdenum and graphite are sufficiently resistant to sulfide attack. However, graphite has a high resistivity, molybdenum is very expensive, and both materials are difficult to fabricate into suitable current collector shapes. Major efforts are presently being directed toward the development of conductive ceramics for use as a coating material on inexpensive metallic current collectors in FeS_2 electrodes. So far, coatings of TiN and TiB_2 look very promising. This effort is being expanded to include studies of other coating materials, both metal and conductive ceramics (or glasses). During the next year, in-cell testing of the promising coating materials is planned.

4. Post-Test Cell Examinations

Post-test examinations are conducted to determine electrode morphology (e.g., microstructure, active material utilization and distribution, reaction uniformity, impurity effects, and cross-contamination); in-cell corrosion reactions and kinetics; and causes of cell failure. These results are evaluated, and appropriate recommendations for improving cell performance are made to engineering personnel.

During the year, 52 engineering cells were subjected to post-test examinations. All of these cells had bicell designs except four, which had multiplate designs. Of the 52 cells, 43 were fabricated by industrial contractors and the rest by ANL. A summary of the causes of cell failure in 46 cells is presented in Table II-7. Six cells completed the scheduled test period and have been included in the table only to complete the record of post-test examinations.

Cell operation has been terminated principally because of electrical short circuits, although in a few cases loss of capacity and declining coulombic efficiency were the causes. For the past year, the major causes of short circuits have been cutting of separators by the current collector (11 cases) and problems with cell assembly (10 cases). The cells with cut separators were fabricated before the recommendation had been made to add protective screens (see last year's report); the screens have proved effective in preventing this problem. Cell assembly difficulties included misaligned (or broken) electrodes, misplaced (or skewed) separators, and contact of ZrO_2

Table II-7. Summary of Cell Failure Modes

Cause of Failure	No. of Cells
Extrusion of active materials (inadequate confinement)	5
Metallic copper deposits in separator[a]	3
Metallic[b] and/or sulfide deposits across separator	4
Separator cut by honeycomb current collector	11
Equipment malfunction[c]	2
Short circuit in feedthrough	4
Cell assembly difficulties	10
Unidentified	
Declining coulombic efficiency	1
Short circuits	3
Loss of capacity/poor utilization	3
End of test	6

[a] FeS cells with Cu_2S additive.

[b] Other than copper.

[c] Resulting in overcharge, temperature excursion, or accidental polarity reversal.

cloth (conductive after reaction with lithium) with both electrodes. Extrusion of active material, a major problem in past years, appears to have been solved in the cells with newer designs. The causes of the short circuits are mechanical and can be avoided by modification of cell designs and by better quality control.

In the four multiplate cells, metallographic examinations showed a significant deficiency of electrolyte in the negative electrodes and separators; the electrolyte deficiency was caused by incomplete filling and/or expansion of the electrodes. These examinations also showed that agglomeration (densification) had occurred to a considerable extent in the center portion of the negative electrode. At this time, Li-Al agglomeration and electrolyte deficiency are believed to be major factors in the high rate of capacity decline presently observed in multiplate cells.

5. Materials Development by Contractors

In the area of materials and components, the Carborundum Co. is developing BN-felt electrode separators, the Illinois Institute of Technology is investigating the electrochemical deposition of molybdenum for joining and plating current-collector structures, and ILC Technology is developing insulated electrical feedthroughs.

G. Cell Chemistry

The cell-chemistry studies are directed toward (1) solving the chemical and electrochemical problems that arise in the cell and battery development work, (2) identifying new cell designs that may improve performance and lifetime, and (3) acquiring an understanding of the processes that occur within the cells. Most of the cell-chemistry studies at ANL this year were concerned with the properties of metal sulfide electrodes. In addition, General Motors Corp. has been contracted to conduct an experimental investigation of the characteristics of the FeS_2 electrode.

Studies are being conducted on the Li_2S-FeS_2-Fe field of the Li-Fe-S phase diagram. The findings of these studies have been incorporated into the phase diagram shown in Fig. II-9.

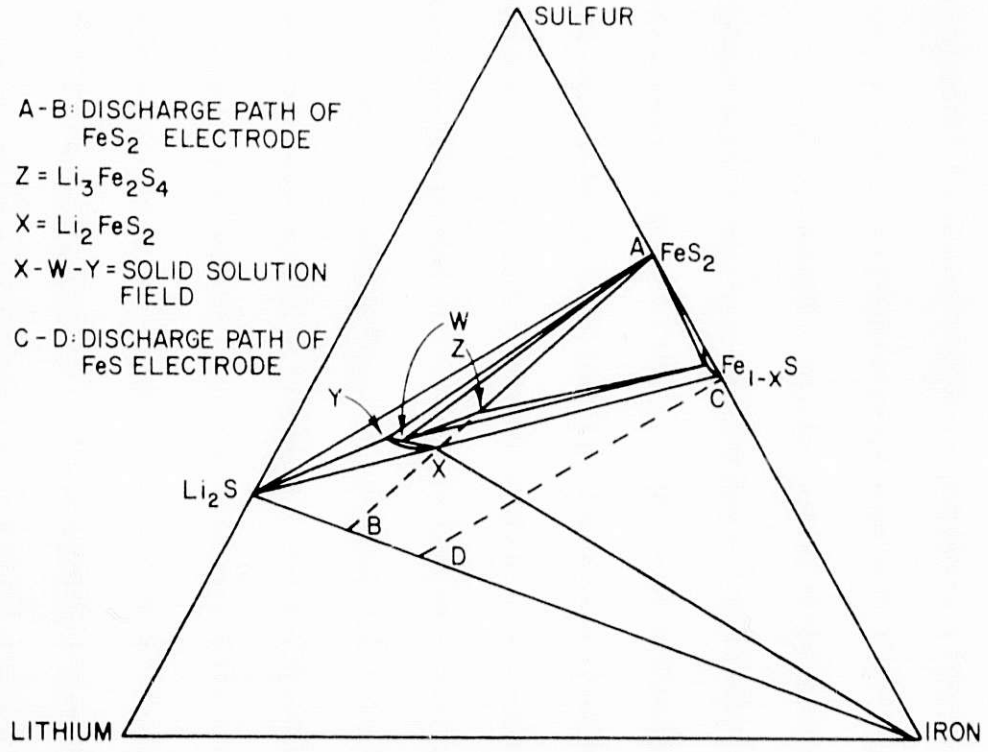

Fig. II-9. Isothermal Section of Li-Fe-S Phase Diagram

The path representing the change in average composition of an FeS_2 electrode as it is charged and discharged at 450°C is indicated by the line A-B. The fully charged electrode contains FeS_2 (point A) and the fully discharged electrode contains Li_2S and iron (point B). Between these extremes, two well-defined compounds are found on the line A-B, namely, Z phase ($Li_3Fe_2S_4$) and X phase (Li_2FeS_2). In addition, more complex phases are found in the region between the Z and X phases, e.g., mixtures of $Fe_{1-x}S$, W (approximate composition, $Li_{12}Fe_4S_{11}$), and Z.

The discharge behavior of FeS_2 electrodes can be described with the aid of Fig. II-9. During discharge, FeS_2 is converted to Z phase. Next, Z phase is converted to a mixture of the compounds $Fe_{1-x}S$ and W. The latter compound lies on the boundary of a solid-solution field labeled X-Y.* The extent of this solid-solution field and the approximate location of the W compound on the field boundary are indicated in the figure. Further discharge of the compounds $Fe_{1-x}S$ and W leads to formation of the single-phase compound, X phase. Finally, X phase is discharged to a mixture of Li_2S and iron. The phases formed during charge are much more complex than those formed during discharge, and are still under investigation.

Cyclic voltammetry studies have been used to elucidate the charge and discharge reactions of the FeS_2 electrode vs. Li-Al in LiCl-KCl electrolyte. The FeS_2 electrode was initially cycled over a broad voltage range (1.0-2.0 V) with a very low voltage scan rate (0.015-0.020 mV/s). In the high-voltage region of the voltammogram (1.5-2.0 V), a large voltage separation, 0.12 V, was found between the charge and discharge reactions, thereby indicating kinetic hindrance of the electrode reaction. In subsequent experiments, voltammograms of the FeS_2 electrode were taken at four discharge cutoff voltages--1.43, 1.56, 1.61, and 1.65 V; and, as the cutoff voltage was increased, the voltage separation was found to decrease due to a shift in the charge peak to a higher voltage (the discharge peak remained fixed). At the 1.65-V discharge cutoff, the voltage separation between the charge and discharge reactions was less than 0.02 V. This result indicates that when the FeS_2 electrode is discharged beyond the Z phase (i.e., the upper voltage plateau) the charge reaction becomes kinetically hindered. Thus, one may conclude that the reactions in FeS_2 electrodes depend strongly on the depth of discharge.

Further investigations of the chemistry of the FeS electrode indicated that, when a Li-Al/LiCl-KCl/FeS cell is charged, the first material to form in the FeS electrode is X phase (Li_2FeS_2). This reaction is followed by the formation of J phase (approximate composition, $LiK_6Fe_{24}S_{26}Cl$), and then by the formation of FeS. The J phase is formed through a reaction with the KCl in the electrolyte, and has been found to adversely affect electrode kinetics. In the absence of J phase, the FeS electrode material traverses

*Approximate composition of Y phase, $Li_7Fe_2S_6$.

two composition triangles during charge and discharge (see line C-D in Fig. II-9). The phases present in the electrode during the first half of the charge (or conversely during the second half of discharge) consist of Li_2FeS_2, Li_2S and Fe (mixture 1). During the second half of charge (or conversely during the first half of discharge) the phases consist of FeS, Li_2FeS_2, and Fe (mixture 2). The two mixtures probably react with electrolyte to form J phase according to the following reactions:

$$6KCl + Fe + 23Li_2FeS_2 \rightleftharpoons J + 5LiCl + 20Li_2S \quad (4)$$

$$6KCl + Fe + 20FeS + 3Li_2FeS_2 \rightleftharpoons J + 5LiCl \quad (5)$$

Preliminary tests by CEN's Basic Energy Sciences program indicated that these reactions are strongly dependent on temperature and on the composition of the electrolyte. Therefore, investigations were carried out to determine the maximum temperature for formation of J phase, T_J, when mixtures (1) and (2) are blended with electrolyte of various compositions. The results showed that the addition of LiCl to LiCl-KCl eutectic significantly decreased T_J. With mixture 2, for example, T_J was 623°C with LiCl-KCl eutectic (58 mol % LiCl), but only 481°C with electrolyte containing about 76 mol % LiCl. Thus, the use of a LiCl-rich electrolyte in Li-Al/FeS cells should result in substantial improvements in performance.

Tests were conducted with Li-Al(10 A·h)/FeS (6.5 A·h) cells having LiCl-KCl electrolytes containing 53, 58 (eutectic), 63, and 67 mol % LiCl to evaluate the effect of electrolyte composition on the utilization of the FeS electrode at 450 and 500°C. (The cells were cycled at current densities of 50 and 100 mA/cm^2.) In the cells with the 53 and 58 mol % LiCl electrolyte, the higher temperature resulted in a significantly increased utilization; this effect was not observed in the cells with the other two electrolyte compositions. In general, the utilization of the positive electrode increased with increasing LiCl content. Thus, the highest utilization (85-90%) was achieved in the cell with an electrolyte containing 67 mol % LiCl.

H. Advanced Battery Research

The objective of this program is to develop high-performance cells that use inexpensive, abundant materials while maintaining the performance levels required for electric vehicles or load leveling. These cells are expected to follow the lithium/metal sulfide cells into commercial production. The present goals for the cells are a specific energy of 160 W·h/kg and a maximum materials cost of $10-15/kW·h in mass production. During the past year, studies were conducted with cells having negative electrodes of either calcium or magnesium alloy, positive electrodes of metal sulfide or metal oxide, and a molten-salt electrolyte. The operating temperature for these cells was between 400 and 450°C.

In testing of magnesium cells, two major problems have been discovered: unacceptably low utilization of the positive electrode, and the formation on the negative electrodes of dendrites which cause short circuits. Therefore, we have decided to concentrate further efforts on development of the more promising calcium cell.

During the past year, a prismatic $Ca(Mg_2Si)/LiCl-KCl-CaCl_2/NiS_2$ cell with a theoretical capacity of 70 A·h was tested to evaluate the behavior of calcium electrodes in an engineering-scale cell. The cell, although not of optimum weight, achieved a specific energy of 42 W·h/kg at the 6-h rate. Operation was terminated after 120 cycles because of declining coulombic efficiency. The results of this test were very encouraging.

The electrolyte used in the cell was relatively expensive because of its high lithium content (54 mol % LiCl); therefore, a search was made for less expensive electrolytes. The most promising salt identified is 29 mol % LiCl-20 mol % NaCl-35 mol % $CaCl_2$-16 mol % $BaCl_2$ (m.p., 390°C).

Small-scale cell (1.5 A·h) tests were conducted to identify promising negative electrodes other than the Ca-Mg-Si system; negative electrodes evaluated included Ca-Si, Ca-Al-Zn, and Ca-Pb. The Ca-Si electrode was the only system that had acceptable utilization. The Ca-Si and Ca-Mg-Si electrodes will be compared in tests of engineering-scale cells during the next year.

In cyclic voltammetry measurements on MS_2 electrodes (FeS_2 and NiS_2) vs. $CaAl_4$, conducted in $LiCl-KCl-CaCl_2$ and $LiCl-NaCl-CaCl_2-BaCl_2$ electrolyte, the high-voltage reactions (>1.6 V) of FeS_2 and NiS_2 exhibited poorer electrochemical reversibility than the lower voltage reactions. The cause of the poor reversibility and methods of correcting it will be sought in future experiments. The utilization of both the FeS_2 and NiS_2 electrodes was much higher in the $LiCl-NaCl-CaCl_2-BaCl_2$ electrolyte than in the $LiCl-KCl-CaCl_2$ electrolyte; thus the $BaCl_2$-containing electrolyte appears more suitable for use in calcium cells.

The results described above are promising. We believe that the cell performance goal (160 W·h/kg) can eventually be achieved in calcium alloy/$LiCl-NaCl-CaCl_2-BaCl_2/FeS_2$ (or NiS_2) cells having multiplate designs. Our goal during the coming year is to design and operate prismatic bicells having specific energies greater than 100 W·h/kg.

III. OFFICE FOR ELECTROCHEMICAL PROJECT MANAGEMENT (OEPM)

The principal activities of OEPM are (1) management of research, development, and demonstration programs on near-term, ambient-temperature batteries for electric vehicles; (2) operation of the National Battery Test Laboratory, in which batteries developed in DOE programs undergo performance verification and qualification testing; (3) research studies in support of electric-vehicle battery development; (4) program planning related to energy conservation in industrial electrolytic processes; and (5) research studies on the battery requirements for photovoltaic systems. These five activities are discussed below.

A. Management of Near-Term Battery Contracts

The OEPM is assisting DOE in the management of industrial contracts for research, development, and demonstration of near-term electric-vehicle batteries. These contracts are part of the DOE program to implement the Electric and Hybrid Vehicle Research, Development, and Demonstration Act of 1976. The battery systems selected were those showing the highest potential for rapid development, namely, the lead-acid, nickel/zinc, and nickel/iron systems, which operate at ambient temperatures. The program is intended to serve as a nucleus for accelerated commercialization of battery technologies and thus includes development of pilot-scale production capability.

The development goals for the near-term batteries, which were established in 1977, are summarized in Table III-1. In large part, the 1977 goals have been surpassed, and most of the 1979 goals will probably be met in 1979 or

Table III-1. Development Goals for Near-Term Electric-Vehicle Batteries[a]

	Lead-Acid			Nickel/Iron			Nickel/Zinc		
	1977	1979	1982	1977	1979	1982	1977	1979	1982
Specific Energy, W.h/kg	30	40	50	44	50	60	70	75	90
Energy Efficiency, %	65	70	70	60	65	70	60	65	70
Specific Power, W/kg									
Sustained	15	20	25	20	30	40	20	40	50
Peak	50	100	150	110	120	150	130	150	200
Cycle Life	700	800	1000	1500	2000	2000	300	500	1000
Price,[b] $/kW·h	100	90	40	120	100	55	180	110	55

[a] Battery duty cycle: 2-4 h discharge; 70-80% depth of discharge; 4-8 h charge.

[b] 10,000-unit selling price to electric-vehicle manufacturer.

1980. If the 1979 goals are met, commuter vehicles should be ready for demonstration in 1980-1981. We are confident that at least one of the ambient-temperature batteries can achieve the goals for 1982 and subsequently capture the market for near-term electric vehicles. In the longer term (after 1985), a more advanced battery such as the lithium/metal sulfide battery (see Section II of this report) may be developed and consequently further broaden the electric-vehicle market.

In the spring of 1978 the following firms were subcontracted to conduct R&D on near-term batteries: Eltra Corp., ESB, Inc., Globe Union, Inc. (lead-acid); Yardney Electric Co., Energy Research Corp., Gould Inc. (Ni/Zn); and Westinghouse Electric Corp., and Eagle-Picher Industries, Inc. (Ni/Fe). Contractual negotiations are in the final stages with ESB for a Ni/Zn battery with a vibrating anode. The contracts extend for periods of three to four years, depending on the complexity of the work; all contracts call for the production of cells (or monoblocks*), prototype batteries, and pilot-line batteries. The contracts on lead-acid batteries call for the development of both improved state-of-the-art batteries and batteries of an advanced design. OEPM provides overall program management, as well as planning, evaluation and technical monitoring of the individual subcontracts. Performance verification and qualification tests of the cells and batteries are conducted in OEPM's National Battery Test Laboratory, described in Section III.C.

During this year, OEPM has concentrated on four areas of near-term battery development: (1) studies of program scope and battery performance projections, (2) creation of battery specifications and standardized testing procedures, (3) recognition of battery problems requiring further analysis, and (4) assessment of the present technical status of the contractor's efforts.

With respect to the first effort, three major studies for DOE were completed: a preliminary analysis of battery cost, a study of the feasibility of program acceleration, and projections of battery performance and cost. The preliminary cost analysis showed that materials would account for approximately 60% of the projected selling price of the near-term batteries; however, the cost projections will remain uncertain until the various technological approaches of the industrial contractors are more clearly defined. The program-acceleration study revealed that technological improvements in the near-term batteries could be accelerated by about six months with significantly increased funding for battery testing, and that the number of prototype batteries produced could be significantly increased through a moderate increase in funding for development of the pilot-line facility. It was also ascertained that the immediate construction of a best-effort prototype battery, followed by an in-vehicle evaluation, would assist in the development program. A program for the construction of this prototype is now being initiated. In the third study, battery performance projections (i.e., specific energy as a function of discharge rate and specific power as a function of depth of discharge and discharge rate) were made for the period 1978-1981; and battery prices were projected for purchases of 1 to 300 electric-vehicle batteries, each with a capacity of 30 kW·h.

*A monoblock is a single module consisting of multiple cells.

For the second effort, preliminary specifications were set for the near-term batteries. The most important specification was the temporary acceptance of module dimensions of a typical "golf-cart" battery with a nominal voltage range of 6-7 V. In addition, standardized test procedures are being formulated; such procedures are required to compare the performance of batteries on a normalized basis.

In the third effort, trade-off studies have been started to relate performance and cycle life to battery design; these studies are needed to identify battery components that require improvement. During next year, careful assessment will be made of battery problems related to thermal management and maintenance such as watering requirements, overcharge requirements and electrolyte maintenance requirements.

For the fourth effort, six contractors have been visited. During these visits, an assessment was made of the contractors' facilities, the technical approach chosen for battery development, and the preliminary experimental success. The status of the near-term battery contracts is discussed below.

Lead-Acid Batteries. With its present performance and low cost, the lead-acid battery should be able to capture a significant portion of the near-term electric-vehicle market. However, to make these batteries even more commercially attractive, the specific energy and cycle life need to be improved without significantly increasing the cost. Using a mathematical model, Globe Union has demonstrated that plate size and width-to-height (or aspect) ratio affect the specific energy. Eltra Corp. is using expanded Pb-Ca-Sn wrought alloy grids for both positive and negative electrodes. These expanded metal grids are especially lightweight and are expected to be maintenance free. In addition, Eltra believes that their wrought alloys will not undergo the same corrosion as Pb-Ca-Sn alloys that are used in cast grids, and thus the life of the battery will be increased. ESB is investigating the effect of changes in battery design on performance and lifetime, and developing tubular positive electrodes that are expected to improve battery lifetime. In addition, ESB is investigating advanced designs for lead-acid batteries such as a bipolar, pile-type battery. An advanced design could produce a significant increase in specific energy for the lead-acid battery.

Nickel/Iron Batteries. The advantageous features of the Ni/Fe system are long cycle life, ruggedness, and insensitivity to cell-voltage reversal; however, this type of battery is very expensive and exhibits inferior performance at low temperatures. Westinghouse Electric Corp. is developing low-cost nickel electrodes and perfecting an electrolyte maintenance system. Eagle-Picher Industries has developed proprietary designs for thick nickel electrodes and thin iron electrodes; these types of electrodes are needed so that state-of-the-art technology can be adapted to electric-vehicle battery designs.

Nickel/Zinc Batteries. The state of technology of the Ni/Zn system is changing rapidly at present. Of the near-term systems, the Ni/Zn battery has the highest specific energy, but the lowest cycle life. However, Yardney Electric Corp., Energy Research Corp., and Gould Inc. are testing many new designs to improve cycle life. Using different approaches, all three contractors are concentrating on the performance of the zinc electrode and the

characteristics of the separator system, as well as on the development of a maintenance-free design. In addition, they are investigating thermal management problems, which are brought about by the high energy density and the unfavorable entropy contribution to the heat generation on discharge.

Public demonstration of the near-term batteries in electric vehicles is planned within the next few years. In the next two years, OEPM must concentrate on recognizing battery problem areas through analysis of data generated by testing the batteries. Once critical areas are recognized, the OEPM must be able to reorient program efforts in order to find solutions.

B. National Battery Test Laboratory

The National Battery Test Laboratory (NBTL)[1] was established to provide a facility for the independent testing and evaluation of various batteries as they are developed. This facility is an integral part of the DOE battery research and development program. Cells and batteries developed within DOE-sponsored programs and those developed by private funds are tested at the NBTL. Applications for these batteries include electric-vehicle propulsion, electric utility load-leveling, and solar and wind energy storage. The laboratory is capable of the simultaneous testing of about 120 cells and five or six full-size (30-40 kW·h) batteries under simulated driving conditions as well as under normal test conditions. Graphical displays of battery performance are directly available through a computer.

1. Facility Operation

During 1978, the following battery modules arrived at the NBTL from near-term battery contractors: improved lead-acid modules from ESB, Inc., a Ni/Zn module from Energy Research Corp., and Ni/Zn modules from Gould Inc.

Figures III-1 and -2 are examples of computer-generated plots available from tests performed in the NBTL. Both of these figures are for a four-cell Ni/Zn module that was discharged at a constant current of 137 A and charged at a constant current and constant voltage of 80 A and 7.8 V, respectively. In Fig. III-1 are plots of battery current, battery voltage, and temperatures of two cells during two successive cycles. The cycle numbers and time of operation are indicated on the abscissa. At the very top of the figure is a computer-generated tabulation of the coulombic and energy capacities, and the average voltage at various times during battery operation. The cycle-to-cycle reproducibility of the measurements is representative of the reliability of the performance of this system. Figure III-2 shows the four individual cell voltages of the Ni/Zn module during the same period of time shown in Fig. III-1. The computer was programmed to terminate the discharge when any cell voltage dropped to 1 V. As can be seen in Fig. III-2, the voltages for all four cells at any given time are similar except at the

[1] The National Battery Test Laboratory Design Report, April 1976-1977, ANL/OEPM-77-4 (1977).

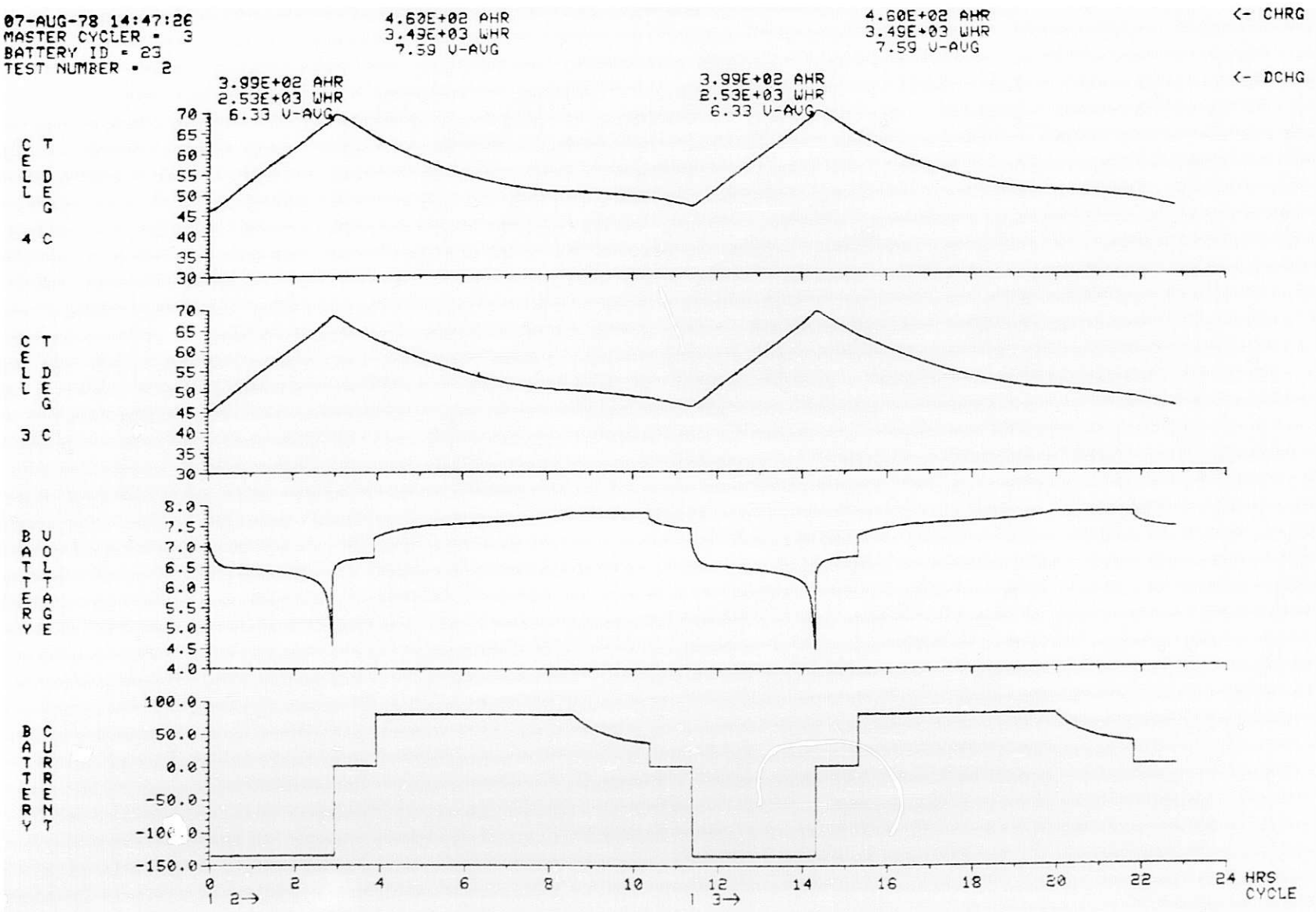

Fig. III-1. Current, Voltage, and Temperature Profiles of Two Cycles of a 400 A·h Ni/Zn Module in NBTL

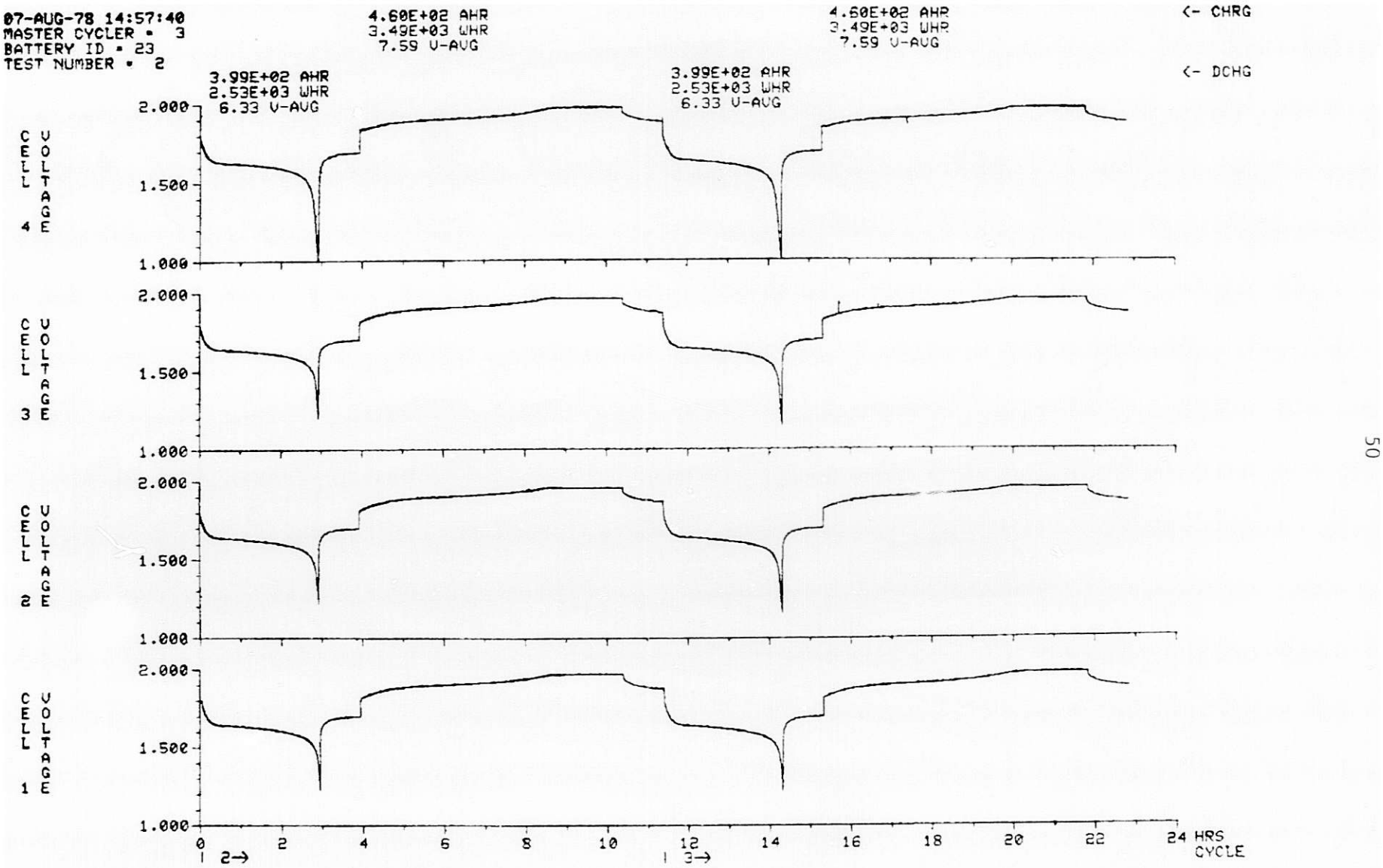

Fig. III-2. Individual Cell Voltage Profiles of a Ni/Zn Module

very end of discharge, where the voltage of Cell 4 is lower than that of the other three cells. It should be noted that the cell voltage at the discharge cutoff is very sensitive to remaining capacity (about 100 mV/5 A·h); as a result Cell 4 may have but 1-2% less capacity than the other three cells. These results indicate that all four cells were rather well matched in this module.

2. Projected Test Schedule

The number of cell and battery tests projected for NBTL through 1981 is as follows: 1979, 68 cells or modules and 18 batteries; 1980, 58-83 cells or modules and 41 batteries; 1981, 23 cells or modules and 22 batteries. Most of these will be lead-acid, Ni/Zn, and Ni/Fe, but tests of other, more advanced systems such as Zn/Cl, Li/S, and Na/S, are also expected. This projection includes cells and batteries from the DOE baseline program, as well as from the additional programs supporting the Electric and Hybrid Vehicle Research, Development, and Demonstration Act of 1976.

3. Ad Hoc National Battery Advisory Committee

The National Battery Advisory Committee (NBAC) was established in 1977 to provide advice to ANL and DOE for planning and implementing battery-related programs. This committee comprises representatives from industrial battery firms and advanced battery developers, electric vehicle developers, universities, the Electric Power Research Institute, government battery testing laboratories, and organizations such as the Electrochemical Society, the Electric Vehicle Council, the Battery Council International, and the Institute of Electric and Electronics Engineers.

The NBAC meets approximately four times a year, and functions in close liaison with OEPM. During this past year, the committee has been active in reviewing standard test procedures for batteries, developing a strategy for data management, studying battery commercialization, and assessing the impact of battery programs on resources.

C. Battery Support Research

One function of the OEPM is to perform basic and applied research in support of the near-term battery program. Research is undertaken in areas of significant interest to OEPM contractors and in areas identified by OEPM as essential to the progress of the program. This work presently includes efforts to improve load-leveling lead-acid batteries, mathematical modeling of electrodes and batteries, and the study of anodes using a simulated porous electrode.

1. Experimental Studies of Load-Leveling Batteries

Lead-acid batteries are being developed for utility load-leveling applications. Thus, support research was conducted during the past year on generation of the highly toxic gases stibine (SbH_3) and arsine (AsH_3) and the loss of water by electrolysis during charging of these batteries.

In previous work, a large industrial battery (5 kW·h) was found to generate a significant amount of stibine and arsine during the overcharge period of a charge cycle and during equalization-charging at 2.65 and 2.55 V, which are normally encountered in the load-leveling applications. During the past year, a stibine/arsine detection kit was developed for use in field evaluation of toxic gas release. The equipment includes a metering pump to provide a constant gas flow rate, an absorption tube to collect the SbH_3 and AsH_3, and the necessary controls, filters, etc. A portable spectrophotometer is used to analyze for antimony. The sensitivity of detection with this field kit is 0.2 mg SbH_3, which is excellent for monitoring cell off-gases. With a more sensitive spectrophotometer, a sensitivity of 25 μg SbH_3 can be obtained, which is sufficient for determining ambient-air toxicity. The absorbed solution is analyzed for arsenic at the laboratory.

Another problem with present load-leveling batteries is loss of water by electrolysis during charging. Two techniques were considered to solve this problem: the periodic addition of water to the battery, and development of a device to recombine the hydrogen and oxygen generated by the cells and subsequently return H_2O to the cells. The latter approach has several advantages: maintenance is reduced, and toxic gases are trapped rather than vented. Specifications for such a device were developed from laboratory data from the 5-kW·h industrial battery, and Varta Batterie AG was contracted to design such devices for batteries with capacities of 5 to 20 kW·h.

During the coming year, work on recombination devices will be continued and means for improving the utilization of the positive electrodes of lead-acid cells will be investigated.

2. Mathematical Battery Models

Testing of Ni/Zn electric-vehicle batteries has shown that they are limited in lifetime and exhibit an increase in temperature during discharge. Consequently, two different models were developed: one to show the effect of variations in electrode design on Ni/Zn cell performance and lifetime, and the other to predict the thermal behavior of a Ni/Zn battery during operation.

In the first case, a three-dimensional model has been developed to predict potential distribution and reaction uniformity in porous electrodes as functions of electrode dimensions, kinetics, component conductivities, and operating current. This model is useful in the design of nickel and zinc electrodes because one can determine the effect of various design parameters on electrode performance. An example of the utility of the three-dimensional model is illustrated in Fig. III-3. By using this figure, one can determine the effect of varying the grid conductivity (σ_g) on the potential distribution and maximum/minimum current density while keeping other battery properties constant. For curves numbered 2 and 3, σ_g was made, respectively, two and ten times as great as for the number 1 curves.

The nomenclature for terms used in the figure is as follows:

F, R, T	Usual electrochemical definitions
i_o	Exchange current density

L_x, L_y, L_z	Electrode length, width, and thickness, respectively
a	Specific surface area of the electrode
I	Total electrode current
R_{max}	Ratio of the maximum-to-minimum current density at a fixed total current (a measure of nonuniformity of reaction)
Φ_m	Electrode/electrolyte potential
κ_e, σ_g	Conductivities of electrolyte and grid, respectively

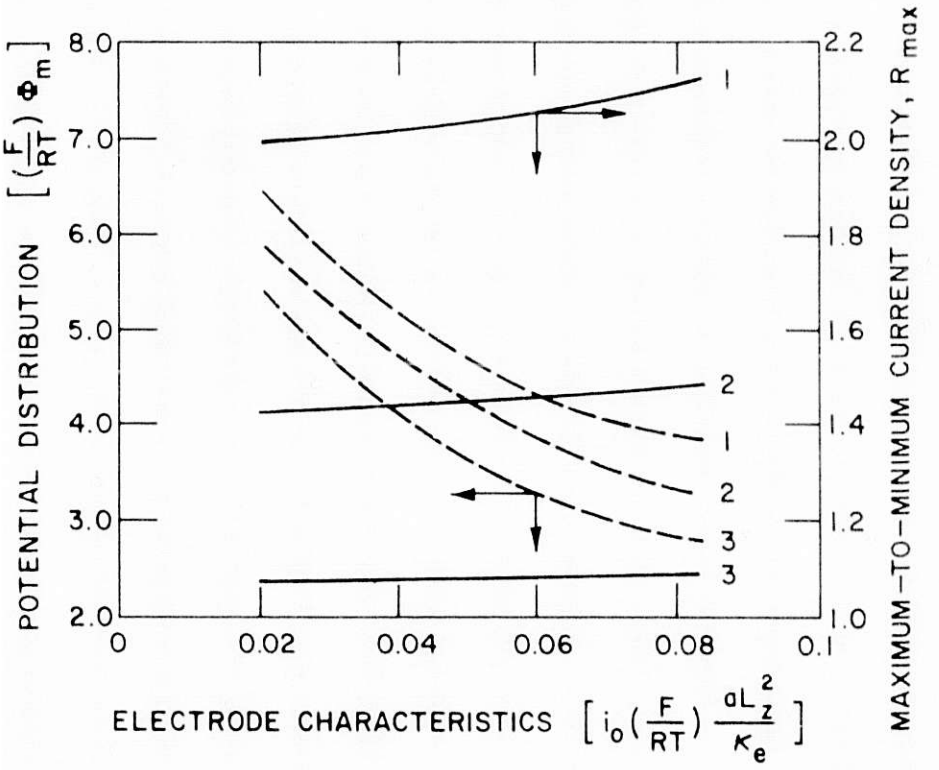

Fig. III-3. Variation in Electrode Potential and Reaction Nonuniformity as a Function of Electrode Properties (all units are dimensionless)

Conditions:

$$\frac{F}{RT} \cdot \frac{I}{L_x L_y} \cdot \frac{L_z}{\kappa_e} = 0.28$$

Center tab location = $\frac{L_x}{5}$

Curves	$\frac{\sigma_g}{\kappa_e} \cdot \frac{L_z^2}{L_x L_y}$
1	0.15
2	0.30
3	1.5

The second model was developed to determine the effect of battery design and operating conditions on the thermal behavior of a Ni/Zn electric-vehicle battery. This model was similar to that formulated earlier for lead-acid batteries.[2] Using this recent model, we predicted the thermal behavior of a contractor-fabricated Ni/Zn battery being tested in the NBTL. The calculated results were nearly the same as those obtained experimentally. Further studies using the model are being carried out to evaluate various engineering approaches for maintaining lower temperatures within Ni/Zn batteries during discharge.

3. Experimental Studies of Porous Electrodes

Previous experimental studies of porous electrodes reported in the literature have used crudely simulated porous electrodes or porous electrodes extracted from post-test cells. During 1977, a simulated porous electrode consisting of a hundred or more cylindrical pores was developed (see last year's report). It is fabricated in a manner to permit the continuous determination of current as a function of the depth within the pore, and is a valuable tool for investigating time-dependent performance parameters occurring within operating porous electrodes.

During this past year, simulated porous electrodes were used to study zinc anodes, which limit the capacity of the nickel/zinc cell. The behavior of zinc anodes in hydroxide electrolyte is complex because of the limited solubility of ZnO as a hydroxylated negative ion, which results in redistribution of the zinc metal during cycling. In turn, this redistribution causes declining performance and electrical short-circuiting of electrodes. With a KOH-zincate electrolyte, the zinc electrode showed an abrupt drop in current after about 3 min of anodization at a current of 411 mA. This abrupt change in current is indicative of passivation. Figure III-4 shows the current-density distribution in the anode as a function of distance from the electrode face, both before and after the onset of passivation. The results indicate that passivation is not uniform, being greatest at the pore entrance and non-existent at a depth of about 0.8 mm within the pore.

Future studies using the simulated porous electrodes will be directed toward measuring electrolyte composition and metal/electrolyte potentials along with the current-distribution determinations. With this type of information, the experimental studies will supplement the theoretical modeling efforts.

D. Industrial Electrolytic Technology

The goal of this program is to increase energy efficiencies for the production of commodities presently, or projected to be, produced by electrolytic processes, thereby resulting in energy savings of 10% in the near term (1985) and about 30% by the year 2000. The efficiencies of these processes can be

---

[2] K. W. Choi and N. P. Yao, An Engineering Analysis of Thermal Phenomena for Lead-Acid Batteries During Recharge Processes, ANL-77-24 (1977).

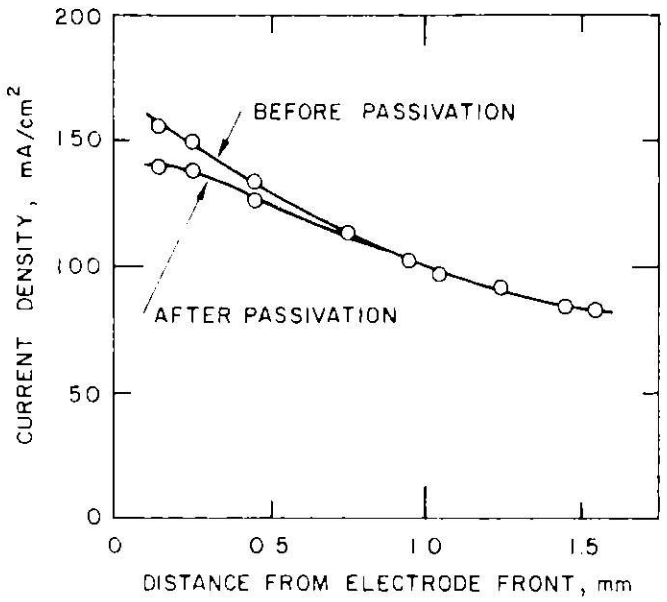

Fig. III-4.

Variation in Current Density Distribution Before and After Passivation

improved by the development of either modifications in major present-day processes or entirely new processes, which may or may not be electrolytic.

A preliminary program plan to assist industry in achieving these improvements was completed in 1977; this plan will be revised during 1979. To promote the interaction of the government with industry and universities, a national ad hoc advisory committee was formed in early 1978. Also during 1978, survey studies to identify energy-efficient electrolytic processes were conducted by industrial firms and ANL.

1. Contracts

The near-term goal of the contracted work is to identify alternative electrolytic processes, project energy savings, and assess the effort needed to develop each process and to demonstrate its commercial feasibility.

Survey studies have been performed by five contractors to assess alternative processes in aluminum (Arthur D. Little, Inc.) and chlorine (Versar, Inc.) production, metal winning (Battelle, Columbus Laboratories), metal recycling (EIC Corp.), and organic electrolytic synthesis (Electrochemical Technology Corp.). The information required for these surveys was obtained from open literature, industrial interviews, and calculations based on data available in the literature. In these survey studies the overall energy of the process alternatives was compared with that of current technology. Those processes for which the energy savings are significant ($>10^9$ MJ/y or 10^{12} Btu/y) were described in detail, and estimates were made on the amount of energy saved, the process cost, and the impact on the environment and natural resources.

The University of Illinois, under a cost-shared contract with ANL, has compiled a bibliography entitled Swan Bibliography of Electroorganic Synthesis Reactions, 1801-1975. The bibliography will serve as a basis for

identifying electroorganic processes that might result in significant energy and resource savings.

During 1979, a contractor will conduct a survey study of the electrolytic production of inorganic chemicals; detailed engineering and economic evaluations will then be carried out for a few of the especially promising processes. In addition, one or two research projects may be initiated in this period.

2. In-House Research

In the past year, ANL has made preliminary evaluations of nearly sixty potential process improvements and new electrolytic processes. These technologies were selected on the basis of information obtained from a number of sources, including the Electrochemical Technology Corporation,* the ad hoc advisory committee, and ANL staff. Table III-2 presents representative results of this preliminary evaluation study and the recommendations made on future actions.

Table III-2. Energy-Saving Technologies

Technology	Evaluation	Recommendation
Aluminum production from sulfides	Promising	Investigate
Aluminum production from Hall-Heroult cells in which anode overpotential decreased	Not likely to succeed	No effort
Chloride production by use of cells with redox-catalyzed O_2 cathodes	Uncertain value	Monitor progress
Electrolysis of HCl to produce chlorine	Limited applicability	No effort
Copper refining using Cu^+	Promising	Investigate
Electrochemical NH_3 production	Advantage limited to H_2 production	No effort
O_3 production	Significant growth likely	Investigate
Application of slurry electrodes	Applications very specific, not amenable for general study	Monitor progress

*From a study performed in 1976.

In predicting the energy consumption of improved or new electrochemical processes, one must consider that industry will operate such processes under conditions optimized to yield the highest profit. In electrochemical processes, the energy cost per unit quantity of product can be decreased by decreasing the current density (because of lower ohmic losses), but investment costs increase. Therefore, a mathematical model was developed to predict the effects of changes in energy price, changes in investment costs, process improvements, and deviations from optimum conditions on energy consumption and product costs for industrial electrolytic processes. Employing this model, we predicted the energy consumption of alternative processes for the production of aluminum and chlorine. Calculations using this model have shown that process improvements do not always save as much energy as would be initially expected. For example, the introduction of an electrolyte with higher conductivity into a given electrochemical cell decreases the ohmic losses, but calculations show that this improvement in ohmic resistance is counteracted by a shift to a higher optimum current density. Consequently, the resulting net energy saving is smaller than was at first expected. Figure III-5 is an illustration of the type of plot that we used to predict the optimum current density (indicated by the vertical dashed line) for electrolytic processes. In this figure, the cost and cell voltage are plotted as a function of current density for two types of chlorine cells--the conventional diaphragm-type cell and a membrane-type cell

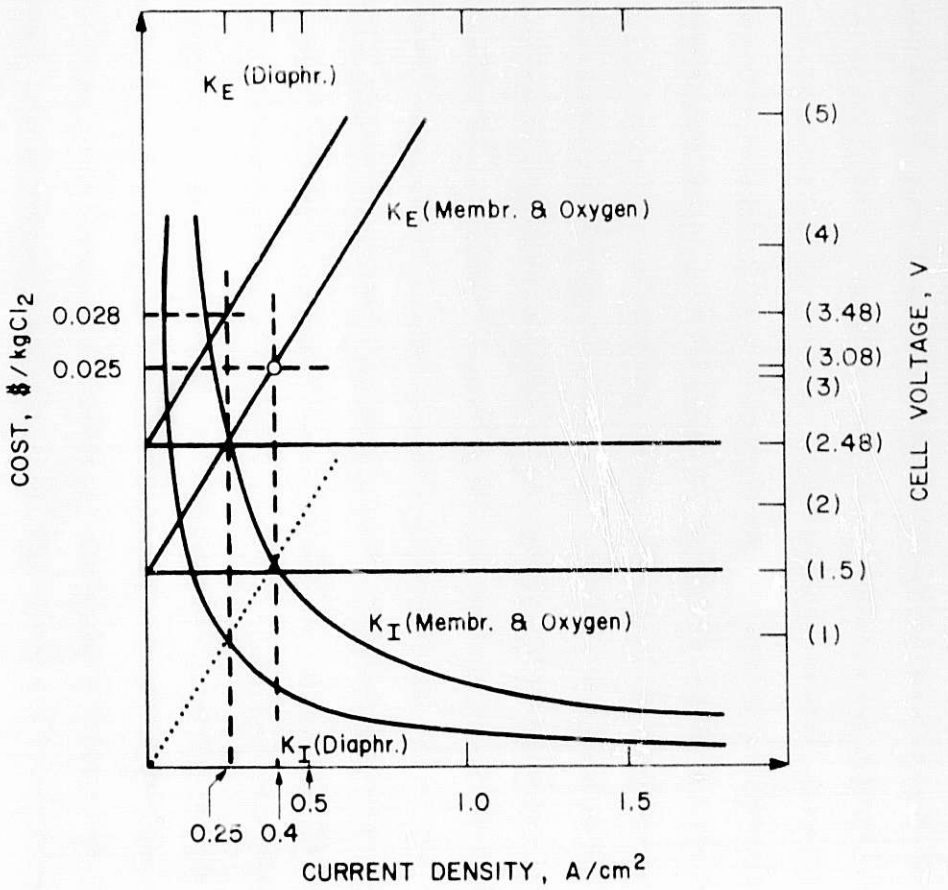

Fig. III-5. Cost vs. Current Density for Two Chlorine Production Processes

with an oxygen cathode. (Both K_I and K_E are components of the total product cost.) From the data in this figure, the energy consumption can be easily computed.

Extensive thermodynamic calculations indicated that the production of aluminum using aluminum sulfide as an intermediate species is an attractive process in comparison to the traditional Hall-Heroult process and a process recently developed by Alcoa ($AlCl_3$ electrolysis). Alumina could be sulfurized to Al_2S_3, which could be subjected to electrolysis to produce aluminum and sulfur; the resulting sulfur could then be recirculated to the sulfurization step. Alternatively, it may be possible to form aluminum subsulfide and to obtain the aluminum from disproportionation of the subsulfide. Additionally, direct sulfurization of aluminous ore is feasible if the sulfides can be efficiently separated. Investigation of crucial process steps and preliminary cost estimates are in progress.

Experimental investigations were started on electrolytes in which stable cuprous complexes form upon anodic dissolution of copper. If such electrolytes were employed in copper refining, only half as much current would be necessary to process a given amount of copper, and an energy savings of about 50% would be possible. Once sufficient laboratory data are obtained, this possibility for energy savings will be analyzed in more detail.

E. Battery Storage for Solar Photovoltaic Systems

Photovoltaic conversion systems provide direct-current electrical energy from an inexhaustible resource with a minimum of adverse environmental effects. To assure commercialization of this technology, DOE has instituted the National Photovoltaic Program Plan.[3] The overall objective of this program is to ensure that photovoltaic conversion systems play a significant role in maintaining the nation's energy supply, with the goal of producing approximately 50 GW(e) of electrical energy by the year 2000. The National Photovoltaic Program will be successful only if inexpensive batteries and power conversion and control equipment are available. Energy storage systems are required to supply energy during the periods when the photovoltaic array is not producing electricity, or to supplement the array output when required. To assist the DOE in defining the role of batteries in various photovoltaic applications, a workshop[4] was held in which 80 government and industrial representatives discussed problems related to the development and commercialization of photovoltaic systems. The workshop focused on three principal applications for battery/photovoltaic energy systems: energy sources for private residences and remote-sites (e.g., microwave repeaters, weather stations), institutions (e.g., shopping centers, high schools), and central power stations.

As a result of the workshop, three conclusions were reached. First, achievement of the near-term (1982-1985) performance and cost goals for the

---

[3] National Photovoltaic Program Plan, U.S. Department of Energy Report DOE/ET-0035 (March 1978).

[4] N. P. Yao and J. J. Barghusen, Eds., Proceedings of the Workshop on Battery Storage for Solar Photovoltaic Energy Systems, ANL/OEPM-78-3 (1978).

National Photovoltaic Program will require the development of lead-acid batteries with a lifetime exceeding 3000 cycles (>10 y). Second, communication between photovoltaic system designers and battery manufacturers is essential; detailed analyses are required to match the battery operating characteristics to the photovoltaic system requirements. Third, studies should be conducted to determine the effect of the use of various photovoltaic systems on electric utilities.

The information collected at the workshop, along with the results of other DOE studies, provided the basis for a program plan covering battery storage systems for solar photovoltaic applications; this plan was submitted to DOE in September 1978.

IV. ADVANCED FUEL CELL DEVELOPMENT

A. Overview

The molten carbonate fuel cell is one of the most promising technologies being developed by DOE to reduce the nation's reliance on petroleum fuels for electrical generation. The Chemical Engineering Division has two responsibilities within the DOE program to develop molten carbonate fuel cell power plants. These are (1) to conduct technical management of the program and (2) to provide supporting research and development that yields fundamental understanding of fuel cell behavior as well as improved cell components.

Molten carbonate fuel cells consist of a porous nickel alloy anode, a porous nickel oxide cathode, an electrolyte structure separating the anode and cathode, and appropriate metal cell housings or, in the case of stacks of cells, cell separator plates. The cell housings (or separator plates) bear upon the electrolyte structure to form a seal (called a wet seal) between the environment and the anode and cathode gas compartments. The electrolyte structure, which is commonly called "tile," is a composite structure of solid $LiAlO_2$ particles and a mixture of lithium and potassium carbonates that is a liquid at the cell operating temperature of 925 K. At the anode, hydrogen and carbon monoxide in the fuel gas react with carbonate ion from the electrolyte to form carbon dioxide and water, giving up electrons to the external circuit. At the cathode, carbon dioxide and oxygen react and accept electrons from the external circuit to form carbonate ion, which is conducted through the electrolyte to the anode. In practical cell stacks, CO_2 for the cathode will be obtained from the anode exhaust.

In a power plant, several hundred cells with parallel gas flows will be assembled in a series electrical connection to form a stack. Depending on plant size, from about ten to more than a thousand stacks will be used to convert fuel gas from a coal gasifier/cleanup subsystem to electrical output. Heat from the cells and gasifier will be used in a bottoming cycle to increase electric output or for industrial processes, depending on the application. The advantages of this type of power plant are (1) use of coal, rather than petroleum or natural gas, (2) very low pollutant emissions, and (3) very high efficiency (about 50%, coal to bus bar, in a baseload plant).

During the past year, the DOE program, under the direction of the Molten Carbonate Fuel Cell Program Office in CEN, has maintained its schedule. The effects of pressure, gas compositions, and major contaminants (primarily sulfur) have been defined, scale-up to pilot-size cells (about 2 ft^2) is proceeding well, operation of cost-effective sheetmetal hardware appears feasible, and significant advances have been made in the manufacture and performance of electrodes and electrolyte tiles. A major thirty-three month competitive procurement for power-plant development has therefore been initiated. This action is intended to bring at least two potential power-plant vendors to the stage of fabrication of the first prototype stacks of power-plant size. Although the bulk of cell development has been and will continue to be carried out by potential power-plant vendors, significant advances have been made by supporting contractors, including CEN, and supporting R&D will be continued.

The total CEN effort comprises only about 5% of the DOE program, but the work has been very productive. The CEN-initiated process for wet-seal corrosion protection, which was described in last year's report, has been adopted throughout the molten-carbonate fuel cell community with complete success, at least to date. In this process, aluminum is first flame-sprayed onto the steel housing in the area of the wet seal; during the subsequent heat treatment the aluminum diffuses into the steel; and after assembly in the cell a corrosion-resistant, aluminum-rich oxidized phase forms on the steel surface exposed to the electrolyte tile. Adaptations of an aqueous method for synthesizing $LiAlO_2$, developed in CEN, are used for all cells at the Institute of Gas Technology (IGT) and for many cells at the General Electric Company and the Energy Research Corporation. The efforts of the research group in CEN are mainly directed toward synthesis of tile materials and definition of the stability of the inert phase ($LiAlO_2$) in the tiles. Significant advances in both these areas have been made during the past year. The group will continue to pursue the development of tiles and to undertake work in other areas of cell technology that are considered basic or critical.

B. Electrolyte Development

The physical properties (allotropic form, surface area, particle shape, and particle size distribution) of the $LiAlO_2$ particles in the electrolyte structure have a significant effect on the performance and life of the molten carbonate fuel cell. For this reason, our research and development effort on electrolyte tiles is focused on the synthesis of $LiAlO_2$ particles that provide good electrolyte retention and mechanical strength. Synthesis procedures are being directed toward production of β- and γ-$LiAlO_2$ rather than α-$LiAlO_2$. Not only is the α-phase less stable, but it is more dense than the β- and γ-phases, and transformation of α- to γ-$LiAlO_2$ is accompanied by a 30% increase in volume. In a continuation of work begun last year we are also assessing the use of low-cost ($0.57/kg) aluminum hydroxide, $Al(OH)_3$, as an alternative starting material to the more expensive ($6.70/kg) high-purity γ-Al_2O_3 previously used for the synthesis of $LiAlO_2$.

We have expanded our capabilities for characterizing the physical properties of $LiAlO_2$ samples. Previously, X-ray diffraction and scanning electron microscopy were the principal methods of characterization; more recently, measurements of particle size and surface area have been incorporated as routine analytical tools. The information obtained by the latter two techniques is already proving useful in relating the physical properties of the $LiAlO_2$ powders and the performance of these materials in electrolyte tiles.

Several new approaches to the preparation of improved $LiAlO_2$ materials were investigated. Three of the most attractive syntheses, which produced spherical "clump-shaped" particles, are (1) the relatively low-temperature (775 K) synthesis of γ-$LiAlO_2$ having a fine particle size (surface area of 17-26 m^2/g) from mixtures of LiOH, γ-Al_2O_3, Li_2CO_3 and K_2CO_3; (2) the synthesis of somewhat agglomerated β-$LiAlO_2$ (surface area of 20-60 m^2/g) by precipitation at 300 K from an alkaline aqueous solution (KOH or LiOH-KOH) containing dissolved $Al(OH)_3$; and (3) the synthesis of β-$LiAlO_2$ having a fine

particle size (surface area of 20 m^2/g) by heat treatment of mixtures of solid LiOH and $Al(OH)_3$ at 725 K. Thermochemical studies indicate that electrolyte structures containing $LiAlO_2$ with surface areas >20 m^2/g exhibit low creep and deformation, and thus, are desirable in molten carbonate fuel cells. The rod-shaped particles of β-$LiAlO_2$ previously produced by impregnation of γ-Al_2O_3 with aqueous LiOH yielded electrolyte tiles that showed poor strength and performance in cells. However, a modification of the latter procedure has been adopted by the Institute of Gas Technology to obtain $LiAlO_2$, and fuel cells incorporating this $LiAlO_2$ showed good performance. Results to date indicate that $Al(OH)_3$ is an attractive low-cost alternative to γ-Al_2O_3 for the synthesis of $LiAlO_2$; however, the $LiAlO_2$ obtained from $Al(OH)_3$ has not been evaluated in fuel cell tests. These studies will begin in the near future.

The thermal stabilities of samples of α-, β-, and γ-$LiAlO_2$ powder were studied at 875 to 1175 K in 16- to 1000-h tests. The results clearly indicated that both the gas- and liquid-phase environments affect the thermal stability of $LiAlO_2$. The allotropic transformation of α- and β- to γ-$LiAlO_2$ occurs at a lower temperature ($\leq$975 K versus $\geq$1125 K) in the presence of molten carbonate (62 mol % Li_2CO_3-38 mol % K_2CO_3) than in its absence. At 875 and 975 K these transformations occur more rapidly in air than in a CO_2 environment. The allotropic transformation is accompanied by a decrease in the surface area and an increase in the average particle size of the $LiAlO_2$. The crystal growth of the three forms of $LiAlO_2$ in molten carbonates appears to be controlled by a solution-redeposition mechanism, whose rate increases as the temperature increases. The inhibiting effect on crystal growth of a CO_2 environment indicates that the dissociation of Li_2CO_3 probably plays an important role in the solution-deposition mechanism. In air, additional oxide and hydroxide ions would be present in the melt and these could enhance particle growth. Further studies are being conducted to determine the limits of temperature and gas composition that will ensure acceptable life for $LiAlO_2$ in electrolyte tile.

C. Cell Testing

Cell testing is essential for understanding and testing the performance of individual and collective components. The 7-cm cylindrical cells previously used for testing have been replaced by cells of a more realistic design (10.6-cm square cells). Figure IV-1 shows one of the two housings that sandwich the electrodes and the tile to form the cell. Figure IV-2 shows the gas-flow pattern within the housing. With the larger cells we have used electrolyte tiles containing Kanthal* wire screen (a technique pioneered by IGT) to improve the mechanical strength of the tiles. In preliminary tests of cells with tiles containing γ-$LiAlO_2$ (26 m^2/g), performance was not as high as had been obtained previously with tiles containing α-$LiAlO_2$ of high surface area (about 80 m^2/g). However, the use of α-$LiAlO_2$ has proved undesirable because, under fuel cell operating conditions, the α-phase is transformed to γ-$LiAlO_2$, with a consequent volume increase of 30% and a surface area loss

*Kanthal Corp., type A-1: 5.75%, Al, 22% Cr, 0.5% Co, balance Fe.

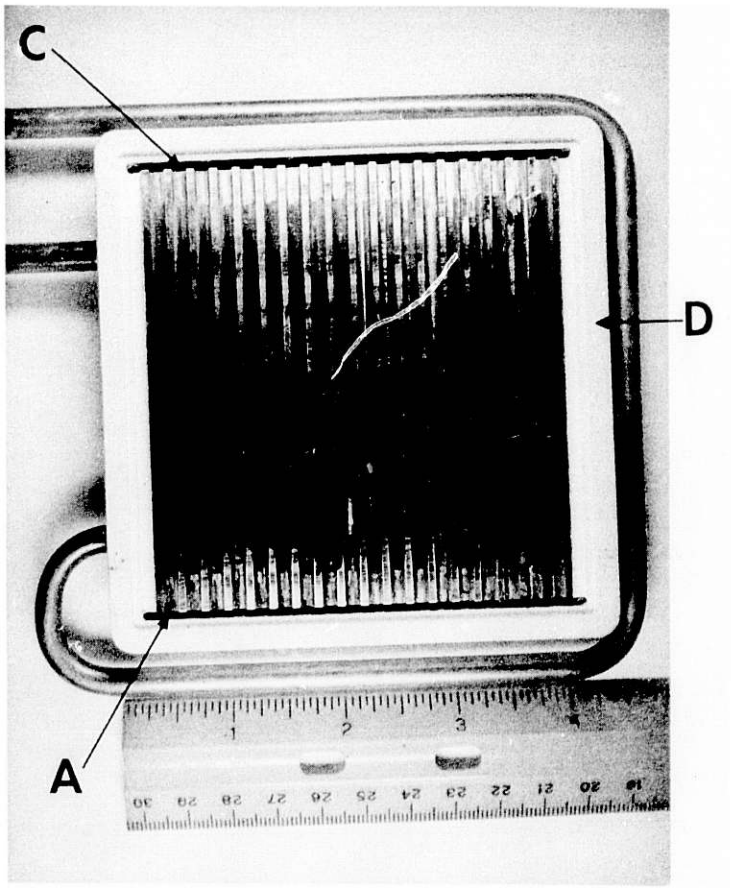

Fig. IV-1

Square Cell Housing
(10.6 x 10.6 cm)

A. Gas entrance slot
B. Gas channels
C. Gas exit slot
D. Wet seal area (light grey color is the area covered by protective aluminum)

due to particle growth. We attribute the poorer performance of the cells with γ-$LiAlO_2$ tiles to poor anode wetting, which resulted from other differences in these particular cells. The tests showed, however, that the γ-$LiAlO_2$ remained unchanged in allotropic form and surface area after 1000 h. Furthermore, an electrolyte tile containing γ-$LiAlO_2$ and a wire mesh screen for reinforcement did not appear to be adversely affected by four thermal cycles between 925 and 575 K. We believe that γ-$LiAlO_2$ is an attractive material for use in the electrolyte structures of molten carbonate fuel cells. Experiments are under way to optimize the cell components to improve the performance of fuel cells containing γ-$LiAlO_2$.

D. Component Analysis and Development

Cell testing is augmented by component analysis and materials development efforts, with the aim of understanding the behavior of components and improving their performance and longevity in fuel cells. Our work on component analysis and development has centered on determining the effects of the physical properties of $LiAlO_2$ on the thermomechanical behavior of electrolyte tiles. To expand our capabilities for studying the thermomechanical behavior of electrolyte structures, two additional pieces of testing equipment have been built. Our test results indicate that the mechanical strength of the electrolyte tile (as measured by the amount of creep and deformation) is

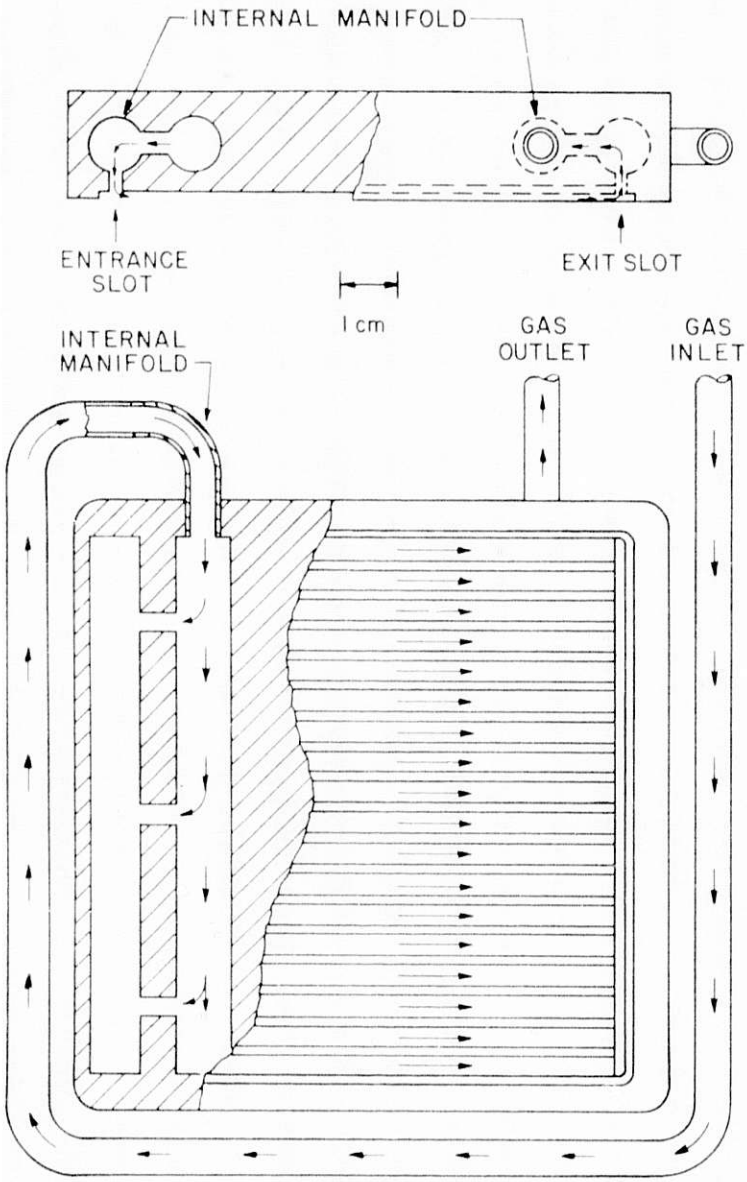

Fig. IV-2.

Schematic of Square Cell Showing Gas-Flow Pattern

a strong function of the surface area of $LiAlO_2$; the mechanical strength of the tile increases with an increase in the $LiAlO_2$ surface area. Studies to determine the effects of $LiAlO_2$ particle shape and particle size distribution on the mechanical strength of electrolyte structures are currently under way.

To provide the additional information required to carry out advanced and engineering development of fuel cell technology, we are undertaking for DOE a critical survey of the literature on the aging and degradation of electrodes in molten carbonate fuel cells. This survey, which includes personal contacts with investigators working in molten-carbonate fuel cell technology, will serve as the basis for defining possible needs for applied research in

such areas as electrode sintering, electrode corrosion, and electrode characterization. The aim is to identify areas in which technical information is needed to accelerate the commercialization of molten carbonate fuel cell technology.

E. Future Direction

The synthesis of $LiAlO_2$ from low-cost aluminas will be continued and synthesis methods to develop alternative matrix materials for electrolyte structures will be considered. The stability tests on $LiAlO_2$ will be extended to longer periods (3000 h) to obtain a more realistic assessment of this material in molten carbonate fuel cells. Of particular interest will be the stability of β- and γ-$LiAlO_2$ to changes in particle shape, size, and surface area under various conditions of temperature and environment.

Our capability for testing 10.6-cm square cells will be increased, so that some longer term (2500 h) tests can be conducted, as required, to evaluate the behavior of electrolyte structures and cell components under realistic operating conditions. Cell tests with improved (stabilized) anodes developed by Energy Research Corp. will also begin, and a detailed analysis of the effects of thermal cycling on cell performance and cross-leakage of reactant gases through the electrolyte tile will be continued.

Our work in component analysis and development also will be expanded. We will continue the study on the thermomechanical characteristics of electrolyte tiles and their correlation with the physical properties of the $LiAlO_2$, and will evaluate nondestructive testing methods to diagnose structural properties of electrolyte tiles. The study on the aging and degradation of electrodes in molten carbonate fuel cells will be completed and the recommendations and findings will be made available to the fuel cell community.

V. UTILIZATION OF COAL

A. Overview

The industrial application of atmospheric pressure fluidized-bed combustion* (AFBC) is one of 20 technologies that have been judged by DOE to be ready for commercialization and one of eight technologies judged likely to make a major impact quickly. A plan has been proposed by a DOE task force to accelerate industrial use and acceptance of AFB coal-fired boilers by building four more large units to be cost-shared by the Federal government and the industrial participants.

In the conversion from oil or gas to coal, large boilers represent the most likely candidates for conversion. Four industries--chemical, petroleum, paper, and primary metals--use 70% of all fossil fuels burned in large boilers. The task force recommended building four large industrial prototypes (200,000 lb steam per hour), one in each of the four industries. These would be in addition to the several industrial AFBC projects already at various stages. The first of these, a 100,000-lb-steam-per-hour boiler at Georgetown University in Washington, D.C., is scheduled for start-up in early 1979 (see Table V-1).

Table V-1. Status of Large-Scale AFBC Projects

Identification	Size	Steam Temp./Pressure	Status
Rivesville, WV[a]	30 MWe	500°C/8600 kPa	Operational in 1977; being rebuilt after fire.
Renfrew (UK)	4 MWe	280°C/2900 kPa	Operational in 1975.
British Steel (UK)	8 MWe	350°C/2900 kPa	Under construction; operational in late 1978.
Enkoping (Sweden)	8 MWe	hot water/low	Operational on oil in 1978; to be operated on coal in the future.
Great Lakes Naval Station[a]	5 MWe	290°C/2500 kPa	Engineering design stage; start-up in 1980.
Washington DC[a] (Georgetown)	10 MWe	230°C/4300 kPa	Construction stage; start-up in 1979.
200-MWe Demo[a]	200 MWe	538°C/16,900 kPa	Planning stage.

[a]DOE project.

*Fluidized-bed combustion is a process in which coal is burned in a fluidized bed of limestone or dolomite, which reacts with most of the sulfur dioxide released during combustion to form calcium sulfate.

Pressurized fluidized-bed combustion (PFBC) units are also being built. The construction of a 20-MWe test unit of the International Energy Agency (IEA) at Grimethorpe, England, is proceeding on schedule. This facility, a joint project of England, Germany, and the United States, is scheduled for start-up in 1979. The Experimental Program Manager for this project is a member of the CEN staff on special assignment. Design of the Curtiss-Wright 14-MWe pilot plant is nearing completion, but DOE has not yet made a decision to begin construction. A privately funded evaluation study by the American Electric Power Company of the desirability of constructing a 170-MWe demonstration facility has proceeded into the second phase of the project. This phase will include a 1000-h test on a small (2-ft by 3-ft cross section) PFBC in Leatherhead, England. That particular test, to study erosion and corrosion of turbine blades and boiler tubes, will be funded jointly by DOE and Electric Power Research Institute (EPRI).

The CEN program in FBC includes laboratory studies and process-development-unit (PDU) studies to support DOE development projects for AFBC and PFBC. The CEN program is aimed at solving problems, filling information gaps, improving process operability and economics, and reducing environmental impacts. Problems associated with efficient limestone utilization, gas cleanup at high temperature and pressure, emission control, combustion efficiency, and minimization of the quantity of solid wastes are among those addressed in this program. To assist in identifying R&D needs, close interaction with industrial developers of FBC is being maintained.

In other divisional work related to coal utilization, the program of support studies for underground coal gasification is continuing; kinetic data are being developed for the mathematical modeling efforts on in situ gasification. Also, technical assessments are being made and technical management efforts carried out to assist DOE headquarters personnel.

B. Regeneration of SO_2 Sorbent for Fluidized-Bed Combustion

The regeneration of partially sulfated limestone sorbent from FBCs for reuse is under investigation as a possible means of reducing the volume of solid wastes. A regeneration process in which the $CaSO_4$ is reductively decomposed into CaO in a fluidized bed operating at about 1100°C continues to show promise. An improved model for material and energy balance allows the performance of the process to be estimated as a function of the various operating and design parameters..

A brief investigation has been made of an alternative process in which the $CaSO_4$ is reduced using carbon in an externally fired rotary kiln. By eliminating the need for fluidizing air, this process offers the potential advantage of high SO_2 concentrations in the off-gas (which reduces the cost of the sulfur recovery step); however, regeneration in a rotary kiln appears to have higher energy costs than the fluidized-bed process does.

The behavior of trace elements during cyclic sulfation-regeneration studies has been investigated; after ten cycles, the trace-element composition of dolomite was what would be expected from the amount of coal-ash buildup on the surface of the particles.

1. Model for Material and Energy Balances

In the process under development for the regeneration of sulfated limestone, $CaSO_4$ is decomposed into CaO and SO_2 by reducing gases derived from the incomplete combustion of coal. This process is carried out in a fluidized-bed reactor operated at about 1100°C. The CEN process development unit regenerator was used earlier in determining the effects of solids residence time and temperature on the extent of regeneration.

Also, earlier cyclic combustion/regeneration studies established the change in SO_2 reactivity of a limestone and a dolomite with repeated cycling. These experimental data have now been used in a mass- and energy-constrained model to relate the regenerator configuration and performance to the operational variables of temperature, pressure, solids- and gas-feed temperatures, gas velocity, fresh sorbent feed ratio,* and solids residence time. How these latter variables affect the SO_2 concentration in the off-gas, the coal consumption in the regenerator, and the bed dimensions has been calculated. The model was used to test various schemes for turning down the regenerator since turndown will be needed if the feed rate from the combustor is decreased. The model was also used to investigate the sensitivity of the cost of the total regeneration system to changes in capital charges, cost escalation, coal cost, limestone cost, operating and maintenance cost, sulfur credit, and utility cost.

When the model was used to predict process performance in other experimental runs done under different conditions, good agreement was obtained between the predicted and observed quantities. The model also allowed the performance to be predicted under conditions which could not be realized in the experimental facility due to physical limitations. For example, the model could be used to study the effect on SO_2 concentration in the exit stream of variations in the reactor dimensions. Studying this in the laboratory would be expensive.

As stated above, the model has been used to study some factors that affect the cost of the process. It was found that sorbent cost is the most important factor, although capital cost and capacity factor are also important. The study showed that for electricity produced with a 635-MW AFBC in combination with a fluidized-bed regenerator and RESOX sulfur-recovery system, assuming a coal cost of $25/ton, sorbent cost of $11.50/ton (including disposal), and no credit for the recovered sulfur, the cost would be the same as for a once-through system (i.e., an AFBC without a regenerator). If the cost of buying and disposing of the sorbent was than $11.50/ton, the AFBC with regeneration would produce cheaper electricity. Increasing the capacity factor or the size of the AFBC would make the AFBC with regeneration more economical, as would an increase in the price of sulfur. Increased capital cost and coal cost tend to make the regeneration process less economical.

---

*The fresh sorbent feed ratio is the mole fraction of CaO as fresh feed to the combustor divided by the total CaO fed to the combustor, including regenerated sorbent.

The model is now being used to identify parts of the process where technical improvements will have the largest effect on the cost.

2. Regeneration in a Rotary Kiln

Externally fired rotary kilns were evaluated for use as regeneration reactors since in kilns there is no dilution of product gas by air needed for fluidization. Consequently, kilns have a greater potential for producing an off-gas having higher SO_2 concentration than could be produced in a fluidized-bed regenerator. This higher SO_2 concentration would improve the economics of subsequent sulfur-recovery processes.

A pilot-plant-scale, externally fired rotary kiln (16.5-cm dia, 344 cm long) was rented for this study. Also, small-scale tests were conducted with a quartz-tube rotary kiln (28-mm-OD tube, 40 cm long) in support of the pilot plant-scale experimental program. Carbon was the reducing agent.

The pilot-plant-scale tests yielded a maximum of about 21% SO_2 in the off-gas at 1050°C, 9.5% at 1000°C, and 4% at 950°C--all approaching equilibrium values--while the highest SO_2 concentration obtained in the fluidized-bed unit was about 10% (at 1100°C). Results similar to the kiln results have been obtained in batch reactors.[1] In addition, regeneration values (percent conversions of sulfated sorbent to regenerated material) approached a maximum of about 85%, thus comparing well with previous results for fluidized beds.[2]

Experimentation was hampered, however, by numerous difficulties. Coal could not be used as the reductant because volatiles caused the sulfated limestone particles to stick to each other and to internal parts. Inferior mixing characteristics of a rotary kiln are believed to have been responsible for the sticking problems. Consequently, coke was used in most of the tests and was much less troublesome. Other problems that appeared were related to materials of construction. Several runs at 1050°C with high concentrations of SO_2 passing through the kiln (>20% SO_2) caused massive pitting along the inside surface of the HH alloy (a high-nickel, high-chromium cast stainless steel) tube. Although this alloy is generally excellent for a reducing gas atmosphere at high temperatures, corrosion caused by reaction of SO_2 with the nickel to form nickel sulfide and oxides could not be prevented. Rapid corrosion of other stainless steel internal parts also occurred.

---

[1] E. T. Turkdogan and J. V. Vinters, Reduction of Calcium Sulphate by Carbon, Trans. Inst. Mining Metall. 85, C117 (1976).

[2] G. J. Vogel et al., Support Studies in Fluidized-Bed Combustion, Annual Report, July 1976-June 1977, Argonne National Laboratory Report ANL/CEN/FE-77-3.

In summary, it appears that externally fired rotary kilns are unsuitable as regeneration reactors for the following reasons: (1) durable construction materials are not available and (2) an expensive clean fuel is required inside an externally fired kiln.

3. Trace-Element Behavior during Cyclic Regeneration

Previously reported results[3] obtained at ANL indicated that the emission of trace elements (such as Hg, F, and Br) to the environment from a fluidized-bed combustor would be less than that expected from a conventional coal-fired boiler. More recent work had the following objectives: (1) to measure the levels of selected trace elements in the sorbent after different numbers of cycles of sulfation and regeneration as an indication of the tendency of a sorbent to be enriched or depleted in trace elements in a cyclic sulfation/regeneration process and (2) to obtain a material balance (based on solid samples only) on a single regeneration experiment for evidence of trace element losses by volatilization.

The samples used in the study were obtained during an earlier 10-cycle combustion-regeneration experiment with Tymochtee dolomite sorbent in the ANL fluidized-bed combustor and regenerator PDUs. Samples were analyzed for trace elements by spark-source mass spectrometry .

The stability of trace elements (which were in the parts-per-million range) in the sorbent during repeated cycling was assessed by comparing the average concentrations of the elements in two samples of sulfated dolomite from the first combustion cycle with average concentrations in two samples of sulfated dolomite from the tenth combustion cycle. Nine elements--Cr, Tl, V, Mo, Zn, Ba, Fe, In, and Sr--were enriched in the sorbent during the ten combustion cycles. The enrichment in these elements was obviously attributable to buildup of coal ash on the surface of the dolomite particles during repeated cycling. Of the 31 elements for which analyses were obtained, none was found to have been depleted over the ten cycles. During the ten cycles, eight elements, which in conventional coal-fired systems have all shown a tendency to be volatile during coal combustion, were either enriched (Cr, Tl, Zn) or remained stable (As, Cd, Pb, Ni, Se) in the dolomite.

To obtain evidence of any volatization of trace elements, the concentrations of the trace elements in a sample from the tenth regeneration cycle were compared with their concentrations in the sulfated sorbent fed to the tenth regeneration cycle: the retention in the sorbent of all 31 elements except nickel was again evident. The material balances (based on solid samples only) for 27 elements in the tenth regeneration cycle ranged from a low of 50% for nickel to a high of about 130% for cadmium and manganese. Nickel showed a slight depletion in the sorbent. Titanium was depleted in the ash from the coal used for regeneration.

---

[3] W. M. Swift, G. J. Vogel, A. F. Panek, and A. A. Jonke, Trace-Element Mass Balances Around a Bench-Scale Combustor, in Proceedings of the Fourth International Conference on Fluidized-Bed Combustion, December 9-11, 1975, MITRE Corp., McLean, VA (1976).

No additional work is planned on trace element characterization in fluidized-bed combustion or regeneration. An effort is planned, however, to characterize emissions of polynuclear aromatics and other complex organics from both the pressurized and the atmospheric fluidized-bed combustion PDUs.

C. Limestone Utilization in Fluidized-Bed Combustion

A major concern in the use of limestone for SO_2 emission control in FBCs is the amount of partially sulfated waste produced. The problem originates in part from the fact that after part of the $CaCO_3$ in the original limestone is converted to $CaSO_4$, the sulfation reaction rate becomes too low for further sulfation. During the past year, a survey was made of the reactivity toward SO_2 of representative limestones from different areas of the United States; the laboratory method previously developed (ANL-78-70) was used to estimate the reactivities in FBCs, and the reactivities of various stones were compared. Studies were continued on the effect of salt additives on the SO_2 reactivity of limestones, including a major investigation of $CaCl_2$.

1. Survey of Limestones

A number of investigators have studied the reactivity of limestones with SO_2. Absent from all of these studies is a method of predicting the limestone requirements in a FBC (kg of stone/kg of coal, or Ca/S ratio) to meet the Federal SO_2-emission standard. Therefore, a convenient laboratory method was developed to predict limestone requirements. In this method, the reaction rate of a limestone with a $SO_2/O_2/N_2$ gas mixture was determined in a thermogravimetric analyzer (TGA). The TGA measurements were made at the FBC operating temperature; the starting material was -50 +70 mesh limestone that had been precalcined in 20% CO_2-N_2.

The agreement of predicted and experimental PDU Ca/S ratios was fair, with a standard deviation for the difference between experimental (PDU) and predicted Ca/S ratios of 1.1. However, the uncertainty (standard deviation) in the experimental Ca/S ratio in the PDU is approximately 0.6, thus indicating that the uncertainty in the predictions can be reduced by improving the measurements on the PDU.

The predictive method was used to estimate limestone requirements for 57 different limestones in an AFBC. The limestone samples were from various locations throughout the United States. For a FBC with a 0.9 m bed depth operating at 2.4 m/s, about 60% of the stones tested were estimated to require less than 0.5 kg/kg of coal; the range was 0.37 to 2.4 kg/kg of coal. When the FBC was operated at 3.6 m/s, the quantity of limestone required generally increased by 50%.

The research suggests that highly reactive limestone that can be used in FBCs to meet the SO_2-emission standard are widely available. Accuracy of prediction of limestone requirements is fair. Refinement of the predictive method will require better experimental results and a better understanding of the reactions which occur in a FBC, in contrast to the reactions that take place in a TGA. Future research will be directed toward a better understanding of limestone-SO_2 reactions in a multiphase FBC.

2. Enhancement of Limestone Reactivity

Study of the effect of inorganic salts on the sulfation of limestones and dolomites, discussed in last year's report, has been continued. The phenomenon of increased sulfation capacity of limestones with salt addition is believed to benefit fluidized-bed combustion by increasing the SO_2 capacity of the limestone or dolomite; thereby, the amount of limestone purchased is reduced, as is the amount of solid waste that must be disposed of.

The goals of this work are (1) to verify the reactivity-enhancement effect for NaCl and other salts, (2) to further elucidate the mechanism of interaction of the salt with the stone, and (3) to arrive at quantitative sulfation capacities provided by the salts for application to fluidized-bed coal combustion systems.

A detailed investigation of the effects of NaCl on both limestones and dolomites has been completed. Synthetic flue gas was used at 850°C in horizontal tube furnaces, and changes in stones were examined by porosimetry and scanning electron microscopy. A mechanism was proposed earlier that is based on interaction of a trace amount of melt (produced at temperatures above 700°C) with the limestone, thereby enhancing decomposition and sulfation by structural rearrangement. This structural change involves migration of pores to form larger pores which favor the permeation of gases and thus allow SO_2/O_2 mixtures to penetrate deeply into the lime particles. The gaseous diffusion is then not so restricted by the $CaSO_4$ product formed (which has a larger molar volume than $CaCO_3$ and tends to choke small channels). Low concentrations of NaCl (<1 mol % limestone) were more effective (up to 60% of the available CaO was converted to sulfate) than high salt concentrations, for which the growth of pores went so far as to cause excessive loss of surface area.

During the past year, a similar study of the effect of $CaCl_2$ on limestones has been completed, and a study of its effect on dolomites is still in progress. This salt also is effective in enhancing limestone sulfation by a mechanism similar to that of NaCl. At high concentrations of $CaCl_2$, however, another mechanism takes effect, namely, the formation of large amounts of liquid that are capable of dissolving CaO. This second enhancement effect can lead to complete sulfation of the stone.

Other salts were examined for similar enhancing abilities in the hope of finding less corrosive species. Of promise are Na_2CO_3 and NaOH, which are effective and do not contain corrosive chloride ions.

The results for NaCl and $CaCl_2$ allowed correlation of average pore diameter with percent conversion to $CaSO_4$ for fifty different limestones and dolomites. They also gave some insight into the structural reasons for some natural limestones reacting to a much greater extent than others and for salt having large positive effects in some stones and very little effect in others.

At present, study of the effects of $CaCl_2$ on dolomites is being concluded, and a series of large-scale tests of salts in a fluidized-bed coal combustor (PDU) is being performed. Along with these confirmatory large-scale combustor tests, a series of corrosion evaluation experiments has been completed, as described in Section E below.

D. Flue-Gas Cleaning for Pressurized Fluidized-Bed Combustion

1. Removal of Alkali Compounds from Hot Flue Gas

Experience obtained from operation of gas turbines with hot flue gas from the combustion of liquid fuels has indicated that alkali metal compounds (such as chlorides and sulfates of sodium and potassium) in the flue gas cause "hot corrosion" of gas turbine hardware. Therefore, for the successful operation of pressurized fluidized-bed combustion (PFBC) combined-cycle power plants, cleanup of alkali metal compounds from the hot flue gas upstream from the gas turbine is imperative. Granular-bed filters are among many devices being actively developed for high-temperature, high-pressure particulate cleanup of flue gas. With a suitable bed material, a granular-bed filter will accomplish removal of alkali metal compounds along with particulate removal. Research work has been under way to develop effective granular sorbents that can be used as bed material in a granular-bed filter for the removal of alkali metal compounds from the hot flue gas of PFBC.

Several commercially available products have been tested as candidate sorbents in a laboratory-scale, fixed-bed combustor. In the tests, gaseous alkali metal compounds were transported to the sorbents in a simulated flue gas of PFBC. Diatomaceous earth and activated bauxite were found to be the two most effective sorbents. Removals of 95-98% of the gaseous NaCl content of a hot gas were readily achieved using these substances. Promising results were obtained in a preliminary economic evaluation, and studies of the effects of some operating variables on the sorption performance for the two sorbents have been continued. Among the variables studied are sorbent bed temperature, superficial gas velocity, gas hourly space velocity, and alkali concentration in the flue gas.

To allow the test to be carried out under pressure, a pressurized sorption test unit is being designed. In this unit the effects of pressure and moisture content of the flue gas on the performance of the sorbents will be investigated. Screening of materials as candidate sorbents will also be continued.

2. Particulate Removal

In pressurized fluidized-bed combustion, the particulate matter in the hot flue gas must be removed to prevent erosion of the gas turbine blades. An experimental program is under way at ANL to test and evaluate promising flue-gas cleaning methods in the off-gas system of the ANL 15-cm-dia FBC (PDU).

Granular-Bed Filter. A granular-bed filter concept being considered at ANL is the use of sulfated limestone from the FBC as the granular material in a fixed-bed filter, with bed material replaced periodically. A small test filter (15.4-cm or 7.8-cm ID) was assembled and was installed in the ANL PFBC for testing.

Experiments were performed to evaluate the effects of particle size, bed depth, and gas velocity on the efficiency of the granular-bed filter. Particle loadings in the flue gas to the filter (from a second-stage cyclone) ranged from 0.3 to 1.4 g/m^3; most loadings were in the range from 0.4 to 0.7 g/m^3.

Over the range of conditions tested, filtration efficiency ranged from about 91 to about 99%. The 99% value was achieved with a 5.1-cm depth of sulfated limestone (mean particle diameter of about 700 μm) and a gas velocity of about 15 cm/s. Particle loadings in the flue gas leaving the granular-bed filter ranged from 0.01 to 0.07 g/m^3, which are at the upper end of the estimated range of acceptable particle loadings for gas turbines of 0.05 to 0.005 g/m^3.

A preliminary analysis of the limestone requirements for a granular-bed filter in an FBC system indicates that limestone usage in the granular bed would slightly exceed the quantity available from the FBC. Additional tests are planned, however, after the installation of a high-efficiency cyclone upstream from the filter. The cyclone will reduce the mass loading in the inlet gas to the filter and theoretically reduce the frequency of replacing the limestone bed material in the filter.

High-Efficiency Cyclones. A Donaldson TAN-JET cyclone, claimed to have a better dust-removal efficiency than conventional cyclones, is being tested. The TAN-JET cyclone employs a secondary flow of clean air to enhance vortex motion and so improve gas-solids separation in the primary air flow of dirty gas from the combustor.

To test the collection efficiency of the cyclone, experiments have been performed (1) at ambient conditions (no combustion, fluidized bed of limestone in the combustor) and (2) at 305 kPa (about 3 atm) with combustion in a fluidized bed of limestone. In these experiments, the mass loading in the flue gas entering the cyclone ranged from about 0.3 to about 3.4 g/m^3. Particle penetration (100% minus cyclone collection efficiency) decreased from about 30% at an inlet loading of about 0.3 g/m^3 to a low of about 5% at an inlet loading of 3.4 g/m^3. These penetrations correspond to mass loadings in the flue gas leaving the cyclone ranging from about 0.08 g/m^3 (at 0.3 g/m^3 inlet loading) to about 0.24 g/m^3 (at 3.4 g/m^3 inlet loading).

At the high inlet mass loadings, an increase in the pressure drop across the secondary air-inlet nozzle in the cyclone dramatically decreased the mass loading in the flue gas leaving the cyclone. At about 3.4 g/m^3 inlet loading, for example, an increase in the pressure drop across the nozzle from 70 kPa to >100 kPa decreased the particle loading in the exiting flue gas from 0.24 to about 0.14 g/m^3. The latter value is approximately three times the maximum loading considered acceptable for a gas turbine. If the particle removals achieved in this preliminary work are not improved, further gas cleanup will be needed downstream from the cyclone.

Additional experiments are planned to test the cyclone at higher pressures (about 810 kPa) and to generate information on separation efficiency as a function of particle size.

Acoustic Dust Conditioning. Acoustic dust conditioning (by exposure to high-intensity acoustic fields) is designed to increase the mean size of dust particles and thereby improve dust collection by downstream collectors.

Efforts to date have been carried out under subcontract at the University of Toronto* for the development and fabrication of a pulse-jet acoustic dust-conditioning (PJ-ADC) system. In this system acoustic power produced by the pulse-jet sound generator is split in the resonant manifold.

The effort at the University of Toronto was divided into three phases: Phase I, the design, fabrication, and testing at atmospheric pressure of a pulse jet-resonant manifold system (PJ-RMS) has been completed. The first pulse jet examined in this phase of the study operated at intensities up to 130 dB and at frequencies of about 300 Hz. Following an intensive program of pulse-jet upgrading, sound intensities as high as 160 dB at a frequency of about 300 Hz were achieved.

Phase II progress is evidenced by the successful operation of the PJ-RMS at pressures as high as 350 kPa. Although, operation of the pulse jet at 810 kPa (the objective of Phase II) has not been demonstrated, there is no reason to believe that this cannot be achieved.

Phase III, the design, manufacture, and testing of a PJ-RMS for installation and evaluation in the flue-gas duct of an ANL process development unit, has not been completed because of the requirement for significantly more developmental work in pulse-jet design than expected. On the basis of this work at the University of Toronto, however, PJ-ADC continues to look promising and technically feasible for PFBC application.

E. FBC Corrosion Studies

1. Laboratory-Scale Studies

The use of alkali salts to enhance the sulfation of limestones in FBC has led to consideration of the possibility of corrosion in the presence of these salts. A laboratory-scale quartz fluidized bed was assembled to screen various alloys and to determine their response to a simulated flue-gas environment with NaCl or $CaCl_2$ added to the bed material. The intent of the preliminary screening of selected alloys was to obtain information for large-scale, long-term corrosion studies. An understanding of the corrosion mechanism produced by these salts in a fluidized-bed environment was also sought.

---

*Investigation directed by Dr. David S. Scott, Professor and Chairman, Dept. of Mechanical Engineering.

Alloy coupons were suspended within and above a fluidized bed of limestone that was at 850°C in a flue gas containing 200-500 ppm SO_2. Salts were added either as dry powder injections into a fixed bed of limestone or by the evaporation of salt slurries on the limestone prior to charging; the salt-treated stone was introduced in a continuous feed.

Experiments on nine alloys exposed to NaCl or $CaCl_2$ were performed, as well as a blank run (no salt); results were reported as the extent of internal penetration and external scale formation. Conclusions from this work were as follows: (1) the addition of NaCl or $CaCl_2$ to the fluidized bed increases the corrosion rate; (2) in the presence of salt, Types 304, 316, and 310 stainless steel perform better than high-nickel alloys do; (3) the corrosion behavior of stainless steels is relatively insensitive to the amounts of NaCl added to the bed; (4) the corrosion behavior of Inconel 600, Inconel 601, and RA333 in the presence of 1.0 mol % NaCl or 0.1 mol % $CaCl_2$ is comparable to that of stainless steels; (5) the internal corrosive attack consists of three distinct zones, namely, an internal oxidation zone, an internal sulfidation zone, and a carburized zone where the carbon from the outer zone reprecipitates as chromium-rich carbides; and (6) specimens exposed above the fluidized bed at 650 and 550°C show extensive corrosive attack; in these specimens, chlorine was detected at the sulfide-oxide interface.

These experiments demonstrated the potential corrosiveness of salt addition for a blank system having no coal combustion. Some steels were rapidly attacked and were not further studied. The unique corrosion due to chloride salts was established, preparing us for future large-scale tests. At present, large-scale corrosion experiments are being carried out in a coal-burning fluidized bed.

The presence of coal ash and alkali halides from coal combustion may have significant effects on the corrosiveness of these salts and their potential application in these systems. Insight into corrosion by alkali salts will also be useful in relation to general corrosion in fluidized-bed combustion.

2. Larger-Scale Studies

As described in the preceding section, there is concern that the use of alkali metal compounds to enhance limestone sulfation might cause unacceptable corrosion of metal components of FBCs. To measure the corrosion rates of metals of construction (represented by metal specimens) in a PDU, a new automated AFBC facility was designed and constructed at CEN. Major components of this new facility are an air preheater, a 152-mm-dia atmospheric-pressure combustor, coal and limestone hopper-feeder assemblies, two parallel off-gas particulate-removal systems, and an off-gas analysis system. Some major components are shown in Fig. V-1.

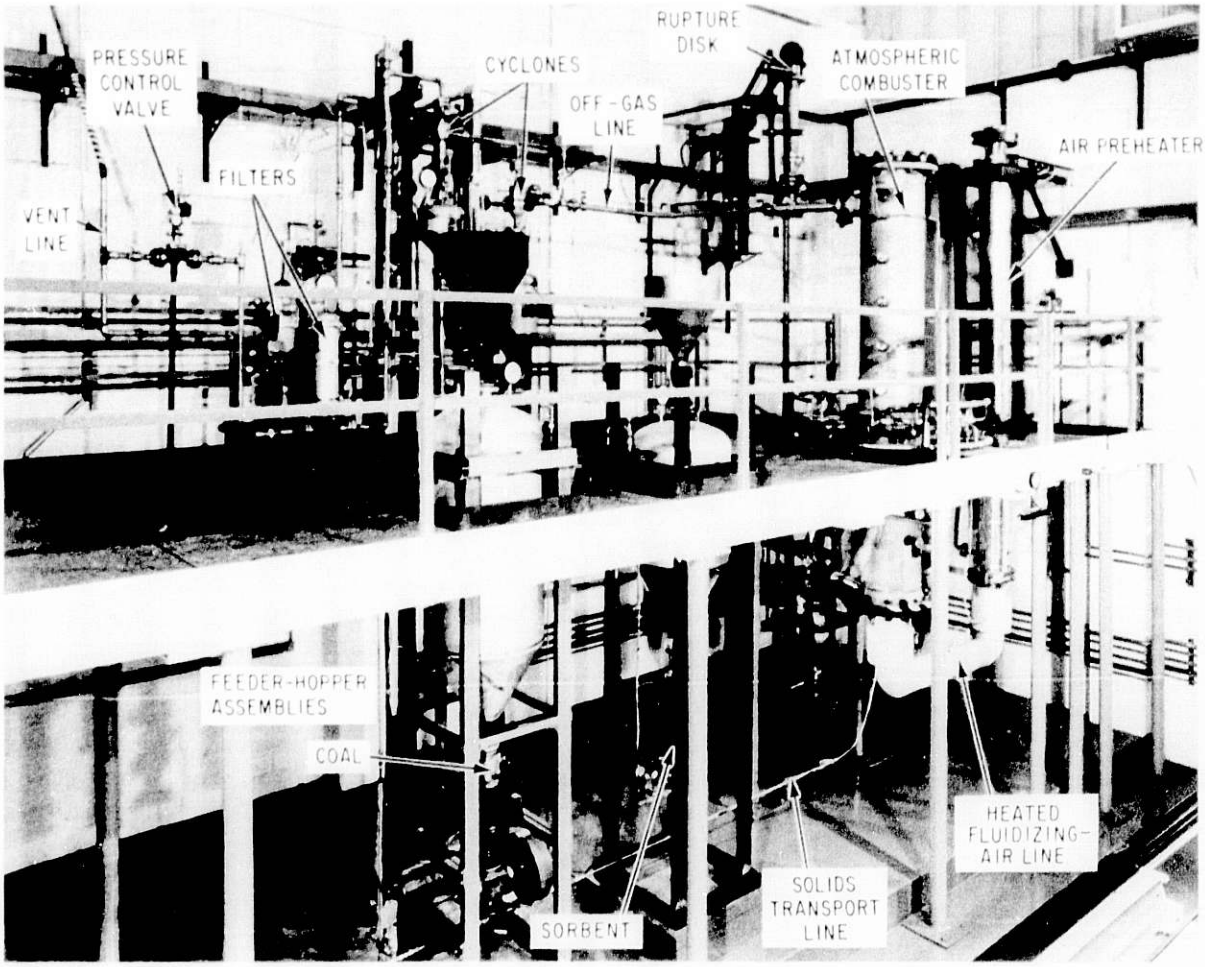

Fig. V-1. Some Major Components of the New AFBC.
ANL Neg. No. 308-78-63A

Three 100-h corrosion test runs have been completed in the new AFBC under the nominal operating conditions listed in Table V-2. In all runs, Sewickley coal (-12 +1[illegible]0 mesh) containing 5.46% sulfur and Grove limestone sorbent (-10 +30 mesh) containing 95.3% $CaCO_3$ were used.

Seven corrosion probes, each holding seven metal specimens were at various locations in the bed and the freeboard sections of the combustor during each of the three 100-h runs. Two probes in the bed section and one in the freeboard section were the air-cooled type to simulate a boiler tube configuration. The remaining probes, two in the bed section and two in the freeboard section, were an uncooled-coupon type to evaluate metals of construction for boiler support plates, hangers, etc.

Table V-2. Nominal Operating Conditions for 100-h Corrosion Test Runs.

Fluidized-Bed Temperature	850°C
Pressure	101 kPa (1 atm)
Fluidizing-Gas Velocity	1 m/s
Fluidized-Bed Height	813 mm
Excess Oxygen	3% (Dry off-gas basis)

In the first run, which was conducted to obtain baseline corrosion data, no alkali metal compound was added. In the second and third runs, about 0.3 mol % $CaCl_2$ and about 0.5 mol % NaCl, respectively, were added to Grove limestone sorbent. During all three runs, the Ca/S mole ratio was adjusted to a value (about 3.5) that would maintain about 700 ppm SO_2 in the dry off-gas and thus meet the present EPA emission standard. (Subsequent experiments have demonstrated that, for noticeable sulfation enhancement in the PDU, higher concentrations of sulfation-enhancing compounds than were used in these two runs are required.) Corrosion behavior of the 147 metal specimens from the three 100-h test runs is being evaluated by personnel of the Materials Science Division of ANL. Techniques used in this evaluation include optical metallography, scanning electron microscopy, and electron microprobe analyses.

Additional 100-h scoping corrosion test runs are planned. The objective will be to test other sulfation-enhancing compounds and to select metals of construction for further evaluation in 1000-h tests.

F. Component Test and Integration Unit

The design of the Component Test and Integration Unit (CTIU) progressed into the detailed engineering phase during the first half of 1978. However, in August, after a detailed examination of the PFBC program, DOE decided to defer construction of the CTIU indefinitely and to use existing facilities with comparable operating conditions and performance characteristics for the achievement of the DOE program objectives in a timely manner. Nevertheless, the CTIU design information will be of value for other elements of the DOE fluidized-bed combustion program.

The CTIU was designed to be a flexible, highly instrumented test facility, capable of relatively easy modification for testing of alternative components for PFB systems. Descriptions of the important systems and their capabilities are given below, along with design features developed during the past year. The design criteria are listed in Table V-3.

Table V-3. Criteria for CTIU Combustor Design

	Reference Operating Conditions	Design Capabilities
Operating pressure	10 atm (147 psia)	3-12 atm
Bed operating temperature	1650°F	1350-1850°F
Bed height	8 ft, 5 in.	1-16 ft
Freeboard height	23 ft	6-25 ft[a]
Fluidized air (dry)	10 lb/sec	--
Feed transport air	0.8 lb/sec	--
Excess combustion air	20%	20-100%
Superficial gas velocity	7 ft/sec	3-9
Ca/S mole ratio	2	0-2.5[b]
Target sulfur removal (minimum)	90%	--
Combustion efficiency	94%	c

[a] Can be changed during shutdown.
[b] At design coal rate.
[c] Determined by operating conditions.

1. Combustor System

The fluidized-bed combustor is contained inside a 12-ft-ID containment vessel having a pressure rating of 260 psig. Combustor details are shown in Fig. V-2. The pressure containment vessel surrounds an internal fluidized-bed module section which has been designed for ease of replacement or modification. Most disassembly of the combustor is through the top of the pressure containment vessel, although the air distributor plate (grid) and some instrumentation can be removed through the bottom of the vessel.

The fluidized-bed combustor is constructed of a stack of flange-connected, refractory-lined modules. The module shells have circular cross sections although the refractory linings for several of the cases considered have square internal cross sections. The bottom module is for feed and air distribution; through it, combustion-fluidizing air and solids feed materials enter the bed. Above this module, are several modules containing bed cooling-tube bundles and specialized test probes. Above the latter modules are several blank or freeboard modules, which may be of various heights, allowing the desired total freeboard height to be achieved.

Many features were designed into the combustor to enhance its usefulness as an experimental facility. Some of them are as follows:

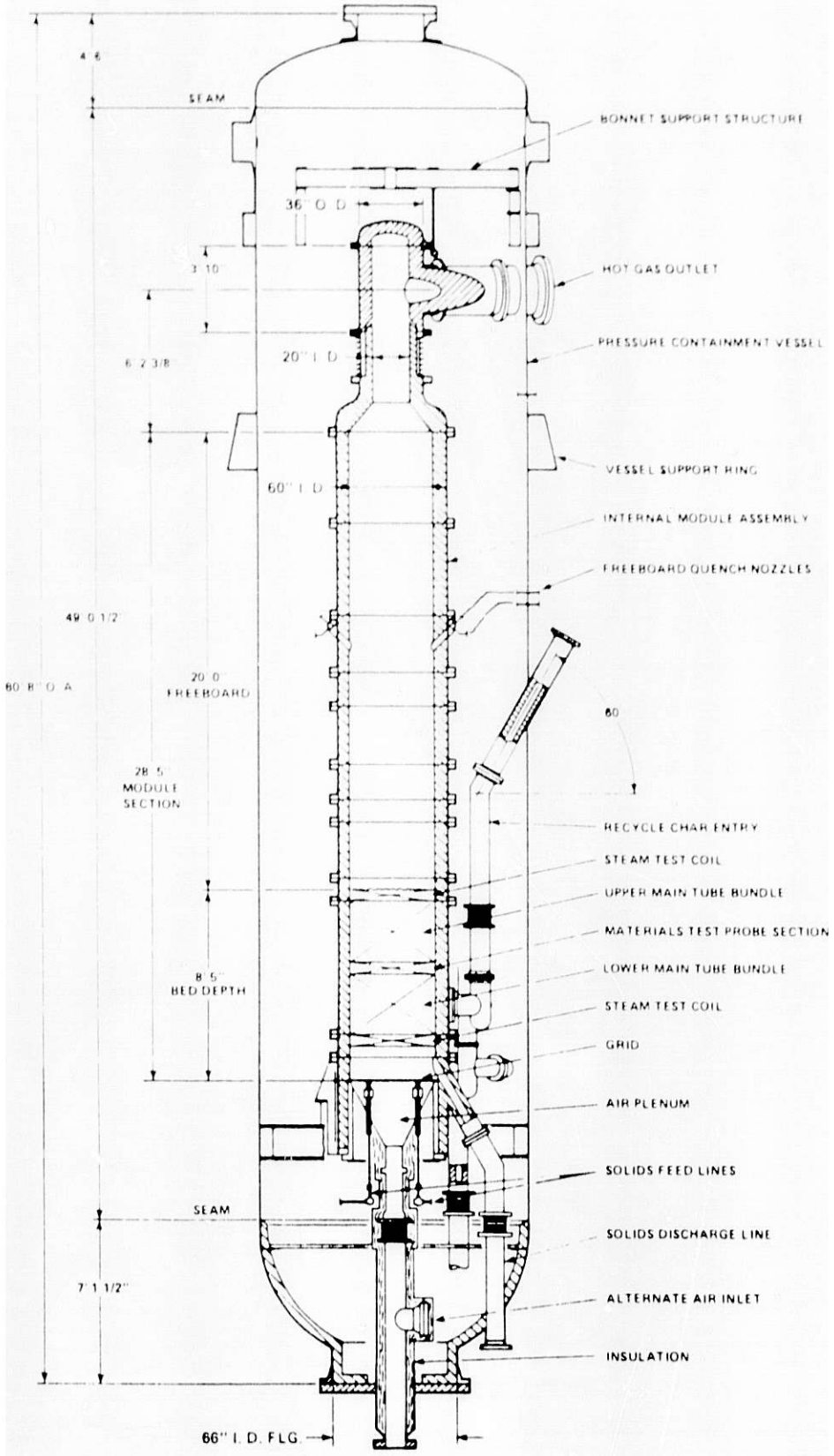

Fig. V-2. CTIU Combustor

(a) Solids feed materials can be introduced into the combustor through five feed nozzles located in the sidewall just above the air distributor (the grid) or through five nozzles projecting upward through the air distributor. Two additional sorbent feed nozzles are placed at higher levels in the bed sidewall. Coal and sorbent are fed through only one or two feed nozzles, with the other nozzles used as spares or to test mixing patterns in the fluidized bed.

(b) The main cooling-tube bundle is split into two sections inside a single module. Between the sections is a U-shaped probe for heat transfer measurement. In addition, on either side of this probe are bayonet-type probes (cooled or uncooled) for testing various tubing materials. These probes are so located that a uniform geometric pattern of the tubes immersed in the bed is maintained.

(c) Above and below the main cooling bundle are two steam-cooled test coils, which are mainly to be used for evaluating corrosion behavior of various tube materials. These, too, are arranged to maintain a uniform geometric pattern of the submerged tubes.

(d) Quench nozzles are located in a module high in the freeboard. By injecting a water mist, these nozzles may be used to reduce temperature excursions caused by afterburning of carbon-containing materials in the freeboard.

(e) Through a pulsed feeder located near the bottom of the fluidized bed, material captured by the primary cyclone can be recycled into the bed in order to investigate how this affects combustion efficiency.

2. Hot Gas Cleanup System

The hot gas cleanup system comprises three stages of particulate removal. The primary or roughing cyclone (just downstream from the combustor) is of moderate efficiency (about 85%), and operation of the plant is possible either with or without recycling of underflow solids materials from the cyclone to the combustor. When solids are not recycled to the combustor, they are discharged through two lockhoppers to the solids coolers. Off-gas from the primary cyclone flows to the secondary cyclone, which has an overall efficiency of about 90%. Off-gas from the secondary cyclone flows to the third-stage particulate cleanup device, which is specified to be a granular-bed filter (such as that offered by Ducon, Inc.) of 95% overall efficiency. Its pressure containment shell is somewhat oversize to accept alternative internals (as yet unspecified). The piping designs allow the filter to be bypassed if desired. Solids from this device are discharged through a single lockhopper into a disposal bin.

The hot gas cleanup system has a provision for extracting a slipstream of up to 1000 acfm downstream from the primary cyclone and for returning this stream to the main gas flow upstream from the third-stage cleanup device. This slipstream may be used to test prototype gas cleanup devices. There are also provisions for both extractive sampling and in situ

monitoring of gas streams, both upstream and downstream from each cleanup device, so that particulate loadings and size distributions can be determined; these data will be used in evaluating the performance of each device.

3. Turbine Cascade System

Hot gas from the third-stage cleanup device flows through a stationary turbine test cascade, which is operated as if it were either a choked or unchoked orifice, depending on the unit's final design. When the cascade is operated in an unchoked condition, system pressure is controlled by the choked orifice downstream from the cascade. If the cascade is operated in a choked condition, system pressure is controlled by the flow through the bypass line cooler and control valve. Gases from the turbine test system flow up a short exit pipe and into the atmosphere. Several sizes of flow orifices are available to allow the system to be operated at pressures and mass flow rates other than those used in the initial test series.

4. CTIU Instrumentation and Control

The CTIU instrumentation and control system is designed in accord with the experimental nature of the facility for which modifications would thus be expected. The system comprises a centralized process-control system, a supervisory control and data-acquisition system, a plant-protection system, instruments, and control elements.

Overall control of the CTIU is normally from a single console in the central control room, but manual control of individual subsections can also be maintained by use of the dedicated controllers. The controllers also have provisions for supervisory input signals. The centralized control system is a stand-alone microprocessor-based system, and one or more keyboards and cathode ray tubes are the primary interfaces with the operator. All subsystem controllers and the data-acquisition system are located in the central control room. The latter system is a real-time digital central processor, such as Honeywell 4500 or Taylor 1010, which performs data recording, supervisory control, data reduction, batch processing, and graphic display support functions. This system is eventually to be used for direct digital control functions.

The central process controller, local process controller, and data-acquisition system have a backup plant protection system that changes operating conditions to safer levels or shuts down the CTIU if the normal systems fail to do so when required. The protection system uses both hardwired logic control schemes and dedicated digital, computer-based logic systems with nonvolatile memories and uninterruptible power sources.

G. Fossil Fuel Conversion and Utilization

1. Support Studies for Underground Coal Gasification

The purpose of this study is to provide data on reaction kinetics in support of the DOE national program for development of underground *in situ* gasification of coal. The DOE program consists of field tests, laboratory studies, and mathematical modeling efforts related to the *in situ* conversion to clean gaseous fuels of lignite western subbituminous, and eastern bituminous coals. The reactions being studied in our effort are those occurring in the gasification zone of the process--*i.e.*, steam-char, CO_2-char, hydrogen-char, water-gas shift, and methanation reactions. The information on reaction kinetics obtained in our studies is used in the global mathematical models being prepared at each of the field test sites. We are using a differential packed-bed reactor equipped with a gas chromatographic analytical system. The coal samples used in our measurements are representative of coals at sites where field tests either are currently being conducted or are under consideration.

During 1978, we have determined kinetic parameters for the reaction of steam with crushed chars prepared from Pittsburgh seam coal. This coal is an eastern high-volatile bituminous coal with a high swelling index and exhibits reaction characteristics very different from those determined earlier for western subbituminous coals. With the Pittsburgh char, the pore structure is apparently fully developed by the time 20% of the carbon is gasified, whereas with the western coal, maximum pore volume (hence, minimum pore diffusion limitations to the steam-char reaction) is not attained until greater than 60% of the carbon has been gasified. However, extensive pore diffusion limitations are observed with the Pittsburgh char, as indicated by the apparent activation energy for the steam-char reaction having a smaller magnitude at higher temperature--*i.e.*, -184 kJ/mol (-44 kcal/mol) at 700°C (reaction activation) and -75 kJ/mol (-18 kcal/mol) (diffusion activation) at 850°C. The reaction of steam with Pittsburgh char was found to be first order with respect to steam, in contrast to fractional orders (0.56 for Hanna and 0.85 for Wyodak) found previously in the case of subbituminous coal. The significance of this finding is not yet apparent.

In another sequence of experiments, we determined the changes in pore structure and surface areas of chars prepared from Hanna subbituminous coal as a function of extent of carbon gasification. A Typical plot of cumulative pore volume *versus* pore diameter is shown in Fig. V-3. At 750°C, as carbon is removed, the total volume of pores having diameters greater than 0.006 μm increases by a factor of >15, up to 65% gasification. During this time, the surface area of the char as determined by nitrogen adsorption (BET method) increased by a factor of six. Kinetic measurements show that under these conditions, the rate of reaction of steam with the Hanna char increases threefold, indicating that the reaction rate is dependent upon the growth of pores having diameters greater than some critical diameter, as well as upon the growth of surface area. More studies in this area will be carried out.

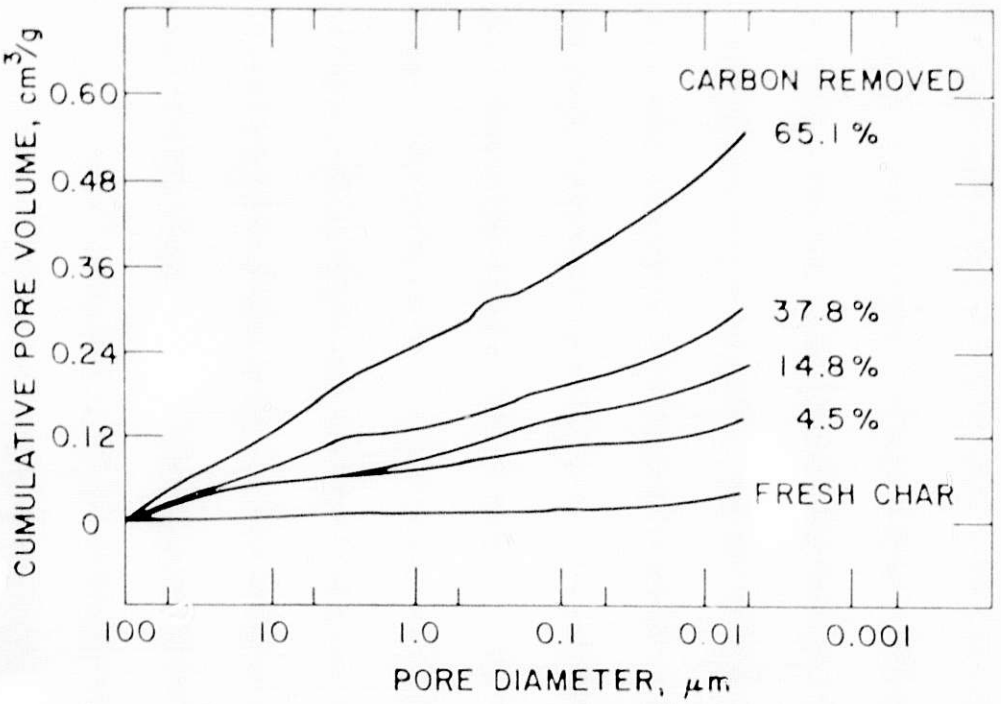

Fig. V-3. Cumulative Pore Volume versus Pore Diameter for Hanna Char

During 1978, we have been developing a rate expression to correlate our previously obtained data on the reaction of steam with chars prepared from Hanna subbituminous coal with operating conditions expected in underground gasification, namely: temperature, 600-850°C; steam partial pressure, 0-300 kPa (0-3 atm). The model found to fit our data best is as follows:

$$r_c = \frac{k_o \left(P_{H_2O}\right)^m \left(X_C\right)^n}{1 - k_1 \left(P_{H_2}\right)^2}$$

where

m = 0.56, reaction order with respect to carbon

n = 0.59, reaction order with respect to steam

k_o = $2.70 \times 10^5 \exp(-25940/RT)$

k_1 = $9.05 \times 10^{-9} \exp(38350/RT)$

r_c = rate of reaction with steam

X_C = fraction of carbon gasified

The form of this rate expression differs somewhat from that generally described in the literature, but for the low values of P_{H_2} and P_{H_2O} which would be expected in underground coal gasification, the correlation using this expression is much improved over other forms.

Future plans include investigation of the reaction of carbon dioxide with both western and Pittsburgh seam chars, as well as expansion of our data-correlation efforts to include Wyodak subbituminous coal and Pittsburgh seam coal.

2. Environmental Control Implications of Generating Electric Power from Coal

The objective of this joint program, managed by Argonne's Energy and Environmental Systems Division, is to provide guidance to the staff of the DOE Office of Environment in their efforts to ensure the development of adequate technology for mitigating the environmental impacts of increased coal utilization. The program focuses on control technology for coal-based power generation. It supplies in-depth evaluations of technical, environmental, and economic aspects of the various options that are available or under development.

CEN's responsibility in this program has been and continues to be technical assessments related to (1) the control of nitrogen oxide (NO_x) emissions from conventional coal-fired boilers, (2) integrated coal gasification/fuel cell power generation, and (3) integrated coal gasification/combined cycle power generation. During FY 1978, a report on NO_x control technology for coal-fired utility boilers was published,[4] and a report on NO_x control technology for coal-fired industrial boilers is in press (ANL/ECT-4). In addition, a preliminary evaluation of the effects of fuel-gas contaminants on molten-carbonate fuel cell performance was completed.

In FY 1979, the Phase II study--an assessment of coal gasification/combined cycle power generation--will be completed, and efforts in this area will then be directed toward utilizing information gathered in Phase II for developing a model. A detailed study of advanced NO_x control technology will also be completed. Finally, an extensive assessment of coal gasification/molten carbonate fuel cell power generation will be initiated.

3. Technical Management of Program to Optimize Fuel Utilization for Fuel Cells

Planning and monitoring services are being supplied by the Division for the DOE-sponsored program for the development of fuel processes appropriate for integration into advanced fuel cell systems. These processes would be capable of utilizing more abundant, lower quality primary fuels (e.g., petroleum distillates and coal-derived liquids), rather than the premium fuels

[4] Environmental Control Implications of Generating Electric Power from Coal, 1977 Technol. Status Report, Appendix D, Assessment of NO_x Control Technology for Coal-Fired Utility Boilers, Argonne National Laboratory Report ANL/ECT-3 Appendix D (December 1977).

(natural gas and naphtha) currently required by first-generation fuel cell systems. ANL is assisting DOE in soliciting and evaluating proposals and providing technical management of investigations in this program.

This effort was initiated at ANL at the beginning of FY 1978. During the past year, contracts were established with the industrial community to provide a base for developing a coordinated program, and familiarity with the ongoing programs was established. Contributions were made to the overall program plan, and additional research contracts were initiated to meet the objectives of this plan. ANL is managing the technical aspects of the contracts.

During FY 1979, technical management of the contracts in this program will be continued. The overall program plan will be reassessed to reflect new developments. In addition, an experimental program will be started in FY 1979 which will be directed toward determining the mechanisms whereby sulfur and carbon deactivate steam re-forming catalysts.

4. Technical Management of Alternative Fuels Technology

The Division provides technical support to DOE in the management of a broad alternative-fuels effort whose objective is to ensure the existence of the fuel technology base required for timely substitution of alternative fuels for petroleum and natural gas. Principal substitute fuels, such as coal-derived liquids, will contribute initially to the nation's liquid fuel needs in the mid-1980s; by the year 2000, about five quads* per year of energy will be derived from liquids made from coal.

The CEN management effort has consisted of providing a program plan establishing objectives, reviewing proposals, reviewing the work of contractors, providing contract procurement documents for DOE, and presenting program overviews at the annual meeting of contractors.

*1 quad = 10^{15} Btu.

VI. MAGNETOHYDRODYNAMICS TECHNOLOGY

A. Overview

Magnetohydrodynamics (MHD) is a developing technology that promises to improve substantially the efficiencies of conversion of coal to electric power. Most of the CEN effort in support of this multidivisional program on open-cycle MHD is directed toward developing the technology required for the components downstream from the MHD channel-diffuser and for processes to recycle the potassium seed material.* The major focus of the CEN effort has been on (1) studies of interactions between coal slag and seed materials in gaseous and condensed phases, and (2) development of a process for removing sulfur from the spent seed material recovered from the MHD power plant. In FY 1979, work in these areas will continue and CEN will assume additional responsibilities for conducting tests of MHD steam-generator components in a 2-MW facility recently constructed at Argonne.

Figure VI-1 is a conceptual representation of the gas system downstream from the MHD channel-diffuser. This portion of the gas system is analogous to the steam-generating portion of a conventional power plant, but it must perform the additional functions of separating slag and seed, recovering heat and nearly all of the seed material, preheating air to high temperatures, and reducing very high NO_x concentrations to acceptable levels. Moreover, because of higher temperatures, fuel-rich gas, and large concentrations of potassium, this system must operate under conditions that are more corrosive than conditions in conventional power plants. The incompletely burned combustion gas leaving the channel-diffuser and entering the steam bottoming plant contains a fraction of the coal slag as small particles and the seed as vaporized potassium species. In the first steam-generator component (the radiant boiler), slag is separated from the combustion gas at a high temperature to minimize the reaction with vaporized potassium species that occurs at lower temperatures. The high NO_x concentrations produced in the primary combustor are reequilibrated to acceptably low levels by providing a low cooling rate in the radiant heater. In the second component, the steam superheater, additional air is injected into the fuel-rich gas to complete the oxidation of CO and H_2 and to convert sulfur to K_2SO_4. The potassium seed material condenses as a mixture of K_2SO_4, K_2CO_3, and KOH and is removed as a liquid in the superheater and as a solid in the heat exchangers that follow. The remaining system components remove solid slag and seed particles from the combustion gas before it is exhausted to the atmosphere.

The overall objective of the Argonne MHD Balance of Plant (BOP) Project is to provide the requisite technical data for designing and operating the downstream gas system and the seed recycle process. The long-range objective is to support the design of the MHD Engineering Test Facility (ETF), which will be built to demonstrate the feasibility of an integrated coal-fired MHD-steam power plant, and a planned 20-MW facility, the Heat Recovery-Seed Recovery Facility, which will be used to test steam-generator components. Support work

---

*The function of the K_2CO_3 seed is to enhance the electrical conductivity of the combustion gases fed to the channel/magnet system.

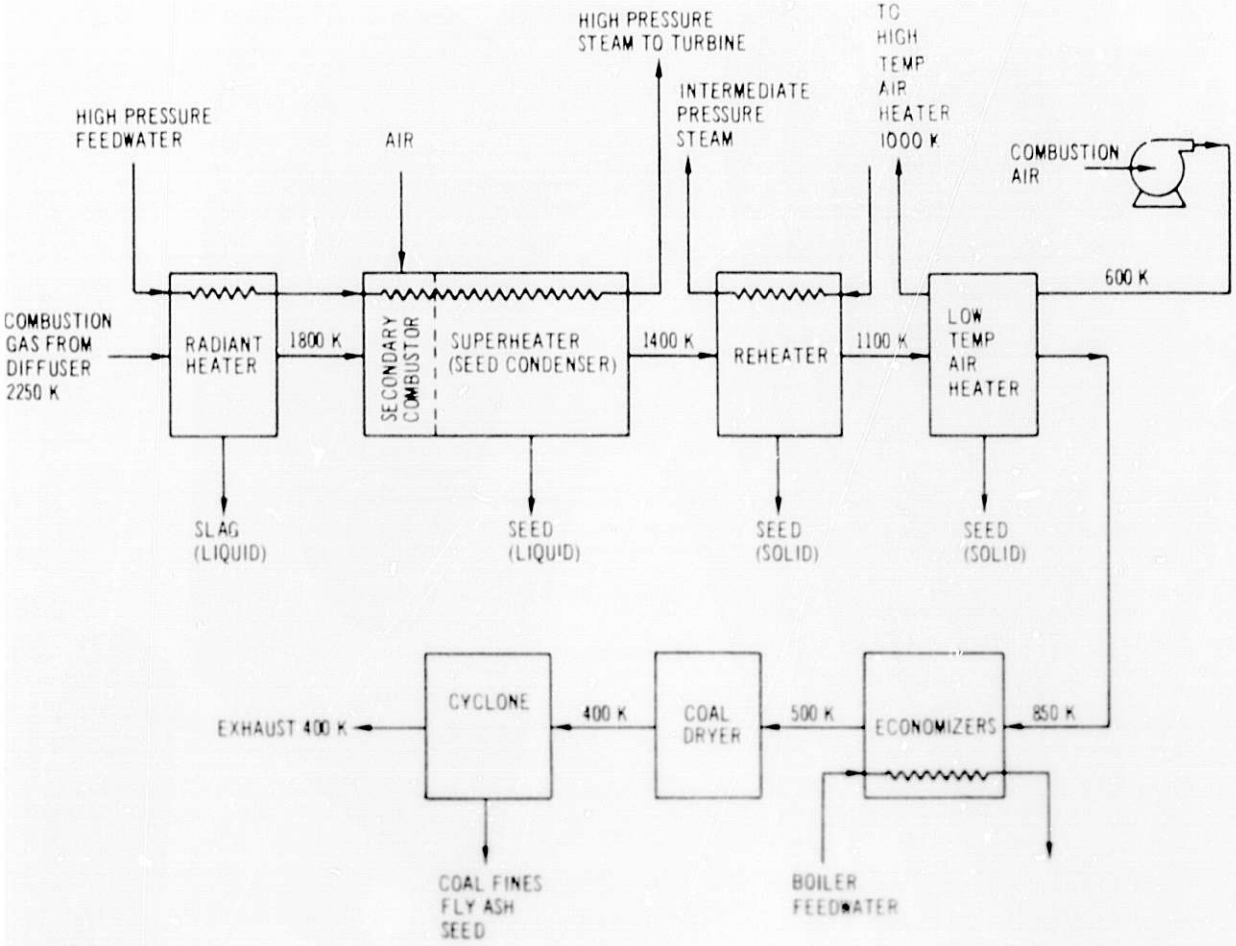

Fig. VI-1. Representative Concept of Downstream Gas System for Open-Cycle MHD Power Plant

covers the general areas of developing analytical models, performing small-scale experiments, and obtaining operating data from prototypic equipment on a 2-MW scale.

B. Thermochemical Support Studies

Studies of slag/seed chemistry in support of Argonne's MHD program include the following: (1) development of computer models to describe vapor/liquid equilibria and the diffusion of potassium in slag and structural materials, and (2) measurement of thermochemical data for compounds critical to the overall potassium seed recovery scheme.

1. Mathematical Model

Vapor-Liquid Equilibria. As mentioned in last year's report, a computer code (MHDGAS) was written to calculate the equilibrium partial pressures and condensed-phase compositions of coal-combustion gases, potassium seed, and coal slag at temperatures typical of those in the coal combustor, MHD generator,

and downstream components. Critical to the development of this model is the assumption that the condensed phase is an ideal solution of stable components formed from the mixture of coal, seed, and slag.

This computer program was checked against a sample of slag/seed from the diffuser section of the coal-fired MHD power channel at the University of Tennessee. The sample contained the usual constituents of coal ash, with approximately 15 wt % potassium and less than 1 wt % sulfate. In a transpiration apparatus, the equilibrium pressure of KOH vapor in a N_2-H_2O mixture over the slag/seed sample was measured in the temperature range from about 1150 to 1800 K. The KOH pressure calculated by the computer code agreed with the measured values within a factor of two.

Most recently, this computer program was used to identify the major potassium and sulfur vapor species in a coal combustion gas system with a low slag content over the temperature range from 1000 to 2000 K, and for conditions in which the stoichiometric ratios of actual air to theoretical air needed for combustion were 0.85, 1.0, and 1.1. The calculations show that in the reference flowsheet (Fig. VI-1) sulfur concentrations in the gas phase can be decreased to acceptable levels if the K/S atom ratio is 1.9 or higher, the stoichiometric ratio is equal to or greater than 1.0, and the loss of potassium to slag is small. However, if the seed is condensed under reducing conditions by carrying out the secondary combustion after the seed is separated, the decrease in sulfur concentrations to acceptable levels requires K/S ratios greater than 2.5 and separation of the condensed potassium-sulfur salts at temperatures between 1200 and 1300 K. The advantage of this flowsheet modification is that potassium reprocessing is simplified because the bulk of the condensed potassium-sulfur is in the form of K_2S, which is readily regenerated. Along with the K_2S, K_2CO_3 and a small amount of K_2SO_4 are also condensed. At temperatures below 1200 K, difficulties may be encountered in condensing the K_2S and K_2SO_4 from the combustion gas before it reequilibrates to form condensed K_2CO_3 and KOH and gaseous H_2S and HS, thereby creating an undesirable stack emissions problem.

Potassium Diffusion. The computer modeling effort has been extended to allow calculations of the thermal diffusion of potassium through a slag layer having a large thermal gradient. In this model, an activity-independent diffusion coefficient was derived and evaluated for potassium diffusion. The calculations indicate a strong driving force for the diffusion of potassium from the hot side of the slag to the cold side. In the calculation, the initial slag-film composition is computed from the equilibrium concentrations of condensed slag and seed. It was assumed at this stage that the film remains in place and potassium from the gas reacts at the hot surface of the film. The potassium transport from the gas to the surface is a combination of gaseous diffusion and turbulence. Potassium moves from the gas into the slag as long as the equilibrium potassium pressure in the slag surface is less than the potassium pressure in the gas.

Figure VI-2 shows the calculated potassium distribution curves in a 2-cm-thick slag layer with a temperature of 1420 K at the hot side and 996 K at the cold side. The potassium diffuses rapidly in the hotter regions and concentrates about 0.7 cm from the cold side because of its lower diffusion rate in the colder portion of the slag layer. This behavior is consistent

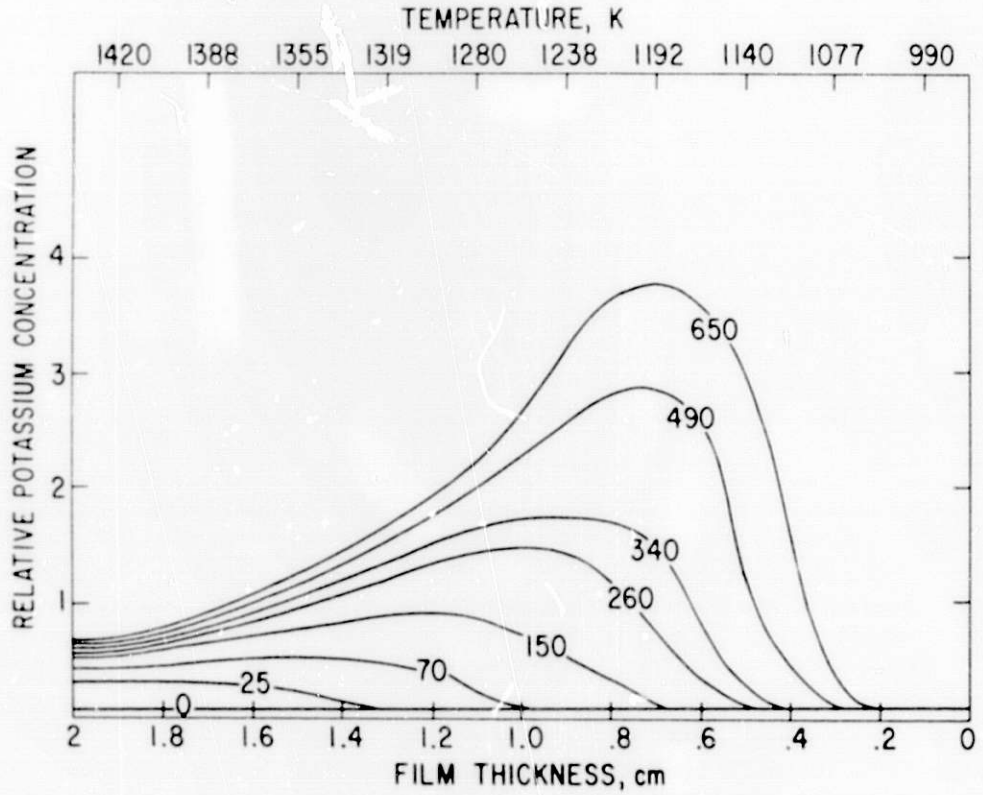

Fig. VI-2. Calculated Potassium Distribution in a 2-cm-thick Slag Layer. (The temperature gradient across the 2-cm thickness is from 1420 K to 996 K; diffusion times are from 0 to 650 h.)

with observations of Jacquin et al.,[1] of potassium attack in ceria-stabilized zirconia under a temperature gradient of 1400 K/cm. These authors found potassium concentrated in the zirconia where the temperature was between 1000 and 1250 K. The attack was believed to be caused by potassium penetration through pores and cracks. The calculations here suggest that ionic thermal diffusion is sufficient to cause the potassium attack of stabilized zirconia. Under high-temperature gradients, the diffusion is considered to be driven by a gradient in the product of the activity-independent coefficient and the potassium partial pressure. This product, $D_{p_k} \cdot P_k$, is an exponential function of 1/T. Thus, the rate of transport is very high at the hot side of the stabilized zirconia, and decreases with the decreasing temperature. At the cold side, the rate is too low for potassium transport. The result is an increase in potassium concentration with time within a region or temperature range of the stabilized zirconia. This peak concentration region shifts toward

[1] M. Jacquin, M. Guillan, A. Montardy and J. M. Phillips, presented at Symposium on MHD Power Generation, Warsaw, Paper SM-107/68; reported in J. B. Heywood and G. J. Womack, Open-Cycle MHD Power Generation, Pergamon Press Ltd., London, p. 562 (1969).

lower temperatures with time. The shift results from the increased potassium pressure as potassium concentration increases. Similar gradients in potassium concentration are expected in the actual slag film where the temperature will vary between 1000 and 1300 K. Again, after long times, the potassium is expected to transport to the lower temperature region.

2. Laboratory Thermochemical Studies

The thermodynamic computer modeling effort has identified two compounds that are critical to the overall MHD operation and seed-recovery scheme; these compounds are potassium sulfide (K_2S) and kalsilite ($KAlSiO_4$). The K_2S is likely to be an intermediate in potassium-recovery schemes and the $KAlSiO_4$ has been identified as a potential source of seed losses in the coal-slag/seed system. Useful thermochemical data for these compounds are extremely limited.

Both compounds have been prepared and purified. Potassium sulfide was made by direct addition of the elements, with excess potassium being removed by distillation. Kalsilite was made by direct addition of $KAlO_2$ and α-SiO_2 in a sealed capsule at 1450°C. Mass spectrometric studies on potassium sulfide have shown the presence of K, S_2, KS, K_2, K_2S, K_2S_2, and KS_2, which are listed in order of decreasing concentration levels in the gas. Thermodynamic analysis of these data is in progress. Similar mass-spectrometric studies on kalsilite are in progress. However, because of a shift in funding, the level of this effort has been greatly reduced.

C. Seed Recycle System

The seed recycle system involves the following steps: (1) collecting and treating the potassium salts separated from the combustion gas stream, usually as K_2SO_4, (2) regenerating seed material by removing sulfur from K_2SO_4, and (3) feeding the seed into the primary combustor. It is estimated that, for economic reasons, seed losses for the entire recycle process should not exceed 5% per cycle.

Two types of processes appear promising for separating sulfur from K_2SO_4. The first is a direct reduction process:

$$K_2SO_4 + xCO + (4 - x)H_2 \rightarrow K_2S + xCO_2 + (4 - x)H_2O$$

$$K_2S + H_2O + CO_2 \rightarrow H_2S + K_2CO_3$$

This process is carried out at near-atmospheric pressure and at temperatures between 700 and 900°C. Similar processes, in which the second step is carried out by stripping H_2S from an aqueous solution of Na_2S, have been developed as a semicommercial process for flue-gas scrubbing and as a commercial process for recovering pulping liquor in the kraft paper industry.

The second promising process involves the production of potassium formate:

$$K_2SO_4 + Ca(OH)_2 + 2CO \rightarrow 2KHCO_2 + CaSO_4$$

The formate reaction is carried out in an aqueous medium at 200°C and 300 kPa pressure. This process has been used industrially to produce K_2CO_3 from K_2SO_4.

These two types of processes and several others with a potential for seed reprocessing have been reviewed on the basis of their energy usage, relative state of development, and costs. A report[2] was prepared summarizing these findings. The more promising processes require a reducing gas that could be produced by coal gasification. Although these processes have had some degree of commercial development, it is not clear that they can meet the requirements of the MHD system for high conversion, low potassium losses, and low energy usage, as well as effecting the separation of slag and other impurities from the seed. A clear-cut choice among the various processes could not be made on the basis of the review, because engineering design data, such as reaction kinetics, effect of impurities, side reactions, and construction materials for the high-temperature reactions, are lacking. Experiments are under way to determine the rate and extent of the reactions involved in the direct reduction process described above.

D. 2-MW Test Facility

A versatile facility for testing MHD steam-generator components under prototypic MHD conditions has been constructed by Argonne's Engineering Division. The facility can supply a mixture of combustion gas, potassium compounds, and coal ash at a rate of 1 kg/s, and at temperatures in the range from 2000 K up to about 2500 K. Initially, the combustion gas will be supplied by a combustor with a feed consisting of a slurry of fuel oil, K_2SO_4 and coal ash, but it is planned to install a coal combustor before the end of 1979. The facility presently includes an oil-slurry feed system, air compressor, air preheater, recirculating-water cooling systems for the experiments, exhaust-gas quencher-scrubber, and data-acquisition system.

CEN has been assigned the lead role in the planning, conceptual design, and execution of the experiments, and interpretation of the results. The experiments fall into three general regimes of combustion-gas temperatures: (1) 2300 to 1800 K, (2) 1800 to 1500 K, and (3) below 1500 K.

The experiments planned for the gas-temperature regime of 2300 to 1800 K are related to the radiant boiler, wherein potassium seed is in vapor form, slag is liquid, and heat is transferred from the gas to the water-cooled walls primarily by radiation. These walls will be coated with a slag film that has a surface temperature in the slag melting range. The radiant-boiler tests will be directed toward measurement of radiant heat transfer from a particle-laden gas, and studies of NO_x reaction kinetics, interactions between seed and slag, and corrosion of refractory and metallic materials by potassium-rich coal slag.

Experiments planned for the 1800 to 1500 K regime are related to the steam heaters and recuperative air heater downstream from the radiant boiler.

---

[2] A. Sheth and T. R. Johnson, Evaluation of Available MHD Seed-Regeneration Processes on the Basis of Energy Considerations, Argonne National Laboratory report ANL/MHD-78-4 (Sept 1978).

In these components, banks (or plates) of steam- or air-cooled tubes will be exposed to a gas stream that contains seed vapor and sub-micrometer particles of slag. Analyses have shown that in this temperature regime, the surface of the seed depositing on the walls will be liquid. These experiments, called "liquid seed condenser" tests, will be directed toward measurement of heat-transfer rates, seed- and slag-deposition rates, and studies of the characteristics of the deposited film and materials corrosion.

Experiments in the lowest temperature range (below 1500 K) will be done first; the planning for these tests is nearly complete. These tests, referred to as the "solid seed condenser" tests, are related to steam and air heaters similar to those considered in the "liquid seed condenser" tests. The objectives of both test series are also similar. However, in the lowest temperature series, the gas temperature is too low to vaporize the seed completely and to maintain a liquid film on the deposited seed material.

The apparatus for the "solid seed condenser" tests, which is to be installed in the 2-MW facility, is shown in Fig. VI-3. Preceding the test section are conditioning and transition sections, which allow the hot gases leaving the combustor to be cooled to the desired test temperature and the vaporized seed material to be condensed in the gas stream. These sections will have instruments to measure gas temperature and flow rates, and means for characterizing entrained particles. The test section consists of a bank of cooled tubes that simulate the configuration of a steam reheater. Instrumentation in this section will allow heat-transfer and solids accumulation rates to be determined. Several tubes can be removed easily to facilitate materials

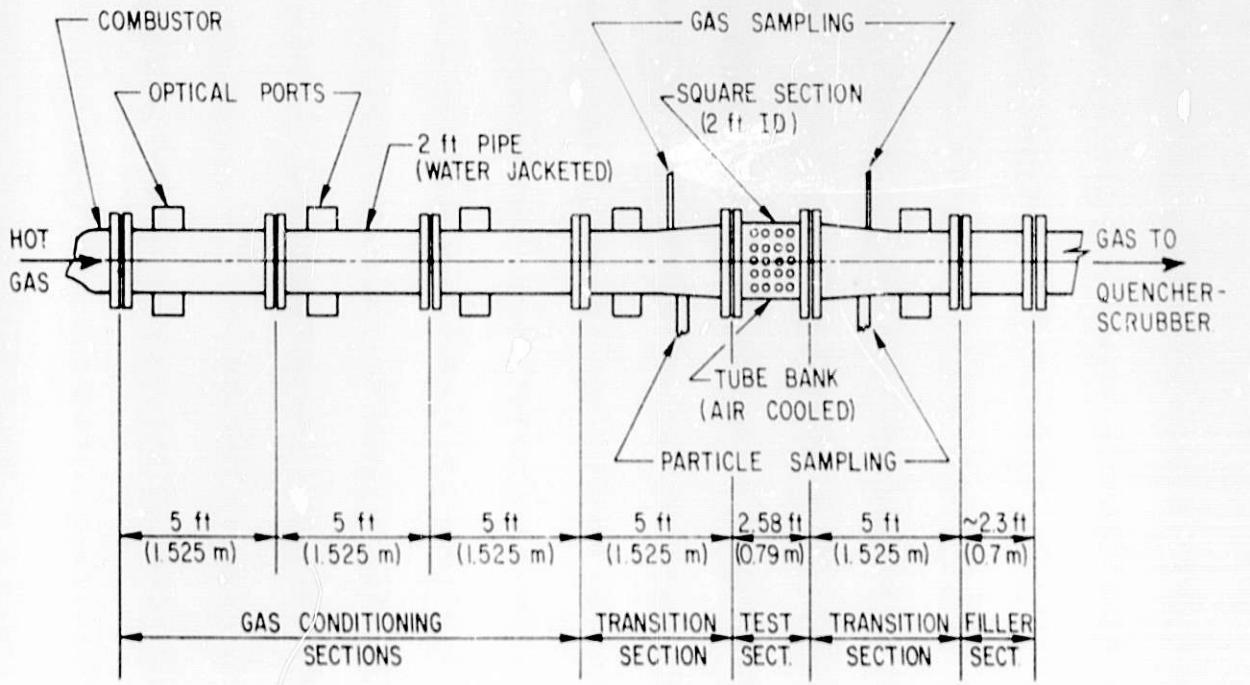

Fig. VI-3. 2-MW Test Train for Solid Seed Condenser

studies. Instrumentation in the transition section following the test section will allow the condition of the gas and entrained solids to be determined as they leave the test section and before the gas is exhausted to the quencher-scrubber.

VII. SOLAR ENERGY DEVELOPMENT

The solar energy program at ANL is an integrated, multidivisional program that includes work on the efficient collection, storage, and utilization of solar energy and the analysis of the near-term status of solar energy technology. The program is directly supportive of the long-range national goal of developing solar energy as an alternative energy source for heating, cooling, and industrial process heat applications. Three of these activities are in the Chemical Engineering Division: the development of improved solar collectors, the development of a method for passive cooling based on seasonal storage of ice, and provision of technical assistance to the National Solar Demonstration Program. Other divisions that have solar programs at ANL include Energy and Environmental Systems, Materials Science, Components Technology, and Engineering Divisions.

A. Development of Improved Solar Collectors

A serious impediment to widespread utilization of solar energy in the United States is the combination of relatively high cost and relatively low performance of available solar collectors. This problem is especially acute in solar cooling of buildings, total energy systems, and high-temperature industrial process heating. Through the development and commercialization of cost-effective solar collectors that operate efficiently in these demanding applications, the CEN collector effort directly addresses the needs of the national solar program.

The CEN solar collectors are based on a new class of nonimaging optical concentrator designs known generically as compound parabolic concentrators (CPCs). Depending on the specific design parameters, CPC trough collectors can function either in a fixed orientation or with a few tilt adjustments throughout the year, while operating efficiently at 100-250°C. A number of factors contribute to the excellent potential for early acceptable cost of CPC-collector-based systems. Because of the higher collector efficiency than that provided by flat plates, fewer collector modules are required for a given application. Reduction in collector mass through the use of optical concentration leads to a lower module cost. Higher operating temperatures result in more efficient performance of the remainder of the system. Finally, the rapid increase in the size of the potential market with increasing operating temperature, induces cost reductions through mass production.

The long-term goal of the solar collector program at Argonne is the establishment of CPC-collector designs as commercially viable options for advanced applications such as space heating and cooling and industrial process heat, in which delivery temperatures up to 250°C are required. Having devised detailed optical and thermal design tools, we are now building on present day-technology and, in close cooperation with industry, developing new technology to provide the required materials, components, and fabrication techniques. By the conclusion of this program, a potential collector vendor will be able to choose a CPC-collector design that best meets his need and, from the established requirements, develop a marketable product. To date, the program has met 80% of the objectives necessary to reach its long-range goal.

The near-term goal of the CPC-collector program has been to successfully commercialize a particular low-concentration collector design suitable for space heating and cooling applications. Engineering prototypes of this design, built at ANL with commercial components and technology have operated efficiently at 180°C. The near-term goal was met this year when two commercial firms introduced their versions of low-concentration collectors.

1. Collectors for Heating and Cooling Applications

A 1.5x CPC cusp collector* developed at ANL provides significant advantages in heating and cooling applications. It operates efficiently at 180°C and yet needs no tilt adjustment, since in stationary operation the useful collection period is at least seven hours per day throughout the year. Freedom from tracking or adjustment greatly simplifies the collector and its mounting structure, and thus lowers capital and maintenance costs. The large angular field of view (70°) of this collector accepts two-thirds of the diffuse sky radiation, in addition to the direct beam solar radiation. The design is particularly attractive, therefore, in non-desert installations (east, south and midwest) where focusing collectors are at a disadvantage because the beam radiation is scattered by haze and cloudiness; similarly, light scattering by dirt on the cover glass is less detrimental to performance of nonimaging collectors. Finally, the collector incorporates existing commercial components and technology, so that there are no hidden development problems, and early cost reductions can be expected. In 1977 the 1.5x CPC cusp collector was selected by Industrial Research Magazine as one of the year's 100 most significant new develoments.

Two licensees of the DOE patent, Sunmaster Corp. (Corning, NY) and Energy Design Corp. (Memphis, TN) are now marketing their versions of the low-concentration CPC cusp collector, optimized for different services. Half a dozen other firms have also become licensees, and others have shown interest.

2. Collectors for Industrial Process Heat

The development of higher temperature collectors (3x to 5x), which are suitable for industrial process heat, is in a less advanced stage than that of the collectors for heating and cooling. For example, suitable components--stable selective surfaces on absorbers, stable heat transfer fluids, higher reflectance surface--are not available commercially and the existing technology is not adequate. A number of laboratory-scale collectors and several full-scale prototypes have been fabricated at ANL using experimental components developed by industry under subcontracts. At the same time, the potential benefits offered by these collectors have been explored in detailed calculations and studies performed by ANL and by A. D. Little, Inc. These studies and the experimental work indicate that the CPC-collector designs are workable and are attractive for use at higher operating temperatures.

---

*The ratio of light intercepted by the combination of collector and cylindrical absorber in a 1.5x CPC is actually 1.5π times that directly intercepted by the absorber; the 1.5x factor refers to the important ratio of total interception area to heat-radiating area of the absorber.

3. Status and Future Direction

The near-term goal of the collector development program was met this year with the introduction of two commercial versions of the low-concentration CPC cusp collector. A final report on the subject will be issued upon completion of some remaining experimental work. Argonne's main effort in FY 1979 on low concentration collectors will consist of providing technical assistance to manufacturers.

To meet the long-range goal, we must continue to identify materials and develop components and fabrication techniques that can be used in mass production and that meet cost and performance criteria. The effort will proceed along the lines already proven to be successful in reaching the near-term goal: building and testing new collectors at Argonne and stimulating intensive industrial interaction through consultation, industrial participation, and contracts. As part of ANL's collector development activity, a unique testing capability has been developed. ANL personnel have the expertise required to test concentrating collectors, and a fully instrumented facility has been built to test collectors operating at temperatures up to 260°C. Figure VII-1 shows several experimental collectors being tested in this facility. Future plans include the use of this facility to evaluate new collector designs and commercial versions of nonimaging concentrators as they are developed.

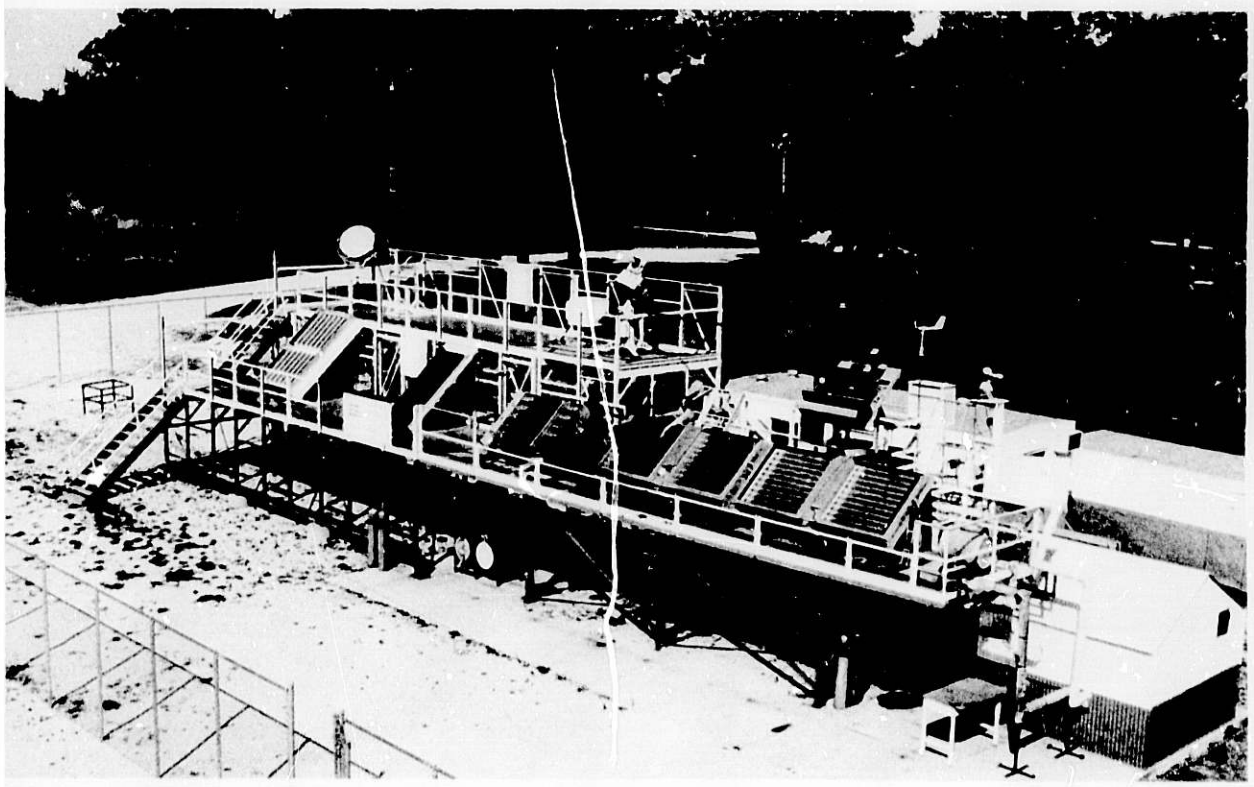

Fig. VII-1. Solar Energy Test Facility. On the right is a 3x collector for process heat application that operates at 200°C; at the center, still covered, is an experimental 3x collector with low-cost plastic mirrors; to its left is a 1.5x collector that operates at 150°C without periodic tilt adjustment.

B. Thermal Energy Storage for Cooling Applications

The objective of this new CEN program is to develop a cost-effective method of passive cooling that uses underground ice formation during the winter for summer cooling needs. This work is an expansion of the CEN effort in applying solar energy to the heating and cooling of buildings. The near-term goal is to determine the feasibility of this passive cooling method by means of comprehensive theoretical analyses and experimental measurements. The long-term goal is to develop the method from the research prototype stage to the stage of industrial commercialization and large-scale utilization by the public sector.

The basic components of the ice-storage cooling method are shown in Fig. VII-2. A large, well-insulated* tank of water is buried underground near the building to be cooled. Freezing units at the tank bottom form and release sheets of ice that float upward. The refrigeration results from vaporization of ammonia in the units, rise of the vapor to above-surface condensers, and gravity return of condensate to the freezing units.

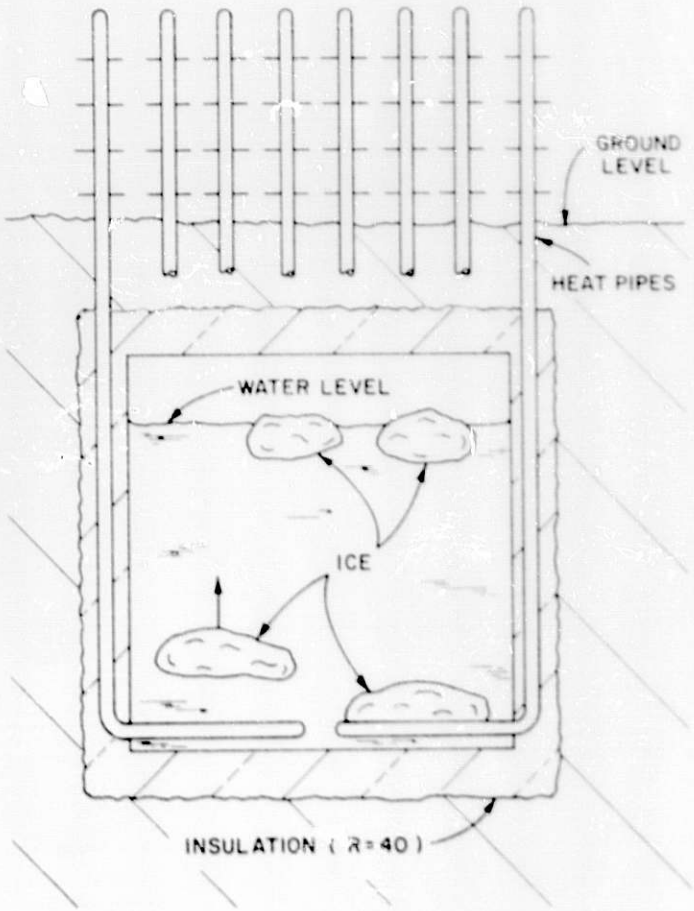

Fig. VII-2. Basic Components of Ice-Storage Cooling Equipment

*Initial results show that an insulation equivalent to R = 40 ($ft^2 \cdot h \cdot °F$)/Btu will be sufficient for seasonal storage.

Operation ceases when air temperatures rise above freezing; consequently, the system is totally passive--no external power is needed. The system will be designed so that the ice formed will fill the storage container during winter operation. It is estimated that a tank with a height and diameter of 10-15 ft could provide sufficient cooling capacity for a well-insulated single family home.

We have begun an extensive survey of literature and recorded data on heat-pipe design, fabrication, and use. Interaction has started with commercial manufacturers of heat pipes. Experimental equipment is now being assembled to test actual evaporator sections for ice formation and automatic release. The future direction of work in this program will be to determine the feasibility of this passive cooling method on the basis of theoretical analysis and experimental data.

C. Support Activities for the National Solar Energy Demonstration Program

As a result of the congressionally mandated solar energy demonstration program, numerous commercial and residential solar energy systems have been constructed throughout the country. ANL has been involved in several aspects of this program, including evaluating proposed solar demonstration systems, performing design reviews during the construction phases, and providing assistance in determining the best methods for solving problems that arise in current systems. This activity directly supports the long-range national goal of developing solar energy as an alternative energy source.

VIII. FAST REACTOR CHEMISTRY RESEARCH

A. Reactor Safety

1. Post-Accident Heat Removal

Work on post-accident heat removal involves heat-transfer modeling and chemical-equilibrium calculations as well as experimental studies of interactions of reactor materials with concrete, steel, and graphite. One phase of this work, which has been of particular interest, is described below.

The current design for gas-cooled fast reactors (GCFRs) employs a lower reactor axial shield consisting of layers of graphite and stainless steel. In a hypothetical core-disruptive accident, core debris consisting of oxide fuel and stainless steel would rest on the shield and interact with the top layer, which is constructed of graphite. Calculations[1] of the heat dissipation for this hypothetical reactor accident attributed removal of 74% of the downward decay heat to chemical reaction between core debris and the graphite in the shield. This analysis, which was based on the endothermic reaction between UO_2 and graphite, did not take into account the effect of steel and the attendant formation of $FeUC_2$ as a reaction product.

Our experiments, designed to study the effect of various amounts of steel on this reaction at a given temperature, suggested that the UO_2-stainless steel-graphite reaction is exothermic. As discussed in last year's report, we found that for small amounts of stainless steel (10% of the weight of UO_2 and steel) the reaction rate was unexpectedly high, the erosion of the graphite was pronounced, and the reaction was unusually violent, as indicated by the ejection of portions of the UO_2 pellet from the reaction site. These results could be attributed to an exothermic reaction with too small an amount of stainless steel to carry the heat of reaction from the reaction site.

To test this hypothesis, an experiment was performed in a graphite crucible with two flat-bottomed cavities. One cavity, which served as a reference, contained only stainless steel, and the other contained a UO_2 pellet plus 10 wt % stainless steel. The temperature of the crucible was maintained at 2400 K for 50 min. During this time, the reaction rate was measured by continuous monitoring of the evolution of CO. The temperature of each cavity was monitored by thermocouples. The temperature in the vicinity of the reaction site showed an increase of 12 K over the temperature at the reference site, with the rate of increase generally corresponding to the rate of evolution of CO (see Fig. VIII-1). Upon completion of the reaction, the temperature of the reaction crucible gradually returned to the reference temperature.

---

[1] C. S. Kang, A. Torri, and L. Yang, The Effect of Chemical Reactions on Post-Accident Fuel Containment in GCFRs, GA-A14680, General Atomic Company (December 1977).

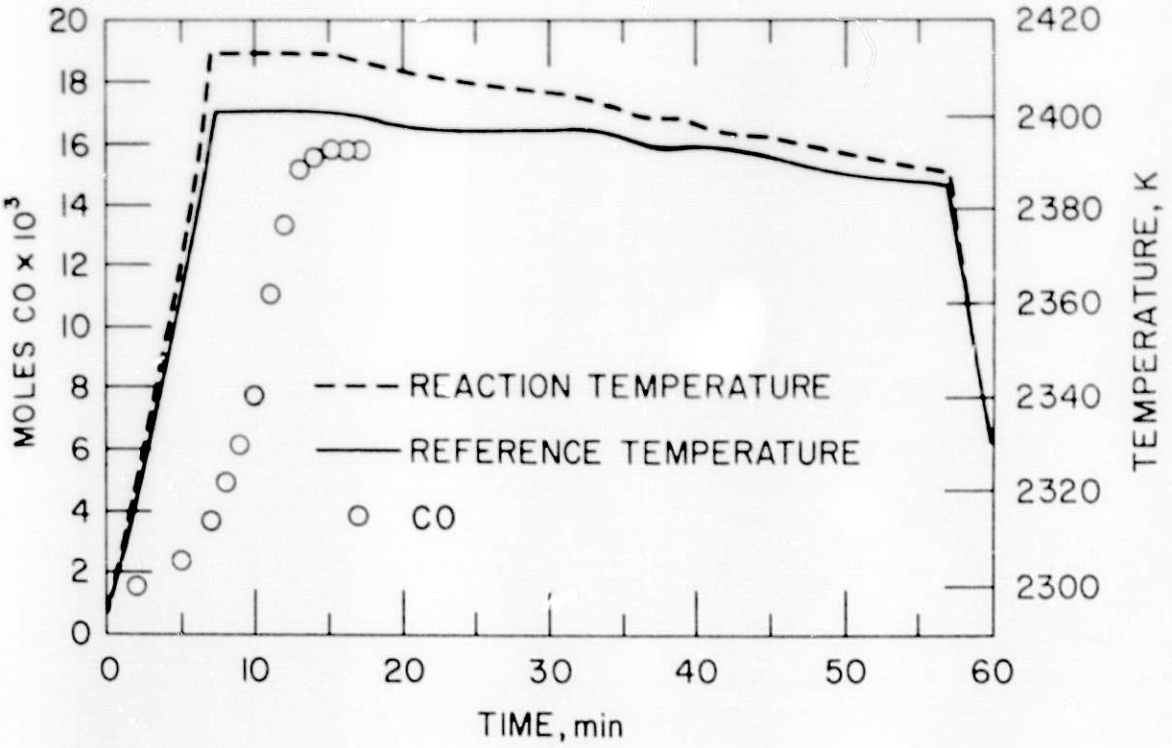

Fig. VIII-1. Temperature and CO Evolution as a Function of Time for UO_2-Stainless Steel-Graphite Interaction. ANL Neg. No. 308-78-129

The unexpected finding that the UO_2-graphite-stainless steel interaction is exothermic has had a significant impact on the calculations of post-accident heat removal and the design of fuel-debris containments. If graphite is used in the containment shield, the heat of reaction of the UO_2-graphite-stainless steel interaction must be dissipated in addition to the decay heat. Because thermodynamic data on this reaction are lacking, we plan to have a pure sample of the reaction product $FeUC_2$ made so that the heat of reaction can be measured by calorimetric methods. Additional studies of this reaction using other metals are also planned.

2. High-Temperature Physical Property Studies

a. Sodium

The reliability of reactor safety analysis is strongly influenced by the thermodynamic and transport property data that are fed into the calculation. Thus, it is essential that consistent and reliable values be used.

Recent experiments of Bhise and Bonilla[2,3] in which the vapor pressure of sodium was determined from 1200 K to the critical point, yielded new values for the critical pressure, critical temperature, and critical density. These new data prompted a reexamination of existing sodium-property data by Padilla.[4] As an extension of the work of Padilla,[4] Das Gupta and Bonilla[5] derived a single equation to fit the existing vapor pressure data,[2,3,6,7] and we derived a single equation for liquid enthalpy to fit the experimental data of Fredrickson and Chasanov[8] (554-1505 K) and those of Ginnings et al.[9] (373-1170 K). Using the new critical parameters, the work of Padilla, and our enthalpy equation for the experimental data as a starting point, we employed thermodynamic relations and extrapolation and estimation techniques to calculate an internally consistent set of thermodynamic property values for saturated, subcooled, and superheated sodium. In addition, values of transport properties of saturated sodium were obtained from fits to experimental data and from extrapolation procedures. An error analysis of the accuracy of the recommended values has been made. Table VIII-1 summarizes our recommended values for saturated sodium at selected temperatures.

These values of thermodynamic and transport properties of sodium, along with detailed discussions of how they were obtained and of their errors, have been compiled to form a revision, now nearing completion, of the sodium section of the handbook, Properties for LMFBR Safety Analysis,[10] which is widely used as input in reactor safety calculations and computer codes. Following completion of this work on sodium data, attention will be directed to revising the oxide fuel section of the handbook.

---

[2] V. S. Bhise, The Critical Point and High-Temperature Thermodynamic Properties of Sodium, Dr. Eng. Sci. Dissertation with C. F. Bonilla, Dept. of Chemical Engineering and Applied Chemistry, Columbia University, Xerox-University Microfilms (1976); also COO-3027-22, NTIS (1977).

[3] V. S. Bhise and C. F. Bonilla, The Experimental Vapor Pressures and Critical Point of Sodium, Proc. Int. Conf. Liquid Metal Technology in Energy Production, Seven Springs, PA, May 3-6, 1977; also COO-3027-21, NTIS (1976).

[4] A. Padilla, Jr., High-Temperature Thermodynamic Properties of Sodium, Hanford Engineering Development Laboratory Report HEDL-TME 77-27 (February 1978).

[5] S. Das Gupta and C. F. Bonilla, private communication (1978).

[6] J. P. Stone, C. T. Ewing, and J. R. Spann, High-Temperature Properties of Sodium, Naval Research Laboratory Report NRL-6241 (September 24, 1965).

[7] R. W. Ditchburn and J. C. Gilmour, Rev. Mod. Phys. 13, 310 (1941).

[8] D. R. Fredrickson and M. G. Chasanov, The Enthalpy of Liquid Sodium to 1505 K by Drop Calorimetry, J. Chem. Thermodyn. 6, 629-633 (1974).

[9] D. C. Ginnings, T. B. Douglas, and A. F. Ball, Heat Capacity of Sodium Between 0 and 900°C, the Triple Point and Heat of Fusion, J. Res. Natl. Bur. Stand. 45, 23-33 (1960).

[10] Properties for LMFBR Safety Analysis, L. Leibowitz, Ed., Argonne National Laboratory Report, ANL-CEN-RSD-76-1 (April 1976).

Table VIII-1. Summary of Thermophysical Properties of Saturated Sodium

Property	Property Values at Indicated Temperature (K)					
	370.98[a]	800	1156.5[b]	1600	2000	2400
Enthalpy, $H_\ell(T) - H_s(298)$, kJ mol^{-1}	4.747	17.67	28.02	41.59	55.69	75.83
Heat Capacity, J mol^{-1} K^{-1}	31.94	29.06	29.29	32.32	39.14	84.75
Vapor Pressure, MPa	1.128×10^{-11}	9.043×10^{-4}	0.1014	1.798	7.851	20.76
Heat of Vaporization, kJ mol^{-1}	103.6	96.77	89.11	78.54	65.15	41.11
Density, kg m^{-3}	927.3	825.6	739.4	632.5	536.4	403.2
Volumetric Thermal Expansion Coefficient, 10^{-4} K^{-1}	2.507	2.912	3.282	3.836	5.037	17.77
Adiabatic Compressibility, 10^{-4} MPa^{-1}	1.714	2.270	3.001	4.709	8.802	42.81
Thermal Conductivity, W m^{-1} K^{-1}		66.8		35.8	22.2	9.5
Thermal Diffusivity, 10^{-5} m^2 s^{-1}		6.40		4.02	2.44	0.609
Viscosity, 10^{-3} Pa·s		0.229		0.130	0.112	0.0992

[a] Melting point of sodium.

[b] Boiling point of sodium.

b. Reactor Fuels

Studies of thermophysical properties of reactor materials have centered largely on properties of oxide fuel, with some attention devoted to carbides and other reactor materials. Measurements of enthalpy, thermal diffusivity, density, and vapor pressure are of interest, and data to about 6000 K are needed in reactor safety analysis. Recent developments in one phase of this work are described in detail below.

Thermodynamic functions of fuel-vapor species may be calculated from spectroscopic data on molecular energy levels. The thermodynamic functions obtained by this method are believed to be more reliable for vapor-pressure calculations at high temperatures than functions obtained by extrapolation of lower temperature data or by experimental methods that have not been calibrated. Thus, these calculated functions are useful for analysis of hypothetical reactor accidents.

Our program combines an experimental part and a calculational part. The goal of the experimental studies is to obtain spectroscopic data on uranium, plutonium, and thorium oxides, nitrides and carbides that are required for the calculations. The goals of the calculational studies are: (1) to estimate data that are not experimentally available; (2) to present results in a form that allows for incorporation of new data; (3) to estimate uncertainties in various contributions to calculated thermodynamic functions; and (4) to provide a consistent "best estimate" of the thermodynamic functions for fuel-vapor species.

Some experimental data are available for known uranium, plutonium, and thorium oxide vapor species; however, these data are incomplete. When experimental data are not available, estimates and modeling are required for the calculation of thermodynamic functions and vapor pressures. Figure VIII-2 shows a scheme for the calculation of vapor pressures that combines experimental data with estimated data to obtain the required set of molecular energy levels. The steps leading to gas-phase thermodynamic functions must be followed for each important vapor species. The condensed-phase data must be known as a function of composition, and both the condensed-phase and gas-phase data must be known as functions of temperature.

Experimental spectroscopic data are being obtained by the matrix-isolation technique. Previously, this technique was used to obtain data on uranium oxides,[11,12] uranium nitrides,[13] and thorium oxides.[14]

---

[11] S. D. Gabelnick, G. T. Reedy, and M. G. Chasanov, J. Chem. Phys. 58, 4468 (1973).

[12] S. D. Gabelnick, G. T. Reedy, and M. G. Chasanov, J. Chem. Phys. 59, 6397 (1973).

[13] D. W. Green and G. T. Reedy, J. Chem. Phys. 65, 2921 (1976).

[14] S. D. Gabelnick, G. T. Reedy, and M. Chasanov, J. Chem. Phys. 60, 1167 (1974).

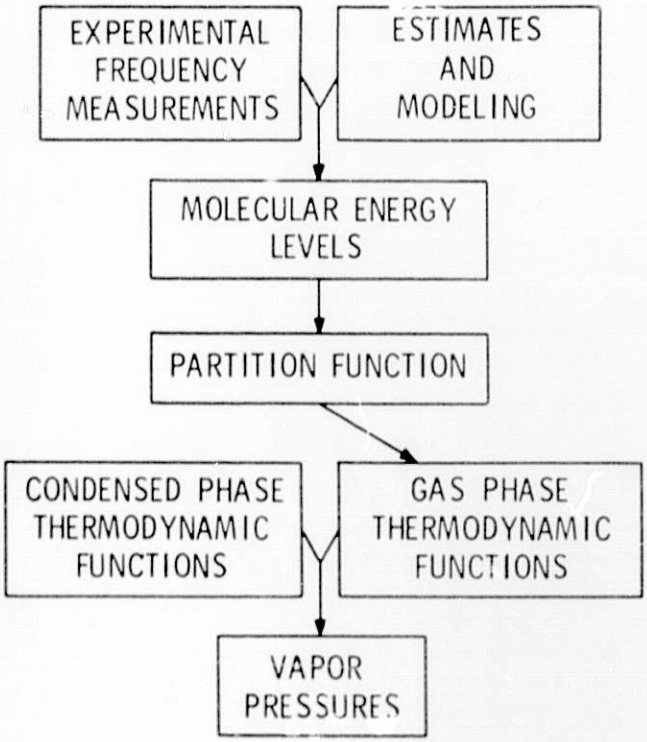

Fig. VIII-2. Scheme for Calculation of Vapor Pressures from Spectroscopic Data. ANL Neg. No. 308-78-269

More recent results for plutonium oxides[15] and nitrides[16] have been published this year. Results have also been obtained for thorium nitride and will be published.[17] The vibrational frequency of ThN was measured and identified by the use of ^{15}N. The harmonic frequency, ω_e, and first anharmonic correction, $\omega_e x_e$, were derived from the measurements. These data are needed for calculation of thermodynamic functions. No dinitride of thorium was observed, in contrast to the cases of uranium and plutonium; however, a dinitrogen complex of thorium was identified.

Preparations have been made for two projects: (1) study of the low-frequency bending modes of ThO_2 (as well as UO_2 and UO_3); and (2) production of thorium carbides and measurement of their vibrational frequencies. A helium-transfer cryostat has been tested. The new cryostat has reduced mechanical vibrations and, as a result, has significantly increased the far-infrared signal-to-noise ratio over that obtained with the closed-cycle helium cryostat previously used. A helium-cooled bolometer is in the final stages of testing. These improvements in the apparatus should enhance our ability to detect weak absorptions by the low-frequency bending modes. Several scoping experiments have been performed to seek a method of

[15] D. W. Green and G. T. Reedy, J. Chem. Phys. 69, 544 (1978).

[16] D. W. Green and G. T. Reedy, J. Chem. Phys. 69, 552 (1978).

[17] D. W. Green and G. T. Reedy, J. Mol. Spectrosc. (to be published).

producing carbides. A thorium cathode was sputtered with mixtures of Ar with CO, CO_2 or C_2H_2 and the reaction products were collected in Ar at 14 K. No thorium carbide species were identified in these preliminary experiments; further experiments are in progress and other means of producing cardides are being sought.

The calculational program has been directed toward fuel-vapor species. Among the special characteristics of these molecules are relatively high dissociation energies and relatively large electronic contributions to the thermodynamic functions. Topics that have been studied include: (1) effects of vibrational anharmonicity, (2) estimates of bond distances, (3) effects of molecular geometry, (4) effects of vibration-rotation interaction, (5) effects of centrifugal stretching, (6) effects of excited-state geometry, (7) estimates of the frequencies of unobserved vibrational modes, (8) effects of various approximations to the partition function including the separation of an electronic portion, and (9) models of the electronic structure. Numerical results have been obtained to determine the possible errors in the calculated thermodynamic functions that result from estimates, models, and approximate methods.

Insufficient empirical data are available to determine the electronic contribution to the partition function and its derivatives for each of the uranium, plutonium, and thorium oxide vapor species. There are no practical methods for obtaining energies of the required electronic states from ab initio calculations. The most promising method appears to be a semi-empirical one in which experimental vapor pressure data are employed to derive the values of model parameters.

We have tried several models of electronic structure to fit the partition function of UO_2. Three models that have proved useful are as follows:

I. A constant-density-of-states model with two variable parameters. The degeneracy, g_i, is constant and the energy-level spacing, x (in cm^{-1}), is constant.

II. An increasing-density-of-states model with three parameters and two variables. The energy levels are identical with Model I, but the degeneracy increases with energy, $g_i = g_o/(1 - \varepsilon_i/A)$, where g_o is a constant and A is the empirical ionization potential.

III. An increasing-density-of-states model with three parameters and two variables. The degeneracy is constant but the energy levels converge: $\varepsilon_i = c_0 - c_1 i^2$ where $c_1 = c_0^2/4A$ and A is the ionization potential.

Values of the variables were determined for each of the models to fit the empirical vapor pressure data for UO_2. At 6000 K, the vapor pressures that are calculated from the corresponding free-energy functions differ by less than 12%. Model I gives a limit to C_p at high temperatures and, thus, is not as realistic as either II or III. We conclude that either Model II or III provides a suitable basis for these calculations. The success of this semiempirical approach for UO_2 has led to its application to other vapor species of interest, including other uranium oxides and plutonium

oxides. The method developed for these molecules should provide a useful way to obtain the electronic contribution to these calculated thermodynamic functions and, by the scheme in Fig. VIII-2, to obtain the pressures of the fuel vapor species at high temperatures.

"Best estimates" of the thermodynamic functions of UO_2 are complete. The contributions to the thermodynamic functions of other fuel-vapor species have been calculated except for the electronic part. Preliminary vapor pressure calculations indicate that the methods employed lead to lower pressures than have been obtained by other methods. A complete comparison will be possible after conclusion of the calculations for molecules other than UO_2.

B. Reactor Fuels Chemistry

The gas-cooled fast reactor (GCFR) program is an incremental program that relies heavily upon LMFBR base technology. However, some features, namely, the use of vented fuel pins, roughened cladding, helium coolant, and direct contact of the primary coolant with the steam generator, are unique to the GCFR and these are being studied to assess their impact on fuel chemistry. The complex chemistry occurring under the large temperature gradients that exist within the uranium-plutonium oxide fuel pins must be understood if problems associated with these features are to be circumvented. To this end, we have continued our investigation of the behavior of fission-product cesium and, during the past year, undertook a study of the reaction of cesium with stainless steel cladding, particularly in relation to possible cladding-attack problems related to vented GCFR fuel pins. However, because of the lack of understanding of the mechanism of cladding attack in LMFBR fuels, our work lead to the development of a model that addresses the more fundamental aspects of fuel-cladding interaction in fast-reactor fuels. This model should contribute significantly to the understanding of cladding attack in both LMFBR and GCFR fuels.

It is generally recognized that the lifetime of fast-reactor uranium-plutonium oxide fuel may be limited by reaction of the stainless steel cladding with fuel containing fission products. Fission products appear to play important roles in fuel-cladding interactions.[18] Cesium is universally observed in the regions of attack and is usually associated with chromium from the cladding. However, the parameters affecting cladding attack have never been adequately defined.

A number of researchers have attempted to correlate the depth of attack with the temperature of the cladding inner surface. There is general agreement that the temperature threshold for attack is a cladding inner surface temperature of 770 K; however, from 770 to 1000 K, widely varying temperature dependencies have been reported. The general trend is that the depth of penetration (a) increases exponentially with increasing temperature in EBR-II pins;[19] (b) increases with increasing temperature from 770 to 870 K and then

---

[18] D. C. Fee, I. Johnson, and C. E. Johnson, ANL-75-53 (1975).

[19] J. W. Weber, R. L. Gibby, E. T. Weber, and R. E. Woodley, Fuel and Cladding Interaction, International Working Group on Fast Reactors, Tokyo, February 21-25, 1977, IWGFR-16 (1977); p. 137 [CONF-770215].

is constant from 870 to 970 K in Rapsodie and DFR pins;[20] and (c) increases with increasing temperature from 770 K to 870 K and then decreases from 870 to 920 K in Phenix pins.[21] None of the existing models of cladding attack predicts the peaking of cladding penetration at 870 K observed in Phenix pins. Thus, it appears that the key parameter(s) affecting cladding attack have not yet been identified.

We have developed a model for cladding attack that is based on the formation of a cesium-fuel compound at the cooler, outer edge of the fuel and the formation of a cesium chromate on the cladding inner surface. These compounds are assumed to be in equilibrium via the gas-phase transport of cesium across the fuel-cladding gap. Using thermochemical data for the species involved, the model successfully predicts the observed temperature dependence of cladding attack in Phenix pins. Furthermore, the model demonstrates that the most important parameter governing cladding attack is the local temperature difference between the fuel outer surface and the cladding inner surface. The importance of this parameter to cladding attack has not been previously demonstrated.

In the model, the cesium pressure in equilibrium with a cesium-fuel compound [$Cs_2(U,Pu)O_4$] is compared with the cesium pressure in equilibrium with a cesium chromate (Cs_3CrO_4) on the cladding inner surface. The cesium-fuel compound was assumed to be [$Cs_2(U,Pu)O_4$] by analogy to the Cs-U-O system where Cs_2UO_4 is the compound that forms over the range of oxygen potentials ($\Delta\bar{G}_{O_2} = RT \ln P_{O_2}$) and temperatures expected at the outer surface of the fuel.[22] Furthermore, the hexavalent cesium-fuel compound, $C_2(U,Pu)O_4$, was selected because analysis of the family of alkali metal actinides showed that stability is strongly correlated with the size of the alkali metal ion and that the valence of the actinide atom is much less important. For example, KUO_3 and $RbUO_3$ are stable, but $CsUO_3$ is not. Consequently, a pentavalent cesium-fuel compound, such as $Cs(U,Pu)O_3$, is not expected to be stable.

The equilibrium cesium pressure above a two-phase region of $Cs_2(U,Pu)O_4$ and $(U,Pu)O_{2\pm x}$ can be calculated from the thermodynamic properties of the phases that are present. The thermodynamic relationship associated with the equilibrium

$$2Cs(g) + (U,Pu)O_2(c) + O_2(g) \rightleftharpoons Cs_2(U,Pu)O_4(c) \qquad (1)$$

is given by

$$2\Delta G_f(Cs,g) + 2\,RT \ln p_{Cs} + RT \ln p_{O_2} + \left\{\Delta G_f[(U,Pu)O_2,c] - \Delta G_f[Cs_2(U,Pu)O_4,c]\right\} = 0 \qquad (2)$$

The dependency of the equilibrium cesium partial pressure over $Cs_2(U,Pu)O_4 + (U,Pu)O_{2\pm x}$ on temperature and oxygen potential is shown in Fig. VIII-3.

---

[20] O. Gotzmann and Ph. Dunner, ibid., p. 43.

[21] M. Conte and J. P. Marcon, ibid., p. 27.

[22] D. C. Fee and C. E. Johnson, J. Nucl. Mater. (in press).

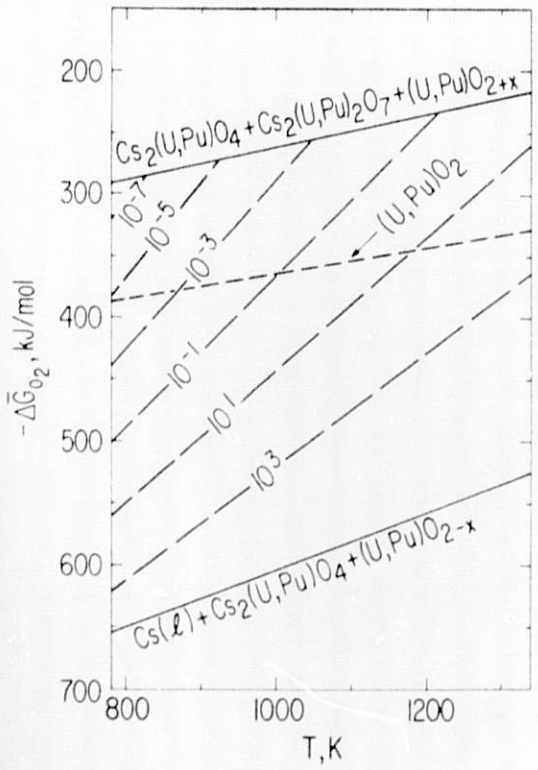

Fig. VIII-3.

Oxygen Potentials in the Cs-U-Pu-O and $(U_{0.8}Pu_{0.2})O_{2.000}$ Systems. Dashed lines are cesium pressures in Pa. ANL Neg. No. 308-77-665

Also shown in the figure are the boundaries of the $Cs_2(U,Pu)O_4$ + $(U,Pu)O_{2\pm x}$ two-phase region. The data in Fig. VIII-3 were calculated with the assumption that the addition of a small amount of plutonium to UO_2 and to Cs_2UO_4 equally affects the free energy of formation of these compounds. As a result, although the thermodynamic properties of $Cs_2(U,Pu)O_4$ have not been measured, the cesium equilibrium pressure over $Cs_2(U,Pu)O_4$ + $(U,Pu)O_{2\pm x}$ can be derived from the thermodynamic data for Cs_2UO_4 and UO_2.

The temperature dependency of the oxygen potential of the three-phase regions of the Cs-Cr-O system is shown in Fig. VIII-4. Also shown in the figure is the dependency of the equilibrium cesium pressure on temperature and oxygen potential for the two-phase regions. The relationships shown in Fig. VIII-4 were calculated using the measured and estimated thermodynamic data of the phases expected to be present in the region of the fuel-cladding gap.

A comparison of the equilibrium cesium pressure of the Cs-U-Pu-O system in the fuel with that in the Cs-Cr-O system at the cladding inner surface defines the temperature conditions in the fuel pin that are required for cladding attack via cesium chromate formation. A preliminary comparison shows that, under isothermal conditions, no cesium chromates would be stable on the cladding inner surface because the equilibrium cesium pressure of the Cs-U-Pu-O system is less than the equilibrium cesium pressure of the Cs-Cr-O system. For example, at 900 K with an oxygen potential set by $(U_{0.8}Pu_{0.2})O_{2.000}$, the cesium pressure above the fuel is 3×10^{-3} Pa (Fig. VIII-3). The cesium pressure necessary to form Cs_3CrO_4 on the cladding inner surface under the same conditions is 3×10^{-1} Pa (Fig. VIII-4). Cesium chromate will be stable at this oxygen potential only when the temperature difference existing between the fuel outer surface and the cladding inner surface is such that the cesium

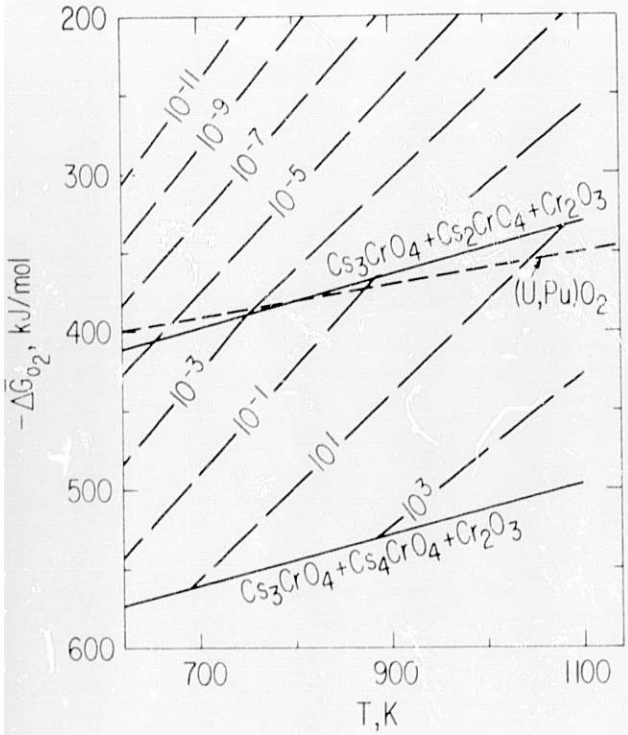

Fig. VIII-4.

Oxygen Potentials in the Cs-Cr-O and $(U_{0.8}Pu_{0.2})O_{2.000}$ Systems Dashed lines are cesium pressures in Pa. ANL Neg. No. 308-77-664

equilibrium pressures of the two regions are equal. For the example given above, this temperature difference is about 125 K.

Several conclusions can be drawn from the above discussion. First, the temperature difference between the fuel outer surface and the cladding inner surface is the most important parameter affecting the stability of cesium chromate on the cladding. Second, because of the shape of the neutron flux profile in the reactor, the maximum thermodynamic driving force for cesium chromate formation occurs at the axial midpoint of the fuel, where the cesium equilibrium pressure of the fuel exceeds the cesium equilibrium pressure of the cladding by the maximum amount. Consequently, the maximum depth of cladding attack is expected at the fuel axial midpoint, not in the region where the cladding inner-surface temperature is highest.

Our model correctly predicts the correlation of maximum depth of attack with cladding inner-surface temperature (axial location) as observed for Phenix fuel pins.[21] Also predicted by the model is the observation that cladding attack increases with increasing temperature from 770 to 870 K and then is constant from 870 to 970 K in Rapsodie and DFR pins.[20] The model predicts a greater extent of cladding penetration in Phenix pins than in Rapsodie and DFR pins because the temperature difference between the fuel outer surface and the cladding inner surface is expected to be larger in the Phenix pins. The fuel sections of the pin are longer in Phenix (85 cm) than in Rapsodie (32 cm), DFR (30 cm) or EBR-II (34 cm). Consequently, the fluence/burnup ratio in Phenix pins is higher at the fuel axial midpoint, and the increased swelling of the cladding produces a larger fuel-cladding gap and, thus, a larger fuel-cladding temperature difference.

Future research efforts will continue to focus attention on those chemical problems that might hinder the success of the pressure-equalization system

and application of vented fuel pins to GCFRs. Because significant quantities of H_2O and H_2 impurities will be present in the helium coolant stream, the impact of these gases on fuel chemistry will be examined.

C. Sodium Technology

1. Tritium Behavior in LMFBRs

A program to study the behavior of tritium in LMFBRs was initiated in 1977. This program involved the collaboration of two laboratories, ANL and Hanford Engineering Development Laboratory (HEDL), with ANL assigned the lead role. In the past year the program has been successfully completed. Below we briefly summarize the work, including some background information, some of our recent results, and the conclusions reached as a result of the study.

Tritium is produced in the LMFBR by mechanisms of ternary fission, activation of boron in the control rods, and activation of lithium and boron impurities in the sodium coolant. Since hydrogen isotopes diffuse readily through steels at elevated temperatures, the tritium enters the coolant stream and spreads throughout the coolant system. More than 99% of the tritium deposits in sodium cold traps, but a small quantity escapes into the environment. The objectives of this work were to determine the important parameters for controlling tritium release to the environment, predict tritium behavior in present and future LMFBRs, and recommend corrective measures, if necessary. These objectives have been met and the program has been terminated.

The complexity of the movement of tritium in the LMFBR system required development of a computer model to calculate tritium transfer rates and concentrations throughout the system. Because the time required for development of steady-state tritium concentrations in the LMFBR is long (of the order of 0.5 to 1 y), it was necessary to calculate the non-steady-state concentrations as well. Data required for these calculations--including cold-trap efficiencies, tritium permeation through stainless steel piping and heat-transfer surfaces, and tritium permeation through steam-generator tubing--were obtained over previous years in this program[23,24] and a related program at HEDL.[25] Using these data and the physical characteristics of EBR-II, FFTF, and CRBR, the tritium transfer rates and concentrations in these reactors were calculated for typical operating conditions. It was possible to make a direct comparison of the model predictions with the behavior of tritium in EBR-II because

---

[23] C. C. McPheeters and D. J. Raue, Control of Tritium in LMFBR Sodium by Cold Trapping, Proc. Int. Conf. on Liquid Metals Technology in Energy Production, Champion, PA, May 3-6, 1976, CONF-760503-P1, p. 298 (1977).

[24] T. A. Renner, D. J. Raue, and C. C. McPheeters, Tritium Permeation Through Steam Generator Materials, Trans. Am. Nucl. Soc. 26, 216 (June 1977).

[25] J. C. McGuire, Tritium Permeation Through Oxidized 304 and 316 Stainless Steels, Symp. on Tritium in Nuclear Systems, 107th AIME Annual Meeting, Denver, CO, February 26-March 2, 1978.

in-sodium tritium meters[26] had been installed on both the primary and secondary sodium systems. The agreement between the model and the measurements on EBR-II is excellent.[27] This agreement increased our confidence in the FFTF and CRBR predictions. The primary release path from the CRBR is expected to be through the steam generator, whereas in the FFTF, release is mainly through the sodium-to-air Dump Heat Exchanger. Other release paths such as leakage from the cover gas and permeation through the secondary system piping are less significant.

The major conclusions reached in this study are as follows: (1) the tritium releases from the FFTF and the CRBR, as currently designed, are expected to be within the limits set by the Code of Federal Regulations, Title 10, Part 20 (10 CFR 20); (2) during the useful life of the sodium cold traps, they retain more than 99% of the tritium released from the core; (3) oxide coatings on the piping and steam-generator surfaces are a major influence in restricting tritium releases; and (4) based on experience at EBR-II, the tritium behavior model adequately describes tritium movement in LMFBR systems.[27] The goals of this program have been achieved, and the work has been concluded.

2. Processing of Radioactive Sodium for Recovery or Disposal

Operation of LMFBRs results in production of radioactive sodium waste. This waste is generated by maintenance and refueling operations and, at the end of the plant life, the entire primary sodium inventory must be managed in a way that minimizes cost and environmental impact. Among the most promising options available for handling radioactive sodium waste are: (1) conversion to an inert compound and isolation in a permanent repository, (2) conversion and burial in a land-fill site, and (3) decontamination and reuse in a new LMFBR plant. Our work has been focused on developing the technology base for option 3 and on extending the technology base for accomplishing either option 1 or 2. Accordingly, we are exploring the potential of fractional distillation for the decontamination of large quantities of sodium for reuse. We are also investigating two methods for converting sodium to a form suitable for disposal, namely, reaction of sodium with NaOH and steam to form NaOH and reaction with oxygen in the presence of SiO_2 to form a Na_2O-SiO_2 glass.

a. Fractional Distillation

Based on the projected cost of disposal of large volumes of radioactive sodium waste, a preliminary cost analysis indicates that it is

---

[26] S. B. Skladzien, T. A. Renner, D. J. Raue, and C. C. McPheeters, Tritium Meters for Use in LMFBR Sodium Coolant, Argonne National Laboratory Report, ANL-78-30 (June 1978).

[27] T. A. Renner and C. C. McPheeters, Tritium and Hydrogen Transport in LMFBR Systems: EBR-II, CRBR, and FFTF, Argonne National Laboratory Report, ANL-78-64 (September 1978).

more economical to decontaminate the sodium for reuse and to dispose of the contaminated residue than to dispose of the entire quantity of sodium. Fractional distillation is being examined as a possible method for decontamination of large quantities of sodium for reuse. Of the large number of soluble impurities likely to be present in contaminated sodium, those having significant radioactivity levels are, primarily, Ba, Cs, I, Rb, Sb, Sr, and Te. Although the radioactivity levels of these contaminants may be high, the corresponding mass concentrations are so low that they may be assumed to form ideal solutions.

A computer program was developed on the basis of this assumption, and the distribution of fission products was calculated for fractional distillation columns having a variety of configurations and operating conditions. These calculations led to the design of an experimental distillation column of approximately 12 theoretical stages and a sodium feed rate of about 13 g/s (100 lb/h); the column is shown schematically in Fig. VIII-5. The packed section of the column is 0.2 m in diameter and 2.4 m high. The feed stream, which enters the column about one-third of the way up the packed section from the bottom, contains ^{137}Cs (as representative of the higher-vapor-pressure species) at an arbitrary concentration of 1×10^{-3} mole fraction and ^{90}Sr (as representative of the lower-vapor-pressure species) at the same concentration. The purified sodium is removed at a point about two-thirds of the way up the packed section, the low-vapor-pressure species are collected in the

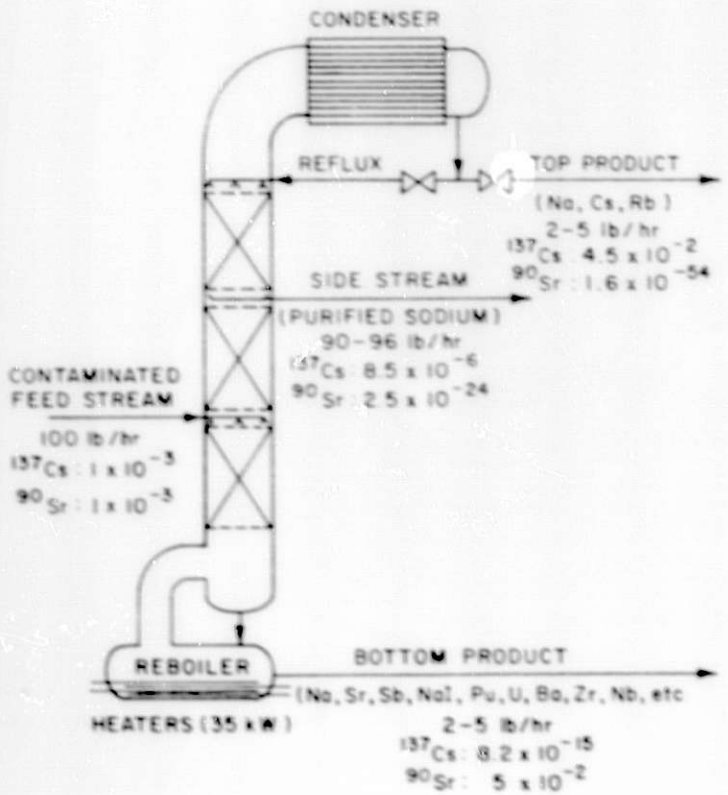

Fig. VIII-5. Fractional Distillation Column for Separation of Fission Products from Sodium (decontamination factors for ^{137}Cs and ^{90}Sr based on arbitrary feed concentrations of 10^{-3} mole fraction)

bottom product, and the high-vapor-pressure species (Cs and Rb) are collected in the top product. Calculations show that the pure sodium product should be decontaminated by a factor of about 120 for ^{137}Cs and about 10^{21} for ^{90}Sr.

A small version of this column (packed section, 0.1 m in diameter and 0.6 m high) is now in operation with total reflux and no feed or side streams; however, impurity distribution data are not yet available. Preliminary work is being done with nonradioactive impurities, and radioactive ^{137}Cs and ^{133}Ba will be used in later tests. A larger column similar to that shown in Fig. VIII-5 has been purchased and is being assembled for testing with radioactive fission products.

b. Formation of NaOH

Conversion of sodium to a form suitable for disposal by reaction with molten NaOH was tested in small-scale experiments. In this method, liquid sodium is introduced onto the surface of a NaOH melt at about 430°C. The sodium reacts according to the equation

$$2Na + NaOH \rightarrow Na_2O + NaH \qquad (3)$$

The Na_2O and NaH are soluble in the melt at concentrations up to about 20%. After the elemental sodium has been consumed, steam is injected into the melt to react with the Na_2O and NaH according to the equations

$$Na_2O + H_2O \rightarrow 2NaOH \qquad (4)$$

$$NaH + H_2O \rightarrow NaOH + H_2\uparrow \qquad (5)$$

Seven small-scale tests were conducted to determine the feasibility of adapting this method for large-scale sodium disposal. In these experiments, a 0.3-kg charge of NaOH was stirred by sparging with helium while 5- or 10-g quantities of sodium were added. After the sodium had been consumed, steam was injected into the helium stream at 1.7 mg/s. Prior to the steam injection, the sodium reaction rate was about 3 $g/m^2 \cdot s$ and hydrogen was slowly evolved (1.5 μg/s) as the NaH decomposed. When the steam was injected, hydrogen was evolved much more rapidly (about 43 μg/s) until the conversion was complete. The reactions are well behaved and neither too rapid nor too slow to prevent adaptation to a large-scale sodium disposal operation.

c. Calcination

Direct oxidation of sodium by calcining has been done on a commercial scale[28] in the production of sodium monoxide. Sodium monoxide is water soluble and thus less than desirable as a disposal product. Yet, calcining is a simple operation. We undertook an investigation to determine the feasibility of preserving the simplicity of the calcining operation while obtaining a product that could be converted to a form that was relatively insoluble in water and which could be used in glass production. For this reason, we evaluated the production, through calcining, of a silica-sodium

[28] Encyclopedia of Chemical Technology, 2nd Edition, Vol. 18, Interscience Publishers, John Wiley & Sons, New York (1969).

monoxide product. In this method silica is mixed with liquid sodium, and the coated silica particles are fed into the calciner. Oxygen is introduced into the calciner and the sodium reacts slowly to form Na_2O. The silica is simply a carrier medium and does not participate in the reaction. The silica-sodium monoxide product can be melted to form a glass that may be suitable for disposal.

Five small-scale sodium oxidation experiments were performed in a batch-type rotary drum reactor. The drum was loaded with the silica-sodium mixture, sealed, and purged with argon. The drum was heated to 110°C; then the heat was turned off, oxygen flow into the drum was started, and the drum was rotated at about 12 rpm. As the reaction proceeded, the drum temperature increased to between 200 and 250°C and then slowly declined as the reaction approached completion. Post-test analysis of the product indicated that as much as 93% of the sodium had been oxidized, leaving 7% as elemental sodium. Sodium peroxide was formed in amounts ranging from 5 to 20% of the original sodium charge. We believe that the sodium oxidation can be increased to 100% in a continuous process with a longer residence time.

d. Future Plans

The primary effort on sodium processing during 1979 will be devoted to the distillation work; experimental data will be obtained on both the small, total-reflux column and the larger, complex column. A lower level of effort will be invested in operating the calcining and NaOH reaction processes on a larger scale than was done in the tests described above.

3. Cold-Trap Development

The Chemical Engineering Division has a lead responsibility in developing methods for optimizing the capacity of cold traps for retaining sodium impurities. The primary impurities in the LMFBR coolant are hydrogen that diffuses through the steam generator from corrosion on the water side and oxygen from moisture and oxides introduced by refueling and maintenance operations. Recent data indicate that the hydrogen diffusion may introduce as much as five times the amount of hydrogen previously expected. Consequently, sodium cold traps that were originally planned to operate five years before becoming filled with sodium hydride are now expected to last only about one year. This reduction in lifetime imposes a significant increase in plant operating costs and creates a strong incentive to find methods or designs for increasing the cold-trap capacity. Because the mechanisms of impurity (hydride and oxide) deposition in cold traps are only dimly understood, the near-term goal of this work is to understand the deposition mechanisms and to develop a computer model to describe impurity deposition in a simple cold trap. Once this goal is achieved, the model will be expanded to include cold-trap designs that are more complex and more realistic. With this model in hand, design parameters can be adjusted to optimize the cold-trap configuration and thereby maximize capacity. The computer model for the simple cold trap has been developed and experiments are being conducted, initially with hydride impurity, in the Apparatus for Monitoring and Purifying Sodium (AMPS) with simple cold traps to test the accuracy of the model.

The computer model is based on the assumption that the rate of deposition of hydrogen (as sodium hydride), dm/dt, in the cold trap is a function of the local supersaturation, the surface area available for deposition, A, and the mass transfer coefficient, k:

$$dm/dt = kA(C - C_e)^n \quad (6)$$

where

C = the local hydrogen concentration in sodium

C_e = the hydrogen saturation concentration at the local temperature

n = the exponent describing the order of the reaction, assumed to be unity in this case

By the use of appropriate mass balance procedures, the model predicts the hydrogen concentration profile within the trap and the mass of sodium hydride deposited along the length of the trap.

A simple Analytical Cold Trap (ACT) was built for experimental testing of the model. The ACT consists of a 19-mm-OD, 0.56-m-long tube containing a 6-mm-OD thermocouple well in the center of the trap along its full length. The incoming sodium is cooled by blowing air through a duct surrounding the ACT. After passing through the length of the trap, the sodium is reheated by electrical power. The ACT is designed to contain a variety of packing materials, ranging from no packing to materials with packing densities considerably greater (about 400 kg/m^3) than that of typical LMFBR cold traps (about 300 kg/m^3).

At the end of each experiment, the sodium in the ACT is quickly frozen, the cold trap is removed and sectioned along its length, and the sections are analyzed for hydrogen content. The results of these analyses are compared with the computer model predictions for the same operating conditions. Although the hydrogen distribution predicted by the model is similar to the experimental distribution, fairly significant differences have occurred; occasionally, the test results show high or low hydrogen levels that are not predicted by the model. The reasons for these differences have not been identified but several possibilities exist: (1) occasional errors in the hydrogen analyses; (2) precipitation mechanisms other than the simple crystal growth implied by Eq. 6, i.e., homogeneous-nucleation growth and settling; and (3) the requirement of a threshold value of supersaturation to induce initial nucleation.

During FY 1979, attempts will be made to refine the cold-trap model to account for the observed hydrogen distributions. The experimental cold-trap work with hydrogen will be completed, and the behavior of oxygen in the cold trap will be determined. The final step in the program will be to modify the model to include the complex flow and temperature variations that occur in full-scale LMFBR cold traps. An underlying goal of this project is to continue a search for new methods or concepts that will result in larger-capacity cold traps for LMFBR systems.

IX. FUEL CYCLE STUDIES

A. Fuel Reprocessing

1. Pyrochemical and Dry Processing Methods

The overall objective of the program on pyrochemical and dry processing methods (PDPM)* is to develop a capability for reprocessing spent reactor fuels while reducing the risk of proliferation of nuclear weapons material. The fuels of interest are uranium-plutonium, uranium-thorium-plutonium, and thorium-uranium. Twelve individual work packages or investigations were established in FY 1978 to evaluate various reprocessing schemes, as well as materials problems associated with their use. This effort is supported by specific contracts or agreements with DOE laboratories and industrial concerns and by efforts in the Materials Science Division (MSD) and the Chemical Engineering Division (CEN) at ANL.

Initially, the work covered reprocessing of light water reactor and fast breeder reactor fuels; however, because of a reduction in funding for FY 1979, DOE is supporting reprocessing of fast breeder reactor fuels only. Accordingly, the PDPM program is being redirected; the effort on some work packages has been terminated, and effort on others has been reduced.

For FY 1979, CEN is managing the program. Experimentation and evaluation are continuing for two of the investigations carried out by CEN: carbide fuel reprocessing and thorium-uranium salt-transport processing. A new investigation, engineering support for PDPM processes, has also been assigned to CEN, beginning in FY 1979.

a. Carbide Fuel Reprocessing

In this work, potential reprocessing methods for carbide fuels are being studied. In principle, carbides can be burned to oxides and then reprocessed like oxide fuel, but a direct reduction of carbides into a metal solvent or an oxidation into a salt phase is more attractive for pyrochemical fuel recovery processes. Two alternatives are presently being considered. In the first, carbides are dissolved and partially separated from fission product elements and each other in liquid bismuth; this is an independent, new process for carbides. In the second process, carbides are oxidized into a salt phase, using zinc chloride or cadmium chloride; the salt phase is then contacted with a liquid metal such as cadmium-magnesium to partially separate the actinides from fission products and each other. This second alternative is a head-end step for salt-transport processes being studied in other segments of the PDPM program.

Reprocessing in Liquid Bismuth. The reaction or dissolution of some of the carbides in bismuth to form bismuthides is the basis for the separation of fission products from the actinides. Some unreacted fission product carbides and bismuthides are lighter than bismuth and, along with free carbon, float on the bismuth and are physically separated. Uranium carbide dissociates to only a limited degree (dependent upon the solubility of

*Previously called the nonaqueous reprocessing program (NARP).

uranium in bismuth). Plutonium is much more soluble in bismuth than is thorium. The solubility of the plutonium is reduced by lowering the temperature, whereupon $PuBi_2$ precipitates. The compounds $PuBi_2$ and $ThBi_2$ are denser than bismuth, are of limited solubility in bismuth, and are expected to settle in the bismuth along with unreacted uranium carbide.

Most of our effort thus far has been directed toward a literature search on the properties of the carbides; a report on the properties and processing of carbide fuels is being prepared. Experimental work will be started upon completion of laboratory renovations.

Molten Cadmium/Salt Reprocessing. The initial steps involve (a) conversion of the actinide and various fission-product carbides to chlorides by reaction with $CdCl_2$ dissolved in $MgCl_2$-NaCl-KCl eutectic (mp, 397°C) and (b) reduction of the salt phase with a cadmium-magnesium alloy, thereby partitioning the fissile, fertile, and fission-product elements between the salt and metal phases. Cadmium-based rather than zinc-based oxidizing and reducing agents were chosen to allow operation at temperatures below 650°C with readily available container materials such as mild steel and series 400 steels. In essence, this processing concept serves as a head-end step for introducing carbide fuels into various pyroprocesses (e.g., salt transport).

Laboratory experiments testing this concept will be carried out in an inert atmosphere because of the sensitivity of actinide monocarbides and anhydrous chlorides to moisture and oxygen. The initial experiments will investigate the rate of reaction of UC or ThC as a function of temperature and $CdCl_2$ concentration in the 50 mol % $MgCl_2$-30 mol % NaCl-20 mol % KCl eutectic.

b. Thorium-Uranium Salt-Transport Processing

The objective of this investigation is to examine concepts for the selective transfer of spent fuel constituents between molten alloys and/or molten salts and to develop process flow sheets for thorium-based oxide fuels and metal fuels. Initially, flow sheets will be constructed that are based on published data and thermodynamic evaluations. These flow sheets will be analyzed in detail. Potential problem areas and missing data are being identified, and laboratory-scale experiments are being done to generate data required to establish the feasibility of selected flow sheets.

Thorium Salt Transport. Pyrochemical processes involving salt-transport and metal-precipitation steps are currently being investigated for use in projected thorium-based fuel cycles. In a salt-transport process, elements dissolved in one alloy (the donor alloy) are oxidized upon being mixed with a salt, enter the salt, are transported in the salt to a second alloy (the acceptor alloy), are reduced, and dissolve in the acceptor alloy. The reference flow sheet has been designed to meet nonproliferation standards and is applicable to plutonium-thorium converter and thorium-uranium breeder fuels. The necessary criteria are that the fissile streams (1) be coprocessed so that the ratio of thorium to uranium-233 or plutonium is no smaller than 4 and (2) be made diversion-resistant by the inclusion of some fission products. A draft of a topical report describing the reduction, solubility, and hydriding aspects of this process has been completed.

As support for the process, experiments investigating both the solubility of thorium in cadmium-magnesium alloys and the reduction rate of high-fired thoria are in progress. Experiments to study the solubility of thorium as a function of temperature and alloy composition have been completed. The apparatus to carry out the reduction studies is being assembled, and the experiments should begin shortly.

Formation of Hydrides in Zinc-Magnesium Alloys. Plutonium and uranium can be separated from noble metal fission products by the salt-transport method. The recovery of both of these actinides from the zinc-magnesium acceptor alloy is accomplished by vaporization of the solvent alloy. Since large quantities of zinc and magnesium need to be distilled, the distillation equipment becomes large. An alternative method of actinide recovery based on precipitation and filtration of the hydrides has been proposed. Hydriding as a means of recovering thorium from liquid magnesium solutions has been investigated by Woerner and Chiotti[1] and by Chilton et al.[2] The former authors extended their work later to alloys of magnesium with zinc or aluminum[3] and found a higher solubility, and hence more difficult recovery, of thorium hydride in the zinc-magnesium solution than in pure magnesium.

We have made calculations to estimate plutonium hydride solubility in a range of zinc-magnesium compositions. The equilibrium concentration of plutonium in a liquid metal under one atmosphere of hydrogen and with a solid phase of PuH_2 is given by[3]

$$\ln X_{Pu} = \frac{1}{RT}\Delta G^{\circ}_{PuH_2} - \ln \gamma_{Pu}$$

where X_{Pu} is the mole fraction of Pu, $\Delta G^{\circ}_{PuH_2}$ is the free energy of formation of PuH_2 and γ_{Pu} is the activity coefficient of Pu in solution. From the free energy of formation of plutonium hydride[3] and the activity coefficients of plutonium found in the literature, the equilibrium concentration of plutonium in pure magnesium was calculated to be 0.027 at. % at 800°C (1073 K). Similar calculations were made for various alloy compositions at 800, 600, and 500°C. Typical plutonium concentrations in acceptor alloys are in the range of 1 to 5 at. %. In a practical process, a recovery of 75% or more of the plutonium would be desirable before recycle of the alloy. Calculations indicate that such recoveries would be possible only with alloys containing at least 75 at. % magnesium.

---

[1] P. F. Woerner and P. Chiotti, Precipitation of Thorium as Thorium Hydride from Thorium-Magnesium Solutions, ISC-928 (1957).

[2] J. D. Chilton, L. Hanson, E. W. Murbach, and F. W. Dodge, Separation of Uranium From Thorium by Liquid Metal Extraction, NAA-SR-6666 (1962).

[3] P. Chiotti and P. F. Woerner, J. Less-Common Met. 7, 111 (1964).

However, for an alloy that is suitable for the hydride step to also be adaptable to the salt-transport process, it must be a feasible acceptor alloy. Since typical acceptor alloys contain high percentages of zinc, the effectiveness of a suitable hydriding alloy as an acceptor alloy needs to be demonstrated. An example is a donor-acceptor system consisting of (1) a Mg-28 at. % Zn (Mg-50 wt % Zn) acceptor alloy (useful for hydride separations) at 600°C and (2) a Mg-79 at. % Cu (Mg-91 wt % Cu) donor alloy at 800°C. Calculations indicate that after ten cycles, >99% of the plutonium has been transferred to the acceptor alloy but only 57% of the uranium has been transferred. Thus, the number of steps required for separation of the uranium from fission products using this acceptor alloy is nearly the same as for more conventional high-zinc acceptor alloys.

c. Recycling of Salt from Calcium-Reduction Process

Several flow sheets under development for reprocessing of oxide fuels include a reduction step utilizing calcium metal, together with a solvent alloy of cadmium, zinc, or copper and a cover salt containing $CaCl_2$. The basic reduction reaction is:

$$MO_x(\text{alloy/salt}) + x\text{Ca(salt/alloy)} \rightarrow x\text{CaO(salt)} + \text{M(alloy)}$$

where

M = uranium, thorium, plutonium, fission products, etc.

With reuse of the salt, CaO builds up to the saturation point in the salt. It then becomes necessary to treat the salt or to discard it as a high-level waste. If the salt is discarded, the volume of waste is about 850 L for each metric ton of oxide fuel that is reduced.

A concept currently being examined for reducing the volume of waste salt is based on fused salt ($CaCl_2$·CaF_2) electrolysis of CaO. The cathode reaction generates calcium metal for recycle. The anode reaction yields oxygen, which reacts *in situ* with the carbon anode to yield CO/CO_2; the latter can be cleaned and released to the atmosphere as a gas. The feasibility of the concept is indicated by earlier work[4] in which gram quantities of calcium metal were produced by electrolysis at 786 to 816°C of fused $CaCl_2$ containing 0.3 to 2 wt % CaO. High current densities (up to 30 A/cm^2) and the absence of anodic chlorine are reported.

Our calculations show that with a current of 30,000 A, about 14 h (at 100% efficiency) would be required to generate the 300 kg of calcium required for the reduction of 1000 kg of uranium oxide. These attractive parameters and the potential for significantly reducing the quantity of wastes from pyrochemical processing stimulated further investigation of this technique. An electrochemical cell is being constructed to examine the fused-salt electrolysis of CaO. The initial cell design provides for collection of the calcium directly in a metal (such as cadmium) convenient for recycle.

---

[4] W. D. Threadgill, Preparation of Metallic Calcium by Electrolysis of Calcium Oxide Dissolved in Molten Calcium Chloride, J. Electrochem. Soc. 111, 1408 (1964).

d. Discussion

The processes in this program are in the early stages of development. It is anticipated that as development continues, one or two of the processes will be shown to be the most likely to achieve the program goal. Emphasis will then be focused on these processes for the large-scale development required to prove any process. In FY 1979, CEN will be involved in providing the engineering development necessary to achieve large-scale operation.

2. Aqueous Reprocessing by Advanced Solvent-Extraction Techniques

Work is continuing in the program to develop advanced solvent-extraction equipment and systems for use in aqueous reprocessing of spent reactor fuels. The equipment-development program is directed toward the design, construction, and testing of laboratory and plant-scale centrifugal contactors based upon an annular-mixing concept. Advanced solvent-extraction systems are being studied in the hope that the short residence times characteristic of centrifugal contactors will improve the decontamination from those fission products whose extraction rates are lower than those of uranium and plutonium. An additional objective of the program is to study the performance of various plutonium reducing agents on partitioning of plutonium and uranium in short residence contactors. Solvent damage and alternative solvent-cleaning techniques are also being investigated in relation to short-residence-time contactors.

The annular centrifugal contactor was first conceived and investigated at ANL in 1970; it is a modified version of the plant-scale contactor in use at the Savannah River Plant (SRP). In the SRP contactor, aqueous and organic process streams are fed into a mixing chamber beneath a vertically suspended rotor. A mixing paddle attached to an extension of the rotor shaft mixes the phases as the rotor spins, and pumps them upward into an orifice in the bottom of the rotor. Within the rotor, the organic and aqueous phases in the mixture are separated under centrifugal force, and the separated phases are then directed to appropriate discharge ports. Multistage countercurrent extraction is achieved by connecting the required number of contactors in series.

In the ANL modification, the separate mixing chamber and paddle are eliminated; instead, the phases are fed into the top of the annulus between the rotor and casing. Here, they are mixed by skin friction as they flow down the annulus and then inward to the rotor orifice. Potential advantages of the ANL design over the SRP design are simpler fabrication and ease of remote maintenance.

During the past year, hydraulic and chemical studies have been carried out in two eight-stage centrifugal contactors (minicontactors) equipped with 2-cm-dia rotors. One of these units is shown in Fig. IX-1. These units have a throughput capacity of about 100 mL/min (total volume of the two phases). Uranium extraction efficiencies were above 85% at high flow rates in a simulated Purex flow sheet.

Studies of the kinetics of uranium, ruthenium, and zirconium extraction in a single-stage minicontactor showed a modest improvement in separation of uranium from the fission products at mixing-zone residence times below 7 s, compared with the separation achieved in a conventional

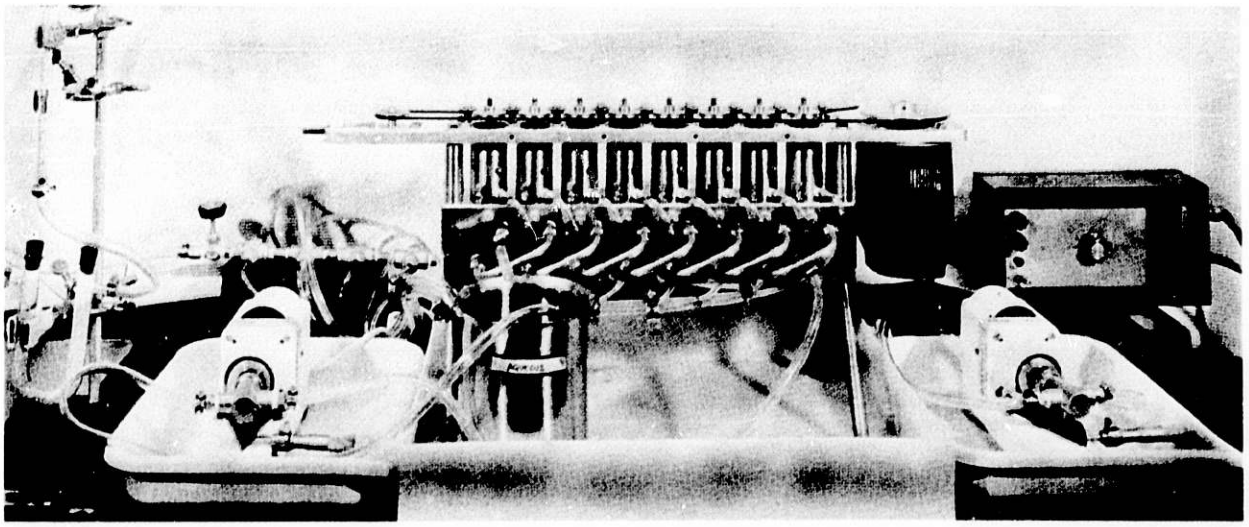

Fig. IX-1. Eight-Stage Miniature Contactor.
ANL Neg. No. 308-77-598

mixer-settler or stage of a pulse column at contact times of several minutes. However, in tests under Purex flow-sheet conditions in an eight-stage minicontactor, the improvement in decontamination was generally lost. Apparently, very short residence times are needed to effect a significant benefit since, in the multistage system, some fraction of the fission products that is not extracted in a single stage because of limited contact time is extracted during the additional contact in succeeding stages.

A modified Purex flow sheet was employed in an eight-stage minicontactor to demonstrate that enhanced decontamination from ruthenium could be achieved when a feed solution low in acid (suppressing the formation of extractable ruthenium) is "spiked" with concentrated nitric acid (needed for extraction of U and Pu) as it enters the contactor. The experiment was successful in showing that during the limited residence time in the contactor, there was no significant conversion of the poorly extractable ruthenium species into the more extractable species present in the usual high-acid feed solution. Adoption of the technique, however, must await additional study of low-acid fuel dissolution.

An eight-stage minicontactor was also used in a successful demonstration of a complex extraction process.* The process involves the use of a high-viscosity organic phase and feeding of up to four separate aqueous streams into the contactor.

In the program on solvent cleanup, various scrub solutions were tested in a single-stage minicontactor to measure their effectiveness in removing zirconium from tributylphosphate/n-dodecane solvent containing the

*An alcohol-extraction process, developed by the Chemistry Division, ANL, for separating the degradation products of tributylphosphate from actinides in high-level aqueous waste containing salt, so that the actinides can be subsequently recovered.

degradation product, dibutyl phosphoric acid. Results confirmed that either sodium carbonate or citric acid in the scrub solution is capable of removing almost 100% of the zirconium. However, alternatives are being sought because sodium carbonate in waste solutions leads to problems in waste disposal, and citric acid in recycled solvent tends to complex the plutonium. A scrub solution of nitrilotriacetic acid removed 70% of the zirconium.

In work funded by Oak Ridge National Laboratory (ORNL), a single-stage contactor (Fig. IX-2) having a 9-cm-dia rotor coupled to a commercial 1800-rpm motorized spindle was put into operation during the past year and its hydraulic and extraction performance characterized. Under simulated Purex conditions, the unit has a capacity of 9 L/min, which meets the requirements for processing LMFBR fuel at a rate of 0.5 Mg/d; operation is stable

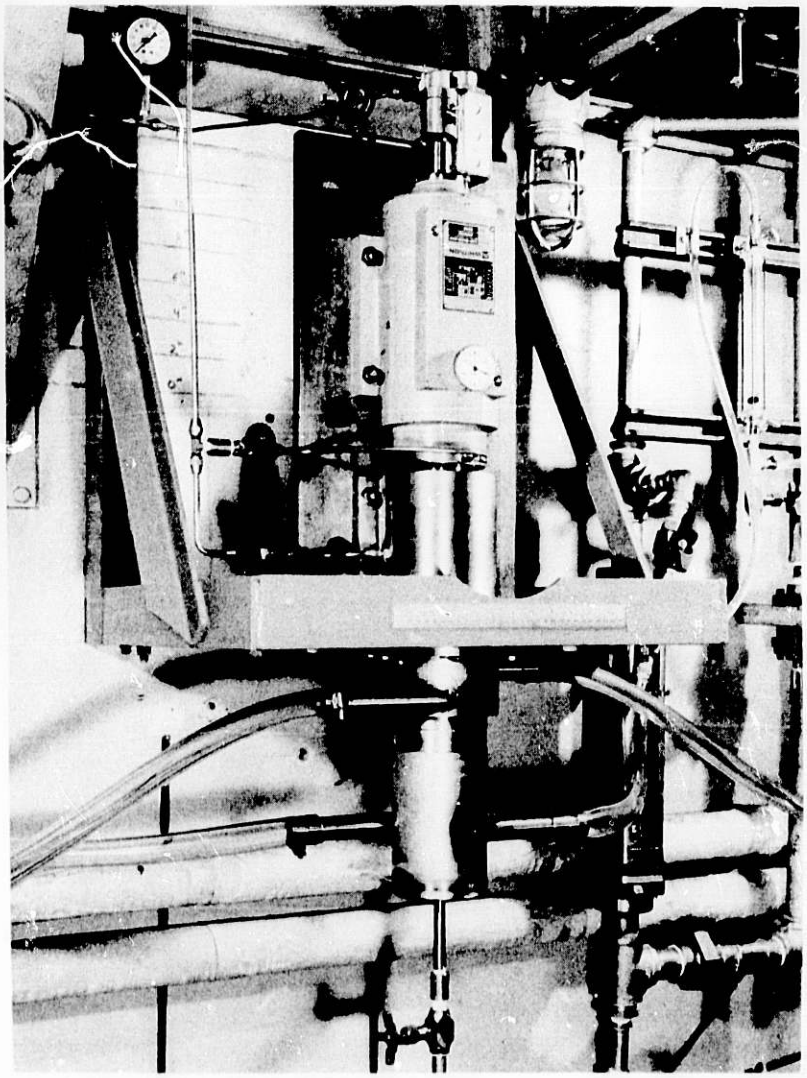

Fig. IX-2. Motorized Spindle and Annular Centrifugal Contactor with a Nine-Centimeter-Diameter Rotor. ANL Neg. No. 308-78-30

over a broad range of organic-to-aqueous flow ratios, and the extraction efficiency is above 98%. A second unit incorporating features for remote maintenance is being designed. A bank of eight such contactors will be built and tested to evaluate contactor performance in a multistage array; this unit will eventually be put into use at ORNL.

A very large contactor (25-cm-dia rotor) similar in design to the unit with a 9-cm-dia rotor is being built with funding from the Savannah River Plant. This unit, which is sized to process light-water reactor fuel at a rate of 10 Mg/d, will be tested for mechanical, hydraulic, and extraction performance.

Future efforts will include studies with the miniature contactor to evaluate proliferation-resistant flow sheets involving partial separation of uranium from uranium-plutonium solution and modifications of thorium-reprocessing systems.

Mechanical and hydraulic testing of contactor designs will continue, with the primary aims of increasing contactor capacity and understanding the behavior of dispersions in a centrifugal field. Information from these tests should lead to improved designs for solvent extraction in nuclear and nonnuclear applications.

B. Nuclear Waste Management

1. Metal Matrix Encapsulation of Radioactive Waste

For containment of high-level wastes, encapsulation of solid waste in a metal matrix is a reasonable alternative to the use of glass monoliths* encased in metal canisters. In metal matrix encapsulation, a metal such as lead or aluminum serves as a continuous matrix in which solid waste fragments are uniformly dispersed.

In our program, a review[5] of the state of the art of waste encapsulation in metal has been completed, and areas have been defined where work is needed to show the feasibility of the process. Experimental work has been carried out on selected topics, including studies of the leaching of waste and the preparation of sound metal-waste composites. An evaluation is under way to design experiments for testing the impact resistance of metal matrix composites at less than full scale.

---

*Potential disadvantages of borosilicate glass as a matrix for high-level waste include: the wide range of conditions under which glass must retain its stability, the lack of homogeneity of the glass beginning with its formation into a glass monolith, and the difficulty of processing wastes by methods involving a liquid phase at the high temperature of molten glass.

[5]L. J. Jardine and M. J. Steindler, A Review of Metal-Matrix Encapsulation of Solidified Radioactive High-Level Waste, Argonne National Laboratory Report ANL-78-19 (May 1978).

Previous studies on the interaction of metal and waste had shown that there is no major reaction when the waste is a stabilized solid. In the case of waste to which silica had been added, prolonged reaction with lead at temperatures well above the melting point of lead produced a film on the waste fragments of rare earth-lead silicates of the general formula, $Pb_3RE_6(SiO_4)_6$. Studies on water leaching of these silicates showed that they are as resistant to dissolution as glass is. Flow sheets have been developed that employ the following well-established process steps: solidification of waste that is originally in acid solution, agglomeration of the fine powders to pellets of manageable size, conversion of these pellets to a stable form by sintering with additives, and encapsulation of the resulting waste. Casting experiments that demonstrated the ability to produce sound ingots in which each waste particle is surrounded by metal (e.g., lead) have been carried out.

A new method for measuring leach rates of solids was developed and tested; the method involves neutron activation of the solid waste form (such as a simulated glass or crystalline ceramic waste), leaching under conditions approximating repository conditions, and simultaneous determination of the concentrations of several nuclides in the leach solutions. When more conventional analytical techniques are used, the surface area of samples is increased by comminution to obtain adequate sensitivity; however, the results of such experiments are not typical of leach rates that would occur under repository conditions.

Results to date indicate that the new method can be used to quickly evaluate solid waste forms of all kinds. Leach studies have shown that lead is reasonably resistant to hot brine of the type likely to be found close to a waste canister in a salt mine, but that aluminum reacts extensively under similar conditions.

Studies published by the Nuclear Regulatory Commission suggest that, of the various steps in the waste-management system, transportation of waste between sites represents the greatest risk to the health and safety of the public. The ability of waste forms to resist dispersion in the event of a transportation accident is an important aspect of the assessment of risk. Work has been done by DOE contractors to evaluate the dispersion of glass on impact under simulated accident conditions; however, no work has been done on dispersion of metal-encapsulated waste upon impact. Owing to the difficulty of testing full-scale waste containers (0.3-m dia by 3 m long), an evaluation is in progress to define the conditions for testing small-size canisters filled with a waste-lead matrix in a way that allows results to be extrapolated to full-size canisters.

The economic factors pertaining to our reference flow sheets are being studied. These results will be compared with similar results for waste management systems that use glass and other waste forms. In other work, studies were made to calculate the temperature profile in canisters containing spent reactor fuel encapsulated in lead.[6]

---

[6] L. J. Jardine and M. J. Steindler, Some Aspects of the Thermal Analysis of Metal Encapsulated Spent Fuel, accepted for publication in Nucl. Sci. Technol.

2. Geologic Migration

The Chemical Engineering Division has two programs related to trace-element migration in geologic bodies, one dealing with nuclear waste and the other with naturally occurring elements.

The goal of the first program is to describe the role of geologic formations in retarding migration of radionuclides from a nuclear waste repository. Because geologic formations immobilize radionuclides, they can play an integral part in the design of waste repositories. In the program, experimental procedures were developed that simulate radionuclide behavior in formations suitable as waste repositories. In a typical experiment, a solution similar in composition to groundwater is maintained at a low oxygen level to represent groundwater in a deep geologic formation. The solution (containing radionuclides) is forced through either a porous rock or a fissure of an impermeable rock to cause movement of the radionuclides. In some experiments, pickup of radionuclides by solutions was accomplished by leaching glass formulated to represent solidified waste; such solutions represented groundwater that had passed through a breached repository.

The experimental results have shown that nuclide migration, in the simpiest cases, depends on the type and extent of reaction of the nuclide with the rock and on reaction kinetics. The interaction among radionuclides, rock, and groundwater is usually considered to be of an ion-exchange type. However, nuclide migration is often complicated by the effects of colloid formation, irreversible reactions, a nonhomogenous geologic medium, or other conditions that preclude a description of migration by simple exchange models.

The goal of the second program is to understand the fundamental mechanisms that underlie immobilization of trace elements by rocks. Fluid-flow experiments were again used so that phenomena are included that exist only under conditions of fluid flow. In these experiments, a hydrated mineral (rather than rock) was used as the geologic medium to provide a few known types of absorption sites for the trace elements. The mineral kaolinite, nominally $Al_2Si_2O_5(OH)_4$, was observed to have an affinity for cesium in the presence of sodium in solution, an affinity that decreases with increasing temperature from 25 to 212°C. The linear relationship between the logarithm of the distribution coefficient for cesium and the reciprocal of temperature is accurately described using the differences in entropies and heat capacities of the cesium and sodium ions, respectively. The results show that partitioning is more strongly dependent on temperature than was calculated from previous work and suggest that, due to heating by radioactive decay, the immobilizing capacity of clay backfills in repositories could be substantially lower than was expected.

C. Evaluations and Studies

1. NASAP/INFCE Studies

In April 1977, President Carter issued a policy statement that indicated concern over the potential diversion of nuclear materials for illicit use (principally, the production of nuclear weapons by a national proliferator). As of that date, he halted efforts directed toward the

commercial processing of spent nuclear fuels in the U.S., encouraged other countries to follow the U.S. lead, and established the basis for an in-depth international study of existing and alternative reactor systems and their fuel cycles to assess their resistance to the diversion of nuclear material and the proliferation of nuclear weapons. This study is known as the International Fuel Cycle Evaluation (INFCE); a parallel domestic study is known as the Non-Proliferation Alternative Systems Assessment Program (NASAP).

The purposes of the studies are (1) to achieve an international consensus on reactor systems and associated fuel cycles having improved proliferation-resistance characteristics and (2) to implement those systems. The Chemical Engineering Division (CEN) is concerned principally with the fuel cycle; other organizations are concerned with reactors, alternative methods of producing nuclear materials, and institutional arrangements and problems.

A determined national proliferator could choose to overtly confiscate a reactor or fuel-cycle facility within its borders along with its inventories of nuclear material. If the nation had previously covertly designed and constructed an appropriate clandestine facility, it might be able to convert those nuclear materials to weapons within a short period of time. One of CEN's principal efforts (together with those of other study participants) was to assess the capability of a nation to accomplish this task for a wide variety of reactors and fuel cycles.

The single outstanding conclusion of a group studying alternative fuel cycles for NASAP (unpublished work) was that a proliferating country (even a developing one) would not be resource-limited (by cost, manpower, or materials) in developing a capability to design and construct clandestine conversion facilities for the production of sufficient material for one nuclear weapon within a period of 10 to 14 days following a successful diversion, irrespective of the form of the material (e.g., spent fuel) or the nature of the reactor fuel cycle (e.g., denatured uranium-thorium cycle in which uranium-233 is associated with uranium-238).

Continuing CEN studies include assessing (1) how attractive it would be for a national proliferator to modify the processes and/or equipment of a confiscated legitimate facility for production of weapons-useful material, and (2) the usefulness of international fuel cycle centers as an institutional method of aiding nonproliferation objectives.

2. Development of Criteria for the Management of Waste Hulls

Special criteria for handling waste fuel-assembly metals from aqueous reprocessing of light water reactor (LWR) fuels were needed because of special combinations of hazards, i.e., possible pyrophoricity of Zircaloy and the radioactivity of neutron-activation products and residual irradiated fuel. Although not related to other current CEN programs, the work, now completed, was an extension of a previous CEN program that evaluated the pyrophoric hazard of Zircaloy hulls, which are the product of the chop-leach step of the Purex process.

The final criteria, developed in 1978, were conceived as a set of general, qualitative guidelines for safety in each of the major operations (e.g., physical or chemical transformations, transport, storage, etc.) likely to be applied to hulls. Criteria were constructed on the basis of a criterion function, which is commonly used for engineering concepts. This basis was considered apt because hulls handling is a set of several engineering operations that convey the waste from the site of generation to the site of terminal storage. Thus, the criterion function was defined as

$$CF = a_1x_1 + a_2x_2 + \ldots + a_6x_6$$

where, in each term, a_n is a weight and x_n is a criterion to guide four categories of factors pertaining to hulls handling, namely, equipment, operations, personnel, and waste-form properties. The inclusion of six terms in the criterion function results from the application of two policies to three types of hazards. The policies are (1) limitation of the impact of normal operation and (2) minimization of the consequences of abnormal operation. The hazards are (1) inhalation/ingestion of radioactive, particulate solids, (2) penetrating radiation, and (3) pyrophoricity. We believe that criteria developed on this basis provide a valuable tool for assessing the factors that affect the entire process of managing hulls safely.

D. LWBR Proof-of-Breeding Analytical Support Project

The Light Water Breeder Reactor (LWBR), now in full operation at Shippingport, Pennsylvania, is the focal point for the national effort to develop technology for breeding in a light water reactor. The LWBR is fueled by a mixture of $^{233}UO_2$ and $^{232}ThO_2$ clad with Zircaloy. Fission of ^{233}U generates power, and additional ^{233}U is bred from ^{232}Th via neutron capture. Thus, LWBRs offer the potential of making use of the relatively abundant ^{232}Th as a nuclear fuel.

Breeding in the LWBR will be evaluated after three years at full power by nondestructively assaying a representative sample of the end-of-life fuel rods. An irradiated-fuel assay gauge (IFAG), which is a delayed-neutron device, is presently being developed for this purpose by the Bettis Atomic Power Laboratory under the sponsorship of the DOE Division of Naval Reactors. ANL's role in this program is to provide destructive physical, chemical, and radiometric analyses of irradiated LWBR fuel rods and fuel rod segments. These analyses will provide calibration factors and overall verification of the performance of the Bettis prototype IFAG; similar analyses will be carried out for the same purpose during the end-of-life analysis of the LWBR core.

Preparation of samples for analysis requires precision cutting of the fuel rod to excise selected fuel rod segments, pulverization of the fuel, and dissolution of the fuel. Cutting is done by high-speed shearing, which simultaneously pulverizes the fuel and largely frees it from the cladding hulls. In the case of sequential segments cut from a rod section, boundaries have to be located accurately, and intersegment cross-contamination must be minimized. After dissolution, the solutions are analyzed for uranium by a mass spectrometric-isotopic dilution method, and for selected fission products (^{137}Cs, ^{144}Ce, ^{95}Zr) by radiometric techniques (see Section XII.B).

Very stringent error requirements have been imposed on each major analytical step and on each analysis; Table IX-1 shows these requirements for the fuel segments, expressed as total allowable error or maximum bias with the relative precision. Error requirements for full-length rods are still under development by Bettis.

Table IX-1. Error Requirements for Analytical Work on Fuel Rod Segments

Determination	Maximum Bias	Relative Precision	Total Error
Location of Fuel Rod Segment, cm (in.)	-	-	2.54×10^{-2}(0.010)
Percent of Fuel in Segment Lost in Shearing	1.0	1.0	-
Total Uranium, %	0.5	1.0	-
Total Fissionable Uranium, %	0.05	0.08	-
Fission Product Monitors, %			
Cesium-137	-	-	2.5
Cerium-144	-	-	5.0
Zirconium-95	-	-	7.5

The proof-of-breeding work at ANL involves several phases (shown in Table IX-2). The current work (Phase 1) has been carried out with a pilot-scale shear and a dissolver initially developed by Bettis. Both systems were installed in the Hot Cave Facility in the ANL Chemistry Division. The work unexpectedly required much developmental effort. In particular, the shear was greatly modified (1) to provide for quantitative sample recovery, (2) to make it remotely operable, and (3) to provide a precision feed system for fuel rods. The feed system utilizes a stepping motor capable of a sensitivity equivalent to 2.54×10^{-4} cm (0.0001 in.); thus, excellent control over rod location and movement is possible.

To determine whether the shear met the requirements of the Division of Naval Reactors, the unit was tested with dummy fuel rods filled with thoria pellets, on the assumption that irradiated fuel would "behave" in a similar fashion to the dummy fuel. The pilot-scale dissolver, comprising a tantalum liner in a stainless steel pressure vessel, was "qualified" by a number of tests in which special $^{233}UO_2$-ThO_2 pellets were dissolved at 195°C and 800 kPa (125 psig) in boiling concentrated nitric acid containing a small amount of HF. The dissolution procedure is one developed by Bettis.

This period of testing and qualification (Phase 1, Table IX-2) allowed the staff and operating crew to be trained and detailed operating procedures to be developed; also, a sample interchange program with Bettis was carried out. The shearing, dissolution, and analysis of an irradiated test rod section completed the test program. All results were completely satisfactory.

Following the test program, three irradiated Zircaloy-clad urania-thoria fuel rod sections were processed. Seven segments (each 6.43 cm long, 0.648 cm in diameter) were excised by shearing from the three sections. All seven segments were dissolved and analyzed for total uranium, uranium isotopes, and selected fission products. Fuel recoveries in the shearing process were slightly below those obtained with the dummy thoria fuel and below the required level (98.1-98.9% as compared with 99.0% minimum requirement). Possibly, the behavior of the two materials differed. A corrosion

Table IX-2. Summary of Activities in LWBR Proof-of-Breeding Analytical Support Project

	Status
Phase 1	
Pilot-Scale Shear and Dissolver System	
Installation and Testing	Complete
Segment Analyses	Complete
Validation Rod Analyses	In progress
Phase 2	
Full-Scale Shear[a]	Being fabricated
Single-Unit Dissolver[a]	Being fabricated
Multi-Unit Dissolver System	Concept being developed
Waste/Scrap Treatment System	Concept being developed
Phase 3	
End-of-life Analytical Campaign (1981-1982)	-
Waste Treatment/Scrap Recovery	-
Cleanup/Waste Disposal (1982-1984)	-

[a]Full-scale shear and single-unit dissolver to be qualified at the end of 1979 by processing a validation rod.

factor has been developed to normalize the shear data. Uranium analyses of dissolved segments by two independent methods showed excellent agreement. All analytical results on segments have been submitted to Bettis for review and for use in calibrating the IFAG.

Work not yet completed with the pilot equipment involves processing of an entire urania-thoria fuel rod section (about 109.2 cm long). The results are intended to validate the performance of the prototyype IFAG.

In the second phase of the ANL program, full-scale shear and dissolver systems are to be built and installed in separate hot cells. The design of the full-scale shear is substantially complete. It will be capable of producing precisely cut segments from 3-m-long LWBR rods having four different diameters, ranging from 0.77 to 2.1 cm (0.30 to 0.83 in.). All major procurements have been initiated, and some components have been received.

A full-scale single-unit dissolver has also been designed and fabricated. It is a prototype for a multi-unit dissolver system to provide samples for analysis at the end of the LWBR core life in 1981-1982. Hot cells are being prepared for installation of the full-scale shear and single-unit dissolver in mid-1979. These units will be installed after a period of out-of-cell checking and shakedown tests. The shearing and dissolving operations will produce a significant quantity of high-level radioactive waste in the form of shearing scrap and radioactive waste solution. Work has been started to identify suitable means for converting the liquid waste to a solid form and for disposing of all wastes.

Work planned for the coming year includes Phase 2 (see Table IX-2)--completion of the procurement, installation, and testing of the full-scale shear and single-unit dissolver systems. After cold testing of these systems, they will be qualified by processing an entire irradiated experimental LWBR fuel rod. Additional work during this year will include beginning the design of the multiple-unit dissolver system and developing a concept for a system for recovering radioactive waste scrap. In the remaining period before ANL begins processing end-of-life fuel from the LWBR, the multi-unit dissolver system will be fabricated, installed, and tested. A waste scrap recovery facility for the treatment and disposal of high-level waste solutions will be designed, built, installed, and tested. Final operating procedures and a data-handling system will be developed, and an operating staff will be trained.

The current schedule for work related to the LWBR end-of-life fuel provides for the processing of 250 segments from 50 fuel rods and five entire rods in a 12-month period from September 1981 to September 1982 (Phase 3). The wastes produced by these operations will be treated concurrently. Some waste may be designated "scrap" and require special treatment. Cell cleanout is scheduled for April 1984.

X. MAGNETIC FUSION ENERGY RESEARCH

A. Introduction

ANL's role in the Magnetic Fusion Energy (MFE) program has shown moderate growth in recent years. A significant fraction (approximately 25%) of the Laboratory's DOE-supported MFE work is conducted within CEN. The CEN effort covers four separate topics: (1) development of technology for handling and processing liquid lithium under conditions anticipated in fusion reactor blanket applications; (2) investigations of the hydrogen-permeation characteristics of candidate structural metals and alloys for fusion reactors; (3) studies of neutron-radiation dosimetry and damage analysis, with emphasis on providing effective service dosimetry for all MFE-supported neutron-irradiation experiments; and (4) a number of systems-type analytical studies encompassing aspects of fusion technology related to design and operational schemes for tritium-handling facilities, alternative breeder blanket concepts, and advanced fusion systems. Objectives and recent accomplishments in the first three areas, which constitute the major part of our work, are summarized below.

B. Lithium Blanket Processing Technology

This program, which is concerned with establishing the technical basis for the use of liquid lithium as a fusion-reactor blanket material, has the following objectives: (1) to demonstrate the capability for recovering the continuously bred tritium from a blanket with a steady-state tritium inventory of less than one weight part per million (wppm), (2) to develop on-line monitoring methods for tritium and other nonmetallic impurities, (3) to test materials and equipment in flowing lithium, and (4) to provide technical input for other lithium-handling facilities. The processing and monitoring methods currently under study include molten-salt extraction of tritium and impurities from lithium, cold-trapping, hot-getter-trapping, on-line monitoring of hydrogen, resistivity measurements, and direct sampling coupled with chemical analysis.

During the past year, significant progress was made in several areas related to lithium processing. The lithium processing test loop (LPTL), described in last year's report and elsewhere,[1,2] was started up in late

---

[1] J. R. Weston, W. F. Calaway, R. M. Yonco, E. Veleckis, and V. A. Maroni, Experimental Studies of Processing Conditions for Liquid Lithium and Solid Lithium Alloy Fusion Blankets, Proc. 3rd Topical Meeting on the Technology of Controlled Nuclear Fusion, May 9-11, 1978, Santa Fe, NM, American Nuclear Society (in press).

[2] J. R. Weston, W. F. Calaway, R. M. Yonco, J. B. Hines, and V. A. Maroni, Control of Impurities in Forced-Circulation Lithium Loop Systems, prepared for presentation at Corrosion 79, sponsored by the National Association of Corrosion Engineers, March 12-16, 1979, and for publication in Corrosion.

1977 and has operated for more than 5000 h with no serious difficulties. Eventually, the LPTL will be used to demonstrate the recovery of tritium from liquid lithium, which is an essential step in closing the D-T fusion fuel cycle.[3] In support of the LPTL studies, a small (about 1 L) lithium loop, the Lithium Mini-Test Loop (LMTL), is being operated as a pilot test-stand for selected materials, hardware, and methods employed on the LPTL.

Initial experiments with the LPTL, which is constructed almost exclusively of Type 304L stainless steel, have examined the effectiveness of cold-trapping and getter-trapping as methods for removing the impurities oxygen, nitrogen, carbon, hydrogen and deuterium from liquid lithium. Control of these impurities is needed to (1) avoid line-plugging problems stemming from precipitation of the less soluble impurities (carbon[4] and oxygen[5]), (2) prevent exacerbation of lithium corrosivity due to nitrogen[6-8] and carbon,[7,8] and (3) eliminate potential embrittlement and tritium-dilution[9] problems associated with the hydrogen isotopes.

Results of cold-trapping studies to date[2] show that (1) the concentration of carbon in lithium can readily be controlled by cold-trapping; (2) the concentration of oxygen can be controlled to a certain extent by cold-trapping, but supersaturation, incomplete crystallization, and/or the existence of stable oxide species other than Li_2O may reduce overall efficiency; and (3) the saturation concentrations of nitrogen and the hydrogen isotopes are too high for acceptable control by cold-trapping alone.

---

[3] W. F. Calaway, Electrochemical Extraction of Hydrogen from Molten LiF-LiCl-LiBr and Its Applications to Liquid-Lithium Fusion Reactor Blanket Processing, Nucl. Technol. 39, 63 (1978).

[4] R. M. Yonco, M. I. Homa, and V. A. Maroni, The Solubility of Carbon in Liquid Lithium (work in progress; see Section XI.B.6, this report).

[5] R. M. Yonco, V. A. Maroni, J. E. Strain, and J. H. DeVan, A Determination of the Solubility of Lithium Oxide in Liquid Lithium By Fast Neutron Activation, J. Nucl. Mater. (in press).

[6] R. M. Yonco, E. Veleckis, and V. A. Maroni, Solubility of Nitrogen in Liquid Lithium and Thermal Decomposition of Solid Li_3N, J. Nucl. Mater. 57, 317 (1975).

[7] J. H. DeVan, J. E. Selle, and A. E. Morris, Review of Lithium Iron-Base Alloy Corrosion Studies, Oak Ridge National Laboratory Report ORNL/TM-4927 (January 1976).

[8] D. L. Smith and K. Natesan, Influence of Nonmetallic Impurity Elements on the Compatibility of Liquid Lithium with Potential CTR Containment Materials, Nucl. Technol. 22, 392 (1974).

[9] E. Veleckis, R. M. Yonco, and V. A. Maroni, Solubility of Lithium Deuteride in Liquid Lithium, J. Less-Common Met. 55, 85 (1977).

Because nitrogen is a major contributor to lithium corrosion phenomena,[7,8] particularly in stainless steel systems, much of our work to date has been on nitrogen control. Experience with the LMTL[1] and LPTL[1,2] (both of which are stabilized with a zirconium getter trap) has been that the nitrogen level tends to rise sharply during the first few hundred hours of operation and then steadily decrease to a level of about 400 to 700 wppm after several thousand hours. A plausible explanation for this behavior is that nitrogen is extracted from the interior surfaces of the loop construction materials in early operating phases; but then, during extended operation, it reequilibrates with the zirconium in the getter trap (forming ZrN) and/or with chromium in the stainless steel (forming Cr_2N). Although chromium might be more active in controlling nitrogen during early operating phases, we expect that over long periods of time most of the nitrogen will migrate to the zirconium. Detailed analyses of the distribution of nitrogen in the LMTL zirconium getter-bed, to be conducted during 1979, should help to resolve this question.

The miniature loop (the LMTL) has now operated for close to 10,000 h at temperatures from 450 to 500°C. During this period, the zirconium-packed getter section[1] was run at temperatures near 600°C. Two materials-related failures were experienced at about 7000 h of operation: A small leak occurred in a cold-worked, highly stressed section of the electromagnetic pump channel and one of the all-welded, bellows-sealed valves, which had been operated (opened and closed) over 300 times, failed due to a series of cracks that developed in the outer edges of the bellows convolutions. However, with the exception of a nickel-depleted ferrite layer about 10 μm thick that has formed on all lithium-contacted surfaces, there is little evidence of serious surface erosion or bulk intergranular attack of the annealed sections of the loop construction material (all 300-series stainless steel). These results suggest that, although flowing lithium is reasonably compatible with austenitic stainless steels at temperatures up to 500°C, there may be some corrosion problems in cold-worked regions with large residual internal stresses or in heavily fatigued components. Accordingly, a number of test probes have been placed in the reservoir tank of the LPTL to provide additional data on lithium/materials interactions in stainless steel systems. In the meantime, the failed components on the LMTL were replaced or repaired and loop operation was continued.

In the coming year we intend to conduct an extensive series of tests in the LPTL salt tank to assess the potential of molten-salt extraction (using LiF-LiCl-LiBr[3]) as a method for removing nonmetallic impurities from liquid lithium. An electrical resistance probe will be inserted in the LPTL reservoir tank to investigate the feasibility of using resistivity measurements to obtain real-time information on gross impurity levels. More experiments with the cold trap, getter trap, and hydrogen meters presently installed on the LPTL are planned. Also, we expect to extend our capabilities for determination of nonmetallic impurities in lithium beyond the elements that are presently done routinely (i.e., oxygen, nitrogen, carbon, hydrogen, deuterium, and tritium) to include chloride, fluoride and bromide (which may be introduced into the lithium during salt extraction operations).

C. Hydrogen Permeation in Candidate Structural Alloys

The principal objective of this program is to investigate the factors that influence hydrogen permeation into and through structural metals and alloys, and thereby obtain a clearer understanding of the rate and extent of tritium migration in fusion reactor systems. Although the focus of work has shifted from development and testing of permeation barriers to measurements of permeation rates, the retardation of permeation in structural materials having excessively high permeation rates continues to be a primary goal.

During the past year, hydrogen-permeation studies were completed for austenitic-, nickel-, and refractory metal-base alloys representative of the classes of alloys that are of primary interest to programs of the DOE/MFE Materials and Radiation Effects Branch. Hydrogen permeation measurements were made from 100 to 800°C and at hydrogen (H_2) driving pressures from 10^{-3} to 10^{4} Pa on the following materials: Type 316 stainless steel (austenitic), Inconel-625 and Inconel-718 (nickel-base), and titanium alloy 5621S (refractory-base). The conditions and results of the experiments are given in Table X-1.

The method used for the permeation measurements has been described elsewhere.[10,11] In brief summary, the apparatus consists of two all-metal, high-vacuum compartments interconnected by a permeation-membrane assembly. The upstream compartment contains a controlled-temperature uranium hydride bed that supplies hydrogen at constant pressure to the membrane, a mass spectrometer (to monitor composition), an ion pump, and assorted pressure-measuring devices. The downstream compartment contains a Zr-Al alloy hydrogen-getter pump, an ion pump, a mass spectrometer, and three standard hydrogen leaks covering a leak-rate range of about four orders of magnitude. The specimen (typically 20 to 40 mm in diameter and about 1 mm thick) is incorporated into the membrane assembly either by electron-beam welding or by gasket-sealing, and functions essentially as a diaphragm between the two compartments.

The sample of Type 316 stainless steel (316-SS) was studied over a wide range of temperatures and driving pressures, as indicated in Table X-1. Even at the lowest pressure studied, namely 10^{-3} Pa, the measured permeabilities showed no significant deviation from the square-root-of-pressure dependence expected for permeabilities that are limited by bulk diffusion. The presence of a gamma source of about 1 mCi in the upstream compartment, near the specimen, had no detectable effect on hydrogen permeation rate. Although the ionizing potential of this source is many orders of magnitude

---

[10] E. H. Van Deventer, Hydrogen Permeability of Haynes Alloy-188, J. Nucl. Mater. 66, 325 (1977).

[11] E. H. Van Deventer, T. A. Renner, R. H. Pelto, and V. A. Maroni, Effects of Surface Impurity Layers on the Hydrogen Permeability of Vanadium, J. Nucl. Mater. 64, 241 (1977).

Table X-1. Conditions and Results of Hydrogen-permeation Experiments

Material	Temp., °C	Pressure, Pa	ϕ_o,[a] $cm^3(STP)/m \cdot s \cdot kPa^{1/2}$	Q_p,[a] cal	Exponent for Pressure Dependence
316-SS	150-750	10^{-3}-10^4	0.182	15,175	0.49-0.57
Inconel-625	150-750	10^{-1}-10^4	0.198	14,371	0.49-0.56
Inconel-718	100-800	10^{-1}-3	--	--	>0.7
	100-800	3-10^4	0.059[b]	13,373[b]	0.5-0.6
5621S[c]	400-650	10^{-1}-10^2	(∿15)[d]	(∿10,000)[d]	0.67-0.70

[a] Permeability = $\phi_o \exp[-Q_p/RT]$, where R = 1.987 and T is in K.
[b] Derived from data obtained at hydrogen pressures >3 Pa.
[c] Ti-5% Al-6% Sn-2% Zr-1% Mo-0.25% Si.
[d] Derived assuming half-power dependence on hydrogen pressure for rough comparison with data for other materials.

lower than that estimated for the radiation field near a fusion reactor first wall, dissociative ionization of H_2 molecules at the surface of the first wall is not expected to increase hydrogen permeabilities beyond the bulk-diffusion-limited rate even in much higher radiation fields.

The test conditions for the Inconel-625 and Inconel-718 samples were similar to those of the 316-SS. Because of the presence of small amounts of aluminum in these alloys (about 0.2% in the 625 and about 0.5% in the 718), their permeabilities to hydrogen showed some sensitivity to the low levels of impurities in both compartments when hydrogen pressures were at the lower end of the range studied. In particular, at pressures <3 Pa, the permeability of the 718 alloy decreased considerably and the pressure exponent increased to values >0.7, thus indicating the onset of surface-limited diffusion, which we believed could be due to the formation of a reasonably uniform aluminum oxide layer. Scanning electron micrographs of the surfaces of both specimens verified the presence of aluminum-rich surface layers and showed that aluminum in the alloys had migrated towards the surface. This finding supports our earlier conclusion, reported last year, that alumina layers formed on the surface of alloys containing aluminum as a bulk constituent tend (1) to impart some resistance to permeation (roughly a tenfold reduction for Inconel-718) and (2) to be rapidly self-healing owing to the continuous diffusion of aluminum to the surface.

During the past year, considerable interest[12] has been generated in the use of titanium-base alloys as fusion reactor construction materials,

12 J. W. Davis and G. L. Kulcinski, Assessment of Titanium for Use in the First Wall/Blanket Structure of Fusion Power Reactors, Electric Power Research Institute Report EPRI ER-386, pp. 53-55 (1977).

mainly because of their availability, strength, low induced radioactivity, and resistance to radiation damage. However, a disadvantage is that titanium is a strong hydride-forming material, and its alloys are expected to exhibit high hydrogen-permeation rates. Accordingly, we are investigating hydrogen dissolution and permeation in selected titanium-base alloys to evaluate possible hydrogen migration problems associated with their use.

A study was completed on the 5621S alloy of titanium (Ti-5% Al-6% Sn-2% Zr-1% Mo-0.25% Si). A special gasket-sealed membrane assembly, developed specifically for titanium-base materials, performed satisfactorily during the 2600-h duration of the tests. The permeability of the sample was about 1000 times greater than that of typical 300-series stainless steels at comparable temperatures and hydrogen pressures. The observed pressure dependence, $P^{0.7}$ (at 10^{-1}-10^{2} Pa, 400-650°C), implies some effect from surface impurity interactions but to a lesser extent than in studies of α-titanium, where a $P^{1.0}$ dependence was found.[13,14] Furthermore, hydrogen permeation rates were 20 to 30 times higher than for α-titanium.[13,14] This difference may be due either to a decrease in surface impurity effects or a higher solubility and/or diffusivity of hydrogen in the 5621S alloy.

Transient data taken during the early stages of a permeation run on the 5621S alloy indicate dissolution of large amounts of hydrogen in the alloy, as expected. Although analysis of the data is incomplete, the magnitudes of the solubility values are in the range anticipated for titanium-base materials,[12] and the derived diffusion coefficients are consistent with a partially surface-limited permeation process.

After study of the 5621S alloy was completed, examination of the specimen showed no visual evidence of change in the appearance or mechanical integrity of the specimen, despite the fact that it had been subjected to about 2600 h of hydrogen infiltration. Of particular interest was the absence of "doming" of the membrane surface (which is usually indicative of hydrogen-diffusion-induced creep). The complete absence of discoloration of either surface of the specimen indicates that the purity of the gas environment was high. Comparative microscopic and microprobe analyses of the permeation specimen and a sample of the as-received 5621S alloy are planned.

In preparation for additional scoping studies of titanium alloys, we have obtained a sample of a Ti-6% Al-4% V alloy and have fabricated several permeation specimens. We plan to investigate the permeation characteristics

---

[13] D. L. Johnson and H. G. Nelson, Determination of Hydrogen Permeation Parameters of Alpha Titanium Using the Mass Spectrometer, Metall. Trans. 4, 569 (1973).

[14] K. K. Shah and D. L. Johnson, Effect of Surface Pre-oxidation on Hydrogen Permeation in Alpha Titanium, Proc. Int. Conf. on the Effects of Hydrogen on Materials Properties, September 23-27, 1973, Champion, PA, pp. 475-481, ASM (1974).

of an as-received specimen, a nitrided specimen,* and possibly an anodized specimen.

In another area of work, we are collaborating with the ANL Materials Science Division in the assembly and operation of a small lithium loop (about 0.5-L capacity) that is constructed from a stainless steel-clad vanadium alloy (V-15 Cr). The loop, which will be used to investigate hydrogen-migration characteristics and materials compatibility in liquid lithium/vanadium alloy systems, is undergoing leak-testing in preparation for lithium filling and startup.

D. Dosimetry and Damage Analysis

Radiation-damage experiments in support of the MFE program are being conducted in a variety of neutron environments, including reactors and particle accelerators. The objectives of the CEN program on dosimetry and damage analysis are to develop techniques for routinely measuring the neutron flux and spectrum at these facilities and to evolve methods for calculating damage parameters, including displacements per atom (DPA) and primary knock-on-atom (PKA) distribution, as well as gas (H and He) and transmutant generation rates. Each irradiation facility must be characterized so that data obtained at different facilities may be correlated and damage effects extrapolated to fusion reactor environments. Our program includes a research and development effort, as well as service dosimetry that is available to all MFE experimenters upon request.

1. Characterization of Irradiation Facilities

Three dosimetry experiments were started at the Oak Ridge Research Reactor (ORR) during FY 1978. These experiments, which are being conducted in conjunction with a series of irradiations sponsored by the DOE/MFE Materials and Radiation Effects Branch, are of particular importance because the ORR has been designated as the primary reactor for MFE materials research for the next three to five years.

Four experiments were conducted at the University of California, Davis Cyclotron (UCDC). A broad spectrum of neutrons is produced at the UCDC, from thermal energies up to about 44 MeV (average, about 14 MeV) by stopping a 30-40 MeV deuteron beam in a thick beryllium target.

---

*Work on applying a nitride coating to the surface of one of the specimens was performed in collaboration with D. M. Gruen (Chemistry Division, ANL) and G. O'Donnell and G. L. Kulcinski (University of Wisconsin), using a procedure described in Ref. 15.

[15] M. B. Liu, D. M. Gruen, et al., Ion Nitriding of Titanium and Zirconium by a D. C. Discharge Method, High Temp. Sci., 10, 53 (1978).

All seven irradiation packages consisted of multiple-foil activation materials; some also included helium accumulation monitors from Atomics International. Integral foil-activation measurements are used to unfold the differential flux and spectrum, from which damage parameters are calculated. Data analysis was completed for previous experiments conducted at the T(d,n) Rotating Target Neutron Source (RTNS-I) at Lawrence Livermore Laboratory (LLL), the Be(d,n) cyclotron source at Oak Ridge National Laboratory, and the LLL Pool-Type Reactor. A Monte Carlo error analysis was provided for all measurements, including errors in the flux, spectrum, and derived damage parameters due to uncertainties in the foil activation measurements, nuclear cross sections, and starting trial solutions.

Considerable research and development work was required for both reactor and accelerator dosimetry. Because the ORR reactor has a mixed neutron spectrum (part thermal and part fast), it is necessary to include self-shielding effects in our spectral unfolding codes. Accordingly, the SAND-II and SANDANL codes, discussed in last year's report, have been revised to include self-shielding and cadmium-cover effects for wires and foils in a beam or isotopic flux.

Dosimetry for high-energy accelerators has been hampered by a lack of reliable activation cross sections above 14 MeV. We have extrapolated a set of 31 activation cross sections to 44 MeV. Integral testing of the data in Be(d,n) fields with deuteron energies of 14, 16, and 40 MeV (by using time-of-flight spectrometry to accurately measure the neutron field) showed [16,17] that 25 reactions are reliable to ±10% in all fields and that they can be used to unfold the differential flux-spectrum with 10 to 30% accuracy in the neutron energy range from 2 to 30 MeV. Since 90% of the damage in materials is produced by neutrons in this energy range, this level of accuracy is sufficient to determine integral damage parameters within ±10% for high-energy accelerator irradiations. We plan to continue the integral testing to include more reactions and different neutron fields. By coupling these results with new measurements and calculations, we expect to improve the accuracy of available dosimetry data.

Considerable effort has also been expended in the past year on planning and reviewing dosimetry for the Fusion Materials Irradiation Test Li(d,n) facility, which is scheduled to be put into operation at Hanford Engineering Development Laboratory by 1983. Much of our dosimetry development effort is focused on the needs of this facility. Experiments are also planned for the RTNS-II T(d,n) source, which is expected to be fully operational at LLL in early 1979. We expect to play a major role in the initial characterization of both facilities.

---

[16] L. R. Greenwood, R. R. Heinrich, R. J. Kennerley, and R. Nedrzychowski, Development and Testing of Neutron Dosimetry Techniques for Accelerator-Based Irradiation Facilities, Nucl. Technol. 41, 109 (1978).

[17] L. R. Greenwood, R. R. Heinrich, J. J. Saltmarsh, and C. B. Fulmer, Integral Tests of Neutron Activation Cross Sections in a $^{9}Be(d,n)$ Field at E_d = 40 MeV, submitted for publication in Nucl. Technol.

2. Damage Analysis

The computer codes for flux-unfolding error analysis and damage analysis, developed in previous years, have been interfaced so that we can routinely provide data on errors due to dosimetry uncertainties for all derived damage parameters. At present, damage calculations can be performed for 21 elements at neutron energies up to 20 MeV, using nuclear data from the ENDF/B-IV files.* However, high-energy accelerator irradiations require the extension of these files up to 40-50 MeV. We have performed such calculations for copper and niobium up to 100 MeV, using cross sections calculated at Oak Ridge National Laboratory for neutron energies up to 32 MeV, and we plan to perform similar calculations for several additional elements in the coming year.

---

*The ENDF/B-IV files (1972-1978) are maintained and issued on magnetic tape by the National Neutron Cross Section Center, Brookhaven National Laboratory.

XI. BASIC ENERGY SCIENCE

A. Homogeneous Catalysis

1. Hydrogenation of Carbon Monoxide

Conversions of the more available fossil fuels--coal, lignite, peat--to increasingly scarce liquid and gaseous fuels or to chemical feedstocks have long been objects of technological attention, and interest in them is still growing. In the present work efforts are made to supplement the vastly researched, but poorly understood, phenomena of heterogeneous catalysis by study of related phenomena in homogeneous catalysis, which are capable of considerably more detailed understanding.

The combination of a theoretical description of a possible initiating step for CO hydrogenation, namely, hydrogen atom transfer from a transition metal hydride complex to CO to form a transient formyl radical, HCO, together with a fortunate observation has led to the discovery[1] of a homogeneous reaction in which syngas is converted to a variety of products that now includes methanol, methyl formate, their higher homologues, ethylene glycol, methane, and carbon dioxide. Of particular interest is the fact that the catalysts for this process that have been so far uncovered--$HCo(CO)_4$ and $HMn(CO)_5$--contain only a single transition metal atom, although it had been previously supposed[2] that multimetal complexes, called clusters, would be required as catalysts.

Recent work has focused on elucidation of the reaction mechanism; in this connection, detailed studies of the net rate of CO hydrogenation ("reaction rate"), product distributions, and kinetic orders have been undertaken, with the following results so far:

(a) The reaction may be carried out in a variety of solvents, including heptane, benzene, p-dioxane, and mixtures of water and p-dioxane. Reaction rates increase as the solvent polarity increases; an optimum dielectri constant, determined by the balance between stabilization of a polar transition state and destabilization of the unionized hydride, may exist.

(b) The principal reaction path is first-order in catalyst, e.g., $HCo(CO)_4$ or $HMn(CO)_5$.

(c) With $HCo(CO)_4$ as catalyst, the reaction is apparently zero-order in CO and first-order in H_2, and has an effective activation enthalpy approximately equal to 40 kcal/mol and an effective activation entropy approximately equal to 0 gibbs/mol.

---

[1] H. M. Feder and J. W. Rathke, J. Am. Chem. Soc. 100, 3623 (1978).

[2] E. L. Muetterties, Science 196, 839 (1977); Bull. Soc. Chim. Belg. 84, 959 (1975); 85, 451 (1976); M. G. Thomas et al., J. Am. Chem. Soc. 98, 1296 (1976); 99, 2796 (1977).

(d) A tentative reaction mechanism is shown in Table XI-1, along with an analysis of the observed rate constant in terms of pre-equilibria[3] and stepwise rates. This specific formulation allows one to devise mechanistic tests via labeling experiments, intermediate trapping experiments, and kinetic isotope-effect experiments that will help validate (or modify) the proposal. A derivative goal for this work will be the modification of catalyst and reaction conditions to enhance the rate and selectivity of formation of products that are of special interest as long-range chemical feedstocks, e.g., ethanol, propanol, and ethylene glycol. It is anticipated that work toward this goal (i.e., toward product optimization) will be undertaken in the future.

2. Catalytic Conversion of Quadricyclane to Norbornadiene

The catalytic conversion of one liquid isomer of C_7H_8 to another at ambient conditions and without the need for other reactants is of such chemical simplicity as to be especially useful for the development of the science of homogeneous catalysis. This reaction exemplifies a class of such isomerizations, which convert highly strained carbocyclic rings to less strained ones with the evolution of sensible heat (about 100 kJ/mol). The reverse transformation may be induced by exposure to light; hence, such pairs of compounds may serve as means of storing solar energy and releasing it rapidly on demand.

One of the catalysts studied was the molecule di-μ-acetato-bis (norbornadiene)dirhodium(I), $[Rh(\mu_2\text{-}O_2CCH_3)C_7H_8)]_2$. In the work completed to date,[4] the valence isomerization of quadricyclane has been shown to (a) yield (about 25%) two norbornadiene dimers (both endo configurations) as well as the monomer, (b) be characterized by the formation of yellow Rh(III) intermediates from the Rh(I) catalyst, (c) obey a rate law which is first-order in original catalyst concentration and zero-order in substrate at high substrate concentrations, but approaches a limiting first-order in substrate at low substrate concentrations, and (d) yield low-temperature trappable intermediates (observed by ^1H and ^{13}C NMR*) formed by the initial insertion of a monorhodium fragment into the carbon-carbon bond of a cyclopropyl ring to form a rhodocyclobutane intermediate.

These results were significant because the mechanism(s) of such catalytic reactions have been discussed repeatedly in the literature without resolving the contending claims of three distinctly different initiating mechanisms that have been proposed. In the present case the actual trapping of an intermediate formed by metal atom insertion is important evidence that such a mechanism operates.

It was thought desirable to ascertain the reason why the acetate-bridged dimer breaks up in the course of reaction. Single crystals were prepared for a crystal and molecular structure investigation[5] in order to

---

[3] C. L. Aldridge and H. B. Jonassen, J. Am. Chem. Soc. 85, 886 (1963).

[4] M. J. Chen and H. M. Feder, accepted for publication in Inorganic Chemistry.

[5] S. Siegel, B. Tani, A. H. Reis, Jr., and C. Willi, accepted for publication in Inorganic Chemistry.

* NMR = nuclear magnetic resonance.

Table XI-1. Tentative Mechanism for Catalytic CO Hydrogenation

Designation	Reactions and Rate Equations	Values of Thermodynamic Functions[a]
1	$CO + HCo(CO)_4 \rightleftharpoons HCO + Co(CO)_4$	$\Delta G^* \sim 43$ $\Delta H^* \sim 40$ $\Delta S^* \sim -7$
2	$HCO + HCo(CO)_4 \rightleftharpoons H_2CO + Co(CO)_4$	$\Delta H \sim -20$
I	$H_2 + CO \underset{k_{-I}}{\overset{k_I}{\rightleftharpoons}} H_2CO$	$\Delta G^\circ_I = 18.8$ $\Delta H^\circ_I = -3.6$ $\Delta S^\circ_I = -49.3$
II	$HCo(CO)_4 \overset{K_{II}}{\rightleftharpoons} HCo(CO)_3 + CO$	$\Delta G^\circ_{II} = 0.4$ $\Delta H^\circ_{II} = 12.7$ $\Delta S^\circ_{II} = 27$
3	$H_2CO + HCo(CO)_3 \overset{k_3}{\rightleftharpoons} Co(CO)_3CH_2OH$	$\Delta G^* \sim 22$ $\Delta H^* \sim 32$ $\Delta S^* \sim 22$
4	$Co(CO)_3CH_2OH \rightleftharpoons Co(CO)_3OCH_3$	
5	$[Co(CO)_3CH_2OH,\ Co(CO_3)OCH_3] \xrightarrow[\text{fast}]{CO,H_2}$ $CH_3OH,\ CH_3OCOH,\ (CH_2OH)_2$	$\Delta G^*_{eff} \sim 41.2$ $\Delta H^*_{eff} \sim 41$ $\Delta S^*_{eff} \sim 0.3$

Rate

$$\frac{dp}{dt} = k_3[HCo(CO)_3][H_2CO]$$

$$= k_3 \cdot \frac{K_{II}[HCo(CO)_4]}{P_{CO}} \cdot \frac{k_I P_{H_2} P_{CO}}{k_{-I} + k_3 K_{II}[HCo(CO)_4]/P_{CO}}$$

$$\simeq k_3 K_I K_{II}[HCo(CO)_4]P_{H_2}, \text{ where } \frac{k_I}{k_{-I}} = K_I$$

[a] ΔG and ΔH in kcal/mol; ΔS in gibbs/mol.

relate structural information to the isomerization mechanism. Each rhodium was found to be approximately in the center of a nearly planar configuration made up of one oxygen atom of each of the bridging acetato ligands and the midpoints of the two olefinic bonds of a norbornadiene ligand. The acetate ligands have "twisted" so that they are not normal to each other, as is usual in multiple acetate bridges, allowing the norbornadiene ligands to avoid an eclipsed configuration. Steric interactions are also found in the norbornadiene ligands, the hydrogen atoms of two ligands of a dimeric unit being within Van der Waals distance of each other. A monomer may form by the breaking of two acetate-rhodium bonds and the incorporation of an additional quadricyclane ligand at a coordinatively unsaturated Rh site. This process would be assisted by the strain evident in the structure of the molecule. No further work on this system is planned.

B. Thermodynamics of Metal and Salt Systems

1. Theory for Ternary Solutions Dilute in One Component

Knowledge of the activities of gases, relatively insoluble materials, and minor constituents dissolved in alloys and ionic (or slag) solvents is important in metallurgy and in a large variety of technological processes. We have developed a statistical mechanical theory that provides a more accurate description of the concentration dependence of activity coefficients of a solute, C, in dilute solution in a binary solvent, A-B, than all other theories of such solutions. Deviations from ideal solution behavior of the solvent enter the theory in an exact manner.

The fundamental equation of the theory expresses the activity coefficient of the solute, γ_C, as follows:

$$\frac{1}{\gamma_C} = \sum_{i=0}^{Z} \frac{Z!}{i!(Z-i)!}\left[\frac{X_A\gamma_A{}^t}{\gamma_C(0)^{1/Z}}\right]^{Z-i}\left[\frac{X_B\gamma_B{}^t}{\gamma_C(1)^{1/Z}}\right]^{i}\left(\exp\frac{-\Delta g_i^E}{2kT}\right) \qquad (1)$$

where X_A and X_B are mole fractions, γ_A and γ_B are activity coefficients of the solvent components, $\gamma_C(0)$ is the activity coefficient of C in pure A and $\gamma_C(1)$ in pure B, i is a running variable related to the number of B atoms (ions) in the coordination shell about C, Z is the coordination number of the nearest shell of A and B about C, and t is a geometric parameter equal to 1/Z for substitutional alloys or additive salt systems and can range from 0.25 to 0.50 for interstitial alloys or reciprocal salt systems. The term Δg_i^E is analogous to an excess free energy of mixing of A and B atoms in the coordination shell. The simplest expression for this term is

$$\Delta g_i^E = i(Z - i)h/2 \qquad (2)$$

which is analogous to that for a regular solution. Equations 1 and 2 have been tested on published data for about twenty different alloy systems and shown to provide descriptions of these systems that are equal to or better

than all prior theories. The results lend confidence in utilizing the theory for metallurgical systems and in the interpretation of experimental results in terms of the energetics and structure of the solutions.

Future work will focus on generalizing the theory for silicate (two-lattice) systems, developing the underlying concepts so that the theory applies to binary systems with complex types of behavior, and extending the theory to multicomponent solvents.

2. Phase Diagrams of Multicomponent Salt Systems

A knowledge of the phase diagram of cryolite-based systems is important for adjusting the Hall-Heroult process for the production of aluminum and could be significant in fine-tuning the process for energy conservation. We have initiated a computer-assisted analysis of the thermodynamics of the $NaF-AlF_3-CaF_2-LiF-MgF_2-Al_2O_3$ system in order to deduce a reliable and thermodynamically self-consistent phase diagram for this system. The calculations combine all known reliable thermodynamic data on the compounds and solutions using an optimization procedure to obtain optimized phase diagrams, as well as a self-consistent set of thermodynamic parameters that describe the stabilities of all the compounds and the properties of all the liquid and solid solutions.

We have completed an analysis of the $NaF-AlF_3$, $LiF-AlF_3$, CaF_2-AlF_3, $LiF-CaF_2$, $NaF-CaF_2$, and CaF_2-AlF_3 binary systems, as well as the ternary system $NaF-LiF-AlF_3$, and have initiated calculations for the $NaF-AlF_3-CaF_2$ ternary. Figure XI-1 shows the results of calculations of liquidus temperatures in the $NaF-LiF-AlF_3$ system. Our calculations lead to thermodynamically

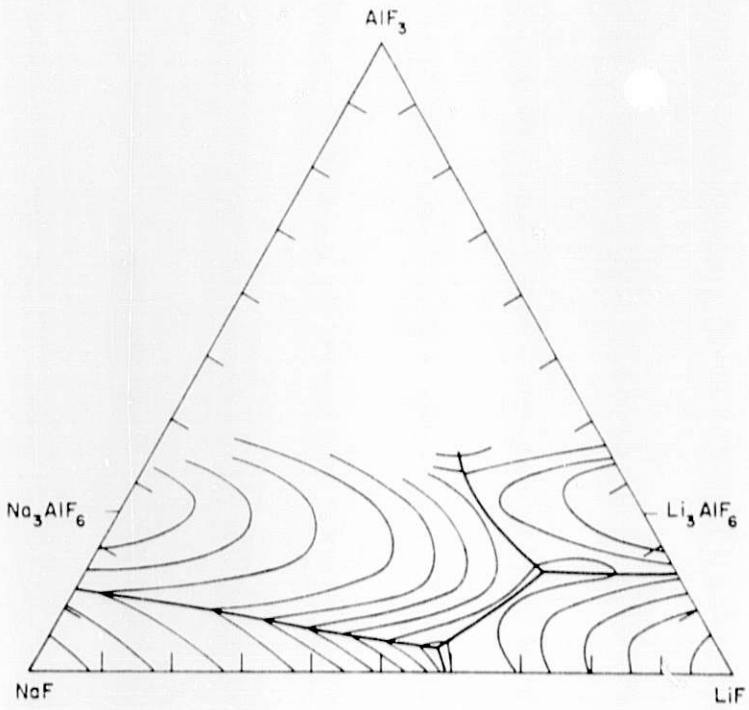

Fig. XI-1. Computer-generated Liquidus Phase Diagram of the $NaF-LiF-AlF_3$ System

valid phase diagrams that have been constructed for unmeasured regions by interpolations and extrapolations from a relatively small number of measurements using theories of solutions that have been developed for these systems. We plan additional calculations on cryolite-based systems to produce a reliable set of phase diagrams for all components of the Hall-Heroult electrolyte.

3. Calculations of Complex Equilibria

Complex equilibria between a multicomponent gas phase and condensed phases occur in several technologies important for major DOE programs. The complete characterization of the chemistry, and a means of obtaining a detailed understanding of condensation processes should prove important in these technologies. Our aims are to develop a computer program to calculate the chemistry of such complex equilibria, to include the possibility of complex multicomponent solution phases, and ultimately, to incorporate certain kinetic constraints into the calculation.

We have used as a starting point, a computer program developed by Gordon and McBride[6] that is capable of performing equilibrium calculations on the condensation of several pure condensed phases from a complex multicomponent gas phase. This computer program has been modified to handle solution phases having up to twelve components. This modified program has been successfully run for a ten-component ideal solution of metals, as well as for several nonideal binary solutions, and can now be applied to a number of technological problems. Our program is perhaps the first to have such a capability in a general form. We plan to extend the program to take into account more complex kinds of solution chemistry; later, some kinetic factors will be included through the imposition of well-defined constraints on the equilibrium calculation. Such kinetic constraints can lead to major alterations in the chemistry and morphology of condensates.[7]

These computer program(s), when coupled with a broad thermodynamic data base, could be an important tool for predicting the chemistry of condensates and for solving a number of important technical and scientific problems. Ultimately, we hope to initiate a parallel experimental program to test the predictions of these computer programs and to provide a basis for making improvements in them.

4. Hydrogen Titration Method

The hydrogen titration method (HTM) has been shown to be useful for the determination of the thermodynamic properties of the Li-Al system. This method, which was described in the last report, has now been applied to the study of the more complex Li-Pb system. Four isotherms were measured over the

---

[6] S. Gordon and B. J. McBride, Computer Program for Calculation of Complex Equilibrium Compositions, Rocket Performance, Incident and Chapman-Janguet Detonations, NASA SP 273 (1971).

[7] M. Blander and L. Fuchs, Geochim. Cosmochim. Acta 39, 1605 (1975).

temperature range from 500 to 600°C for two initial starting compositions (Pb/Li = 0.261 and Pb/Li = 0.286). The data verified the existence of three known phases (Li_7Pb_2, Li_3Pb, and Li_8Pb_3) and indicated a new and fairly broad homogeneous phase (β) whose lead-rich boundary corresponds to $Li_{11}Pb_3$. Constant-pressure plateaus in each of the three two-phase regions (β + Li_7Pb_2, Li_7Pb_2 + Li_3Pb, and Li_3Pb + Li_8Pb_3) were used to derive the corresponding lithium activities and to determine the predicted galvanic cell emfs. The latter values show good agreement with those recently determined for the same system by the coulometric titration technique.[8]

The success of the HTM in accounting for the thermodynamics of two binary lithium-containing systems (Li-Al and Li-Pb) has prompted us to apply the method to a calcium-containing system, namely, Ca-Al, which may prove useful for hydrogen storage application.* We expect the Ca-Al system to absorb hydrogen according to the mechanism postulated for the HTM. Upon completion of this study, the applicability of the HTM will have been demonstrated and no further work with it is planned.

5. Measurement of the Solubility of Carbon in Liquid Lithium

Measurements of the solubility of carbon in liquid lithium have been completed. Sixteen filtered samples of carbon-saturated lithium were taken at random intervals over the temperature range from 204 to 635°C. Carbon concentrations were determined by quantitative gas chromatographic analysis of the carbonaceous gases evolved on hydrolysis of each sample. The dominant carbon-bearing species present in lithium is expected to be the acetylide, Li_2C_2, which on hydrolysis should give only acetylene. However, since a large quantity of lithium metal is necessarily hydrolyzed along with the acetylide, some hydrogenation of the acetylene to ethylene and ethane is expected. Accordingly, since all three gases (C_2H_2, C_2H_4, and C_2H_6) were observed during each hydrolysis, the carbon (as Li_2C_2) assays were determined by summing the individual contributions from each C_2 species. The low level of CO_2 which was also observed in the gas chromatographs was attributed to background effects and was not included in the carbon assay.

The temperature dependence of the solubility of carbon in liquid lithium, as determined by least-squares refinement of the solubility data points, may be represented by the equations

$$\ln S(\text{mol \% } Li_2C_2) = 3.61 - 6200/T$$

$$\log S^*(\text{wppm C}) = 6.11 - 2700/T$$

where T is the Kelvin temperature. The solubility values given by these equations are several orders of magnitude lower than those reported previously by Federov and Su.[9] Because the overall experimental technique of Federov

---

[8] M. L. Saboungi and J. Marr, Argonne National Laboratory, work in progress.

[9] P. I. Federov and M.-T. Su, Hua Hsueh Hsueh Pao 23, 30 (1951); see also Chem. Abst. 52, 19377 (1958).

*In this connection, the hydrogen sorption of a Ti-6Al-4V alloy will also be studied.

and Su has been criticized by other investigators[10] and because their solubility points appear to have been read from a thermoanalytical cooling curve, which may not have represented equilibrium conditions, our data are much more likely to represent the true solubility of carbon in liquid lithium.

The results of this study have (1) defined the lithium-rich hypereutectic for the liquidus Li-Li_2C_2 system, (2) supplied information on the solubility limits for carbon in cold-trapped lithium (this has already been of value in analyzing results from the LPTL,* see Section X.B), and (3) provided guidance in evaluating sensitivity requirements for on-line carbon monitors to be used in conjunction with large circulating liquid-lithium systems. These results are also expected to contribute to the general understanding of materials compatibility limits in a liquid-lithium environment.

In the light of recent findings[11] concerning the presence of a chemical interaction between nitrogen and carbon in lithium and the existence of the compound Li_2NCN,[12] work on this project is now being directed toward (1) the preparation of Li_2NCN and (2) the elucidation of the nature of the C-N interaction in lithium in the dilute solution range.

6. Resistometric Studies of Impurity Interactions in Liquid Lithium

Operational performance of systems in existing and advanced energy technologies could be seriously impaired by materials interactions, particularly those between high-temperature fluids and containment materials. Thus, basic information on the rates and mechanisms of these interactions is essential to a thorough understanding of corrosion phenomena. The principal objective of the resistivity studies program is to provide real-time measurements of the rates and extents of impurity interactions in liquid metal/transition metal systems. These studies have also proven to be useful in generating data on distribution coefficients and redistribution rates for impurity elements between the liquid metal and the transition metal. A reliable experimental method has been reasonably well worked out and a number of enlightening results have been obtained during the past year. The method and results are briefly discussed below.

The electrical resistance studies are being done in the specially designed flushable resistivity apparatus shown in Fig. XI-2. The apparatus consists of a stainless steel pot, outfitted with a stirrer and thermocouple well, into which the charge of lithium is loaded. One end of a thin-walled, coiled stainless steel tube is attached to the side of the pot at a point well below the normal liquid level of the lithium in the pot. The opposite end of the tube is connected to a small side reservoir located at a height near that of the liquid level in the pot as shown in Fig. XI-2. In this configuration,

---

[10] P. F. Adams, P. Hubberstey, and R. J. Pulham, J. Less-Common Met. 42, 1 (1975).

[11] See Section X.B.6.

[12] M. G. Down et al., J. Chem. Soc./Chem. Commun. 1978, 52.

*Lithium Processing Test Loop.

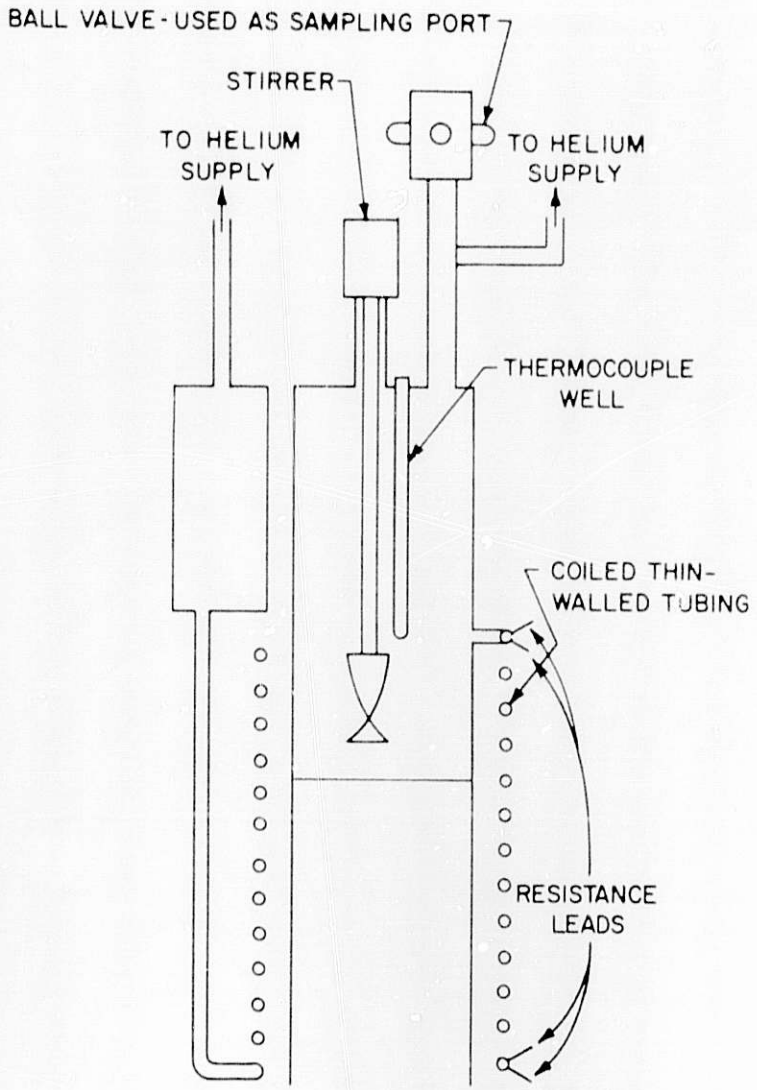

Fig. XI-2. Flushable Resistivity Apparatus Used to Conduct Liquid Lithium Resistivity Experiments

the lithium in the pot can be flushed back and forth through the coil by adjusting the cover-gas pressure in the small reservoir. The resistivity of the lithium is determined from the resistance of the filled tube and the known resistance of the empty tube by treating the tube and lithium as parallel resistors. The electrical resistance leads are located as shown in Fig. XI-2. There are two leads at each end of the coiled tube: one set is used to supply the current and the other set, to measure the potential drop.

The entire apparatus shown in Fig. XI-2 is supported by a ceramic superstructure and inserted in a stainless steel furnace well that is attached to a helium atmosphere glove box. The apparatus is appropriately packed with nonconductive spacers and thermal insulation so that (1) a constant temperature (within ±2°C) is maintained within the pot, while a reproducible temperature gradient of <5°C is obtained along the tubing, and (2) the tube and pot are everywhere insulated (electrically) from the glove box and everywhere insulated from each other except at their point of attachment.

Initial experiments were devoted to measuring the resistivity of "pure" lithium. Our measurements agreed, within experimental uncertainty, with published literature values[13-15] for the resistivity of pure liquid lithium. Our subsequent experiments focused on observing the effects of chemical transformations in lithium on the resistivity. In a typical experiment, following the initiation of some type of chemical transformation in the lithium held in the pot (i.e., by addition of an impurity or a gettering metal), the lithium is flushed back and forth through the coil; after thermal equilibrium is attained, the resistance is measured and the temperature recorded. Using these data and the previously determined resistivity of the empty tube, the actual resistance and resistivity of the lithium are determined. Through a series of such measurements, it is possible to obtain kinetic data on the rate of the initiated transformation in the pot.

The effect of adding controlled quantities of several impurity species (e.g., Li_3N, Li_2C_2, Li_2O, LiH, and LiBr) on the resistivity of liquid lithium was measured during the past year. Typical results of these kinds of experiments are shown in Fig. XI-3. Resistivity-increase coefficients (expressed as $n\Omega \cdot m$ of increase per mol % of impurity added) for nitrogen, oxygen, and hydrogen additions to lithium, derived from data like those shown in Fig. XI-3, are in reasonably good agreement with previously published values.[16,17] Nitrogen (about 70 $n\Omega \cdot m$/mol %) has the greatest impact on resistivity, with hydrogen (53 $n\Omega \cdot m$/mol %) and oxygen (24 $n\Omega \cdot m$/mol %) following closely behind.

An interesting feature in Fig. XI-3 is the sharp drop in resistivity following the addition of about 0.03 mol % Li_2C_2 to the high-nitrogen (about 0.3 mol %) lithium used in this series of experiments. This effect could well be a manifestation of the chemical interaction between nitrogen and carbon in lithium reported recently by Down et al.,[12] in that the added carbon may be interacting with nitrogen to form an Li-N-C species that precipitates from the lithium and/or has a lower resistivity-increase coefficient than Li_3N. The overall resistivity drop in Fig. XI-3, assuming that it were due totally to removal of nitrogen from the lithium, corresponds to 0.06 mol % nitrogen or a nitrogen/carbon interaction ratio near 1. This particular ratio, although interesting in its own right, is not obviously consistent with the formation of Li_2NCN as reported by Down et al.[12] However, the solutions from which Down et al. crystallized Li_2NCN from lithium were more concentrated in carbon and nitrogen than the one that resulted in the data in Fig. XI-3. Clearly, the existence and characteristics of carbon/nitrogen interactions in liquid lithium need further study.

---

[13] G. K. Creffield, M. G. Down, and R. J. Pulham, J. Chem. Soc. Dalton Trans. 21, 2325 (1974).

[14] J. F. Freedman and W. D. Robertson, J. Chem. Phys. 34, 769 (1961).

[15] S. M. Kapelner, USAEC Report PAWC-349 (1961).

[16] P. F. Adams, M. G. Down, P. Hubberstey, and R. Pulham, J. Less-Common Met. 42, 325 (1975).

[17] M. N. Arnol'dov, M. N. Ivanovskii, V. I. Subbotin, and B. A. Shmatko, High Temp. 5, 723 (1967).

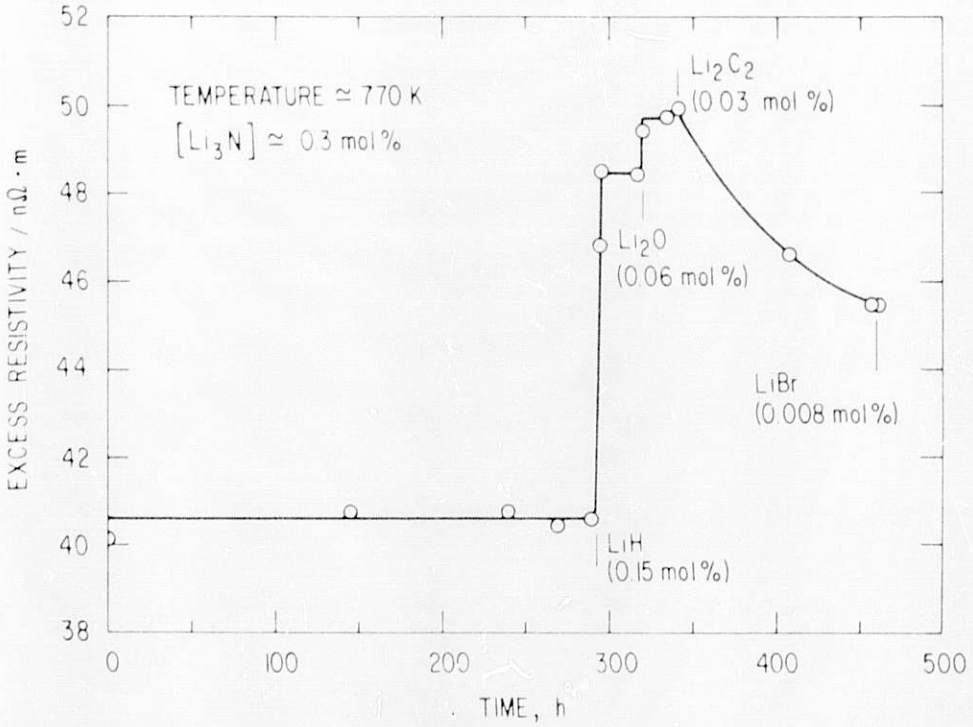

Fig. XI-3. Results of Studies of Resistivity-Increase Coefficients for Selected Impurities in Liquid Lithium

In other experiments conducted with the resistivity apparatus, the impurity-gettering characteristics of a series of refractory metals were investigated. At 500°C, vanadium proved to be ineffective in removing impurities from lithium; in fact, the resistivity measurements indicated that lithium actually leached impurities (probably hydrogen and oxygen) from the vanadium. Zirconium showed only limited capacity to remove impurities from lithium. Yttrium, which was by far the best, did appear to remove nitrogen at a reasonable rate when nitrogen concentrations in the lithium were high, but its effectiveness dropped off steadily with decreasing nitrogen level.

In another interesting experiment, the precipitation characteristics of Li_3N were investigated. The experiment showed that Li_3N crystallites readily separate from liquid lithium. Also, the measured and calculated excess resistivities at the break points in the resistivity curves (due to the onset of precipitation of Li_3N) were in very good agreement with the known saturation solubility of Li_3N in liquid lithium.

Work on this program in the coming year will proceed along much the same lines as described above. The Li-N-C interaction and the Li-N-Cr interaction (which also appears to be significant in stainless-steel-contained lithium systems) will be investigated in greater detail. More work will be done to investigate optimum conditions and materials for gettering impurities from liquid lithium. It is expected that, in the longer range, the results of this program will lead to the identification of the dominant mechanisms by which lithium attacks and corrodes various classes of structural metals.

C. Thermochemistry

The objectives of this program are to (1) measure thermochemical properties of selected organic and inorganic compounds, and (2) interpret and predict thermodynamic properties such as enthalpies of formation by means of group- and bond-energy schemes and other theoretical approaches. These objectives are being met in our studies of heteroatomic polyaromatic "building-block" molecules of coal; sulfides and zeolite minerals related to geothermal energy sources; and transition-metal alloys that exhibit excellent hydrogen adsorption and desorption properties.

1. Thermochemistry of Coal Components

A large number of complex aromatic compounds are obtained when coal is pyrolyzed.[18] These compounds are considered to be related to the basic building-block molecules of coal, the structure of which is not well understood. Thermochemical data for these building-block molecules would be of value in contributing to a better understanding of coal structure, defining possible paths of decomposition, and identifying the effects that variables such as temperature might have on processes of coal liquefaction and gasification. Standard enthalpies of formation have been determined for xanthone, chromone, benzonaphthofuran, anthrone, and fluorenone by oxygen-bomb calorimetry. From these limited data we have developed a predictive capability based on a group additivity approach that is being used to estimate the enthalpy of formation of compounds of interest. Since group-energy schemes are applied to gaseous molecules and all our enthalpy of combustion measurements were performed on solid substances, it has been necessary to measure, or estimate, the enthalpies of sublimation for the molecules of interest.

Because of its structural complexities, fluorenone has thus far afforded the most rigorous test of our predictive capabilities. Our estimated value of $\Delta H_f^\circ(g)$ for fluorenone agreed within 3 kJ with the experimentally derived value based on measurements of $\Delta H_f^\circ(s)$ and the enthalpy of sublimation.

Currently, studies are continuing on benzofuran and γ-pyrone which will improve our capability to handle strained-ring molecules and molecules containing keto groups. In order to expand our data base of group-energy contributions, calorimetric measurements are planned on nitrogen- and sulfur-containing molecules, as well as on compounds with phenyl-phenyl bonds.

2. Studies of Geothermal Materials

The thermodynamic properties of sulfide minerals are of interest in the geothermal energy program because of the environmental and corrosion problems associated with them. A program was initiated last year to obtain the thermodynamic properties of a number of such sulfides at room and higher temperatures. The enthalpies of formation of $As_4S_4(\alpha)$ and As_2S_3 (orpiment),

---

[18] R. Hayatsu, R. G. Scott, L. P. Moor, and M. H. Studier, Nature 257, 378 (1975).

determined by fluorine-bomb calorimetry, were -33.1 and -17.1 kcal/mol, respectively. These values differed by about a factor of two from the values based on oxygen-bomb calorimetry.[19-23] Because of the complexity of the combustion reaction in oxygen-bomb calorimetry as contrasted with the simplicity of the fluorine-bomb reaction, the fluorine-bomb values are considered to be more reliable. Measurements of the high-temperature enthalpy functions, $(H_T - H_{298.15})$ up to 850 K, have also been completed on these materials. These measurements extend about 300 K into the liquid region.

Studies on Sb_2S_3 have been initiated because of the discordant values reported for its enthalpy of formation and lack of high-temperature thermodynamic properties. A sample of Sb_2S_3 was synthesized and high-temperature enthalpy functions were determined to 1050 K. Measurements of the enthalpy of formation by fluorine-bomb calorimetry are planned.

Measurements of the enthalpies of hydration of zeolite minerals have begun. These data are of interest in connection with the exploitation of "hot dry-rock" geothermal resources. Water is introduced through a drill hole into the hot rock; the water circulates through natural and induced fractures to another drill hole where it is pumped to the surface and the heat extracted. Commonly found in these sources are layer lattice minerals, zeolites and feldspar glasses, which are characterized by open structures in which the adsorption and desorption of water readily occur. The understanding of conditions that may limit the exploitation of these geothermal sources would be enhanced by the availability of enthalpy of hydration data.

In a collaborative phase of this effort, synthetic minerals are being prepared by C. C. Herrick of Los Alamos Scientific Laboratory. Zeolite M, having an approximate composition of $K_{14}[(AlO_2)_{14}(SiO_2)_{14}]\cdot 12\ H_2O$, has been received and will be used to develop calorimetric procedures. The minerals chabazite, phillipsite, and mordenite, which are characteristically found in "hot dry-rock" geothermal sources, will also be studied when procedures are finalized.

3. Enthalpy of Hydrogen Absorption in $LaNi_x$ and Related Alloys

Certain transition metal alloys, typified by $LaNi_5$, are capable of incorporating large amounts of hydrogen into their structures. In the AB_5H_n series of hydrides, the replacement of lanthanum or nickel by a different metal can frequently bring about orders-of-magnitude changes in the

---

[19] E. V. Britzke, A. F. Kapustinsky, and L. B. Tschenzova, Z. Anorg. Allg. Chem. 213, 58 (1933).

[20] K. C. Mills, Thermodynamic Data for Inorganic Sulfides, Selenides and Tellurides, Butterworths, London (1974).

[21] W. W. Weller and K. K. Kelly, U.S. Bureau of Mines RT 6511 (1964); NBS Tech. Note 270-3 (1968).

[22] P. B. Barton, Geochem. Cosmochim. Acta 33, 841 (1969).

[23] K. Jellinek and J. Zakowski, Z. Anorg. Allg. Chem. 142, 1 (1925).

hydrogen decomposition pressure. There has been a growing interest in compounds that can reversibly absorb and desorb hydrogen at moderate temperatures and atmospheric pressure. These compounds have been considered for a variety of energy applications, e.g., heat pumps, hydrogen storage, the gettering of tritium in fusion reactor systems, and other uses connected with the role of hydrogen in energy conservation programs.

In collaboration with Argonne's Chemistry Division personnel who have been making vapor pressure measurements on hydride systems, a program has been undertaken to measure directly, by calorimetry, the energies of absorption and desorption of hydrogen by $LaNi_5$ and $LaNi_xAl_{(5-x)}$ alloys. For this study, a calorimetric system and associated gas-handling apparatus were set up. Measurements were made of the energy released when accurately measured amounts of hydrogen were admitted to the calorimeter reaction vessel containing the alloy being studied. These measurements were carried out in the region of limited solubility of hydrogen in the metallic α-phase, in the region in which the saturated α-phase is in equilibrium with the separate hydride (β-phase), and in the region where single-phase metallic hydride is in equilibrium with hydrogen at rapidly increasing pressures. Data obtained to date indicate that the enthalpy of hydriding of $LaNi_5$ in the $\alpha \rightarrow \beta$ two-phase region is -31.36 ± 0.80 kJ $(g\ atom\text{-}H)^{-1}$, which is in good agreement with vapor-pressure measurements.

D. Environmental Chemistry

The goals of the environmental chemistry program include the determination of the chemical composition of the condensed material in the atmosphere and its variation with time and location, development of techniques for sampling and characterizing the emissions from advanced and emerging energy-production systems, determination of the significant mechanisms for the formation of primary (at the source) and secondary (in the atmosphere) sulfates and nitrates, and the determination of reaction rates and mechanisms associated with the production and control of atmospheric pollutants from coal combustion at their source. To achieve these goals, we are developing sensitive instruments and analytical techniques, participating in field programs for aerosol sampling and analysis, conducting laboratory experiments to investigate the formation of primary and secondary sulfates and nitrates, and studying dolomite sulfation and regeneration using various analytical tools.

1. Development of Instruments and Analytical Techniques

Sensitive and accurate techniques are needed for the sampling and physical and chemical characterization of the fine particles suspended in the atmosphere. For some time now, we have been developing the Fourier-transform infrared analytical technique for the determination of nitrate, neutral and acidic sulfate, ammonium ions, and total hydrocarbons in samples of particles collected by an impactor or a filter. More recently, we have initiated the development of a technique for the analysis of samples for their content of specific heavy organic compounds.

Some of the problems of quantifying the infrared spectra of fine particles were addressed this year. By working with carefully prepared standards, it was determined that, for some of the absorption bands, the peak area was a better measure of the quantity of the respective ion than the peak height, at least as determined with our system using an 8 cm^{-1} resolution. Also, the absorption band at 1400 cm^{-1} for the ammonium ion was found to give different Beer's law plots depending upon the associated anion: sulfate or nitrate. These changes have been incorporated into the current version of the computer program that analyzes the infrared spectra. Efforts are presently under way to quantify the spectra of samples containing acidic sulfate. In this regard, it was demonstrated that our freeze-drying technique for the analysis of filter-collected samples changes the acidity of acidic as well as neutral ammonium sulfate samples. This procedure is therefore not being used at present.

We are currently developing an instrument that enables us to use the attenuated total internal reflection phenomenon for the infrared spectroscopic analysis of fine particles. Due to multiple internal reflections within a single internal reflection element, with an attendant attenuation at each reflection, such a device provides a highly sensitive analytical system. In the prototype that we have built, a head-end centripeter removes particles greater than 1 μm in aerodynamic diameter from the air stream; two opposed jets then deposit 0.3- to 1.0-μm particles on the two opposite faces of an internal reflection element by impaction. A number of such elements are moved past the air jets at a controlled rate to provide time resolution. Atmospheric sampling tests have shown that, using this device, the detectable limit for sulfate, nitrate, and ammonium ions is lowered by at least a factor of six. This makes possible very short sampling times in relatively polluted air, such as urban, industrial, or power-plant plumes.

We have also developed a sample-handling device that allows relatively rapid analysis of organic compounds in filter- or impactor-collected samples. The sample is placed in a vaporizer and rapidly heated to the desired temperature. The organic compounds that are vaporized are carried by an inert gas to an unheated capillary tube where they condense. The organic compounds are thus greatly concentrated and can be analyzed by any of a number of analytical techniques. A temperature-programmed vaporizer provides a means for an initial separation of the organic compounds according to their volatility. This device has been successfully used for direct on-column injection of the organic fraction of the sample into a gas chromatograph; the organic material condensed in the capillary has also been successfully analyzed using thin-layer chromatography. In either case, the analysis is relatively rapid and sensitive enough for many of the organic compounds present in ambient samples.

2. Chemistry of Atmospheric Particulate Materials

Our efforts in this area may be divided into two broad categories. One is the measurement of the chemical composition of the atmospheric fine particles; and the other is an investigation into the mechanisms that are effective in the formation of these chemical species.

We are presently participating in a major field program, the Multistate Atmospheric Power Production Pollution Study (MAP3S). Samples of nonurban aerosols are being collected at College Town, PA; Charlottesville, VA; Rockport, IN; and Upton and Racquette Lake, NY. Fine particles in the size range of 0.3- to 0.1-μm aerodynamic diameter are analyzed by the infrared spectroscopic technique for sulfate, ammonium, and nitrate ions and sulfate acidity. One of the results obtained so far is that the atmospheric aerosol is essentially neutral at Rockport, IN, but highly acidic at Upton, NY. Aerosol at College Town, PA, and Charlottesville, VA, is slightly lower in acidity than that at Upton, NY, but is considerably more acidic than the aerosol at Rockport, IN. (There is very little information from Racquette Lake, NY, since that sampler has only recently started operating.) Aerosol loadings in the 0.3 to 1.0 μm size range were observed to be highest at Rockport, IN; lower at College Town, PA, and Charlottesville, VA; and lowest at Upton, NY. Distinct, and as yet unexplained, diurnal patterns were observed for the aerosol loading and acidity at each of the sampling sites. Very low levels of nitrate were found at all of the MAP3S sites.

Our observation that aerosol acidity is considerably greater in the Eastern States than in the Midwest is in contrast to the fairly uniform acidity of the precipitation (rain and snow) in much of the MAP3S region. We are attempting to see if the fine particle aerosol loading and acidity that we have observed can be correlated with the precipitation chemistry and atmospheric turbidity at these sites.

Measurement of the stable oxygen isotope ratio, $^{18}O/^{16}O$, in atmospheric sulfates, sulfur dioxide, water vapor, and precipitation is being used as a tool to distinguish between different mechanisms of formation of sulfate. Previous work had indicated that sulfates dissolved in precipitation are most likely formed by the oxidation of sulfur dioxide in the aqueous phase, and that the sulfate in the fine particle aerosol is also formed in a similar fashion. These conclusions were based on the observations that three of the four oxygen atoms of the sulfate ion dissolved in precipitation are apparently contributed by the water of precipitation, and that the long-term average oxygen isotope ratio in the aerosol sulfate is the same as that in sulfate associated with precipitation.

However, the sulfate in precipitation is more enriched in ^{18}O ($\delta^{18}O$ greater by 6-10°/₀₀) than that obtained by the laboratory oxidation of sulfur dioxide in water of the same oxygen isotopy as that of the precipitation.

Several mechanisms for SO_2 oxidation in the atmosphere have been proposed by other workers. Using our oxygen isotope ratio measurement technique, we are attempting to determine which, if any, lead to an ^{18}O-enriched sulfate product.

This phase of the work has begun with an examination of the effect of carbon. It has been speculated that carbon plays a significant role in the atmospheric oxidation of sulfur dioxide. Experiments are being conducted in the laboratory using activated charcoal as a surrogate for atmospheric carbon. While an ^{18}O enrichment in product sulfate has not yet been confirmed, the results to date indicate that the mechanism of sulfate formation on charcoal (and the associated oxygen isotopy) is indeed very different from that of

sulfate formed in aqueous solution. Additional experiments are being planned to investigate the isotopic effects of sulfur dioxide conversion to sulfate on a variety of particulate materials or catalysts likely to be present in the atmosphere.

3. Sulfur Emissions Control Chemistry

These studies are directed toward determining the kinetics and mechanisms of the reactions that are significant in the cyclic use of SO_2 sorbents in fossil fuel combustion. Whereas previous work had been concentrated on the reactions pertaining to the calcination and sulfation of dolomite, and the $CaSO_4$-CaS reaction for the regeneration of sulfated dolomite, more recently we have been investigating the regeneration of sulfated dolomite by reduction with hydrogen according to the reaction:

$$[CaSO_4 + MgO] + H_2 \rightarrow$$

$$u[CaS + MgO] + v[CaO + MgO] + w\ H_2S + x\ H_2O + y\ SO_2 + z\ S_2$$

Preliminary work had indicated that the reaction-product distribution, i.e., relative magnitudes of the reaction coefficients u, v, w, etc., is strongly dependent on reaction temperature and hydrogen concentration, indicating that several competing reactions occur in this system. The reaction most favored thermodynamically is

$$[CaSO_4 + MgO] + 4\ H_2 \rightarrow [CaS + MgO] + 4\ H_2O$$

However, CaO is the more desirable product of the regeneration reaction, and it is therefore of interest to learn what factors promote or inhibit its formation.

Varying the hydrogen concentration between 0.1 and 6% in He in the reducing gas, and varying the gas flow rate between 0.1×10^{-3} and 5×10^{-3} m^3/min, showed that, as the amount of available hydrogen was decreased, relatively greater amounts of CaO were produced. Even at the high hydrogen concentrations and gas flow rates, at 1223 K, more CaO than CaS is formed in the early stages of the reaction; the final product, however, contains more CaS than CaO. CaO is preferentially formed when low hydrogen concentrations and low reducing-gas flow rates are used, even though the overall reduction rates are lowered. Interestingly, when hydrogen availability is low, much of the CaO is formed in the interiors of the particles; this is in contrast with a shrinking-core behavior that is observed when hydrogen availability is high. Annealing the sulfated dolomite at high temperature tends to make CaO production more uniform throughout a particle when low hydrogen availability conditions are used. Such annealing increases the average pore diameter within the particles, with the increased porosity being most pronounced at the exterior surfaces of the particles. It was also observed that the presence of small amounts of water vapor, $\leq$1% H_2O, in the reducing gas has a small retarding effect on the reduction reaction kinetics but has a significant effect on the product distribution. As the water vapor concentration is increased from 0.1 to 1%, relatively greater amounts of CaO are formed; with water vapor concentration at 1% or higher, no CaS is observed in the final product. By comparison of kinetic data with the rate behavior predicted by the various reaction mechanisms, it was found that the dominant mechanism changes, as a function of both

the temperature and the reducing-gas composition, from a phase-boundary-controlled (at high temperatures and hydrogen concentrations) to a nucleation-controlled, and finally, to a diffusion-controlled (at low temperatures and hydrogen concentrations) mechanism.

The future direction of this research will be to complete the high-temperature structural studies of the CaS-$CaSO_4$ reaction, as well as the studies on the reduction of sulfated dolomite by hydrogen. The scope of this general area of research will be expanded to include studies of NO_x-dolomite reaction mechanisms.

E. Physical Properties of Associating Gases and Salt Vapors

1. Associating Gases

Experimental and theoretical studies have continued on the properties of associating gases that are promising candidates for heat transfer and power cycle working fluids. In these studies, analyses of enhanced thermal conductivities are used to determine the thermodynamic properties of the associated species and *ab initio* molecular orbital calculations are used to determine their structures.

A technique has been developed for measuring the thermal conductivity of a binary mixture of gases of known composition using a thick-hot-wire cell.[24] The measured pressure dependence of the thermal conductivity of two compositions of methanol-water mixtures is shown in Fig. XI-4. Analysis[25] of the results indicated the presence of a methanol-water dimer and trimer, methanol tetramer,[24] and water dimer,[26] with the trimer being composed of two methanol molecules and one water molecule. The enthalpy and entropy of association of this trimer are given in Table XI-2. These measurements are among the few available of the association properties of binary mixtures in the gas phase.

Table XI-2 also includes the results of analysis of the thermal conductivity data of four other gases in which the dimer was found to be the predominant associated species. Trifluoroacetic acid associates very strongly causing a large enhancement in its thermal conductivity similar to that found for acetic acid.[27] Measurements on trifluoroethanol-water mixtures, a commonly used working fluid, also indicate the presence of a 1:1 mixed species, as well as dimers of the two components.

---

[24] T. Renner, G. Kucera, and M. Blander, J. Chem. Phys. 66, 177 (1977).

[25] J. N. Butler and R. S. Brokaw, J. Chem. Phys. 26, 1636 (1957).

[26] L. A. Curtiss, D. J. Frurip, and M. Blander, Chem. Phys. Lett. 54, 575 (1978).

[27] D. J. Frurip, L. A. Curtiss, and M. Blander, unpublished results.

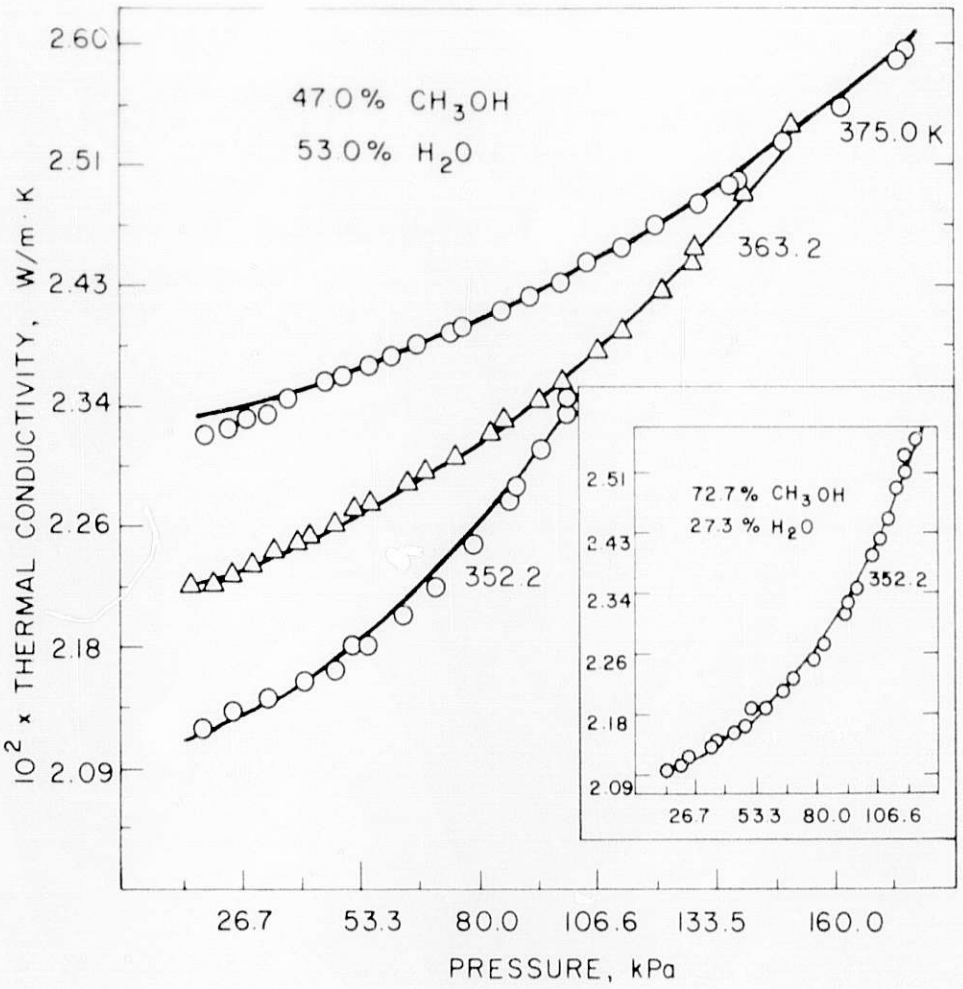

Fig. XI-4. Thermal Conductivity as a Function of Pressure for a Binary Mixture of Methanol and Water at Two Different Compositions (mole percent). [The theoretical fit to the data is represented by the solid lines. Included in this fit are $(H_2O)_2$, $(CH_3OH)_2$, $(CH_3OH)_4$, $(CH_3OH)(H_2O)$, and $(CH_3OH)_2(H_2O)$.]

Table XI-2. Enthalpies and Entropies of Various Associated Species

Substance	Species	ΔH, kcal/mol (kJ/mol)	ΔS, kcal/mol·deg (kJ/mol·deg)
Pyridine	dimer	-5.14 (-21.52)	-22.9 (-95.8)
Hexafluoropropanol	dimer	-4.88 (-20.43)	-18.6 (-77.9)
Pentafluorobutanol	dimer	-4.78 (-20.02)	-17.5 (-73.3)
Trifluoroacetic acid	dimer	-14.60(-61.13)	-38.7(-162.0)
Methanol-Water	2:1 trimer	-10.43(-43.67)	-38.0(-159.1)

Ab initio molecular orbital calculations have been carried out on the monomers and dimers of acetic acid, trifluoroacetic acid (TFA), and pyridine. The acetic acid and TFA dimers are quite similar in geometry. Both form two parallel hydrogen bonds, C=O...H-O, in a cyclic array in consonance with electron diffraction results. The equilibrium pyridine structure contains a linear C-H...N hydrogen bond involving the proton para to the nitrogen. The molecular planes of the monomers in the equilibrium structure are perpendicular.

We plan thermal conductivity experiments on other mixed systems that have possibilities as working fluids. These include acetic acid-water and TFA-water. The thermal conductivity technique provides a novel way to determine, unambiguously, the nature and thermodynamic properties of mixed associated species.

Some of the substances studied such as trifluoroethanol, pyridine, and trifluoroacetic acid show promise as constituents of advanced working fluids. We plan to phase out the experimental part of the program, continuing only with calculations that would indicate the potential usefulness of such fluids in power cycles.

2. Salt Vapors

Our program on the thermodynamic and physical properties of ionic vapors is aimed at developing fundamental theories of such systems as well as the study of classes of ionic vapors that have potential uses or are important in technology.

a. Dimensional Analysis of Partition Functions for Ionic Vapor Molecules

We have evaluated the relative values of the free energy functions, $(G_T^\circ - H_0^\circ)/RT$, and the entropies, S_T°, for ionic substances from a dimensional analysis[28] of the configurational integral using a model pair potential. The results permit one to minimize the amount of spectroscopic data and simplify the procedure used for calculating these two thermodynamic properties. For the case where the electronic partition function, q_e, is separable, we obtain:

$$-\frac{(G_T^\circ - H_0^\circ)}{RT} = \gamma(T) + \ln\left[d^{3(a+x-1)}(m_+^a\, m_-^x)^{3/2} q_e\right] \qquad (3)$$

and

$$\frac{S_T^\circ}{R} = \sigma(T) + \ln\left[d^{3(a+x-1)}(m_+^a\, m_-^x)^{3/2} q_e\right] \qquad (4)$$

where $\gamma(T)$ and $\sigma(T)$ are universal functions, d is the cation-anion separation, a and x are the stoichiometric coefficients of the atoms in the salt, and m_+ and m_- are ionic masses. The substances tested and found to be

---

[28] M. Blander, J. Chem. Phys. 41, 170 (1964).

adequately represented by the model include the alkali halides, alkaline earth dihalides, and even gaseous diatomic ions. This theory allows one to calculate, with relative accuracy, the unknown thermodynamic properties of a large number of substances from the known properties of a few.

b. Ab Initio Molecular Orbital Calculations of High-Temperature, Metal-Halide Complexes

Ab initio molecular orbital theory has been very useful in providing information on the structures, energies, and bonding for many different types of molecules. During the past year we have undertaken a study of the use of ab initio molecular orbital theory as an aid in the characterization of complexes present in high-temperature salt vapors. The species considered include the aluminum halide dimers, Al_2F_6 and Al_2Cl_6; the complexes between an aluminum halide molecule and ammonia, $AlF_3 \cdot NH_3$ and $AlCl_3 \cdot NH_3$; and complexes between lithium fluoride and aluminum trifluoride.

The most stable structures of several of these complexes are illustrated in Fig. XI-5. The geometries obtained are in good agreement with those determined by electron diffraction studies. There has been some disagreement experimentally as to the structure of $LiAlF_4$. Using an extended basis set, a structure with two fluorines in the bridge (Fig. XI-5b) is predicted to be most stable, in agreement with the most recent experimental studies.

The results so far have indicated that ab initio molecular orbital theory can provide useful structural information on metal-halide complexes not studied experimentally and can complement experimental studies of salt vapors.

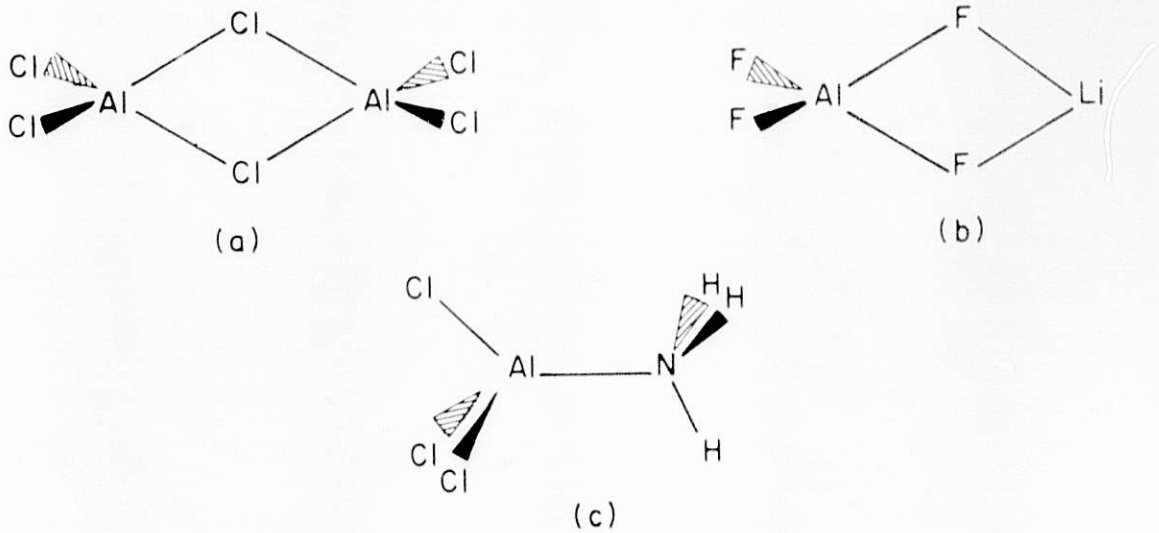

Fig. XI-5. The Predicted Most Stable Structures for Al_2Cl_6, $LiAlF_4$, and $AlCl_3 \cdot NH_3$ Using ab initio Molecular Orbital Theory

Our aims are to further develop our theoretical statistical mechanical and quantum mechanical calculations to make them useful tools in high-temperature chemistry. We plan studies of more molecules using molecular orbital calculations and are developing techniques for making P-V-T, vapor density, and thermal conductivity measurements of ionic vapors.

c. Spectroscopic Studies of High-Temperature Molten-Salt Vapors and Vapor Complexes

The formation of stable gaseous complexes between many metal halide and "acidic gases"[29,30] (e.g., A_2X_6; A = Al, In, Fe....., X = halide) leads to a potentially useful method for the volatilization of involatile halides. Our studies are directed to the preparation of a variety of vapor complexes and the determination of their structural and thermodynamic properties.

We have partially updated and redesigned the laser-Raman system for high-temperature measurements of vapors and vapor complexes.

The formation of vapor complexes between transition metal chlorides MCl_2 (M = Fe, Co, Ni, Cu, Zn) and indium(III) chloride has been investigated. Simple tube-furnace experiments showed the existence of these complexes. Raman spectroscopic studies for all these systems were conducted. At elevated temperature, the vapor mixture formed contains vapors of MCl_2, which, in most cases, yield resonance Raman and/or strong fluorescence spectra. It was thus necessary to investigate the spectra of the MCl_2 vapors to distinguish their vibrational frequencies from those of the vapor complex. Of all systems studied, only the Cu-In-Cl system gave rise to resonance Raman signals characteristic of the $CuInCl_5$ molecule. Examples of the spectra are presented in Fig. XI-6.

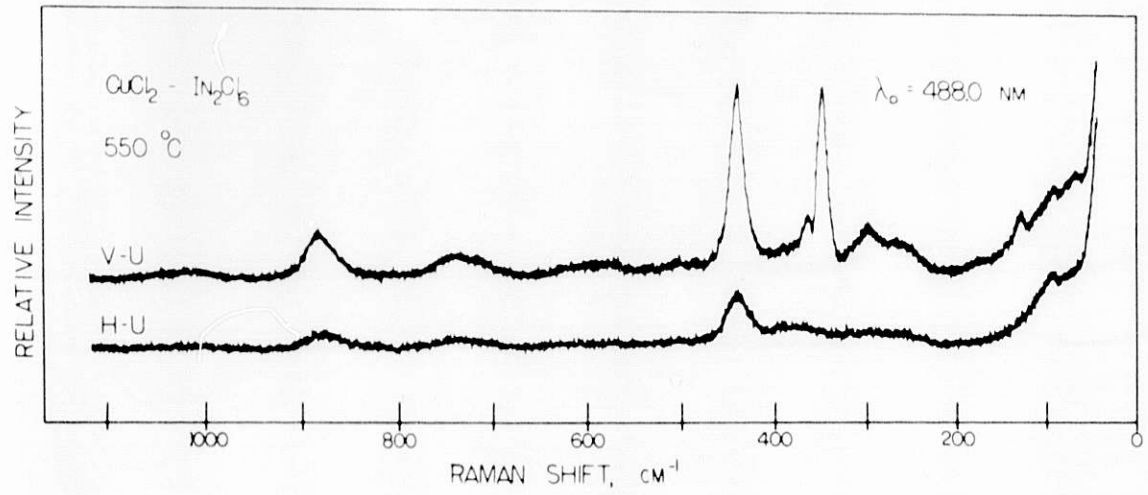

Fig. XI-6. Polarized Raman Spectra of the Cu-In-Cl Vapors. [Observed bands are attributed to $InCl_3(g)$ and $CuInCl_5(g)$.]

[29] G. N. Papatheodorou and G. H. Kucera, Inorg. Chem. 16, 1006 (1977) and references therein.

[30] H. Schafer, Angew. Chem., Int. Ed. 15, 713 (1976).

Spectra obtained with the Zn-In-Cl system consisted of a superposition of the indium chloride fundamentals and the symmetric stretch of the MCl_2 triatomic molecule. At temperatures above 700°C, the Co-In-Cl and Ni-In-Cl spectra were dominated by the fluorescence spectra of $CoCl_2$ and $NiCl_2$, respectively. At lower temperatures, where the MCl_2 pressures were low, only the characteristic indium chloride frequencies were observed.

New methods have been devised and used for the preparation of anhydrous chemicals by simultaneous chlorination and vapor transport of the oxides with acidic gases, e.g.,

$$6UO_2(s) + 4Al_2Cl_6(g) + 3Cl_2 \xrightarrow{300°C} 6UCl_5(s) + 4Al_2O_3(s)$$

$$\downarrow \; Al_2Cl_6 \text{ (vapor transport)}$$

$$U_2Cl_{10} \text{ (crystals)}$$

Raman spectra of U_2Cl_{10} vapors and of the vapor complex[31] $UAlCl_8$ have also been measured. Resonance enhancement of the Raman intensities of the U-Cl_t stretching mode has been observed. Furthermore, measurements of Raman band intensities using variable laser power (Fig. XI-7) have shown that with increasing power the spectroscopic temperature increases and the $UAlCl_8$ vapor complex partially dissociates:

$$2UAlCl_8(g) \xrightarrow{h\nu} U_2Cl_{10}(g) + 2AlCl_3(g)$$

We are presently involved in similar spectroscopic studies using transition metal halides with Al_2Cl_6 and Fe_2Cl_6 gases as carriers. Such volatility enhancement holds promise for use in chemical separations, crystal growth, and the construction of high-efficiency lamps[32] and high-power lasers.[33] Furthermore, knowledge of vapor complexes is important to the understanding of new industrial processes aimed at energy conservation. Examples are the uses of Al_2Cl_6 in the aluminum industry and of Fe_2Cl_6 for the extraction of nickel chloride in the nickel industry.

In the future, emphasis will be given to the $TiCl_x$, $NiCl_2$, and $CuCl_2$ complexes with Fe_2Cl_6 as the carrier gas. The uses of vapor complexes for preparing graphite intercalates of paramagnetic transition metal halides are to be studied.

---

[31] D. M. Gruen and R. L. McBeth, Inorg. Chem. 8, 2625 (1967).

[32] Proceedings of the Symposium on High-Temperature Metal Halide Chemistry, D. L. Hildenbrand and D. C. Cubicciotti, Eds., Electrochem. Soc., Inc., pp. 95-105 (Dec. 22, 1978).

[33] Laser Program Annual Report, Lawrence Livermore Laboratory Report, UCLR 50021-75 (March 1976).

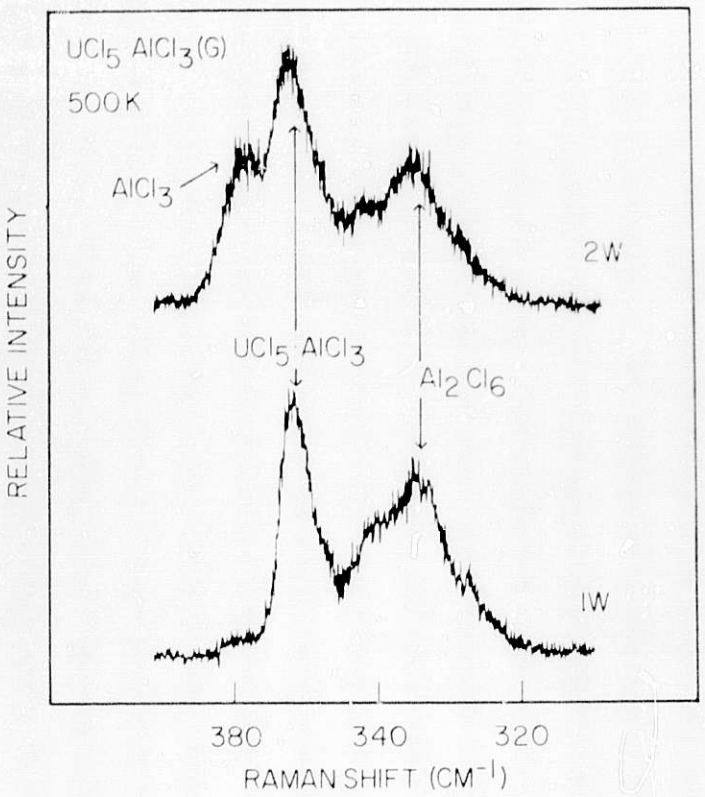

Fig. XI-7. Effect of the Intensity of the Excitation Line on the Raman Spectra of $UAlCl_8$ Vapors

F. Electrochemistry

1. EMF Studies of Sulfide Solubilities in Molten Salt Systems

The solubilities of lithium sulfide and solubility products of lead sulfide in the LiCl-KCl and LiCl-LiF eutectic compositions have been measured by an electrochemical titration method in the temperature range of 673 to 823 K using a cell represented schematically as

$$Ag/AgCl \text{ in eutectic}//\text{eutectic} + PbCl_2 + Li_2S/Pb$$

At 823 K, the solubility of Li_2S in the LiCl-LiF eutectic was much larger than in the LiCl-KCl eutectic (in mole fraction units, 2.0×10^{-2} compared with 3.5×10^{-3}). The measured solubility product of PbS in the LiCl-KCl eutectic is 1.0×10^{-10} and in the LiCl-LiF eutectic, 6.8×10^{-11} at 823 K. A priori calculation of the solubility product of PbS in the LiCl-KCl eutectic leads to a value that agrees with the measurements well within the uncertainties in the calculated value. A theoretical analysis was made of the differences between the two solvents utilizing theories of molten salt solutions developed at this laboratory. This analysis indicates that the calculated activity coefficient of Li_2S is higher and that of $PbCl_2$ is lower in the LiCl-KCl eutectic

than in the LiCl-LiF eutectic. The first factor explains the higher solubility of Li_2S in the LiCl-LiF eutectic and the cancellation of these two factors leads to solubility products of PbS in the two mixtures that differ little.

2. Studies of Electrocatalysis

These investigations are designed to elucidate the action of certain substances in catalyzing the electrochemical reduction of simple molecules. Initial studies deal with the kinetics and mechanism of electroreduction of oxygen on carbon-supported iron phthalocyanine electrodes. These electrodes are known to catalyze oxygen reduction, but the mechanisms of the reduction reaction and of electrode deactivation are poorly understood. Spectroscopic and electrochemical techniques are being employed to determine the role of surface interactions and interfacial structure on the kinetic behavior of the oxygen-phthalocyanine-carbon electrode system and ultimately on the mechanisms.

Initial work has concentrated on the electrode substrate. We have shown that, at vitreous carbon rotating disk (with ring) electrodes in 6N H_2SO_4 solution, oxygen reduction proceeds *via* the production of hydrogen peroxide as intermediate, *i.e.*

$$O_2 + 2H^+ + 2e^- = H_2O_2 \qquad E^\circ = 0.682 \text{ V } \underline{\text{vs.}} \text{ SHE}^* \qquad (5)$$

$$H_2O_2 + 2H^+ + 2e^- = 2H_2O \qquad E^\circ = 1.77 \text{ V} \qquad (6)$$

Moreover, the reduction of hydrogen peroxide appears to be kinetically hindered by a slow charge-transfer step. Deposition of iron(II) phthalocyanine (FePc) on a vitreous carbon support was accomplished and the anticipated catalytic effect on oxygen reduction was observed. Mössbauer spectroscopy studies of adsorption of FePc on carbon showed a strong interaction of the iron with the carbon support leading to partial oxidation of the iron. Oxygen-containing functional groups on the carbon surface are believed to be responsible for this oxidation. It was also found that classical procedures for preparing FePc-on-carbon electrodes, *e.g.*, precipitation from a concentrated H_2SO_4 solution and the use of a pyridine solution, invariably result in a change in electronic structure around the central iron atom. The results obtained so far, which are preliminary, give us confidence that our approach may lead to a better understanding of a process that is important in fuel cells, metal-air batteries, and human metabolism.

Future work will involve characterization of the iron-oxygen interaction by surface chemical techniques (*e.g.*, ESCA†) and "*in-situ*" Mössbauer and optical (*e.g.*, UV, visible, and Raman) spectroscopy. Differential capacitance measurements will be undertaken to obtain information on double-layer structure. In addition, measurements of rate constants will be made in acid and neutral solutions, which we hope to correlate with interfacial structure and surface interaction of the catalyst.

---

*Standard hydrogen electrode.

†Electron spectroscopy for chemical analysis.

3. Electrode Reaction Kinetics

Studies of electrode reaction kinetics of metal deposition/dissolution in molten salts are under way to gain fundamental insights into these processes, many of which have significance in metallurgical and battery technologies. The first system being investigated is that of iron in the LiCl-KCl eutectic melt for which the reaction is so fast that it is outside the range of most relaxation techniques used for electrode kinetics investigations.[34-37] An analysis was made of the most promising method, the double-pulse technique, to establish the technique's applicability for such fast reactions before starting on an extensive experimental approach. This analysis indicated that the double-pulse technique needed modification to be applicable to our purposes. This modification has been made and we have shown, through an error calculation, that the technique will be limited only by experimental random error rather than by instrumental characteristics.

Finally, a cell has been designed which we believe will fulfill the rigorous requirements of the modified double-pulse technique. This cell will be utilized to perform measurements on Fe in the LiCl-KCl eutectic in order to test our theoretical development and the technique. In the future, we plan to study the deposition/dissolution kinetics of iron sulfides and of other metals, such as Ni and Mo, in the LiCl-KCl eutectic to understand the fundamentals of these processes and to gain information related to the high-energy-density batteries under development at Argonne.

---

[34] D. J. Kooijman and J. H. Sluyters, J. Electroanal. Chem. Interfacial Electrochem. 13, 152 (1967).

[35] H. P. Van Leeuwen and J. H. Sluyters, ibid., 42, 313 (1973).

[36] H. Gerischer and M. Krause, Z. Phys. Chem. (Frankfurt) 10, 264 (1957).

[37] H. Matsuda, S. Oka, and P. Delahay, J. Am. Chem. Soc. 81, 5077 (1959).

XII. ANALYTICAL CHEMISTRY LABORATORY

A. Overview

The Analytical Chemistry Laboratory (ACL) is operated by CEN as a central analytical facility for Argonne's scientific and engineering programs. Its principal functions are (1) to provide assistance to scientists and engineers in solving analytical problems that arise in the course of their normal programmatic activities; (2) to perform routine analyses, thereby utilizing the laboratory's resources efficiently; and (3) to conduct research and development activities as required to provide the ACL with the capability of meeting the present and projected needs of the Laboratory's programs.

A summary of the activities of the ACL is presented in Table XII-1. The ACL, which is operated as a full-cost-recovery service center, has

Table XII-1. Summary of ACL Activities

Major ACL Users:		% of Total
Chemical Engineering		
Nuclear Waste Management	3.8	
Nuclear Fuel Cycle	7.0	
LWBR Proof of Breeding	13.4	
Sodium Technology	1.5	
Battery Development	5.4	
Fluidized-Bed Combustion	7.6	
Fuel Cell	2.5	65.8
Atmospheric Chemistry	6.8	
Dosimetry	4.1	
Lithium Processing Technology	0.6	
Analytical Instrument Development	0.8	
EPRI-EXXON Pu Recyle	7.7	
Others	4.6	
Materials Science		5.4
Biological and Medical Research		3.8
Reactor Analysis and Safety		0.7
Applied Physics		0.8
Chemistry		6.6
Research Reactor Operations		0.5
Radiological and Environmental Research		4.9
SAREF Project Control		0.8
Energy and Environmental Systems		4.4
Work for Others		1.7
Other ANL Divisions		4.6
		100.0

Personnel: thirty

Current Level of Effort:

Approximately 1,500 jobs per year requiring more than 16,000 separate analyses of all types

continued to grow during the past several years--both in personnel and capabilities. However, new Laboratory-wide guidelines from DOE on manpower limitations and Laboratory management's views on the role of service centers in meeting ANL's programmatic objectives must be clarified before an assessment can be made of the prospects for continued growth of the ACL.

B. Role of the ACL in Major R&D Programs

During the past year, the single largest user of ACL services has been CEN's Proof-of-Breeding Project, the purpose of which is to determine the extent of breeding in a Light Water Breeder Reactor (see Section IX.D). In this project, fuel-rod segments, cut with high precision, are dissolved, and samples of the solution are assayed for uranium content and isotopic composition and for selected fission products, namely, ^{137}Cs, ^{144}Ce, and ^{95}Zr. During the development phases of the dissolution process, the ACL provided support by preparing samples for dissolution and developing the appropriate separations and cleanup procedures necessary for the mass-spectrometric measurements.

Results for the Proof-of-Breeding Project must meet stringent error limits (see Section IX, Table IX-1) for accuracy and precision. A particularly difficult problem has been the very high precision required for mass-spectrometric results, which is near the limit of instrumental capability. The requisite precision has been achieved as a result of the extreme care exercised by all personnel involved and the use of an innovative approach, namely, introduction of the natural uranium "spike" into the dissolver solution rather than into individual aliquots. This procedure is an example of the advantages to an R&D program of involving the ACL in the planning of experiments.

Another program that has become prominent in the past year is the Coal Toxicology Program in the Division of Biological and Medical Research (BIM). In support of this program, the ACL is fractionating and characterizing crude samples from coal conversion and combustion processes, with the objective of preparing the material for mutagenicity and toxicity testing by BIM. Data on biological effects and chemical composition will then be correlated to assess the biological hazards of coal-utilization processes. Samples studied to date include condensed vapors from the effluent stream of a pressurized fluidized-bed combustor (FBC), fly-ash samples collected from the precipitators of a conventional coal combustion facility, and oil and quench-water samples obtained from a pilot-scale high-Btu gasification facility. The techniques employed in analyzing these samples include various types of extractions (separatory funnel, Soxhlet, and column), distillation, vacuum sublimation, and column chromatography. Samples have been "fingerprinted" by gas chromatography and infrared spectroscopy, and selected samples have been sent to commercial laboratories for gas chromatographic/mass spectrometric analysis. The material from the pressurized FBC effluent appears to be primarily polynuclear aromatic hydrocarbons; material from the fly ash is significantly more polar; and that from the high-Btu gasification process contains the whole spectrum of organic compounds, especially cycloparaffins and phenols.

C. New Capabilities and Procedures

During 1978, the Analytical Chemistry Laboratory expanded its capabilities in a number of areas. Requests from the Materials Science Division, as well as several programs within CEN, for surface-area measurements led to the acquisition of a state-of-the-art BET surface-area apparatus. A scanning electron microscope (SEM), complete with nondispersive X-ray detection for the identification of specific elements, is now in operation in the ACL. With the SEM, a new mode of user/ACL interaction has been introduced, namely, that qualified operators trained by ACL personnel also have direct access to the use of the instrument; for this particular instrument, this method of operation appears to be working very well. A recently developed instrument, an ion chromatograph, which is suitable for the analysis of multiple anions or cations in a water solution, has been acquired and placed in operation. Ion chromatography shows considerable promise as a rapid, accurate and dependable technique with wide applicability in wet-chemical analysis.

We have made significant improvements in a laser-beam sampling method for determining the radial distribution of fission gas (primarily ^{85}Kr) in irradiated nuclear fuels. This work has been done in support of programs in the Materials Science Division and the Reactor Analysis and Safety Division. The method involves the use of a pulsed laser beam, focused by means of microscope optics on a selected area of fuel cross section, to ablate a micro-portion (about 10-μm dia) of the fuel and thereby release retained fission gas. The released gas, after dilution with a carrier gas of inactive krypton, is collected and the ^{85}Kr content determined. Improvements in the method have resulted from installation of new equipment--a closed-circuit television system for sample viewing and on-line proportional gas counting equipment--and, most important, from advances in data-interpretation techniques. The improved data interpretation has made it possible to determine not only the fission gas content of various regions of the fuel, but the distribution of gas between intra- and inter-granular sites.

A plutonium analytical facility has been planned and constructed during the past two years. This facility has been placed in operation on a limited basis to support the EPRI/EXXON Plutonium Recycle Program in CEN, as well as the Proof-of-Breeding Project. When fully operational, the facility is expected to meet the ACL's needs for the foreseeable future in the analysis of samples of plutonium and other transuranic elements.

D. Development of Instrumentation for Organic Analysis

The acquisition of direct funding from DOE for analytical instrument development for organic materials was reported last year. This program has proceeded very satisfactorily during 1978, the principal result being the acquisition of a PDP-11/60 computer system* and a CVC time-of-flight mass spectrometer.† These devices, together with a gas-chromatograph inlet system for the mass spectrometer, are expected to produce a gas-chromatograph/mass-spectrometer/data-system (GC/MS/DS) package that will appreciably advance

---

*Digital Equipment Corp., Maynard, MA.

†CVC Products, Inc., Rochester, NY.

the state of the art in this field. Specific features that are expected to make the system superior to existing systems are: (1) unattended operation, with automatic sample injection and automated data acquisition, analysis, and output; (2) adequate sensitivity to identify picogram levels of unknown compounds; (3) resolution of multiple-component GC peaks by the mass spectrometer and data system; (4) significantly lower run time per sample; (5) high-performance, general-screening analysis for diverse sample types without the need for changing equipment operating parameters; and (6) special inlet capabilities on the mass spectrometer that will provide for the analysis of organic constituents from sources other than the outlet of the gas chromatograph. The Electronics and Applied Mathematics Divisions at Argonne will participate in full development of this system by assisting as necessary to develop those features of the system that are currently beyond the state of the art. It is expected that the development of this advanced GC/MS/DS unit will give the ACL the capability for organic analysis necessary to meet the increasing needs, already established, of programs in the BIM Division, as well as the less well defined needs of programs dealing with fossil fuels throughout the entire Laboratory.

E. Future Plans

During the coming year, the ACL will continue to provide a high level of analytical support to various divisions within the Laboratory. Because of a manpower ceiling placed on the Laboratory, a manpower limit can be expected to be imposed on the ACL. It is likely, therefore, that a significant portion of the ACL work will have to be subcontracted to other analytical facilities in the Chicago area. Maintenance of proper quality assurance on these samples presents a new dimension for the Analytical Laboratory in the future. It can be expected that these quality assurance requirements, together with increasing consciousness of the need for quality assurance by programs within ANL, will require new initiatives in the Analytical Chemistry Laboratory to document the quality of the results produced.

XIII. COMPUTER APPLICATIONS

The computer applications group provides assistance to Division staff members in all phases of computer-related activities. The major areas of effort consist of (1) computer modeling and simulation, (2) laboratory automation, (3) data-base development, and (4) general support (e.g., consulting, equipment specification, etc.). Some of the major contributions in these areas are described below.

A. Computer Modeling and Simulation

1. A program has been developed to calculate potential surfaces, equipotential contours, and current-density distributions for a single collector plate in a Li/MS_x cell. To date, the program (which is based on the DISPL code[1]) has been utilized for rectangular plates of various thicknesses. Typical results are given in Fig. XIII-1, where a normalized electrical potential is shown as a function of distance from the top and center of the collector plate. The equipotential curves represent the loci of points defined by the intersection with the potential surface of planes parallel to the R and Z axes. Further efforts will include the addition of special current collectors and variation of geometry with the goal of optimizing cell design by reducing weight and minimizing potential drop and heating effects.

2. A mathematical model was constructed to calculate tritium concentrations during release and cleanup after a hypothetical accident in a fusion reactor plant. Solution to a set of nonlinear differential equations containing experimentally determined parameters yields time-dependent variation of resultant compounds. The model accounts for permeation through walls by HT and for adsorption and release of HTO at wall surfaces. Clean-up is accomplished by forcing air through the plant and subsequently through a scrubber.

3. A NASA code[2] for the calculation of complex chemical equilibria has been modified to allow for the formation of a multicomponent, nonideal solution from pure condensed species. The program provides for up to 12 components in solution. Calculations have been performed on a system containing a ten-component ideal solution. This system approximates the condensation of refractory metals from a dense solar nebula, from which it is believed the solar system formed 4.6 billion years ago. Work is proceeding on utilizing the program for nonideal solutions, and the method has been successfully tested for several nonideal binary systems.

---

[1] G. K. Leaf, M. Minhoff, G. D. Byrne, D. Sorenson, T. Bleakney, and J. Sultzmarn, DISPL: A Software Package for One and Two Spatially Dimensioned Kinetics Diffusion Problems, Argonne National Laboratory Report ANL-77-12 (May 1977).

[2] S. Gordon and B. M. McBride, Computer Program for Calculation of Complex Chemical Equilibrium Compositions, Rocket Performance, Incident, and Reflected Shocks, and Chapman-Jonguet Detonations, National Aeronautics and Space Administration Report NASA SP-272 (1971).

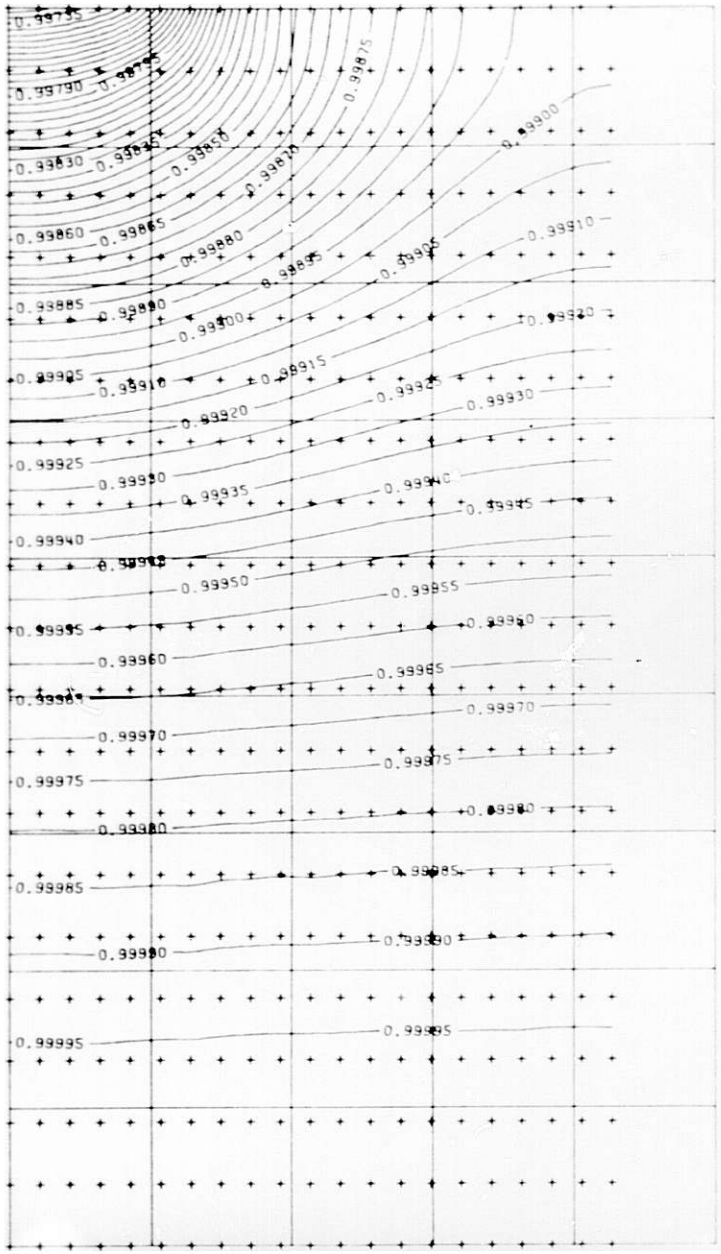

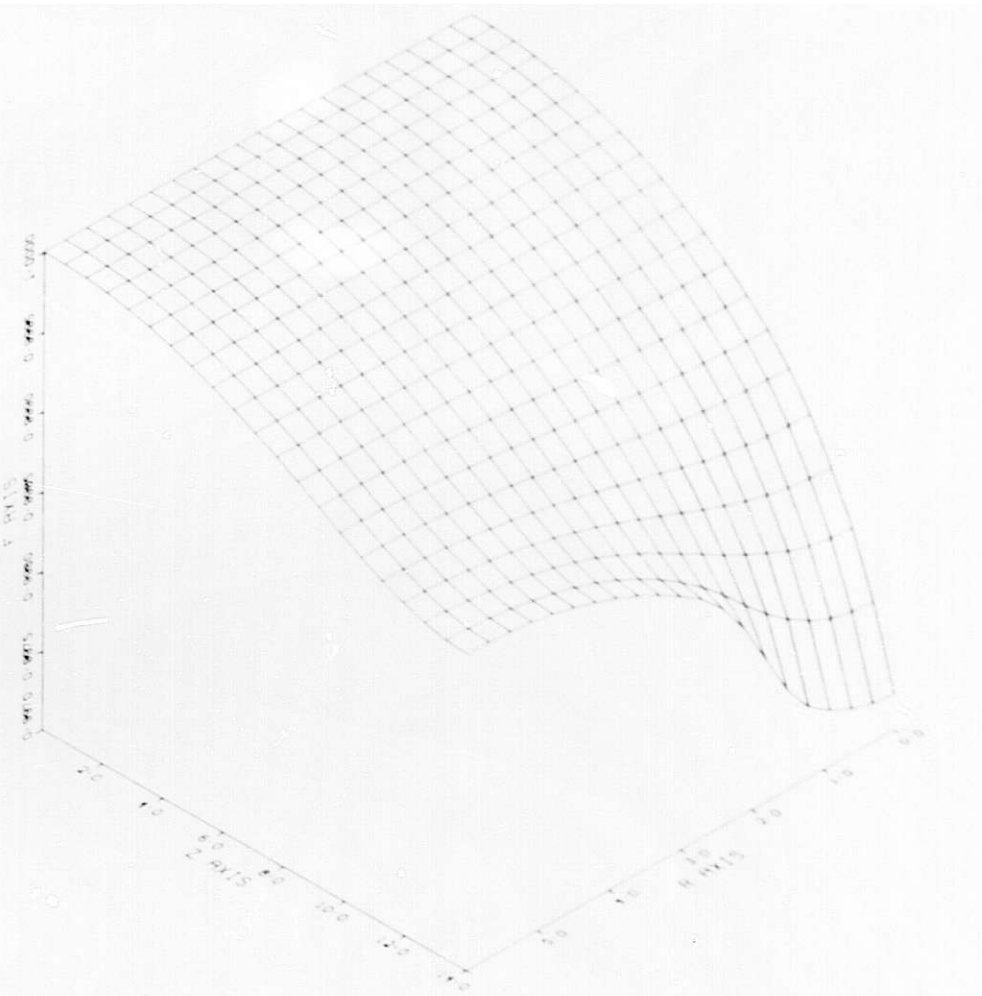

Fig. XIII-1.

Potential Surface and Equipotential Contours for Flat-Plate Collector for Li/MS_x Cell.

4. A model has been developed for fluidized-bed combustion of coal char coupled with sulfur retention by limestone, based on a mechanism of noncatalytic, single-particle gas-solid reaction. Formulation of the model included setting up the heat and mass balance equations pertaining to a single particle exposed to a varying reactant concentration along the height of the bed, with accompanying change in particle size during the course of reaction. These equations were then solved numerically to account for all sizes of particles in the bed in order to obtain the overall carbon conversion efficiency and resultant sulfur retention.

B. Laboratory Automation

Support of laboratory automation activities has continued for the National Battery Test Laboratory, the ambient-temperature and lithium/metal-sulfide high-temperature battery programs, and the ion-microprobe facility. In addition, during the past year, several major improvements to CEN's data-acquisition capabilities have been made. Three systems based on a Digital Equipment Corporation PDP 11 family of processors have been installed and are in initial programming phases. The first of these will be used to acquire data from a 50-cell Li/MS_x life-test facility and to acquire data and control cell tests for the Li/MS_x battery program's cell development and engineering group. Another system will be used by the reactor safety group to automate a number of experiments, including viscosity, calorimetry, density, and thermal diffusivity measurements of reactor materials. The third large system will be used to control the collection and processing of data from the Analytical Chemistry Laboratory's new gas-chromatograph/mass-spectrometer system (see Section XII.D). A small system is also being planned for the automation of some new analytical X-ray equipment. Several microcomputer systems have been purchased as ancillary processors and development aids for the National Battery Test Laboratory.

C. Data-Base Management and Development

Data bases have been set up to assist CEN staff members having the responsibility of reviewing or coordinating the review of proposals solicited by the Department of Energy. The data bases have been used to centralize information collection and to generate reports and statistical data. One such project, in which approximately 500 proposals on solar heating were reviewed, has been completed. Another, involving over 1200 proposals for "energy-related appropriate technology," is in progress. Data bases are also being set up to assist Divisional administrative personnel in various types of record keeping (e.g., personnel directories and author files).

D. General Support

In addition to offering general consulting and data management services, the computer applications group maintains a computer documentation library, and is responsible for the Division's time-sharing and batch-entry facilities and its audio-visual minicomputer course materials.

E. Future Plans

The CEN Division is currently participating in an experimental program of the Applied Mathematics Division (AMD) to develop a laboratory-wide minicomputer network. Through nodes such as the one in CEN, minicomputers will be able to send data and submit jobs to the batch-computing facility at AMD and will further be able to transfer files from one minicomputer system to another. Current thinking at AMD leans toward development of a distributed computer system to off-load time-sharing from the central computing facility. CEN will be exploring this concept carefully with AMD to determine how best to provide sorely needed improvements in the over-burdened time-sharing facilities presently available to the ANL user community.

XIV. ADDENDUM.

CHEMICAL ENGINEERING DIVISION PUBLICATIONS--1978

A. Open-Literature Publications

M. A. Abdou, R. G. Clemmer, et al.
Systems Studies on Technology and Economics of Tokamak Power Plants
Trans. Third Topical Meeting on Technology of Controlled Nuclear Fusion, Santa Fe, NM, p. 163 (May 1978)

J. E. Battles, J. A. Smaga, and K. M. Myles
Materials Requirements For High Performance Secondary Batteries
Metall. Trans. 9A, 183 (February 1978)

M. Blander
Inconsistencies in a Criticism of the Flood-Grjotheim Treatment of Slag Equilibria
Metall. Trans. 8B, 529-530 (December 1977)

M. Blander and M. L. Saboungi
Thermodynamic Properties of Molten Salt Slags
Extended Abstracts Electrochem. Soc. Meeting, Seattle, WA, May 21-26, 1978, Vol. 78-1, pp. 1080-1081 (1978)

M. Blander
The Thermodynamics of Solid Solutions Based on the Two Site Model
Proc. CALPHAD VII Workshop, Stuttgart, Germamy, pp. 159-163 (April 1978)

M. Blander and H. R. Leribaux
Equations of State for Alkali Metals Near their Critical Point
Proc. Seventh Symp. on Thermophysical Properties, ASME, pp. 882-886 (1977)

R. A. Blomquist, J. K. Fink, and L. Leibowitz
Viscosity of Molten Alumina
J. Am. Ceram. Soc. 57(5), 522 (May 1978)

L. Burris and P. A. Nelson
Advanced Batteries for Vehicle Propulsion
Soc. of Automotive Engineers, Earthmoving Industry Conf., Peoria, IL, April 10-12, 1978, Technical Paper 780458 (1978)

W. F. Calaway
Electrochemical Extraction of Hydrogen from Molten LiF-LiCl-LiBr and Its Application to Liquid Lithium Fusion Reactor Blanket Processing
Nucl. Technol. 39, 6 (June 1978)

M. A. Capote and G. N. Papatheodorou
Spectrophotometric and Raman Spectroscopic Studies of the Palladium(II) Bromide-Aluminum Bromide Vapor Complexes
Inorg. Chem. 17(12), 3414-3418 (1978)

M. A. Capote, G. H. Kucera, and G. N. Papatheodorou
Spectra and Thermodynamics of Palladium(II) Bromide-Aluminum Bromide and Palladium(II) Chloride-Indium Chloride Vapor Complexes
High Temperature Metal Halide Chemistry, D. D. Cubicciotti and D. L. Hildenbrand, Eds., p. 367 (1978)

M. J. Chen and H. M. Feder
Chloro-meso-tetraphenylporphyrinatocobalt(III) as Catalyst for Quadricyclane Isomerization
J. Catal. 55 105 (1978)

K. W. Choi and N. P. Yao
Thermal Analysis of Lead-Acid Cells for Load-Leveling Applications
J. Electrochem. Soc. 125(7), 1011-1019 (July 1978)

K. W. Choi and N. P. Yao
Heat Transfer in Lead-Acid Batteries
ASME Publication 78-HT-52 (1978)

R. G. Clemmer
Impact of Plasma Performance Parameters Upon the Vacuum and Tritium System Design Requirements for Near-Term Tokamak Reactors
Fusion Reactor Design Concepts, International Atomic Energy Agency Report IAEA-TC-145/34, pp. 537-546 (December 1978)

R. G. Clemmer, R. H. Land, and A. G. Rogers
Computer Modeling and Bench-Scale Testing of Air Detritiation Operations
Trans. Am. Nucl. Soc. 30, 41 (November 1978)

E. H. P. Cordfunke and P. A. G. O'Hare
The Chemical Thermodynamics of Actinide Elements and Compounds. Part 3. Miscellaneous Actinide Compounds
International Atomic Energy Agency, Monograph, Part III (1978)

L. A. Curtiss, D. J. Frurip, and M. Blander
A Study of Dimerization in Water Vapor by Measurement of Thermal Conductivity
Chem. Phys. Lett. 54(3), 575 (March 15, 1978)

L. A. Curtiss, D. J. Frurip, and M. Blander
Studies of Hydrogen Bonding in the Vapor Phase by Measurement of Thermal Conductivity and Molecular Orbital Calculations. 2,2,2-Trifluoroethanol
J. Am. Chem. Soc. 100, 79 (1978)

L. A. Curtiss
Molecular Orbital Studies of Al_2F_6 and Al_2Cl_6 using a Minimal Basis Set
Int. J. Quantum Chem. XIV, 709-715 (December 1978)

D. C. Fee and C. E. Johnson
Phase Equilibria in the Cs-U-O System in the Temperature Range From 873 to 1273 K
J. Inorg. Nucl. Chem. 40, 1375-1381 (September 15, 1977)

D. C. Fee and C. E. Johnson
The Interactions of Cesium with Urania in Urania-Plutonium-Oxide Fast Reactor Fuel Pins
J. Nucl. Mater. 78, 219-224 (1978)

J. K. Fink, J. J. Heiberger, and L. Leibowitz
Interactions of UO_2 with Reactor Materials
Proc. Third Post-Accident Heat Removal Information Exchange, pp. 415-423 (November 2-4, 1977)

P. A. Finn, K. Kinoshita, G. H. Kucera, and J. W. Sim
Synthesis of Lithium Aluminate for Molten Carbonate Fuel Cell Applications
Extended Abstracts, 1978 National Fuel Cell Seminar, DOE/EPRI, San Francisco, CA, July 11-13, 1978, p. 110 (1978)

P. A. Finn
The Thermal Stability of Lithium Aluminate
Extended Abstracts Electrochem. Soc. Meeting, Pittsburgh, PA, October 15-20, 1978, Vol. 78-2, p. 696 (1978)

D. J. Frurip, L. A. Curtiss, and M. Blander
A Comparitive Study of Associated Species in Vapors of Alcohols and Water by Measurement of Thermal Conductivity
Proc. Seventh Symp. on Thermophysical Properties, ASME, p. 721 (1978)

D. J. Frurip, L. A. Curtiss, and M. Blander
Characterization of Molecular Association in Acetone Vapor: Thermal Conductivity Measurements and Molecular Orbital Calculations
J. Phys. Chem. 82(24), 2555-2561 (1978)

L. H. Fuchs, E. L. Nielsen and B. R. Hubble
Use of Oil Shale for Control of Sulfur Dioxide Emissions from the Combustion of Coal
Thermochim. Acta 26, 229-239 (1978)

R. Graven, A. Corski, W. Schertz, and J. E. A. Graae
Modular Assembly of a Photovoltaic Solar Energy Receiver
U.S. Patent No. 4,118,249 (October 3, 1978)

O. Gotzmann, C. E. Johnson, and D. C. Fee
Attack of Stainless Steel by Liquid and Vaporized Cesium Hydroxide
J. Nucl. Mater. 74, 68 (1978)

D. W. Green and G. T. Reedy
Matrix-Isolation Studies with Fourier Transform Infrared
Chapter 1 in Fourier Transform Infrared Spectroscopy.
Applications to Chemical Systems, J. R. Ferraro and
L. J. Basile, Eds., Academic Press, New York, Vol. 1 (1978)

D. W. Green and G. T. Reedy
Infrared Spectra of Matrix-Isolated Plutonium Nitrides
J. Chem. Phys. 69, 552 (1978)

D. W. Green and G. T. Reedy
Infrared Spectra of Matrix-Isolated Plutonium Oxides
J. Chem. Phys. 69(2), 544-551 (July 15, 1978)

D. W. Green and G. T. Reedy
Matrix Isolation Studies with Fourier Transform IR
Ber. Bunsenges. Phys. Chem. 82, 90-91 (1978)

D. W. Green, G. T. Reedy, and L. Leibowitz
Thermodynamic Functions and Vapor Pressures of Uranium and Plutonium Oxides at High Temperatures
Proc. Seventh Symp. on Thermodynamic Properties, ASME,
pp. 379-385 (1978)

L. R. Greenwood
Damage Analysis and Fundamental Studies Quarterly Progress Reports,
January-March, 1978, DOE/ET-0065/1; April-June, DOE/ET-0065/2;
July-September, DOE/ET-0065/3; October-December, DOE/ET-0065/4

L. R. Greenwood, R. R. Heinrich, R. J. Kennerley, and R. Medrzychowski
Development and Testing of Neutron Dosimetry Techniques for Accelerator-Based Irradiation Facilities
Nucl. Technol. 41(1), 109 (November 1978)

J. J. Heiberger, J. K. Fink, and L. Leibowitz
Observations on Effects of Stainless Steel on UO_2-Graphite Interactions
Trans. Am. Nucl. Soc. 28, 527-528 (June 1978)

B. D. Holt, M. F. Bouchard, P. T.Cunningham, A. Engelkemeir, E. L. Nielsen, S. A. Johnson, and R. Kumar
Oxygen Isotopes in Atmospheric Sulfates, Sulfur Dioxide, and Water Vapors, Field Measurements, July 1975
U.S. Environmental Protection Agency Report No. EPA-600/3-78-045 (April 1978)

B. D. Holt, R. Kumar, P. T. Cunningham, M. F. Bouchard, A. G. Engelkemeir, S. A. Johnson, E. L. Nielsen, and J. D. Shannon
Regional ^{18}O Variations in Particulate Sulfate and Water Vapor at Three Sampling Sites about 100 km Apart
Environ. Sci. Technol. 12, 1394-1398 (1978)

B. D. Holt, P. T. Cunningham, and A. G. Engelkemeir
Application of Oxygen-18 Analysis to the Study of Atmospheric Sulphate Formation
Stable Isotopes in the Earth Sciences, B. W. Robinson (comp. and ed.), New Zealand DSIR Bulletin 220, pp. 105-109 (1978)

F. Hornstra and N.P. Yao
Test Methods and Facilities at the National Battery Test Laboratory
Extended Abstracts Electrochem. Soc. Meeting, Pittsburgh, PA, October 15-20, 1978, Vol. 78-2, No. 102 (1978).

C. C. Hsu and M. L. Saboungi
Calculations of Isothermal Sections of the Ca-Li-Mg System
Z. Metallkd. 69, 581-586 (March 3, 1978)

B. R. Hubble, S. Siegel, and P. T. Cunningham
Regeneration of Sulfated Metal Oxides and Carbonates
U.S. Patent 4,081,522 (March 28, 1978)

A. H. Jaffey, H. Diamond, W. C. Bentley, D. G. Graczyk, and K. F. Flynn
The Half-Life of ^{240}Pu
Phys. Rev. C. 18, 969 (1978)

A. H. Jaffey, H. Diamond, W. C. Bentley, K. F. Flynn, D. J. Rokop, A. M. Essling, and J. Williams
The Half Life of ^{239}Pu: By Specific Activity Measurements and by Mass Spectrometric Determination of Daughter Growth
Int. J. Appl. Radiat. Isotopes 29, 505-507 (1978)

L. J. Jardine and M. J. Steindler
Metal Matrix Encapsulation of Waste
Proc. Waste Management and Fuel Cycles '78, Tucson, AZ, March 6-8, 1978, p. 388 (1978)

C. E. Johnson and D. C. Fee
Oxygen Getters for Fast Reactor Fuel Pins
Nucl. Technol. 40, 89-97 (August 1978)

G. K. Johnson and P. A. G. O'Hare
Thermochemistry of Uranium Compounds. XI. Standard Enthalpy of Formation of γ-UO_3
J. Chem. Thermodyn. 10, 577-580 (September 6, 1978)

C. S. Kim, R. A. Blomquist, J. Haley, R. Land, J. Fischer, M. G. Chasanov, and L. Leibowitz
Measurement of Thermal Diffusivity of Molten UO_2
Proc. Seventh Symp. on Thermodynamic Properties, ASME, pp. 338-343 (1978)

K. Y. Kim, R. E. Winans, W. N. Hubbard, and C. E. Johnson
Thermochemistry of Coal Components. 1. Xanthone
J. Phys. Chem. 82(4), 402 (1978)

K. Kinoshita and J. P. Ackerman
Method of Preparing Electrolyte for Use in Fuel Cells
U.S. Patent 4,115,632 (September 19, 1978)

K. Kinoshita, J. W. Sim, and J. P. Ackerman
Preparation and Characterization of Lithium Aluminate
Mater. Res. Bull. 13, 445-455 (1978)

K. Kinoshita, J. W. Sim, and G. H. Kucera
Synthesis of Fine Particle Size Lithium Aluminate
Extended Abstracts Electrochem. Soc. Meeting, Pittsburgh, PA October 15-20, 1978, Vol. 78-2, p. 694 (1978)

N. Koura, N. P. Yao, and J. Kincinas
Development of FeS_2 Electrode Current Collector for the Secondary Li-Al/FeS_2 Battery
J. Jap. Electrochem. Soc., 46, 395 (July 1978)

W. G. Lyon, T. W. Osborne, H. E. Flotow, F. Grandjean, W. N. Hubbard, and G. K. Johnson
Thermodynamics of the Lanthanide Trifluorides. I. The Heat Capacity of Lanthanum Trifluoride, LaF_3 from 5 to 350°K and Enthalpies from 298 to 1477°K
J. Chem. Phys. 69(1), 167-173 (July 1, 1978)

F. J. Martino, T. D. Kaun, H. Shimotake, and E. C. Gay
Advances in the Development of Lithium-Aluminum/Metal Sulfide Cells for Electric-Vehicle Batteries
Proc. 13th Intersociety Energy Conversion Engineering Conf., Soc. Automotive Eng., San Diego, CA, August 20-25, 1978, Vol. 1, pp. 709-716 (1978)

F. J. Martino, L. G. Bartholme, E. C. Gay, and H. Shimotake
Development of Li-Al/FeS Cells with LiCl-Rich Electrolyte
Extended Abstracts Electrochem. Soc. Meeting, Pittsburgh, PA,. October 15-20, 1978, Vol. 78-2, pp. 100-103 (1978)

J. P. Mathers, C. W. Boquist, and T. W. Olszanski
Powder Electrode Separators for High Temperature Lithium-Aluminum/Iron Sulfide Batteries
J. Electrochem. Soc. 125(12), 1913-1918 (December 1978)

C. A. Melendres, S. Siegel, and J. Settle
Polarization Behavior and Structure of LiAlMg Alloy Electrodes
J. Electrochem. Soc. 125(11), 1886 (1978)

C. A. Melendres and B. Tani
Mössbauer Spectra and Lattice Parameters of Some New Sulfide Phases of Iron
J. Phys. Chem. 82, 1117 (December 1978)

C. A. Melendres and C. C. Sy
Structure and Cyclic Discharge Behavior of LiAl Electrodes
J. Electrochem. Soc. 125(5), 727 (May 1978)

J. C. Montagna, W. M. Swift, G. W. Smith, G. J. Vogel, and A. A. Jonke
Regeneration of Sulfated Dolomite by Reductive Decomposition with Coal in a Fluidized Bed Reactor
AIChE Symp. Series No. 176, Vol. 74, pp. 203-211 (1978)

J. C. Montagna, F. F. Nunes, G. W. Smith, G. J. Vogel, and A. A. Jonke
High Temperature Fluidization and Limestone Regeneration for Fluid Bed Boilers
CEP Technical Manual, Coal Processing Technology, AIChE, Vol. IV, pp. 87-93 (1978)

Z. Nagy
A Modified Galvanostatic Double Pulse Technique for the Investigation of Fast Electrode Reactions
Extended Abstracts, Electrochem. Soc. Meeting, Seattle, WA, May 21-26, 1978, Vol. 78-1, pp. 1358-1361 (1978)

Z. Nagy
On the Effect of Finite Rise Time of Pulse Generators on Some Relaxation Techniques for Electrode Kinetic Investigations
J. Electrochem. Soc. 125(11), 1809-1811 (1978)

T. W. Olszanski and H. Shimotake
Engineering-Scale Li-Al/FeS Cells with Magnesium Oxide Powder Separators
Extended Abstracts Electrochem. Soc. Meeting, Pittsburgh, PA, October 15-20, 1978, Vol. 78-2, pp. 148-149 (1978)

G. N. Papatheodorou
Magnetic Susceptibilities and Electronic Absorption Spectra of Liquid Aluminum(III) Chloride-Palladium(II) Chloride Mixtures
Inorg. Nucl. Chem. Lett. 14, 249-253 (1978)

G. N. Papatheodorou and M. A. Capote
Resonance Raman Spectra of Inorganic Salt Vapors. I. Palladium(II) and Copper(II) Chloroaluminates
J. Chem. Phys. 69(5), 2067-2075 (September 1, 1978)

G. N. Papatheodorou and M. A. Capote
Resonance Raman Spectra of Divalent Transition Metal Chloroaluminate Vapors
High Temperature Metal Halide Chemistry, D. D. Cubicciotti and D. L. Hildenbrand, Eds., p. 320 (May 1978)

J. E. Parks, I. O. Winsch, C. E. Stevenson, and N. M. Levitz
Analytical Shearing of Fuel Rods in a Hot Cell
Trans. Am. Nucl. Soc. 30, 753 (November 1978)

A. D. Pelton, P. L. Lin, P. Cerisier, and M. L. Saboungi
Phase Diagrams of the $LiF-AlF_3$, $NaF-AlF_3$ and $Li_3AlF_6-Na_3AlF_6$ Systems: Survey and Computations
Extended Abstracts Electrochem. Soc. Meeting, Seattle, WA, May 21-26, 1978, Vol. 78-1, pp. 1082-1083 (1978)

W. Podolski and R. Crawford
Pressurized Fluidized-Bed Combustion/Component Test and Integration Unit Preliminary Design Report
Proc. 13th Intersociety Energy Conversion Engineering Conf., San Diego, CA, August 20-25, 1978, Vol. 3 (1978)

J. Purcell, R. Kustom, R. Clemmer, V. A. Maroni, J. M. Mintz, et al.
GAC-ANL TNS Scoping Studies
General Atomic Company Report GA-A14614, Vol. V, Support Engineering, Tritium and Neutronics (January 1978)

A. Rabl
Optical and Thermal Properties of Compound Parabolic Concentrators
Sol. Energy 1, 479-511 (1976)

P. L. Radloff and G. N. Papatheodorou
Raman Spectra of Indium Halide Vapors
High Temperature Metal Halide Chemistry, D. D. Cubicciotti and D. L. Hildenbrand, Eds., p. 320 (May 1978)

J. W. Rathke and H. M. Feder
Catalysis of Carbon Monoxide Hydrogenation by Soluble Mononuclear Complexes
J. Am. Chem. Soc. 100, 3623 (1978)

K. Reed
Inclination Dependence of Pyranometer Sensitivity
Proc. Society of Photo-Optical Instrumentation Engineers, Vol. 161, p. 106 (1978)

K. Reed and J. Allen
Solar Thermal Collector Testing: Calorimetric Ratio Technique
Proc. 1978 Annual Meeting of International Solar Energy Soc., Vol. 2.1, p. 345 (1978)

A. Rehmat, S. C. Saxena, R. Land, and A. A. Jonke
Noncatalytic Gas-Solid Reaction with Changing Particle Size: Unsteady State Heat Transfer
Can. J. Chem. Eng. 56, 316-322 (June 1978)

E. Rytter, S. Goates, and G. N. Papatheodorou
High Temperature Raman Band Contours and Vibrational Analysis of Arsenic Oxide Vapors
J. Chem. Phy. 69(8), 3717-3722 (1978)

M. L. Saboungi and C. C. Hsu
Estimation of Isothermal Sections of Ternary Phase Diagrams of Lithium Containing Systems: The Al-Li-Mg System
Proc. Workshop on Applications of Phase Diagrams in Metallurgy and Ceramics, NBS Special Publication 496, Vol. 2, pp. 1109-1138 (March 1978)

M. L. Saboungi and M. Blander
Theoretical Concepts Useful in the Calculation or Storage of Phase Diagrams of Ionic Systems
Proc. Workshop on Applications of Phase Diagrams in Metallurgy and Ceramics, NBS Special Publication 496, Vol. 2, pp. 1093-1108 (March 1978)

M. L. Saboungi, J. Marr, and M. Blander
Solubility Products of Metal Sulfides in Molten Salts: Measurements and Calculations for Iron Sulfide (FeS) in the LiCl-KCl Eutectic Composition
J. Electrochem. Soc. 125(10), 1567-1573 (1978)

M. L. Saboungi, P. Cerisier, and M. Blander
Variations of the Activity Coefficient of a Minor Element Dissolved in a Binary Alloy: Interstitial and Substitutional Alloys
Proc. Calphad-VII, Max-Planck Institute, Stuttgart, Germany, pp. 164-174 (1978)

M. L. Saboungi, J. Marr, and M. Blander
Solubility Products of PbS in Molten LiCl-KCl and Molten LiCl-LiF Eutectics: Measurements and a Priori Calculations
Extended Abstracts Electrochem. Soc. Meeting, Pittsburgh, PA, October 15-20, 1978, Vol. 78-2, pp. 917-918 (1978)

M. L. Saboungi and A. E. Martin
Electrochemical and Metallographic Investigations of the Stability of the J(= $LiK_6Fe_{24}S_{26}Cl$) Phase in Several Molten Salt Mixtures
Extended Abstracts Electrochem. Soc. Meeting, Pittsburgh, PA, October 15-20, 1978, Vol. 78-2, pp. 919-920 (1978)

M. L. Saboungi, P. Cerisier, and M. Blander
Theory for Ternary Solutions Dilute in One Component
Extended Abstracts Electrochem. Soc. Meeting, Pittsburgh, PA, October 15-20, 1978, Vol. 78-2, pp. 976-977 (1978)

M. L. Saboungi, P. Cerisier, A. D. Pelton, and P. L. Lin
Determination Theorique de la Temperature du Liquidus du Melange Ternaire Fluorure de Sodium - Fluorure de Lithium - Fluorure d'Aluminum
Bull. Soc. Chim. Fr. (1978)

M. L. Saboungi, P. Cerisier, and M. Blander
Les Alliages Interstitiels Liquides: Thermodynamique d'un Constituant Faiblement Dilue dans un Solvant Binaire Metallique - Extension aux Sels Fondus
Bull. Soc. Chim. Fr. (1978)

M. L. Saboungi, J. Marr, and M. Blander
Thermodynamic Properties of a Quasi-Ionic Alloy from Electromotive Force Measurements: The Li-Pb System
J. Chem. Phys. 68(4), 1375-1384 (February 15, 1978)

W. W. Schertz
Fabrication of Trough-Shaped Solar Collectors
U.S. Patent No. 4,099,515 (July 11, 1978)

M. G. Seitz, P. Rickert, A. Friedman, S. Fried, and M. J. Steindler
Transport Properties of Nuclear Waste in Geologic Media
Office of Waste Isolation Progress Reports Y/OWI/TM-43/3, 43/4, 43/6, 43/8, and 43/9 (1978)

H. Shimotake, E. C. Gay, and P. A. Nelson
The Design and Cost Optimization of Li-Al/FeS_x Cells
Extended Abstracts Electrochem. Soc. Meeting, Pittsburgh, PA, October 15-20, 1978, Vol. 78-2, pp. 93-96 (1978)

A. A. Siczek and M. J. Steindler
A Review of the Chemistry of Ruthenium and Zirconium in the Purex Solvent Extraction Process
At. Energy Rev. 16, 3 (1978)

S. Siegel, L. H. Fuchs, B. R. Hubble, and E. L. Nielsen
Relationship between the Morphological Properties of Half-Calcined Dolomite and the Kinetics of the Sulfation Reaction
Environ. Sci. Technol. 12, 1411-1416 (December 1978)

S. Siegel
Bond Strength-Bond Length Relationships for Some Metal-Oxygen Bonds
J. Inorg. Nucl. Chem. 40, 275 (1978)

J. W. Sim, K. Kinoshita, G. H. Kucera, and J. P. Ackerman
Effects of Electrolyte Matrix Structures on Molten Carbonate Fuel Cell Performance
Extended Abstracts Electrochem. Soc. Meeting, Pittsburgh, PA, October 15-20, 1978, Vol. 78-2, p. 137 (1978)

J. A. Smaga, F. C. Mrazek, K. M. Myles, and J. E. Battles
Materials Requirements in LiAl/LiCl-KCl/FeS_x Secondary Batteries
Materials Considerations in Liquid Metals Systems in Power Generation, N. J. Hoffman and G. A. Whitlow, Eds., NACE, Houston, TX, pp. 52-64 (1978)

W. M. Stacey, Jr., M. A. Abdou, J. N. Brooks, I. Charak, R. G. Clemmer, V. A. Maroni, B. Misra, et al.
Tokamak Experimental Power Reactor
Fusion Reactor Design Concepts, International Atomic Agency Report IAEA-TC-145/10, pp. 131-153 (December 1978)

W. M. Stacey, Jr., R. G. Clemmer, V. A. Maroni, et al.
Tokamak Experimental Power Reactor
Trans. Third Topical Meeting on the Technology of Controlled Nuclear Fusion, Santa Fe, NM, May 9-11, 1978, p. 368 (1978)

R. B. Swaroop, C. W. Boquist, and J. E. Battles
Development of Electrode Separators for Lithium-Aluminum/Metal Sulfide Batteries
Extended Abstracts Electrochem. Soc. Meeting, Pittsburgh, PA, October 15-20, 1978, Vol. 78-2, p. 145 (1978)

R. B. Swaroop, J. A. Smaga, and J. E. Battles
Materials for High-Performance Lithium-Alumium/Iron Sulfide Secondary Batteries
Proc. V Inter-American Conf. on Materials Technology, Sao Paulo, Brazil, November 5-10, 1978, pp. 137-145 (1978)

R. B. Swaroop, J. W. Sim, and K. Kinoshita
Corrosion Protection of Molten Carbonate Fuel Cell Gas Seals
J. Electrochem. Soc. 125(11), 1799-1800 (November 1978)

M. Tetenbaum
Some Aspects of High Temperature Vaporization Behavior and Valence Effects in Actinide Oxide Rare-Earth-Oxide Systems
Rev. Hautes Temp. Refract. 15, 20 (1978)

M. Tetenbaum, W. A. Shinn, and C. E. Johnson
Compatibility of Cladding Materials with Thorium-Uranium Alloys
Trans. Am. Nucl. Soc. 28, 168 (June 1978)

M. Tetenbaum and R. J. Ackermann
High Temperature Vaporization Behavior of Oxygen-Deficient Thoria
Trans. Am. Nucl. Soc. 28, 166 (June 1978)

D. R. Vissers, P. A. Nelson, T. D. Kaun, and Z. Tomczuk
Electrode Including Porous Particles with Imbedded Active Material for Use in a Secondary Electrochemical Cell
U.S. Patent No. 4,086,404 (April 25, 1978)

G. J. Vogel, A. A. Jonke, and R. B. Snyder
Method of Removing Sulfur Emissions from a Fluidized-Bed Combustion Process
U.S. Patent No. 4,091,076 (May 23, 1978)

G. J. Vogel, J. Montagna, W. M. Swift, and A. A. Jonke
Experiences in Regenerating Sulfated Limestone from Fluidized-Bed Combustors
Proc. Second Engineering Foundation Conf., J. F. Davidson and D. L. Kearins, Eds., pp. 394-400 (1978)

B. Papers Accepted for Publication in Open Literature

M. J. Chen and H. M. Feder
Valence Isomerization of Quadricyclane Catalyzed by Di-μ-acetatobisnorbornadienedirhodium: Evidence for a Rhodocyclobutane Intermediate
Accepted for publication in Inorg. Chem.

K. W. Choi and N. P. Yao
Heat Transfer in Lead-Acid Batteries Designed for Electric-Vehicle Propulsion Application
Accepted for publication in J. Electrochem. Soc.

L. Curtiss
Ab Initio Molecular Orbital Studies of Some High Temperature Metal Halide Complexes
Accepted for publication in Proc. Tenth Materials Research Symp.

M. M. Farahat
Thermal Energy Storage TES Applications for Highway Vehicles with Stirling Engines
Accepted for publication in Proc. Third Annual Thermal Storage Contractors' Information Exchange Meeting, December 1978

D. C. Fee and C. E. Johnson
Cesium Chemistry in GCFR Fuel Pins
Accepted for publication in Proc. Int. Conf. on Fast Breeder Reactor Fuel Performance, March 5-8, 1979

D. C. Fee, K. Y. Kim, and C. E. Johnson
Phase Equilibria in the Cs-Cr-O System
Accepted for publication in J. Nucl. Mater.

J. K. Fink
A Review of Studies on the Compatibility of Sodium with Refractory Ceramics
Accepted for publication in Rev. Coat. Corros.

P. A. Finn, A. C. Sheth, and L. Leibowitz
Equation of State of Uranium Dioxide
Accepted for publication in J. Nucl. Mater.

K. F. Flynn, L. J. Jardine, and M. J. Steindler
Method for Determining Leach Rates of Simulated Radioactive Waste Forms
Accepted for publication in 1978 Am. Chem. Soc. Symp. on Radioactive Waste in Geologic Storage

K. F. Flynn, L. J. Jardine, and M. J. Steindler
Leach Rate Characterization of Solid Radioactive Waste Forms
Accepted for publication in Proc. 1978 Mater. Res. Soc. Symp. on Science Underlying Waste Management

D. J. Frurip and M. Blander
Dimensional Analysis of Partition Functions for Ionic Molecules: Thermodynamic Properties of Vapors
Accepted for publication in Proc. Tenth Materials Research Symp. on Characterization of High Temperature Vapors and Gases

D. W. Green and G. T. Reedy
Identification of Matrix-Isolated Thorium Nitrides and the Thorium-Dinitrogen Complex
Accepted for publication in J. Molecular Spectroscopy

L. R. Greenwood and N. R. Chellew
Improved ^{10}B-loaded Liquid Scintillator with Pulse-Shape Discrimination
Accepted for publication in the Rev. Sci. Instr.

L. R. Greenwood, N. R. Chellew, and G. A. Zarwell
^{6}Li-loaded Liquid Scintillators with Pulse-Shape Discrimination
Accepted for publication in Rev. Sci. Instr.

B. D. Holt, P. T. Cunningham, and R. Kumar
Seasonal Variations of Oxygen-18 in Atmospheric Sulfates
Accepted for publication in Int. J. Environ. Anal. Chem.

C. C. Hsu and C. E. Johnson
Seed Activities in Open Cycle MHD System Predicted from a Multiphase Multicomponent Solution Model
Accepted for publication in Proc. Tenth Materials Research Symp. on Characterization of High Temperature Vapors and Gases, Gaithersburg, MD, September 18-22, 1978

W. N. Hubbard, G. K. Johnson, and V. Ya Leonidov
Combustion in Fluorine and Other Halogens
Accepted for publication as Chap. 12 in Combustion Calorimetry, Experimental Thermodynamics, Vol. 1

L. J. Jardine and M. J. Steindler
Some Aspects of the Thermal Analysis of Metal Encapsulated Spent Fuel
Accepted for publication in Nucl. Sci. Technol.

G. K. Johnson
The Enthalpy of Formation of Uranium Hexafluoride
Accepted for publication in J. Chem. Thermodyn.

G. K. Johnson and K. H. Gayer
The Enthalpies of Solution and Formation of the Chlorides of Cesium and Rubidium
Accepted for publication in J. Chem. Thermodyn.

M. A. Kirk and L. R. Greenwood
Determination of the Neutron Flux and Energy Spectrum in the Low-Temperature Fast-Neutron Facility in CP-5, Calculations of Primary-Recoil and Damage - Energy Distributions, and Comparisons with Experiment,
Accepted for publication in J. Nucl. Mater.

M. A. Kirk, R. A. Conner, D. G. Wozniak, L. R. Greenwood, R. L. Malewicki and R. R. Heinrich,
The Sputtering of Gold by Fast Neutrons
Accepted for publication in Phys. Rev.

S. H. D. Lee and I. Johnson
Removal of Gaseous Alkali Metal Compounds from Hot Flue Gas by Particulate Sorbents
Accepted for publication in Trans. ASME Conf., March 12-15, 1979

F. J. Martino, L. G. Bartholme, E. C. Gay, and H. Shimotake
Development of Lithium-Aluminum/Metal Sulfide Cells with LiCl-Rich Electrolyte
Accepted for publication in Proc. Symp. on Battery Design and Optimization, Electrochem. Soc. Meeting, Pittsburgh, PA, October 15-20, 1978

J. C. McGuire and T. A. Renner
Control of Tritium in Liquid Metal-Cooled Fast Breeder Reactors (LMFBRs)
Accepted for publication in At. Energy Rev.

P. A. Nelson, A. A. Chilenskas, and R. K. Steunenberg
Lithium-Iron Sulfide Batteries for Electric Vehicles
Accepted for publication in Proc. Fifth Int. Electric Vehicle Symp., Philadelphia, PA, October 2-5, 1978

G. N. Papatheodorou and G. H. Kucera
Vapor Complexes of Samarium(II) and Samarium(III) Vapor Complexes with Aluminum Chloride
Accepted for publication in Inorg. Chem.

G. N. Papatheodorou, Ø. Waernes and T. Østvold
Thermodynamic Studies of Binary Charged Unsymmetrical Fused Salt Systems: Calorimetric and Electromotive Force Measurements of Liquid Yttrium(III) Chloride-Alkali Chloride Mixtures
Accepted for publication in Acta Chem. Scand.

G. N. Papatheodorou
Resonance Raman Spectra of Metal Halide Vapor Complexes
Accepted for publication in Proc. Tenth Materials Research Symp. on Characterization of High Temperature Vapors and Gases

G. N. Papatheodorou and D. A. Buttry
Resonance Raman Spectra and Laser-Induced Dissociation of Uranium(V)-Aluminum(III) Chloride Vapors
Accepted for publication in Inorg. Nucl. Chem. Lett.

T. A. Renner and D. J. Raue
Tritium Permeation Through Fe-2 1/4 Cr-1 Mo Steam Generator Material
Accepted for publication in Nucl. Technol.

A. Reis, Jr., C. Willi, S. Siegel, and B. Tani
The Molecular and Crystal Structure of Di-μ-Acetato-Bis (Norbornadiene) Dirhodium(I): A Catalyst for the Reaction of Quadricyclane to Norbornadiene
Accepted for publication in J. Inorg. Chem.

P. G. Rickert, R. G. Strickert, and M. G. Seitz
Nuclide Migration in Fractured or Porous Rock
Accepted for publication in Am. Chem. Soc. Symp. Ser., Symp. on Nuclear Waste Disposal

H. Shimotake, E. C. Gay, and P. A. Nelson
The Design and Cost Optimization of Li-Al/FeS_x Cells
Accepted for Publication in Proc. Symp. on Battery Design and Optimization, Electrochemical Soc. Meeting, Pittsburgh, PA October 15-20, 1978

L. E. Trevorrow and M. J. Steindler
Technology Assessment in the Management of Nuclear Waste
Accepted for publication in CHEMTECH

E. Veleckis
Decomposition Pressures in the (α+β) Fields of the Li-LiH, Li-LiD, and Li-LiT Systems
Accepted for publication in J. Nucl. Mater.

D. R. Vissers, K. E. Anderson, C. K. Ho, and H. Shimotake
Effects of the LiCl-KCl Electrolyte Composition on the Performance Characteristics of the Li-Al/FeS Cells.
Accepted for publication in Proc. Symp. on Battery Design and Optimization, Electrochem. Soc. Meeting, Pittsburgh, PA, October 15-20, 1978

N. P. Yao, F. A. Ludwig, and F. Hornstra
Overview of Near-Term Battery Development
Accepted for publication in Proc. Fifth International Electric Vehicle Symposium, Philadelphia, PA, October 2-5, 1978

R. M. Yonco, V. A. Maroni, J. E. Strain, and J. H. Devan
A Determination of the Solubility of Lithium Oxide in Liquid Lithium by Fast Neutron Activation
Accepted for publication in J. Nucl. Mater.

C. ANL Reports

J. P. Ackerman, K. Kinoshita, J. W. Sim, R. Swaroop, and P. A. Nelson
Advanced Fuel Cell Development, Progress Report for July-September 1977
ANL-77-79

J. P. Ackerman, K. Kinoshita, P. A. Finn, J. W. Sim, and P. A. Nelson
Advanced Fuel Cell Development, Progress Report for October-December 1977
ANL-78-16

J. P. Ackerman, P. A. Finn, K. Kinoshita, G. H. Kucera, J. W. Sim, and R. B. Swaroop
Advanced Fuel Cell Development, Progress Report for January-March 1978
ANL-78-40

J. P. Ackerman, P. A. Finn, K. Kinoshita, G. H. Kucera, and J. W. Sim
Advanced Fuel Cell Development, Progress Report for April-June 1978
ANL-78-71

P. E. Blackburn
GASCON and MHDGAS: Fortran IV Computer Codes for Calculating Gas and Condensed-Phase Compositions in the Coal-Fired Open-Cycle MHD System
ANL/MHD-77-4

R. A. Blomquist, J. K. Fink, and L. Leibowitz
The Viscosity of Molten Alumina
ANL-78-28

L. Burris, D. S. Webster, F. A. Cafasso, A. A. Jonke, P. A. Nelson, and M. J. Steindler
Chemical Engineering Division Research Highlights 1977
ANL-78-70

F. A. Cafasso, L. Leibowitz, C. C. McPheeters, and C. E. Johnson
Reactor Fuels and Materials Chemistry Research: July 1976-September 1977
ANL-78-15

F. A. Cafasso, M. Blander, V. A. Maroni, C. E. Johnson, R. Kumar, and S. Siegel
Basic Energy Sciences Research: July 1976-September 1977
ANL-78-42

K. W. Choi and N. P. Yao
Computer Program for the Thermal Analysis of Lead-Acid Cells for Load-Leveling Applications
ANL/OEPM-78-1

L. S. H. Chow and T. R. Johnson
Slag Transport Models for Vertical and Horizontal Slag Surfaces
ANL/MHD-78-1

R. G. Clemmer, R. H. Land, V. A. Maroni, and J. M. Mintz
Simulation of Large Scale Air Detritiation Operations by Computer Modeling and Bench Scale Experimentation
ANL-FPP-77-3

M. Collares-Pereira and A. Rabl
Simple Procedure for Predicting Long-Term Average Performance of Nonconcentrating and of Concentrating Solar Collectors
ANL-78-67

G. Fabris, E. S. Pierson, A. K. Fischer, and C. E. Johnson
Experimental Two-Phase Liquid-Metal Magnetohydrodynamic Generator Program
ANL/MHD-78-2

J. K. Fink, M. G. Chasanov, and L. Leibowitz
Thermophysical Properties of Thorium and Uranium Systems for Use in Reactor Safety Analysis
ANL/CEN/RSD-77-1

J. Fischer, J. E. Young, J. E. Johnson, and A. A. Jonke
Laboratory Support for In Situ Gasification Reaction Kinetics
Quarterly Report for the Period April-June 1977
ANL/CEN/FE-77-6

F. C. Franklin, E. R. Ebersole, and R. R. Heinrich
Analysis of EBR-II Low-Power Dosimetry Run 78C,
ANL-77-76

D. R. Fredrickson, J. E. Young, J. Fischer, and E. D. West
Development of a Calorimeter to Determine Heats of Reaction of Hydrogen with Coal and Coal Slurries
ANL/CEN/FE-78-6

C. C. Hsu, Irving Johnson, and M. Blander
Chemical Activities of Alkali Sulfates in Hot Corrosion
ANL-77-84

C. C. Hsu, R. H. Land, and M. Blander
Binary Solution Model for Computation of Equilibrium Compositions
ANL-77-83

L. J. Jardine and M. J. Steindler
A Review of Metal-Matrix Encapsulation of Solidified Radioactive High-Level Waste
ANL-78-19

I. Johnson, G. J. Vogel, S. H. D. Lee, J. F. Lenc, F. F. Nunes, J. A. Shearer, R. B. Snyder, G. W. Smith, E. B. Smyk, W. M. Swift, F. G. Teats, C. B. Turner, W. I. Wilson, and A. A. Jonke
Support Studies in Fluidized-Bed Combustion, Quarterly Report, October-December 1977
ANL/CEN/FE-77-11

I. Johnson, G. J. Vogel, S. H. D. Lee, J. A. Shearer, R. B. Snyder, G. W. Smith, W. M. Swift, F. G. Teats, C. B. Turner, W. I. Wilson, and A. A. Jonke
Support Studies in Fluidized-Bed Combustion, Quarterly Report, January-March 1978
ANL/CEN/FE-78-3

I. Johnson, G. J. Vogel, S. H. D. Lee, J. A. Shearer, R. B. Snyder, G. W. Smith, E. B. Smyk, W. M. Swift, F. G. Teats, C. B. Turner, W. I. Wilson, and A. A. Jonke
Support Studies in Fluidized-Bed Combustion, Quarterly Report, April-June 1978
ANL/CEN/FE-78-4

A. A. Jonke, E. L. Carls, G. J. Vogel, and I. Johnson
Highlights of Studies on Fluidized-Bed Combustion of Coal - 1977
ANL/CEN/FE-78-1

B. J. Kullen, N. M. Levitz, and M. J. Steindler
Management of Waste Cladding Hulls. Part II. An Assessment of Zirconium Pyrophoricity and Recommendations for Handling Waste Hulls
ANL-77-63

C. C. McPheeters and R. D. Wolson
Disposal of Radioactive Sodium Waste
ANL-78-87

J. C. Montagna, G. W. Smith, F. G. Teats, G. J. Vogel, and A. A. Jonke
Evaluation of On-Line Light-Scattering Optical Particle Analyzers for Measurements at High Temperature and Pressure
ANL/CEN/FE-77-7

J. C. Montagna, G. J. Vogel, G. W. Smith, and A. A. Jonke
Fluidized-Bed Regeneration of Sulfated Dolomite from a Coal-Fired FBC Process by Reductive Decomposition
ANL-77-16

P. A. Nelson, N. P. Yao, R. K. Steunenberg, A. A. Chilenskas, E. C. Gay, J. E. Battles, F. Hornstra, W. E. Miller, M. F. Roche, and H. Shimotake
High-Performance Batteries for Stationary Energy Storage and Electric-Vehicle Propulsion, Progress Report for the Period April-June 1977
ANL-77-68

P. A. Nelson, N. P. Yao, R. K. Steunenberg, A. A. Chilenskas, E. C. Gay, J. E. Battles, F. Hornstra, W. E. Miller, M. F. Roche, and H. Shimotake
High-Performance Batteries for Stationary Energy Storage and Electric-Vehicle Propulsion, Progress Report for the Period July-September 1977
ANL-77-75

P. A. Nelson, R. K. Steunenberg, A. A. Chilenskas, E. C. Gay, J. E. Battles, F. Hornstra, W. E. Miller, M. F. Roche, and H. Shimotake
Development of Lithium/Metal Sulfide Batteries at Argonne National Laboratory: Summary Report for 1977
ANL-78-20

P. A. Nelson, R. K. Steunenberg, A. A. Chilenskas, E. C. Gay, J. E. Battles, F. Hornstra, W. E. Miller, M. F. Roche, and H. Shimotake
High-Performance Batteries for Stationary Energy Storage and Electric-Vehicle Propulsion, Progress Report for the Period October-December 1977
ANL-78-21

P. A. Nelson, R. K. Steunenberg, A. A. Chilenskas, E. C. Gay, J. E. Battles, F. Hornstra, W. E. Miller, M. F. Roche, and H. Shimotake
High-Performance Batteries for Stationary Energy Storage and Electric-Vehicle Propulsion, Progress Report, January-March 1978
ANL-78-45

M. Petrick, K. E. Tempelmeyer, and T. R. Johnson
MHD Balance of Plant Technology Project, First Quarterly Report for the Period 1 January-31 March 1978
ANL/MHD-78-3

M. Petrick, K. Tempelmeyer, W. C. Redman, C. V. Pearson, D. H. Bomkamp, L. W. Carlson, K. H. Im, L. S. Chow, B. K. Snyder, T. R. Johnson, C. E. Johnson, P. E. Blackburn, C. C. Hsu, A. Sheth, R. B. Poeppel, J. W. Hafstrom, R. N. Singh, and K. Natesan
Program Plan for Development of Heat and Seed Recovery Components for a Coal-Fired, Open-Cycle MHD Power Plant
ANL/MHD-78-6

R. Razgaitis
An Analysis of the High-Temperature Particulate Collection Problem
ANL-77-14

T. A. Renner and C. C. McPheeters
Tritium and Hydrogen Transport in LMFBR Systems: EBR-II, CRBR, and FFTF
ANL-78-64

S. C. Saxena and W. M. Swift
Fast Removal From Hot and Compressed Gas Streams By Fibrous- and Granular-Bed Filters: A State of the Art Review
ANL/CEN/FE-77-9

M. G. Seitz, P. G. Rickert, S. M. Fried, A. M. Friedman, and M. J. Steindler
Studies of Nuclear-Waste Migration in Geologic Media, Annual Report, November 1976-October 1977
ANL-78-8

J. A. Shearer, I. Johnson, and C. B. Turner
The Effect of Sodium Chloride on the Reaction of SO_2/O_2 Mixtures With Limestones and Dolomites
ANL/CEN/FE-78-8

A. C. Sheth and T. R. Johnson
Evaluation of Available MHD Seed-Regeneration Processes on the Basis of Energy Considerations
ANL/MHD-78-4

S. B. Skladzien, T. A. Renner, D. J. Raue, and C. C. McPheeters
Tritium Meters for Use in LMFBR Sodium Coolant
ANL-78-30

L. M. Southwick and W. Thomas Atkins
Regeneration of Calcium Sulfate From Fluid Bed Combustion of Coal: Process Design and Cost Estimate
ANL/CEN/FE-78-9

M. J. Steindler, M. Ader, R. E. Barletta, G. J. Bernstein, K. F. Flynn, T. J. Gerding, L. J. Jardine, B. J. Kullen, R. A. Leonard, W. J. Mecham, R. H. Pelto, B. B. Saunders, W. B. Seefeldt, M. G. Seitz, A. A. Siczek, L. E. Trevorrow, A. A. Ziegler, D. S. Webster, and L. Burris
Chemical Engineering Division Fuel Cycle Programs, Progress Report, January-September 1977
ANL-78-11

M. J. Steindler, Milton Ader, R. E. Barletta, J. K. Bates, C. H. Bean, G. J. Bernstein, T. R. Cannon, K. F. Flynn, T. J. Gerding, L. J. Jardine, B. J. Kullen, R. A. Leonard, W. J. Mecham, K. M. Myles, R. H. Pelto, B. B. Saunders, W. B. Seefeldt, M. G. Seitz, A. A. Siczek, L. E. Trevorrow, A. A. Ziegler, D. S. Webster, and Leslie Burris
Chemical Engineering Division Fuel Cycle Programs, Progress Report, October-December 1977
ANL-78-37

R. V. Strain, G. L. Fogle, H. R. Thresh, R. R. Heinrich, R. M. Fryer, S. Y. C. So, and J. D. B. Lambert
EBR-II Fission-Product-Source Test No. 1
ANL-78-58

R. Varma and N. P. Yao
Stibine and Arsine Generation From a Lead-Acid Cell During Charging Modes Under a Utility Load-Leveling Duty Cycle
ANL/OEPM-77-5

G. J. Vogel, I. Johnson, S. H. Lee, J. F. Lenc, A. S. Lescarret, J. Montagna, F. F. Nunes, J. A. Shearer, R. B. Snyder, G. W. Smith, W. M. Swift, F. G. Teats, C. B. Turner, W. I. Wilson, and A. A. Jonke
Supportive Studies in Fluidized-Bed Combustion, Annual Report, July 1976-June 1977
ANL/CEN/FE-77-3

G. J. Vogel, I. Johnson, S. H. Lee, J. F. Lenc, J. C. Montagna, F. F. Nunes, J. A. Shearer, R. B. Snyder, G. W. Smith, E. B. Smyk, W. M. Swift, F. G. Teats, C. B. Turner, W. I. Wilson, and A. A. Jonke
Supportive Studies in Fluidized-Bed Combustion, Quarterly Report, July-September 1977
ANL/CEN/FE-77-8

G. J. Vogel, I. Johnson, J. F. Lenc, R. B. Snyder, E. B. Smyk, F. G. Teats, and A. A. Jonke
Regeneration of Sulfated Limestone From FBCs and Corrosive Effects of Sulfation Activators in FBCs, Quarterly Report, October-December 1977
ANL/CEN/FE-77-10

G. J. Vogel, I. Johnson, J. F. Lenc, R. B. Snyder, G. W. Smith, E. B. Smyk F. G. Teats, and A. A. Jonke
Regeneration of Sulfated Limestone From FBCs and Corrosive Effects of Sulfation Accelerators in FBCs, Quarterly Report, January-March 1978
ANL/CEN/FE-78-2

G. J. Vogel, I. Johnson, J. F. Lenc, R. B. Snyder, G. W. Smith, E. B. Smyk, F. G. Teats, and A. A. Jonke
Regeneration of Sulfated Limestone from FBCs and Corrosive Effects of Sulfation Activators, Quarterly Report, April-June 1978
ANL/CEN/FE-78-5

G. J. Vogel, W. Swift, M. J. McDaniel, G. Smith, and A. Ziegler
Testing of a Pulsed L-Valve Feeder for Use in Fluidized-Bed Combustion and Sorbent Regeneration Units
ANL/CEN/FE-78-12

N. P. Yao and J. J. Barghusen (eds.)
Proceedings of the Workshop on Battery Storage for Solar-Photovoltaic Energy Systems
ANL/OEPM-78-3

R. W. Zygmunt
A Study of the Production of Well-Characterized Aerosols Using a Flow Reactor
ANL-77-90

D. Papers Presented at Scientific Meetings

M. A. Abdou, C. C. Baker, R. G. Clemmer, et al.
Impact of Technology and Maintainability on Economic Aspects of Tokamak Power Plants
Presented at Seventh International Conf. on Plasma Physics and Controlled Nuclear Fusion Research, Innsbruck, Austria, August 23-30, 1978

J. P. Ackerman
Development of Central Station Power Plants Integrated with Coal Gasifiers
Presented at Fifth Energy Technology Conf., Washington, D.C., February 27-March 1, 1978

G. Bandyopadhyay, D. G. Graczyk, and D. Stahl
Determination of Retained Fission Gas in Irradiated Oxide Fuels by Laser-Sampling Technique
Presented at Am. Ceramic Soc. 80th Annual Meeting, Detroit, MI, May 6-11, 1978

J. E. Battles
Electrical Energy Storage
Presented at ACEA Materials Science Conf., Argonne National Laboratory, June 1-2, 1978

J. E. Battles
Electrochemical Engineering of Batteries - lecture series
Presented at Univ. of California, Los Angelos, CA, May 15-19, 1978

G. J. Bernstein, R. A. Leonard, A. A. Ziegler, and M. J. Steindler
An Improved Annular Centrifugal Contactor for Solvent Extraction Reprocessing of Nuclear Reactor Fuel
Presented at AIChE 84th National Meeting, Atlanta, GA, February 26-March 1, 1978

M. Blander, M. L. Saboungi, and P. Cerisier
A Statistical-Mechanical Theory for Ternary and Binary Solutions
Presented at Seventh Euchem Conf. on Molten Salts, Lysekil, Sweden, June 18-23, 1978

M. Blander, C. Horowitz, and R. Land
Refractory Metal Condensation From a Nebula
Presented at Meteoritical Soc. 41st Annual Meeting, Sundbury, Ontario, Canada

M. Blander
Computer Modeling of Gas-Condensed Phase Equilibria: Present Status and Some Future Needs in Science and Technology
Presented at Tenth Materials Research Symp. on Characterization of High Temperature Vapors and Gases, September 18-22, 1978

S. Bourne
Chemical Preparation of Fossil Fuel Samples for Biological Studies
Presented at USDOE Workshop on Review and Development of Biotesting Programs for Energy Utilization, Boca Raton, FL, November 11-14, 1978

M. J. Chen and H. M. Feder
Valence Isomerization of Quadricyclane Catalyzed by Di-μ-acetato-bisnorbornadienedirhodium: Evidence for a Rhodocyclobutane Intermediate
Presented at Am. Chem. Soc. National Meeting, Miami Beach, FL, September 10-15, 1978

K. W. Choi and N. P. Yao
Heat Transfer in Lead-Acid Batteries
Presented at Second AIAA/ASME Thermophysics and Heat Transfer Committee, Palo Alto, CA, May 24-26, 1978

K. W. Choi and N. P. Yao
A Mathematical Model for Porous Nickel Electrodes in Zinc/Nickel Oxide Cells
Presented at Electrochem. Soc. Meeting, Pittsburgh, PA, October 15-20, 1978

K. W. Choi and N. P. Yao
Potential Distributions in Rectangular Electrodes
Presented at Electrochem. Soc. Meeting, Pittsburgh, PA, October 15-20, 1978

L. S. H. Chow, R. Viskanta, and T. R. Johnson
Slag Transport Models for Radiant Heater of an MHD System
Presented at ASME 1978 Winter Meeting, San Francisco, December 1978

R. A. Couture, M. G. Seitz, and M. J. Steindler
Experimental Trace-Element Transport By Fluid Flow at Elevated Temperatures: Ion Exchange on Kaolinite
Presented at AGU Fall Meeting, San Francisco, CA, December 4-8, 1978

P. T. Cunningham
Application of Infrared Spectrophotometric Methods to the Determination of Sulfur- and Nitrogen-Containing Species in Airborne Particulate Material
Presented at EPRI Workshop on Chemical Speciation of Sulfur and Nitrogen Compounds on Particulate Matter in the Atmosphere Palo Alto, CA, February 12-13, 1979

P. T. Cunningham
Overview of Activities of the Analytical Chemistry Laboratory at ANL
Presented at Conf. on Analytical Methods, Sandia Laboratories, Albuquerque, NM, November 8-9, 1978

P. T. Cunningham and B. D. Holt
Transformation Studies Using ^{18}O
Presented at MAP3S Review Meeting, Brookhaven National Laboratory, February 13-16, 1978

P. T. Cunningham and B. R. Hubble
High Temperature Reaction of Sulfurous Gases with Limestones and Other Minerals
Presented at Gordon Research Conf. on High Temperature Chemistry, Wolfeboro, NH, August 7-11, 1978

P. T. Cunningham and J. S. Bogard
The Identification and Determination of Nitrogenous Contaminants in the Environment
Presented at Symposium on Environmental Analytical Chemistry, Brigham Young University, Provo, UT, June 21-23, 1978

L. A. Curtiss
Molecular Orbital Studies of Metal Halide Complexes
Presented at Am. Conf. on Theoretical Chemistry, Boulder, CO, June 25-30, 1978

L. A. Curtiss
Ab Initio Molecular Orbital Studies of High Temperature Metal Halide Complexes
Presented at 10th Materials Research Symp. on Characterization of High-Temperature Vapors and Gases, National Bureau of Standards, Gaithersburg, MD, September 18-22, 1978

D. G. Doran, H. Farrar IV, A. N. Goland, L. R. Greenwood, R. R. Heinrich, et al.
The Damage Analysis and Fundamental Studies Program
Presented at Third ANS Topical Meeting on Technology of Controlled Nuclear Fusion, Sante Fe, NM, May 9-11, 1978.

R. C. Elliott and E. C. Gay
Computer Aided Design of Lithium/Metal Sulfide Cells
Presented at Electrochem. Soc. Meeting, Pittsburgh, PA October 15-20, 1978

A. M. Essling, R. J. Meyer, and D. J. Rokop
Purification of Uranium in UO_2-ThO_2 Fuel for Mass Spectrometry
Presented at 22nd Conf. on Analytical Chemistry in Energy Technology, Oak Ridge National Laboratory, Gatlinburg, TN, October 10-12, 1978

D. C. Fee, A. Smith, and C. E. Johnson
Cesium Thermochemistry in Nuclear Fuels
Presented at Am. Ceram. Soc. Meeting,, San Diego, CA, October 25-28, 1978

A. K. Fischer and C. E. Johnson
Foaming and Surface Tension in Liquid Metals. The Na-K-Ba System
Presented at Am. Chem. Soc. National Meeting, Miami Beach, FL, September 10-15, 1978

K. F. Flynn, L. J. Jardine, and M. J. Steindler
Method for Determining Leach Rates of Simulated Radioactive Waste Forms
Presented at Am. Chem. Soc. National Meeting, Miami Beach, FL, September 10-15, 1978

K. F. Flynn, L. J. Jardine, R. E. Barletta, and M. J. Steindler
Leach Rate Characterization of Solid Radioactive Waste Forms
Presented at International Symp. on Science Underlying Radioactive Waste Management, Boston, MA, November 29-December 1, 1978

D. J. Frurip and M. Blander
Estimation of the Thermodynamic Properties of Ionic Vapors By a Dimensional Theory
Presented at Electrochem. Soc. Meeting, Pittsburgh, PA, October 15-20, 1978

L. Fuchs and M. Blander
Refractory Metal Particles In Calcium-Aluminum Rich Inclusions in Allende
Presented at Meteoritical Soc. 41st Annual Meeting, Sudbury, Ontario, Canada

E. C. Gay, W. E. Miller, R. F. Malecha, R. C. Elliott
Review of Industrial Participation in the ANL Lithium/Iron Sulfide Battery Development Program
Presented at Intersociety Energy Conversion Engineering Conf., San Diego, CA, August 20-25, 1978

D. G. Graczyk
Laser Sampling of Retained Fission Gases in Irradiated Fuels
Presented at Conf. on Analytical Methods, Sandia Laboratories, Albuquerque, NM, November 8-9, 1978

R. Graven, A. Gorski, and W. McIntire
On the Design of CPC Photovoltaic Solar Collectors
Presented to International Solar Energy Soc., New Delhi, India, January 1978

D. W. Green and G. T. Reedy
Matrix-Isolated High-Temperature Molecules Studied with Fourier Transform Infrared Spectroscopy
Presented at the Am. Chem. Soc. Joint Central-Great Lakes Regional Meeting, Indianapolis, IN, May 24-26, 1978

D. W. Green and G. T. Reedy
Identification of Matrix-Isolated Plutonium Oxides, Plutonium Nitrides, Thorium Nitride and the Thorium-Dinitrogen Complex
Presented at 33rd Annual Symp. on Molecular Spectroscopy, Ohio State University, Columbus, OH, June 12-16, 1978

D. W. Green and G. T. Reedy
Matrix Isolation Infrared Spectroscopy of Reactor Fuel Vapor Species
Presented at Tenth Gordon Research Conf. on High Temperature Chemistry, Wolfsboro, NH, August 7-11, 1978

B. D. Holt, R. Kumar, and A. G. Engelkemeir
Interference By Isotopic Exchange in the Determination of Oxygen-18 in Atmospheric Sulfur Dioxide
Presented at the Third International Conf. on Stable Isotopes, Oakbrook, IL , May 23-26, 1978

B. D. Holt, M. Bouchard, P. T. Cunningham, A. Engelkemeir, E. Nielsen, S. Johnson, and R. Kumar
Simultaneous ^{18}O Variations in Atmospheric Sulfates, Sulfur Dioxide, and Water Vapor at St. Louis, Mo., Auburn, Ill., and Glasgow Ill., July 1975
Presented at 58th Annual Meeting with the Eighth Conf. on Weathercasting (Radio and TV) of the American Meteorological Soc., Savannah, GA, January 29-February 2, 1978

B. D. Holt
^{18}O Studies of Atmospheric Sulfate Formation
Presented at Chemistry Department Seminar, Chalmers University of Technology, Gothenburg, Sweden, March 30, 1978

L. J. Jardine and M. J. Steindler
Some Thermal Analysis Aspects of Metal Encapsulated Waste
Presented at Am. Nucl. Soc. Meeting, Savannah, GA, March 19-23, 1978

L. J. Jardine and M. J. Steindler
A Perspective of Metal Encapsulation of Waste
Presented at Materials Research Soc. Meeting, Boston, MA, November 29-December 1, 1978

C. E. Johnson and D. C. Fee
Cesium Chemistry and Behavior in GCFR Mixed-Oxide Fuel Pins
Presented at Information Meeting on Fast Breeder Reactor Fuel Element Development, Richland, WA, May 2-4, 1978

C. E. Johnson
Surface Analysis in Energy Research
Presented at 22nd Conf. on Analytical Chemistry in Energy Technology, Oak Ridge National Laboratory, October 10-12, 1978

C. E. Johnson
SIMS Studies of Surface Effects of Materials Related to Fission and Fusion Reactors
Presented at U.S.-Japan Seminar on Secondary Ion Mass Spectrometry, Takarazuka, Japan, October 23-27, 1978

G. K. Johnson and C. E. Johnson
The Thermodynamic Properties of Realgar
Presented at 144th National AAAS Meeting, Washington, DC, February 12-17, 1978

G. K. Johnson and C. H. P. Cordfunke
Enthalpies of Formation of Some Uranium Nitrides by Fluorine Bomb Calorimetry
Presented at 33rd Annual Calorimetry Conf., Utah State University, Logan, UT, July 25-29, 1978

I. Johnson, J. Shearer, R. Snyder, and G. J. Vogel
Factors Limiting Limestone Utilization Efficiency In Fluidized-Bed Combustors
Presented at Intersociety Energy Conversion Engineering Conf., San Diego, CA, August 20-25, 1978

I. Johnson
Fluidized-Bed Combustion--Enhancement of SO_2 Emission Control by the Use of Salt
Presented at Salt Institute Meeting, Chicago, IL, October 26, 1978

I. Johnson, R. B. Snyder, W. M. Swift, S. H. D. Lee, G. W. Smith, and A. A. Jonke
Flue Gas Cleaning for Pressurized Fluidized-Bed Combustors
Presented at USDOE Environmental Control Symp., Washington, DC, November 28-30, 1978

S. A. Johnson, R. Kumar, and P. T. Cunningham
Measuring Sulfate Acidity
Presented at Multi-state Atmospheric Power Production Pollution Study (MAP3S) Review Meeting, Brookhaven National Laboratory, Upton, NY, February 13-16, 1978

T. R. Johnson, K. H. Im, L. S. H. Chow, P. E. Blackburn, and R. Singh
MHD Downstream Gas Management
Presented at Fourth US/USSR Colloquium on MHD Power Generation, Washington, D.C., October, 1978

A. A. Jonke
Design Alternatives for Improved Sorbent Utilization (SO_2 Removal)
Presented at Atmospheric Fluidized-Bed Combustion Workshop, Electric Power Research Institute, Palo Alto, CA, August 25-26, 1977

A. A. Jonke
Status and Future Promise of Fluidized-Bed Coal Combustion
Presented at Miami International Conf. on Alternative Energy Sources, Miami, FL, December 5-7, 1977

A. A. Jonke
Clean Electric Power by Fluidized-Bed Combustion of Coal
Presented at 70th Annual AIChE Meeting, New York, NY, November 13-17, 1977

R. Keller
Energy Conservation in an Optimized Electrochemical Process
Presented at Int. Soc. of Electrochem. 29th Meeting, Budapest, Hungary, August 28-September 2, 1978

R. Keller
Predicting the Energy Consumption of a New Electrochemical Process
Presented at Electrochem. Soc. Meeting, Pittsburgh, PA, October 15-20, 1978

K. Kim and C. E. Johnson
Thermochemistry of Coal Components. Benzonaphthofuran and Chromone
Presented at 33rd Annual Calorimetry Conf., Utah State University, Logan, UT, July 25-29, 1978

K. Kim, G. K. Johnson, and C. E. Johnson
Thermochemistry and Structures of Rare Earth Sesquioxides, Trichlorides, and Trifluorides
Presented at 33rd Annual Calorimetry Conf., Utah State University, Logan, UT, July 25-29, 1978

K. Kinoshita
Electrocatalyst-Support Interactions
Presented at Workshop on the Electrocatalysis of Fuel Cell Reactions, DOE, Brookhaven National Laboratory, May 15-16, 1978

K. Kinoshita
Electrolyte Structures for Molten Carbonate Fuel Cells
Presented at DOE/EPRI Workshop on Molten Carbonate Fuel Cells, Oak Ridge National Laboratory, Oak Ridge, TN, October 30-November 2, 1978

M. A. Kirk and L. R. Greenwood
Determination of the Neutron Flux and Spectrum in the Low-Temperature Fast-Neutron Facility in CP-5
Presented at Int. Conf. on Neutron Transmutation Doping, University of Missouri, Columbia, MO., April 23-26, 1978

J. H. Kittel and J. K. Bates
Recycle Technology for Thorium Metal Fuels
Presented at Am. Nucl. Soc. Meeting, San Diego, CA, June 18-23, 1978

V. M. Kolba
The Development of High Energy Lithium-Metal Sulfide Batteries for Improved Electric Vehicle Performance
Presented at ASME Meeting, Fox Valley Section, December 6, 1978

R. A. Leonard, G. J. Bernstein, A. A. Ziegler, R. H. Pelto, and M. J. Steindler
Laboratory Centrifugal Contactor for Rapid Liquid-Liquid Extraction
Presented at Am. Chem. Soc. National Meeting, Miami Beach, FL, September 10-15, 1978

V. A. Maroni, T. A. Renner, D. J. Raue, and E. H. Van Deventer
Effects of Surface Environment and Bulk Composition on the Permeation of Hydrogen Isotopes Through Iron- and Nickel-Base Alloys
Presented at AIME Annual Meeting, Denver, CO, February 26-March 2, 1978

V. A. Maroni
Control of Tritium Permeation Through Fusion Reactor Structural Materials
Presented at DOE Environmental Control Symp., Washington, DC, November 28-30, 1978

B. Misra, C. C. McPheeters, and R. D. Wolson
Feasibility of Decontamination of LMFBR Coolant by Low Pressure Distillation
Presented at Am. Nucl. Soc. Meeting, San Diego, CA, June 1978

K. M. Myles
The Role and Status of Pyrochemical Nuclear Fuel Technology
Presented at American Society of Metals Meeting, Savannah River Chapter, September 21, 1978

P. A. Nelson, W. J. Walsh, and A. A. Chilenskas
Battery Requirements for Electric Vehicles
Presented at Electrochem. Soc. Meeting, Pittsburgh, PA, October 15-20, 1978

P. A. Nelson
Energy Projects in Relation to Fuel Cells and Batteries
Presented at First Seminar on Energy and Battery Electrochem. Soc. of Japan, Osaka, October 31-November 2, 1978

P. A. Nelson
U.S. Projects on Electric Vehicles and Other Energy Related Projects
Presented at First Seminar on Energy and Battery Electrochem. Soc. of Japan, Osaka, October 31-November 2, 1978

N. Otto
Failure Analysis of Two LiAl/LiCl-KCl/FeS_2-CoS_2 Electrolyte Cells
Presented at 11th Annual International Metallographic Society Convention, Montreal, Canada, July 16-19, 1978

G. N. Papatheodorou
Structural and Thermodynamic Studies of Salt Vapors
Presented at Euchem. Conf. on Molten Salts, Lysekil, Sweden, June 18-23, 1978

G. N. Papatheodorou and T. Østvold
Thermodynamics of Yttrium-Alkali-Chloride Mixtures
Presented at Euchem. Conf. on Molten Salts, Lysekil, Sweden, June 18-23, 1978

G. N. Papatheodorou
Laser-Induced Decomposition of Vapor Complexes
Presented at Gordon Research Conf., Wolfsboro, NH, August 7-11, 1978

G. N. Papatheodorou
Resonance Raman Spectra of Metal Halide Vapor Complexes
Presented at Tenth Materials Research Symp. on Characterization of High Temperature Vapors and Gases, National Bureau of Standards, Gaithersburg, MD, September 18-22, 1978

G. N. Papatheodorou
Lecture series on Spectroscopy and Spectrophotometry of Vapors
Presented at Chemistry Dept. of Technical Univ. of Denmark, Lyngby, Denmark, November-December 1978

A. D. Pelton, P. L. Lin, P. Cerisier, and M. L. Saboungi
Phase Diagrams of the $LiF-AlF_3$, $NaF-AlF_3$ and $Li_3AlF_6-Na_3AlF_6$ Systems: Survey and Computations
Presented at Electrochem. Soc. 154th Meeting, Seattle, WA, May 21-26, 1978

R. D. Pierce
Fuel Cell Systems
Presented at Workshop on Hydrocarbon Processing - Mixing and Scale-up Problems, Washington, DC, December 13-15, 1978

S. K. Preto, Z. Tomczuk, A. E. Martin, and M. F. Roche
Reactions in FeS_2 Electrodes Operated in Molten LiCl-KCl Elecrolyte
Presented at Electrochem. Soc. Meeting, Pittsburgh, PA, October 15-20, 1978

S. K. Preto, S. von Winbush, and M. F. Roche
Electrochemical Reversibility of FeS_2, CoS_2, and NiS_2 in Molten LiCl-KCl
Presented at Electrochem. Soc. Meeting, Pittsburgh, PA, October 15-20, 1978

P. L. Rawlings and W. N. Hubbard
The Enthalpy of Hydriding of $LaNi_5$
Presented at 33rd Annual Calorimetry Conf., Utah State University, Logan, UT, July 25-29, 1978

G. T. Reedy, S. Bourne, and P. T. Cunningham
Infrared Analysis of Gas Chromatographically Separated, Matrix-Isolated Compounds
Presented at Pittsburgh Conference, Analytical Chemistry and Applied Spectroscopy Societies, Cleveland, OH, February 28, 1978

G. T. Reedy, S. Bourne, and P. T. Cunningham
Matrix-Isolation Infrared Spectroscopy of Gas Chromatographically Separated Compounds
Presented at the Am. Chem. Soc. Joint Central-Great Lakes Regional Meeting, Indianapolis, IN, May 24-26, 1978

A. Reis, Jr., C. Willi, S. Siegel, and B. Tani
The Structure of Di-μ-Acetato-Bis (Norbornadiene) Dirhodium(1): A Catalyst for the Reaction of Quadricyclane to Norbornadiene
Presented at ACS National Meeting, Miami Beach, FL, September 1978

M. L. Saboungi
Solubility of FeS in Molten LiCl-KCl Eutectic
Presented at Institute of Inorganic Chemistry, Norwegian Institute of Technology, June 15, 1978

M. L. Saboungi, A. D. Pelton, P. L. Lin, and P. Cerisier
Analyses of the Thermodynamic Properties of Binary and Ternary Solutions Containing AlF_3
Presented at Seventh Euchem. Conf. on Molten Salts, Lysekil, Sweden, June 18-23, 1978

M. L. Saboungi, J. J. Marr, and M. Blander
Measurements of the Solubility of Sulphides in Molten Salts
Presented at Seventh Euchem. Conf. on Molten Salts, Lysekil, Sweden, June 18-23, 1978

W. W. Schertz
Material Constraints on Evacuated Tube Concentrating Collectors
Presented at Arizona State University Materials for Solar Energy Conversion Symp., Tuscon, AZ, January 1978

W. W. Schertz
Concentrating and Evacuated Tube Insulated Collectors
Presented at SEIA National Solar Heating and Cooling Workshop, February 4-8, 1978

H. Shimotake
High Temperature Batteries
Presented at the First Seminar on Energy and Battery, Electrochem. Soc. of Japan, Osaka, Japan
October 31-November 2, 1978

A. B. Smith, D. L. Smith, L. R. Greenwood, and R. R. Heinrich
Nuclear Data for High-Energy Neutron-Damage Sources
Presented at Northern European and American Data Committee Meeting, Oak Ridge National Laboratory, April 3-7, 1978

R. K. Steunenberg
Lithium Batteries
Presented at Am. Chem. Soc. Meeting, Hunt Valley, MD, April 5-7, 1978

R. K. Steunenberg
Molten Salt Batteries
Presented at Am. Chem. Soc. Meeting, Miami Beach, FL, September 10-15, 1978

A. L. Taboas, R. N. Singh, and T. R. Johnson
Plasma Duct for Instrumentation, Materials, and Process Analysis
Presented at ANL-DOE-ISA Symp. on Instrumentation and Control for Fossil Demonstration Plants, San Francisco, CA, June, 1978

M. Tetenbaum and H. E. Flotow
The Heat Capacity and Thermodynamic Properties of $^{242}Pu_2O_3$ from 8 to 350 K. Evaluation of the Magnetic Entropy
Presented at 33rd Annual Calorimetry Conf., Logan, UT, July 25-29, 1978

M. Tetenbaum and R. J. Ackermann
High Temperature Vaporization Behavior of Oxygen-Deficient Thoria
Presented at Tenth Gordon Research Conf. on High-Temperature Chemistry, Wolfsboro, NH, August 7-11, 1978

M. Tetenbaum and R. J. Ackermann
Thermodynamic Properties of Oxygen-Deficient Thoria
Presented at ASME-AIME Fall Meeting, St. Louis, MO, October 15-19, 1978

M. Tetenbaum and C. E. Johnson
Low-Temperature Oxygen Potential Measurements Above Hypostoichiometric U-Pu-O Compositions
Presented at Am. Ceram. Soc., San Diego, CA, October 25-28, 1978

L. E. Trevorrow
The Back End of the Nuclear Fuel Cycle
Presented at Argonne Conf. on the Energy Dilemma and the Environment, AUA-ANL Biology Symposium, April 19, 1978

L. E. Trevorrow and M. J. Steindler
Control of Environmental Impact of Low-Level Aqueous Fuel Reprocessing Wastes by Deep-Well Disposal
Presented at 71st Annual AIChE Meeting, Miami, FL, November 12-16, 1978

E. H. Van Deventer and V. A. Maroni
Hydrogen Permeation Characteristics of 316-SS, 321-SS, and Inconel-625
Presented at Am. Nucl. Soc. Meeting, San Diego, CA, June 18-23, 1978

R. Varma
Stibine and Arsine Generation from Lead-Acid Batteries
Presented at VARTA Research and Development Center, VARTA Batterie AG, Keklheim/TS, West Germany, June 23, 1978

G. J. Vogel, J. Montagna, W. Swift, and A. A. Jonke
Experiences in Regenerating Sulfated Limestones from Fluidized-Bed Combustion
Presented at Engineering Foundation Conf. on Fluidization, Cambridge, England, April 1-6, 1978

S. Vogler
Current Status of the Pyrochemical and Dry Processing Methods Program at ANL
Presented at Fuels Refabrication and Development Program Review, Battelle Seattle Research Center, September 13-15, 1978

J. R. Weston, W. F. Calaway, R. M. Yonco, E. Veleckis, and V. A. Maroni
Experimental Studies of Processing Conditions for Liquid Lithium and Solid Lithium Alloy Fusion Blankets
Presented at Am. Nucl. Soc. Third Topical Meeting on the Technology of Controlled Nuclear Fusion, Santa Fe, NM, May 9-11, 1978

Y. Yamazaki and N. P. Yao
Measurement of Current Distribution in a Porous Zinc Electrode Using Photoengraved Electrode-Stacks
Presented at Electrochem. Soc. 153rd Meeting, Seattle, WA, May 21-26, 1978

N. P. Yao
Advanced Secondary Batteries for Electric Vehicle Propulsion
Presented at 1978 Advanced Transit Assoc. International Conf., Washington, DC, April 25-28, 1978

J. E. Young, S. H. Y. Wong, and J. Fischer
Reaction Characteristics for Steam Gasification of Pittsburgh Seam Coal Under Simulated In Situ Conditions
Presented at 4th Annual Underground Conversion Symp., Steamboat Springs, CO, July 17-20, 1978

J. E. Young and J. Fischer
Reaction Characteristics During In Situ Gasification of Western Subbituminous Coals
Presented at Am. Chem. Soc. 176th National Meeting, Miami, FL, September 10-15, 1978

J. E. Young, J. Fischer, and S. H. Y. Wong
Laboratory Studies of Gasification Kinetics for Western Coals Under Conditions Expected During In Situ Conversion
Presented at 53rd Annual Technical Conf. and Exhibition of the Society of Petroleum Engineers of AIME, Houston, TX, October 1-4, 1978

J. E. Young
Current Fuel Cell Fuels Processing R&D
Presented at Workshop on Hydrocarbon Mixing and Scale-up Problems, Washington, DC, December 13-15, 1978